

The Degradation of Lubricant and Fuel Due to Nitrogen Dioxide

Neil Harris

Doctor of Philosophy

University of York
Chemistry

September 2016

ABSTRACT

Due to the recent trends to improve fuel economy and reduce emissions there have been changes to engine design, resulting in higher temperatures and more nitrogen dioxide in the engine, as well as increased biodiesel usage. Overall, this has led to a more severe environment for the engine lubricant, increasing degradation; an understanding of the mechanism is required to prevent this degradation.

Squalane has been used as a model base oil and degraded in an environment of nitrogen dioxide at 150 °C. GC x GC has been used to separate the resultant product mixture, and time of flight mass spectrometry identified products as the squalane alcohol, ketones and alkane fragments. Nitrogen containing products have been identified using a GC x GC with nitrogen chemiluminescence detector, the highest concentration of product has been identified as nitromethane. Other nitroalkanes have been proposed based on retention index. The experiments have been repeated for mixtures of nitrogen dioxide and oxygen and no unique products have been identified.

The impact of biodiesel degradation has been assessed using methyl linolate as a model compound and applying the same techniques as used for the base oil model system. The products have been identified as being due to fragmentation of the methyl linolate and the formation of ketones. The largest nitrogen containing product concentration being the nitromethane, other nitroalkanes which have been identified.

This experimental evidence has led to the elucidation of the mechanism for nitration which is presented and compared with the autoxidation mechanism. The nitration is hydrogen abstraction initiated by NO_2 . The second stage is the addition of NO_2 to form an alkyl nitrite. The CO-NO bond is comparable to a peroxide, therefore decays to an alkoxy radical. The alkoxy radical can then follow the established mechanisms in autoxidation to form the observed products.

Contents

Abstract	3
List of figures	10
List of tables	16
Acknowledgements	18
Authors Declaration	20
1 Introduction	23
1.1 Introduction	24
1.2 Types of base oil	26
1.3 Bio-derived base oil	29
1.4 Autoxidation of oil	30
1.5 Oxidation of branched alkanes	33
1.6 NO _x introduction	36
1.7 Production of NO _x in the engine	37
1.8 Nitration and nitrooxidation of engine oils	39
1.9 Liquid phase reaction of hydrocarbons with NO _x	42
1.10 Gas phase reactions of NO _x	43
1.11 Interactions of NO _x with antioxidants	44
1.12 Analytical techniques for degraded oils	44
1.13 Other useful analytical techniques	47
1.14 Engine operation conditions	49
1.15 Conclusions	52
2 Experimental	55
2.1 Introduction	56
2.2 Reaction set up	56
2.3 Materials	59
2.4 Reaction procedure	60
2.5 Risk assessment handling with NO ₂	62
2.5.1 Risk phrases	62

2.5.2	Safety phrases	63
2.5.3	Exposure limits	63
2.5.4	Controlling the risk from using NO ₂	63
2.5.5	Controls to minimise the risk during the experiment	64
2.5.6	Controls to minimise the risk to those outside of the laboratory	64
2.5.7	Action to take in case of accidental release	64
	Fume cupboard extraction failure during the normal running of an experiment	64
	Fume cupboard extraction and alarm failure during the normal running of an experiment	65
2.5.8	Risk calculation	65
	Concentration of NO ₂ emitted from exhaust stack	65
	Time to fill a fume hood	65
	Time to fill area surrounding the fume hood	65
2.6	Infrared spectroscopy (IR)	66
2.7	Gas phase infrared spectroscopy	66
2.8	Gas chromatography mass spectrometry (GC-MS)	67
2.8.1	Silylation of the alcohol	67
2.8.2	GC x GC – time of flight (TOF) MS	67
2.8.3	GC x GC nitrogen chemiluminescence detection (NCD)	68
2.9	Synthesis of nitroalkanes	68
3	Major products of nitration and nitrooxidation of squalane	69
3.1	Introduction	70
3.2	Previous work to identify the products from nitration of alkanes	70
3.3	FT-IR analysis of squalane nitration and nitrooxidation	70
3.4	GC x GC MS analysis of squalane nitration and nitrooxidation	73
3.5	Product identification by GC x GC MS analysis	76
3.5.1	Alkanes	76
	Mass fragmentation of alkanes	79
	Analysis of retention indices for confirmation of molecular size	80
	Product identification of alkanes	81
	Mechanism of alkane formation	82
	Alkane ratio	83
3.5.2	Ketones	84
	Mass fragmentation of ketones	84
	Product identification of ketones	86
	Mechanism of alkanes and ketones formation	86

3.5.3	Alcohols and lactones	87
	Mass fragmentation of alcohols and lactones	88
	Alcohols	89
	Lactones	92
3.6	Conclusions	94
4	Identification of nitrogen containing products	97
4.1	Introduction	98
4.2	Previous work to identify nitrogen containing degradation products of base oils	98
4.3	Maximum nitrogen concentration	98
4.4	Infrared absorption bands due to nitro functional groups	100
4.5	GC x GC-NCD analysis of squalane nitration and nitrooxidation	104
4.6	Synthesis of nitroalkanes	105
4.7	Retention indices calculation of nitroalkanes in GC X GC NCD	107
4.8	Carbon number calculation	109
4.9	Quantification of the nitro alkane products	113
4.10	Identification of nitromethane	115
4.11	Quantification of detected nitrogen containing species	117
	4.11.1 Percentage identified nitrogen	119
4.12	Nitration of pristane	121
4.13	Conclusions	121
5	Analysis of the reaction gases	123
5.1	Introduction	124
5.2	Previous work into reaction gas analysis	124
5.3	Gas phase IR of exhaust gases	124
5.4	Gas phase IR of nitrogen dioxide	126
5.5	Gas phase IR of nitric oxide	126
5.6	Gas phase IR spectra of carbon monoxide and carbon dioxide	128
5.7	Summary of gas phase infra red analysis	131
5.8	Infra red spectroscopic analysis of the contents of the cold trap	132
5.9	Production of the oxygen due to the decay of nitrogen oxide	134
5.10	Conclusions	136
6	Nitration and nitrooxidation of methyl linolate	137
6.1	Introduction	138
6.2	Previous work into the nitration of methyl linolate	138

6.3	Identification of the major product of nitration of methyl linolate	139
6.3.1	Mass spectrum identification of dec-2,4-dien-1-al	140
6.3.2	Mass spectrum identification of the formation of methyl octanoate	142
6.3.3	Mass spectrum identification of the formation of methyl nonano-1-al	144
6.3.4	Mass spectrum identification of the formation of methyl dec-2-eno-1-al	146
6.4	NCD analysis of the nitration and nitrooxidation of methyl linolate	148
6.5	Identification of the nitro alkane products of nitration of methyl linolate	151
6.6	Stability of the identified nitroalkanes	153
6.7	Quantification and stability of other nitrogen containing products	155
6.8	Total amount of nitrogen containing products in nitrogen and nitrogen dioxide	157
6.8.1	Percentage identified nitrogen	159
6.9	Conclusion	160
7	Discussion	163
7.1	Introduction	164
7.2	Initiation	164
7.3	Propagation	165
7.4	Chain branching	167
7.5	Termination	169
7.6	Overall mechanism	170
7.7	Nitromethane	172
7.8	Comparison with oxidation	173
7.9	Effects on lubricant performance the engine	174
7.10	Measurement of the nitrate esters	175
8	Comparison of the model system with the materials used commercially	177
8.1	Introduction	178
8.2	PAO	178
8.3	PAO nitration and nitrooxidations by GC x GC NCD	179
8.4	Biodiesel	180
8.5	Biofuel nitration and nitrooxidations by GCxGC NCD	181
8.6	Field trials of lubricants in heavy duty diesel engines	183
8.7	Conclusions	184
9	Conclusions and Future Work	185
9.1	Conclusions	186
9.2	Future work	187

List of Abbreviations	190
A1 : Appendix for chapter 3	193
A2 : Appendix for chapter 4	197
A3 : Appendix for chapter 6	199
Bibliography	201

CONTENTS

List of Figures

1.1	The types of chemical structures found in mineral base oils	27
1.2	The correlation between the tertiary alkanes in base oils and the oxidation stability by PDSC	29
1.3	Radical initiation and peroxy radical formation	30
1.4	Peroxide radical hydrogen abstraction	31
1.5	Autoretardation of oxidation	31
1.6	Adol condensation to a product which can undergo further condensations	32
1.7	The structure of squalane	33
1.8	Functionalisation and fragmentation of squalane in oxidation	34
1.9	Autooxidation products of squalane	35
1.10	Resonance forms of nitrogen oxide	37
1.11	Resonance forms of nitrogen dioxide	37
1.12	Formation of NO by the Zel'dovich mechanism	38
1.13	Formation of NO by the Fenimore mechanism	38
1.14	Formation of nitrogen dioxide	39
1.15	Nitration mechanism as presented by Coultas ¹	41
1.16	A modified version nitration mechanism as presented by Coultas to explain oxygen loss	41
1.17	Liquid phase reactions of NO _x	42
1.18	Oxidation of NO by peroxy radicals	42
1.19	Nitrogen dioxide products in the gas phase	43
1.20	Structure of nitro and nitrate esters	45
1.21	A schematic representation of GC x GC set up	48
1.22	Schematic of the NCD to form excited state of NO from the organic nitrogen in the sample	49
1.23	Pressure in the engine cylinder calculated by <i>Han et al.</i> ²	51
2.1	Schematic of reaction set-up used for nitration and nitro-oxidations under continuous flow of NO ₂ , O ₂ in N ₂	56

2.2	Photograph of reaction set up used for nitration and nitro-oxidations under continuous flow of NO ₂ , O ₂ in N ₂	57
2.3	Photographs of reactor including lid showing inlets and outlets, side view of reactor base, top view of reactor	58
2.4	Schematic of reaction set up for gas phase IR	66
2.5	The reaction scheme for conversion of primary bromides to nitroalkanes .	68
3.1	FT-IR spectrum of squalane nitration at 150 °C of the liquid samples at 20 minute intervals between 0 and 120 mins	71
3.2	FTIR of squalane nitrooxidation at 150 °C of the liquid samples at 20 minute intervals, measured against a background of squalane	71
3.3	GC x GC-TOF-MS of squalane nitration at 150 °C after sample two hours	74
3.4	GC x GC-TOF-MS of squalane nitrooxidation at 150 °C after two hours .	75
3.5	GC x GC TOF MS of nitrooxidation with identified products numbered .	76
3.6	fragmentation pattern of 2,6,10,15,19-pentamethyl heneicosane in TOF-MS (product 2)	80
3.7	Analysis of retention times of alkanes identified by GC x GC-TOF-MS to confirm molecular size	81
3.8	Structures of alkanes identified by GC x GC TOF MS	82
3.9	Mechanism of alkane fragments formation from squalane during nitration	83
3.10	Mechanism of McLafferty ion formation for ketones	84
3.11	Structures of ketones identified by GC x GC-TOF-MS	86
3.12	Mechanism of alkane and ketone fragments formation from squalane during nitration	87
3.13	TIC of the GC-MS analysis of the squalane oxidation and after silylation	89
3.14	Mass spectra of the three peaks formed on the silylation of oxidised squalane	90
3.15	Structures of alcohols identified by GC x GC TOF MS	91
3.16	Structures of silylated alcohols identified by GC x GC TOF M	91
3.17	Scheme of alcohol formation from squalane during nitration	92
3.18	Characteristic fragmentation of lactones	93
3.19	Structures of lactones identified by GC x GC TOF MS	93
3.20	Mechanism of lactone formation from squalane by autooxidation as proposed by stark et al. ³	93
3.21	Mechanism of lactone formation from squalane by autooxidation with squalane	94
4.1	Infrared spectra of nitromethanetrispropanol and 2-methyl propan-1-ol . .	101
4.2	Infrared spectrum of nitromethane	102

4.3	FTIR spectrum of squalane nitration end of reaction sample for 2 hours at 150 °C	103
4.4	GC x GC-NCD analysis of squalane nitrated at 150 °C for 2 hours	104
4.5	Numbered products and regions of GC x GC NCD analysis of squalane nitrated at 150°C for 2 hours	105
4.6	¹ H NMR shift changes between a bromoalkane and nitroalkane	106
4.7	Crude ¹ H NMR spectrum of nitroalkanes synthesised from bromoalkanes .	106
4.8	Nitroalkanes synthesised from bromoalkanes	107
4.9	Retention indices of nitroalkanes in the GC x GC NCD	109
4.10	Chemical structures of the proposed nitro alkane products from the nitration and nitrooxidation of squalane	111
4.11	The scheme to form primary nitroalkanes from the fragmentation of squalane	112
4.12	The quantification of the identified nitro alkanes from NCD for the nitration of squalane at 150 °C for two hours	114
4.13	Quantification of the identified nitro alkanes from NCD for the nitro oxidation of squalane at 150 °C for two hours	115
4.14	GC x GC NCD analysis of nitromethane	116
4.15	Formation of nitromethane from attack at position two of squalane . . .	117
4.16	Quantification of total nitrogen containing alkanes form nitration and nitrooxidation	118
4.17	Quantification of nitromethane nitrooxidation of squalane	119
5.1	The gas phase infra red spectrum of the exhaust gases	125
5.2	The gas phase infra red spectrum of NO ₂ region of the exhaust gases . .	126
5.3	The gas phase infra red spectra of NO region of the exhaust gases . . .	127
5.4	Schematic of reaction set up	127
5.5	Infra red spectra of carbon monoxide and carbon dioxide reported by Coblentz ^{4,5}	128
5.6	The gas phase infra red spectra of CO and CO ₂ region of the exhaust gases	129
5.7	Scheme of carbon monoxide and carbon dioxide formation by autoxidation ^{6,7}	130
5.8	Scheme of carbon monoxide and carbon dioxide formation under nitration	131
5.9	Infra red spectrum of the sample collected in the cold trap during nitration of squalane for two hours at 150 °C compared to spectrum of H ₂ O . . .	133
5.10	Scheme for the formation of water from nitrous acid decay	133
5.11	The concentration of oxygen formed by the decay of nitrogen dioxide with varying temperature	135

6.1	The structure of methyl linolate	138
6.2	GC x GC chromatogram of methyl linolate nitration at 150 °C of the liquid samples at 20 minute intervals	139
6.3	Initiation of methyl linolate by hydrogen abstraction and resultant resonance structures	140
6.4	Comparison of the mass spectra to identify dec-2,4-dien-1-al	141
6.5	Mechanism for the formation of dec-2,4-dien-1-al from methyl linolate during nitration	142
6.6	Comparison of the mass spectra to identify methyl octanoate	143
6.7	Mechanism for the formation of methyl octanoate from methyl linolate during nitration	143
6.8	Comparison of the mass spectra to identify methyl nonano-1-al	144
6.9	Mechanism for the formation of methyl nonano-1-al from methyl linolate during nitration	145
6.10	Alternative mechanism for the formation of methyl nonano-1-al from methyl linolate during nitration	146
6.11	Comparison of the mass spectra to identify methyl dec-2-eno-1-al	147
6.12	Mechanism for the formation of methyl dec-2-eno-1-al from methyl linolate during nitration	148
6.13	GCxGC NCD analysis of methyl linolate nitration at 150 °C for 1 hour .	149
6.14	GCxGC NCD analysis of methyl linolate nitrooxidation at 150 °C for 1 hour	150
6.15	Mechanism for the formation of the the nitro alkanes from methyl linolate nitration and nitrooxidation	152
6.16	The concentration of nitroalkanes identified from the nitration and nitrooxidation of methyl linolate	153
6.17	The concentration of nitroalkane products identified from the nitration of methyl linolate at 150 °C after heating under nitrogen for 1 hour	154
6.18	Quantification of other nitrogen containing species by NCD from the nitration of methyl linolate for 1 hour at 150 °C	155
6.19	Quantification of other nitrogen containing species by NCD from the nitrooxidation of methyl linolate for 1 hour at 150 °C	156
6.20	Quantification of other nitrogen containing species by NCD from the nitration of methyl linolate for 1 hour at 150 °C with heating under nitrogen for 1 hour	157
6.21	Quantification of total nitrogen containing products from nitration and nitrooxidation	158
6.22	Quantification of nitro methane from nitration and nitrooxidation	159

7.1	Initiation of alkanes by NO_2	164
7.2	Proposed propagation steps for the nitration of branched alkanes	165
7.3	Nitrogen dioxide resonance	166
7.4	Mechanism for tertiary nitrite decay	167
7.5	HONO fragmentation	167
7.6	Oxidation of NO to NO_2	168
7.7	NO_x cycle	168
7.8	Fragmentation of a tertiary alkoxy radical to form a ketone	169
7.9	Autonitration cycle of hydrocarbons by NO_2	171
7.10	Mechanism the nitration of engine oil as proposed by Coultas ¹	172
8.1	Comparison between squalane and PAO nitrooxidation	180
8.2	Comparison between nitrooxidation methyl linolate and biodiesel NCD	182
8.3	Oxidation and nitration value by IR from a field trial of heavy duty trucks	183
9.1	Fragmentation pattern to identify 2,6,10,15,19 pentamethyl hencosane	193
9.2	Fragmentation pattern to identify 2,6,10,15,19 pentamethyl eincosane	194
9.3	Fragmentation pattern to identify 2,6,10,15 tetraamethyl eincosane	195
9.4	ragmentation pattern to identify dec-2,4-dien-1-al	199
9.5	Fragmentation pattern to identify methyl octante	199
9.6	Fragmentation pattern to identify methyl nonano-1-al	200
9.7	Fragmentation pattern to identify dec-2-eno-1-al	200

LIST OF FIGURES

List of Tables

1.1	The classification of base oils according to API ⁸	26
2.1	The equipment used in the experimental set-up	59
2.2	Chemical used in this study	60
2.3	The standard reaction parameters used	61
2.4	Definitions of the samples taken	62
3.1	Mass spectrum fragmentation pattern peaks for identified alkanes	77
3.2	The ratio of alkanes formed during the nitrooxidation of squalane at 150 °C for 2 hours	83
3.3	Mass spectrum fragmentation pattern peaks for identified ketones	85
3.4	The mass spectra fragmentation of squalane alcohol and lactone products	88
4.1	The nitro compounds used for the retention index calculation	108
4.2	The calculated carbon number based on the primary retention time of the nitroalkanes from the nitrated squalane	110
4.3	Retention times for nitromethane peaks and product 21	116
5.1	The reaction conditions used for gas phase infrared spectroscopic analysis	125
5.2	Summary of the infra red signal of species analysed for in the gas phase infra red spectra	132
5.3	Rate constants for the decay of nitrogen dioxide to nitric oxide and oxygen between 150 °C and 200 °C using the Arrhenius parameters of Rosser and Wise ⁹	134
6.1	Calculated carbon numbers from the primary retention times of products from the nitration nitrooxidation of methyl linolate at 150 °C for 1 hour	151
6.2	Total nitrogen quantification and percentage for nitration and nitrooxidation of methyl linolate	160
9.1	Calculated concentrations of NO ₂ and O ₂ in the reactor	197

Acknowledgements

I must extend my thanks to my supervisors, Dr Stark, Dr Hamilton and Dr MacQuarrie for their support and guidance over the last four years. They have been key in helping to keep the project progressing when the difficulties that come with research have been experienced.

Secondly I must be very thankful to my industrial supervisors, Dr Brown and Dr Ransom for their continued support through the project. I also must be extremely grateful for them being prepared to take a risk and employ placement students, with it this all I know I wouldn't be in the same situation I am today. Afton Chemical have kindly sponsored this work for which I am beholden.

The NCD has been an essential piece of equipment in this study. I am much indebted to Naomi Farren for her work to keep this piece of equipment working to the highest standard. Without this I do not know the route the project would have taken to achieve the same results. I am also grateful to my friends and colleagues at the University of York who were always supportive and offered assistance when required.

Friends were also extremely supportive throughout my PhD, most of all Rachael, Lyndsay and Julia who help not just with the chemistry also the socialising which is required to get through the tougher times. They were also a great personal support during the times even helping me get to the university when fracturing my back.

Finally but most importantly I must extend my gratitude to my family for their support especially with the birth of my daughter Beatrix during my studies. I would not have been able to complete this study without their support.

Authors Declaration

I declare that this PhD thesis entitled “The Degradation of Lubricant and Fuel Due to Nitrogen Dioxide” has been researched and written by myself under the supervision of Dr Stark, Dr Hamilton and Dr MacQuarrie. This work has not previously been presented for an award at this, or any other, University. All sources are acknowledged as References.

The field trial data of oxidation and nitration by infra red used in chapter 8 was compiled by a team at Afton Chemical under the leadership of Frank Bellgardt.

Chapter 1

Introduction

1.1 Introduction

Lubricants are used in engines to perform a variety of roles, which improve the lifetime and performance of the engine. The main functions of the lubricant are to dissipate heat, reduce friction, reduce wear and improve the engine cleanliness. A majority of the lubricant consists of a base oil, which will be the focus of this study, and also additives which are also used to enhance to performance of the oil. These additives including detergents and dispersants to solubilise polar contaminants, friction modifiers to improve fuel economy, and antiwear agents such as zinc dithiodiphosphate (ZDDP).¹⁰

The lubricant reduces the friction between moving parts, increasing the efficiency of the engine. The reduction in friction in boundary lubrication occurs by providing a surface between the metal parts with a lower coefficient of friction than the metal. Boundary friction occurs when two surfaces are close together, moving over each other at relatively low speed, this is typically the highest coefficient of friction is measured for the surface. It is suggested that the film is strengthened by organometallics from reactions of the cylinder with the oil, this film is then strengthened by additives.¹¹ The lubricant film also prevents wear and damage occurring to the metal parts in the engine as they are not directly in contact, with the additives forming a sacrificial layer.¹²

Oxidation is of high concern to engine manufacturers, oil producers and additive companies, as oxidised oil can be seriously detrimental to the engine. Acids and peroxides are formed as oxidation products which will corrode the metal surfaces on the engine causing inefficient performance and reduced lifetime.¹³ Sludge and deposits are high molecular weight species formed as results of the oxidation process.¹⁰ The formation of high molecular weight species also causes poor lubrication as they will not pump round the engine efficiently due to viscosity increase. The increase in viscosity is observed in oxidation testing as an exponential and can cause rapid catastrophic engine failure.¹⁰ Hard deposits and varnish which form on the pistons can cause wear and damage to the engine, this will reduce engine durability and performance.¹⁴

Due to environmental concerns, smaller engine sizes are being used in cars, to reduce emissions and keep costs down to the user by increasing the fuel economy.¹² However, the same performance is required as with large engines. To achieve this level of performance engines are required to run at higher temperatures and pressures than previously. These more severe operating conditions can result in quicker oil degradation due to oxidation.¹² Health concerns have also caused significant interest in the emissions from vehicles which

has led to the addition of after-treatment devices to engines, some of which, such as exhaust gas recirculation, have affected lubricant operating conditions.¹⁵

The second major change recently is the common usage of biofuels. Biodiesel contain unsaturated carbons which can further increase the rate of oxidation.^{16,17} During engine operation the lubricant can become diluted with unburnt fuel, impacting on the oxidation. Kowalski found that the temperature dependence for oxidation for the oil was equivalent to activation energy of 135-170 kJ mol⁻¹ for oil, however, for rape seed oil it much lower at 84.3 kJ mol⁻¹.¹⁶ Biofuel usage is mandated by the EU which aim to have all member states using at least 20% biofuel (including biodiesel and biogasoline by 2020).¹⁸ There is also many ethical concerns about the use of biofuels due to the conflict with crops grown for fuel or food.

There is a significant body of work looking at biofuels in the recent years, it is expected these will be more widely used, possibly legislated.¹⁹⁻²² Areas of the world where biofuel is produced such as Brazil in the case of bioethanol, utilise these fuels in much higher concentrations due to the availability and low cost.²³ Standards have been set for the property requirements of B100 biodiesel and B5 is the legal minimum in pump fuel, representing 5% biodiesel in conventional diesel.²⁴

Antioxidants such as hindered phenols, aminic compounds and sulphurised olefins are used as additives to reduce the lubricant oxidation.^{11,25} However, understanding the mechanisms of oxidation could allow the optimisation of the additives to minimise oxidation. These types of molecules have a labile hydrogen which can be easily abstracted, with the resultant radical being stabilised. Aromatic systems are often present to enable delocalisation of the radical causing the stabilisation, steric hindrance further reduces the reactivity of the radical. On top of resonance stabilisation and steric hindrance, relief of strain and enabling of free rotation can often be employed as a driving force for rapid reaction with radicals in the oil but can shift the equilibrium constant toward the radical form of the antioxidant.²⁶ The scavenging of the radicals by the stabilised molecules causes the interruption of the radical autoxidation chain reaction, stopping further oxidation.

There is a significant body of work published on the autoxidation mechanism of hydrocarbons. However NO_x is another oxidative gas formed in the combustion process. The degradation of hydrocarbons by NO_x is not as well studied as degradation by oxygen.

1.2 Types of base oil

There are several different types of base oil used in lubricants, the amount of processing affects the properties of the oil due to the changes in the chemical composition. The source of the oil also affects the chemical compositions as mineral oil is not a pure substance but a mixture of hydrocarbon of varying size and structure. Although this can cause base oils to have slight batch and supplier variation, it is considered that base oils of the same group have similar properties in regard to their performance. However, between the groups there is significant variation in the observed performance of the oils. The American Petroleum Institute classifies the base oils with regard to its physical properties into five groups which are summarised in Table 1.1.⁸ When commercial lubricants are formulated the base oils is selected to balance performance with cost, as the amount of processing increases the cost of the base oil. Groups I-III are considered mineral and groups IV-V are synthetic in Europe, however in the USA group III oils are classed as synthetic as the crude oil is heavily processed. The properties which are used to characteristic the base oil are the sulfur content, saturate level and the viscosity index. Viscosity index is a measure compared to standards of how much the viscosity changes with varying temperature, higher numbers show a more constant viscosity with temperature. These properties have been deemed critical with regard to the performance of the lubricant.

Table 1.1: The classification of base oils according to API⁸

Group	Saturates %	Sulfur %	Viscosity Index
I	<90	>0.03	80-120
II	>90	<0.03	80-120
III	>90	<0.03	≥ 120
IV	Poly Alpha Olefins (PAO)		
V	Other- Not in group I-IV		

The structure of the bases oil compounds varies more than is described by the API classification. Base oils are made up of a variety of hydrocarbon type, normally with a carbon number in the range C_{18} - C_{40} , in a mixture of paraffinic, naphthenic and aromatic compounds as shown in figure 1.1.²⁷ Nitrogen and sulfur heteroatoms are also commonly found in the carbon chain or heterocycles, these can cause significant difference in the oil performance. All base oils undergo hydrocracking, dewaxing and solvent extraction to improve the properties of the base oil. The amount of the processes that take place

will reduce the heteroatoms and the unsaturation in the base stocks, therefore more processing is required to produce group III base oils than group I. The unsaturated species, including aromatics, are hydrated from group I to group II increasing naphthenic compounds. Naphthenics are processed further to form paraffinic molecules in group III oils, this improves the properties of the base oil with regard to viscometrics as well oxidative stability, freezing point amongst others.

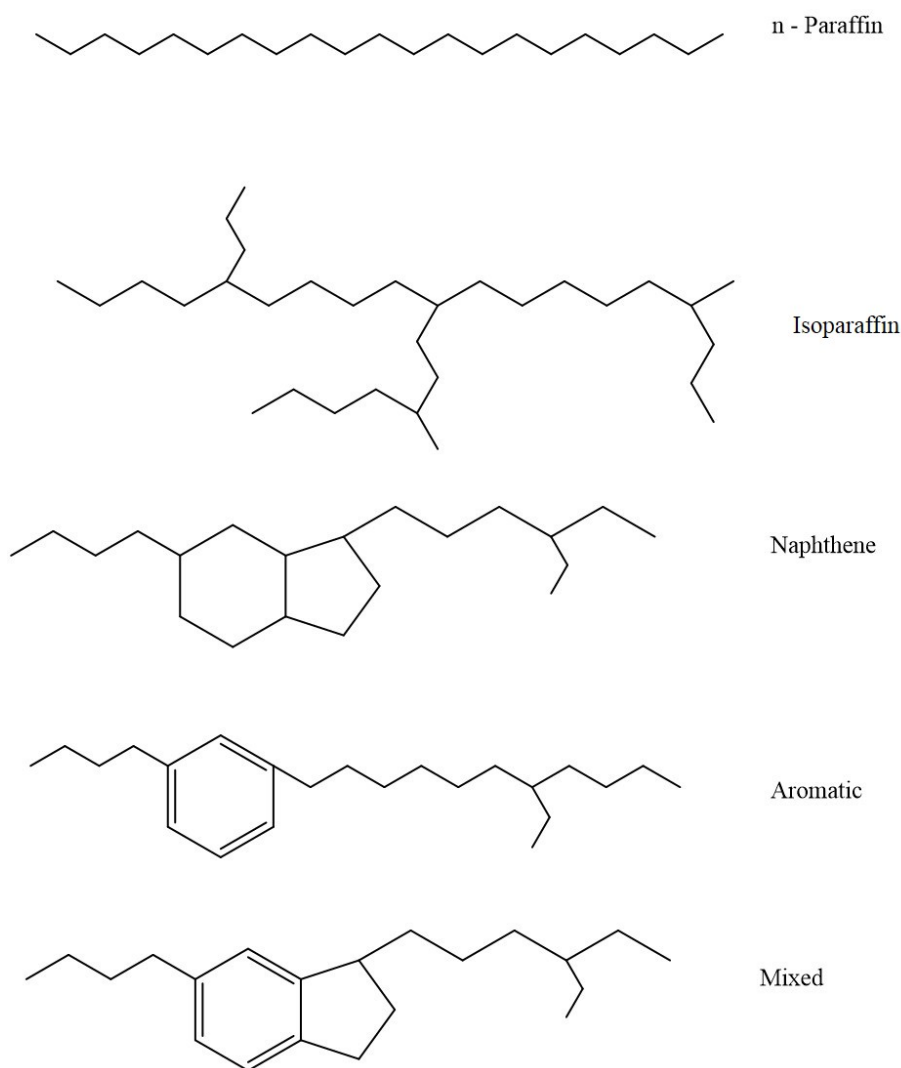


Figure 1.1: The types of chemical structures found in mineral base oils

The differences in the molecules can cause a different performance in oils as the groups vary, particularly with regard to oxidation.²⁸ The labile hydrogen atoms alpha to the aromatic rings are susceptible to radical abstraction as the benzyl radical formed has significant resonance stabilisation²⁹ and this weakens the C-H bond making abstraction easier. Double bonds in unsaturated hydrocarbon will form radicals more rapidly due to the weakened allylic C-H bond lowering the activation energy of initiation. Once

initiated, the autoxidation reactions will proceed in the base oil rapidly, *via* a radical chain mechanism resulting in an increased overall rate of oxidation, this is discussed in more detail in section 1.4. This means that it would be expected that group III oil will perform much better than group I in oxidation testing. However another factor to consider is the heterocyclic molecules found in group I base oils, in particular those which are containing sulphur or nitrogen. The aromatic heterocyclic compounds contain some inherent antioxidant performance,¹³ because they contain similar functionality to the supplementary antioxidants used as additives to enhance performance.²⁵ This results in an improved natural antioxidant level in group I oils compared to group III. Therefore the type of molecule may have a significant effect on oxidation dependent upon the types of compounds present. The base stock changing between group I and group II was found to be significantly different in research carried out by Barman.³⁰ The amount of tertiary carbons has been quantified by ¹³C NMR spectroscopy in Group II and III base oil, this has been presented to show a correlation with the oxidative stability when measure by pressure differential scanning calimetry (PDSC). The onset temperature is seen to decrease when there are higher levels of branching present as shown in fig 1.2. This study shows the difference in oxidation performance due to different structures in the base oil even within the same API classification.³¹

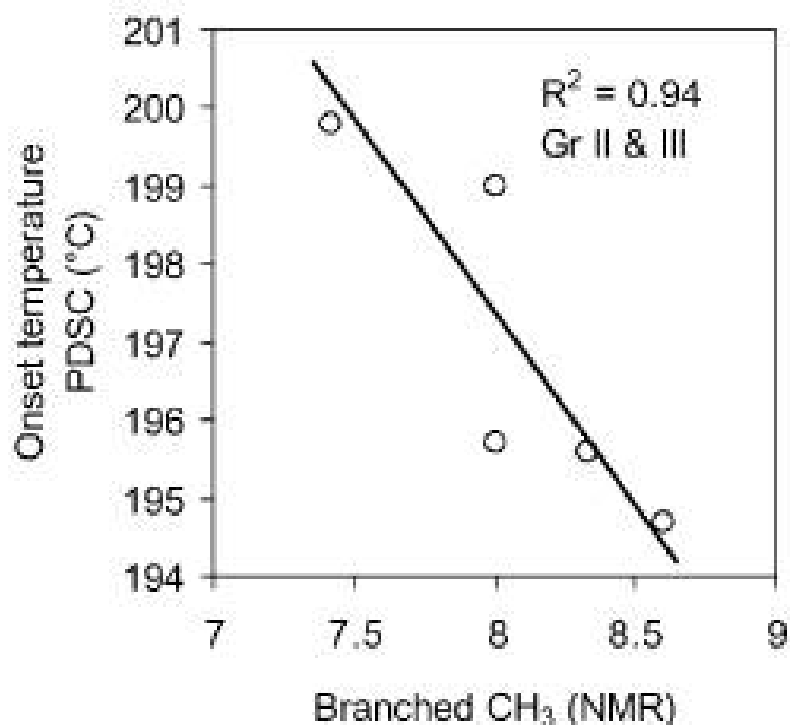


Figure 1.2: The correlation between the tertiary alkanes in base oils and the oxidation stability by PDSC

1.3 Bio-derived base oil

As crude oil prices increase and more environmentally friendly solutions are used in many applications of daily life, there have of been several reports on the possibility of biologically derived plant material to act as base oil in 'biolubricants'. One of the main issues with the biolubricants is that to achieve the same performance requires a very different additive package to what is traditionally used. However, a formulation using 15 % w/w soybean oil was used in both engine and bench testing by has been found to have good performance in low temperature, metal corrosion, oxidation and heat stability once the additive package had been optimised. Although this found some weakness some evidence is shown that with further development in the processing of the oil, the genetic modification of soy beans and greater additive optimisation then soy bean oil does represent a possible engine lubricant, however this evidence is based on minimal engine testing.³² Some derivatisation have been reported to help chemically change the features of the natural oils which have a negative impact upon the performance. One such reaction is to remove the oxidatively reactive double bonds by forming epoxides which can be then ring opened to form two esters.³³ Esters are a comparatively stable

functionality and enzymes have also been used to esterify oleic acid with fuel to form stable base oil which is reported to be very similar to low viscosity lubricating reference oil.³⁴ Fully understanding the mechanism of the degradation of these bioderived species will allow better technologies to be developed.

1.4 Autoxidation of oil

Autoxidation is the uncatalysed reactions of organic compounds in the presence of molecular oxygen or air. The oxidation takes place via a radical pathway which can cause a variety of products, however the main functional groups formed are ketones, aldehydes, peroxides, esters, alcohol and carboxylic acids.^{10,35–37} All of the products are as a result of the same key mechanistic steps. The first stage of the radical mechanism is initiation, which is a hydrogen abstraction by the di-radical oxygen species (O_2) to form a carbon-centred radical and a hydroperoxyl radical^{10,37,38}.

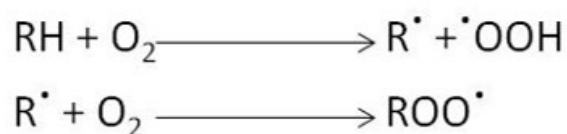


Figure 1.3: Radical initiation and peroxy radical formation

Overall, initiation is a very slow reaction often considered to be the rate determining step in the oxidation reaction.¹⁰ The selectivity of initiation by abstraction of hydrogen is due to the weakest C-H bond in the hydrocarbon. As explained in section 1.1, biofuels and biolubricants made using vegetable oil contain unsaturation in the carbon chain, the amount of which is dependent upon the plant source. The carbon-carbon double bond can resonate the radical formed giving electronic stabilisation of the radical, leaving it much more susceptible to radical attack. Due to the increase in effective concentration of labile hydrogens when unsaturation is present, the rate of hydrogen abstraction is increased causing an increase in the overall rate of reaction for the oxidation process.^{17,39} Some literature also has the mechanism to be a simply decay of the hydrocarbon species upon heating to a hydrogen radical and a carbon-centred radical.^{17,38,40} In the absence of any catalyst this seems like an unlikely process and no evidence is presented supporting spontaneous decay at these temperatures, particularly when there is a natural di-radical initiation species present in the form of oxygen. The reactions do converge later in the

mechanism resulting in the same products.

The next stage of the oxidation is propagation where the carbon-centred radical reacts with a second oxygen molecule to form a peroxy radical.^{10,17,38,40} Hydrogen abstraction by the peroxy radical can then occur, to reform an alkyl radical and also form an alkylhydroperoxide, which and continue the chain reaction leading to a variety of product to be formed, shown in figure 1.4. However this step is dependent upon the hydrocarbons involved. In some cases a more favoured reaction is the intramolecular hydrogen abstraction, forming a hydroperoxide and another carbon-centred radical on the same carbon backbone.¹⁰



Figure 1.4: Peroxide radical hydrogen abstraction external or internal

The new radical can then react on to form a second hydroperoxide. At high concentrations and temperatures the peroxide can decay leading to chain branching reactions;¹⁰ different sources suggest different stages in the mechanism dependent upon the molecules which are studied, however, they all result the formation of ketones, aldehydes and alcohols. The peroxide decay reactions are known as autocatalytic as they cause an increase in the rate that alkyl hydroperoxide is formed, resulting in an accelerating rate of reaction.

The radical chain reaction mechanism can be terminated *via* combination of two carbon-centred radicals, or the combination of two peroxyradicals, and the transition state formed will then decay to a ketone, alcohol and oxygen (Figure 1.5) in an autoretardation reaction.¹⁰

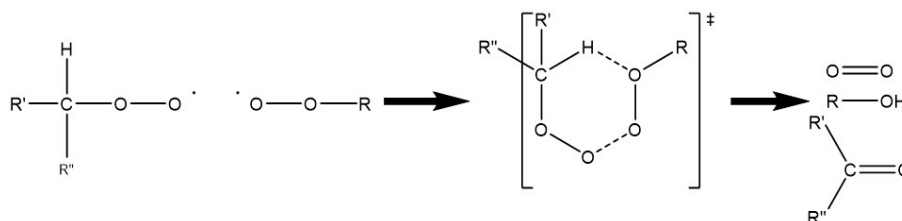


Figure 1.5: Autoretardation of oxidation

Following the primary oxidation a secondary phase takes place as the primary oxidation products react further.¹⁰ In some cases the peroxides formed will decay and form species

with low molecular weight, chain cleavage is more prevalent when the supply of oxygen is limited by diffusion.¹⁰ These volatile organic compounds can quickly evaporate from an open heated sample. Secondly, the difunctional oxidation compounds produced in the autocatalytic oxidation by intramolecular hydrogen abstraction can polycondense and polymerise in adol condensations (reaction 6, Figure 1.6) to form long chains of high molecular weight.^{10,17,33,40} Mono-functional compounds can also condense, however, di-functionality is required for further polymerisation. These species will initially form viscous materials increasing the overall viscosity of the oil. Further polymerisations and polycondensation will result in the molecules reaching a size where the product is no longer oil soluble, these insoluble products will then form sludge and deposits in the engine.

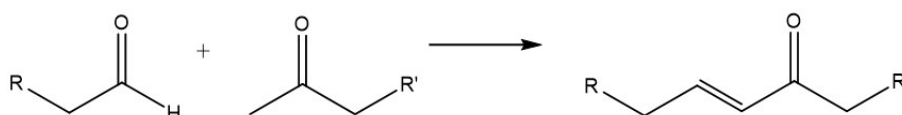


Figure 1.6: Adol condensation to a product which can undergo further condensations

The polar molecules formed from oxidation such as carboxylic acid can react with the metal parts of the engine to form ligands, these metal complex then can be soluble in oil and catalyse further reactions, particularly the polymerisation.⁴¹⁻⁴⁴ The catalysis can be either heterogeneous or homogeneous depending upon whether they dissolve into the oil, with different radical mechanism proposed depending upon the distance from the metal surface to where the oxidation takes place.⁴³ The type of metal surface has also been shown to have a great effect with low carbon steels observed as the most catalytic with lead showing signs of reducing oxidation.^{41,42}

The radical mechanisms will form a variety of products, however, there has been some selectivity shown in the products. At lower temperatures the hydrogen which is abstracted will be that with the lowest bond strength, although this is also the case at higher temperature the reaction has sufficient energy to also remove stronger bound hydrogen atom.¹⁰ In a study with ketones Hammond *et al.*⁴⁵ showed that there was a preference for the reaction was at the α position (62%) over the β and γ (21%, 17%). This observation is due to stability of the radical which is formed, the α position is stabilised by resonance with the C=O rather than the polarity of the compound.⁴⁵

1.5 Oxidation of branched alkanes

Due to base oils being a complex mixture of different compounds, mechanistic studies to understand the degradation into the multiple compounds formed from radical oxidation can be problematic. In order to remove some of the complications, pure model compounds are often used in studies to gain information that can be transferred into understanding about mineral oils, therefore compounds similar to oil need to be selected. To analyse the oxidation on different molecules a selection of compounds have been used, including decane, octane,³⁷ n-hexadecane^{46,47} and nonane-5-one has been used as a primary oxidation product.⁴⁵ Some the models worked to show the mechanism of oxidation under engine condition, as well as outside the engine, however careful consideration is required when combined to understand mineral base oils. Squalane (2,6,10,15,19,23-hexamethyltetracosane) (Figure 16) is a similar compound due to its structure with regard to the ratios of primary, secondary and tertiary carbons and molecular size (C₃₀), therefore it has been used as a model paraffinic compound in oxidation studies, and has be found to be a successful model in several pieces of research.^{36,37}

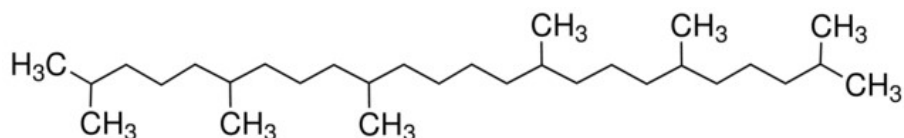


Figure 1.7: The structure of squalane

The oxidation of squalane was studied in depth by Stark *et al.*,³ as well as the oxidation of a related C₁₉ branched alkane, pristane. Mathur *et al.*³⁶ also carried out mechanistic studies into the oxidation of squalane, though some variation may be observed as their work was photo-thermal oxidation, rather than just thermal which is the case in the engine environment.

Despite the variation in experimental set up both papers find that the initial stage is a hydrogen abstraction to form a carbon centred radical, this then reacts further to form peroxides. However, following this the mechanisms vary, Stark *et al.*³ base the next stage on the peroxide decomposition as opposed the and intramolecular hydrogen abstraction.³⁶ These initial stages are summarised in section 1.4. The conditions in the engine are more closely related to that used in the work of Stark *et al.*³ therefore study of their mechanism and products form is of more relevance and will be focused upon. The intial reaction is the same as that discussed earlier.

The decay of peroxide to form the alkoxy radical, $RO\cdot$ then leads to a series of reactions resulting this functionalisation or fragmentation of the squalane molecule, shown in figure 1.8. As explained in section 1.4 there is selectivity in the oxidation due to the branching. All of the products observed using GC-MS, by Stark *et al.*,³ are in figure 1.9 suggesting the mechanistic steps involved initial abstraction of tertiary hydrogen atoms and whether a 2, 6 or 10 – squaloxy radical leads to the formation of the product.

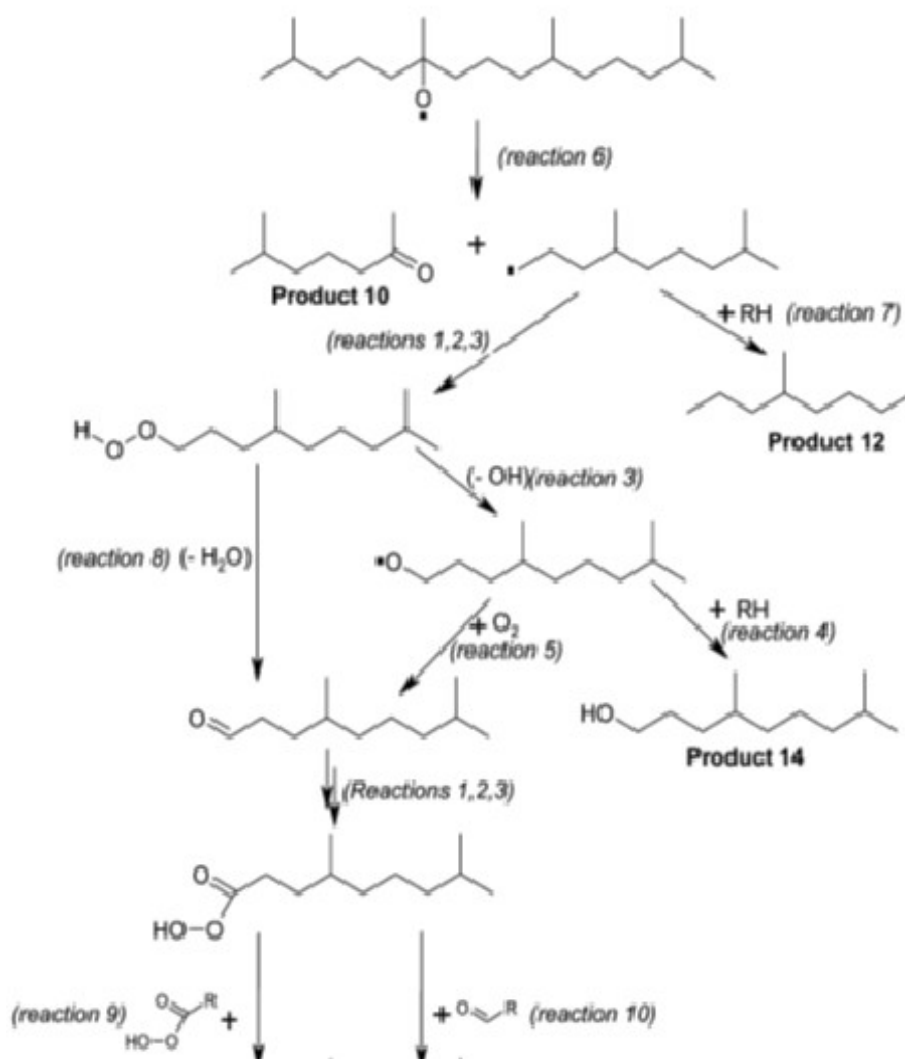


Figure 1.8: Functionalisation and fragmentation of squalane in oxidation³

Product	squaloxyl radical	Structures
propanone	2-squaloxyl	
2-methylpentane	6-squaloxyl	
6-methylhept-2-one	6-squaloxyl	
2,6-dimethylnonane	6-squaloxyl	
6,10-dimethylundecan-2-one	6-squaloxyl	
2,6,10-trimethyltetradecane	10-squaloxyl	
7,11,15-trimethylhexadecan-2-one	10-squaloxyl	
2,6,10,15-tetramethyloctadecane	6-squaloxyl	
6,11,15,19-tetramethyleicosan-2-one	6-squaloxyl	
2,6,10,15,19-pentamethyldocosane	2-squaloxyl	

Figure 1.9: Autooxidation products of squalane³

Lactones were also observed in pristane oxidation and are likely in squalane due to the structural similarities, although none were detected. Due to the formation of lactones from two tertiary radicals the mechanism proposed by Goosen⁴⁸ for lactone formation does not work in this case as it involves two hydrogen abstractions from the same carbon.⁴⁸ Therefore an alternative mechanism based on the esterification of the carboxylic group in the 2 position and alcohol in the 6 position was presented.

There is significant reporting on the effect of oxidised engine oil forming deposits, sludge, causing viscosity increase and corrosion.^{13,14} Thermally initiated radical chemistry has been studied using a range of techniques to gain information on the products formed leading to the bulk changes affecting the engine performance.^{10,36–38,40} Use of model compounds for branched alkanes to simulate Group III base oils has led to mechanistic models for the oxidation.³ However, there is little work confirming the mechanism in mineral base oil, nor is there evidence on how other types of base oil are affected by the non-paraffinic compounds, such as heterocycles, in terms of the autoxidation mechanism. The mechanistic work show no species larger than the initial model and the polymerisation reported in real life cases has not been seen, longer experimental runs to understand this

may be key.

NO_x is known to be a strong oxidising agent, particularly reactive with hydrocarbons due to the radical nature of N-O bonding. There is evidence that NO_x is oxidatively reactive toward lubricants causing varnish in the engine.⁴⁹ Significant production of NO_x takes place in the engine due to the heat in the combustion chamber. However, there is no detailed mechanistic understanding of how the nitration takes place in oils in the presence of NO_x .⁵⁰⁻⁵² Nitrooxidation is also reported to have significant effects in both the mechanism and the kinetics compared to autoxidation, the condition of having both oxygen and NO_x present represent the real engine environment and this understanding would be the most valuable to understanding the degradation of the oil.

Usage of biofuel and biolubricant is increasing rapidly and biofuels and biolubricants are likely to become more widely used in the near future.^{19-22,24} Due to unsaturation resulting in a weaker C-H bond, bio-derived hydrocarbons have a much lower activation energy with regard to radical oxidation.¹⁶ Whilst there is plenty of evidence of the reduced activation energy, there is little comparison of the mechanism or products beyond that.

Overall, while there is significant understanding of the initial oxidation of the lubricant oil, there is still more work required to understand the mechanisms of other types of compounds, mineral oil, nitration, nitrooxidation, secondary oxidation, biolubricants and biofuels. Studies into each of these areas will enable a more complete picture of lubricant degradation to be built.

1.6 NO_x introduction

This thesis focuses on the degradation of lubricants and biodiesels by reactive gases in the engine, in particular oxygen and nitric oxides, NO_x . NO_x is a collective term for nitrogen monoxide (NO) and nitrogen dioxide (NO_2). The presence of these gases in the atmosphere is mainly from anthropogenic combustion although small amounts are formed in the high temperature from lightning, the formation from combustion is discussed in more detail in section 1.7.¹⁵

Nitrogen monoxide is a paramagnetic compound, with a radical structure in two main resonance forms (Figure 1.10). The radical structure explains the reactivity, particularly towards other radicals, due to the resonance structures it can react via the nitrogen or the oxygen, although the nitrogen is electroincally preferred.^{35,53} This reactivity is due to

the doublet spin nature of nitrogen oxides. In its ground state it has C_{∞v} symmetry.



Figure 1.10: Resonance forms of nitrogen oxide

Nitrogen dioxide is also a paramagnetic radical with resonance forms (figure 1.11), stabilising the radical distributed through the molecule. In its ground state it has C_{2v} symmetry

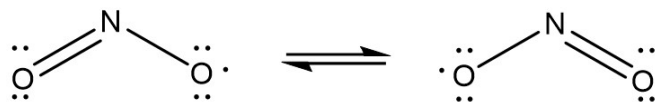


Figure 1.11: Resonance forms of nitrogen dioxide

The radical and charged nature of the NO_x species leads to their high reactivity particularly towards other radical species. The reactivity toward the lubricant is reviewed in section ??.

1.7 Production of NO_x in the engine

Due to the high temperatures reached in the combustion chamber from the combustion of fuel, nitrogen and oxygen gases in the air have been reported to react to form nitric oxides (NO_x) emissions.⁵⁴ The formation of NO takes place via a series of reactions shown in figure 1.12.^{50,51} NO is only formed in the extremely hot parts of the engine due the high activation energy, as a result of the nitrogen triple bond or an oxygen double bond that is required to be broken, which are extremely strong bonds, in the case of nitrogen the activation energy is $\approx 315 \text{ kJ mol}^{-1}$.⁵⁰ The NO_x emissions are a small proportion of the combustion products when oxygen and nitrogen are exposed to temperature $>1600 \text{ }^\circ\text{C}$ for seconds or $>2000 \text{ }^\circ\text{C}$ for milliseconds.⁵⁵ The thermal mechanism proposed by Zel'dovich is now commonly accepted as the dominant mechanism for NO_x formation in fuel lean environments, and has subsequently been extended for fuel rich environments.⁵²

Zel'dovich Mechanism



Extended for fuel rich environments



Figure 1.12: Formation of NO by the Zel'dovich mechanism

An alternative has been proposed for the prompt formation of NO by Fenimore,⁵⁶ which is a reaction between C-H and atmospheric nitrogen to form hydrogen cyanide to aid the breaking of the strong nitrogen triple bond. (figure 1.13).



Figure 1.13: Formation of NO by the Fenimore mechanism

Measurements have been made in engines to calculate how much nitrogen oxide is formed via the thermal or prompt mechanism. The major component is the Zel'dovich mechanism accounting for 88% of the formation with the Fenimore mechanism leading to 8%.⁵⁶

Hanson *et al*⁵⁷ found that the NO_x produced in the engine originates from the hot gases in the engine cylinder, the cylinder temperature affects the amount of NO_x produced with the higher temperatures increasing the rate of production. The engine load also affects the rate of NO_x production, increasing with the increase in load. They also noted that on changing the oil a lower level of NO_x production was observed for the first 20h period after which it returned to previous levels.

The residence time of NO in the crankcase is sufficiently long enough for the NO to react on to form NO_2 (Figure 1.14).⁵⁷ However, it is expected that the concentration of ozone at the elevated temperature is minimal, resulting in a negligible effect due to ozone. Due to the electronic structure of the NO bond nitrogen dioxide is a strong oxidising agent and it may autoxidise with oil or other species found in the engine.

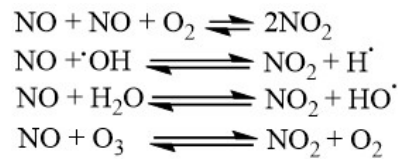


Figure 1.14: Formation of nitrogen dioxide

There are several factors that will vary the amount of nitrogen fixing that takes place in the engine, intake pressure, air fuel ratio and engine combustion ratio.^{50,57} Spindt *et al.*⁴⁹ reported that using these factors can allow the flame temperature to be calculated. Then using equations in their paper the concentration of NO can be estimated. The residence time can have a strong effect, NO is the major component of NO_x in exhaust emissions the study indicated that the NO is largely prevented from forming NO₂ in the piston by rapid cooling after the combustion as a result of the expansion stroke, while keeping the residence time at high temperature leads to more NO₂ formation.⁵⁸

Use of biodiesel causes an increase in NO_x production in the engine,⁵⁹ rises of NO_x concentration as high as 13% has been measured.³⁹ The level of oxygen in the fuel is one hypothesised cause, the other suggestion is that higher levels of biodiesel are required to be injected to produce the same engine torque compared with the standard diesel used in engine testing.³⁹

Josefsson *et al.*⁶⁰ modelled the amount NO_x produced in the engine, the model core is based around the engine geometry and the combustion processes. The key variables in the model are the temperature, flame area, fuel, O₂ concentration and N₂ concentration. On quantitatively measuring the NO_x production in the engine using KrF excimer laser to monitor NO levels, the experimental data showed good correlation with the modelled data. The flame temperature has been found to have strong effects, with negligible NO formed below 1800 K, however, significant formation takes place over 2000 K with a 100 K increase doubling the rate of formation.⁶¹

1.8 Nitration and nitrooxidation of engine oils

Spindt *et al.*⁴⁹ reviewed evidence from his own work as well as work by others, all of which observed under different circumstance that the addition of nitrogen containing compounds (NO_x or HONO) caused an increased amount of varnish to be formed in the engine. Diamond *et al.*⁶² subsequently reported that nitrogen dioxide does not cause varnish when in the presence of oil alone but when fuel is also in the mixture

the varnish level significantly increases. Spindt *et al.*⁴⁹ analysed the low temperature resins found in the engine, this showed an approximate 1:1 ratio between molecules forming varnish and the nitrogen atoms they contained. Oil and fuel do not contain enough nitrogen to provide this concentration, however the level of NO_x produced as a by-product of combustion is enough to produce this ratio. On testing the effect of NO_x dilution on the oil it was noticed that a 'gumming', to form highly viscous polymer material, was observed. It was proposed that this was due to the oxidation of the oil being catalysed by NO_x although no suggestion of made on the mechanism by which this may be happening.⁵⁷

In heavy duty diesel engines with normal and excessive wear the effect of nitro-oxidation was studied and the degraded oil showed significant infra-red absorbance due to the formation of nitrate ester, giving evidence that, as with gasoline engines, nitrooxidation takes place.⁶³ Further blocking of the oil filter with insoluble material from polymerisation and soot was observed when the engine was exposed to high level of NO_x. The level of wear in the crankcase, which has been measured to increase with the increase in NO_x, was attributed to part of the sludge, a thick deposit consisting of soot and polymeric oxidation products, which are polymerised resin due to the nitrate esters from the nitrooxidation.

More recently a study by Coultas¹ on the nitration of engine oils has been carried out, using data from both bench and vehicle testing. This study used the industry standard method for nitration, DIN 51453, measuring the change in intensity of absorbance due to the nitrate ester peak at 1710 cm⁻¹. As a result, of this work a temperature dependence was found with higher temperature resulting in the level of nitration increasing to a maximum concentration observed at approximately 150 °C after which the concentration decreased. As a result of this study the following mechanism was proposed (figure 1.15 for nitrooxidation of lubricants.

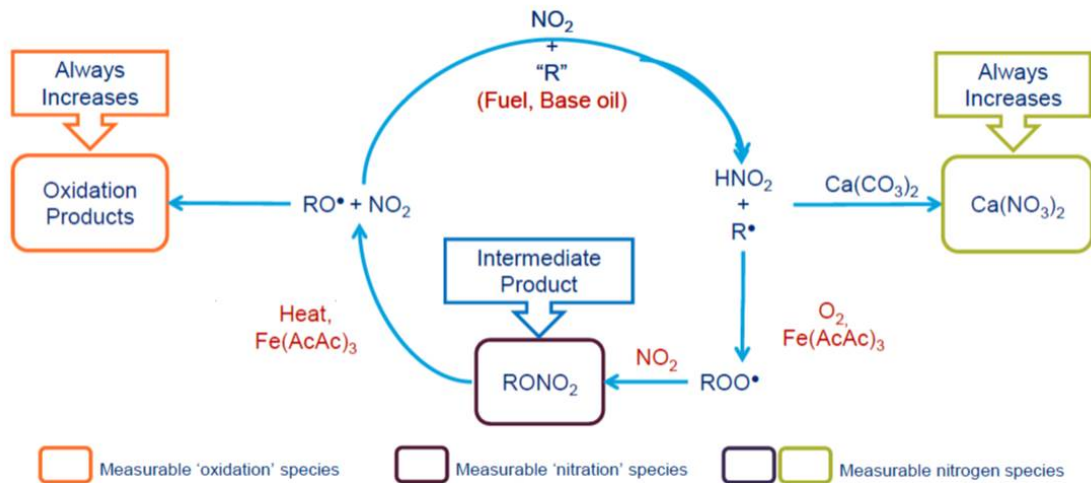


Figure 1.15: Nitration mechanism as presented by Coultas¹

However this mechanism assumes nitrate ester are the only products formed containing organic nitrogen. The more significant problem with the mechanism is the peroxy radical to the nitrate ester does not account for the loss of the oxygen atom. If stages have been missed to form the oxy radical and then follow by the addition of nitrogen dioxide to form the nitrate ester, then the species presented as the decay products are the starting material. A corrected mechanism is proposed in this thesis, shown below as an oxidation cycle as previously well reported with a initiated by NO₂ and the formation of a radical sink in the form of nitrate ester. This proposed corrected is presented below (figure 1.16) with the additions in purple.

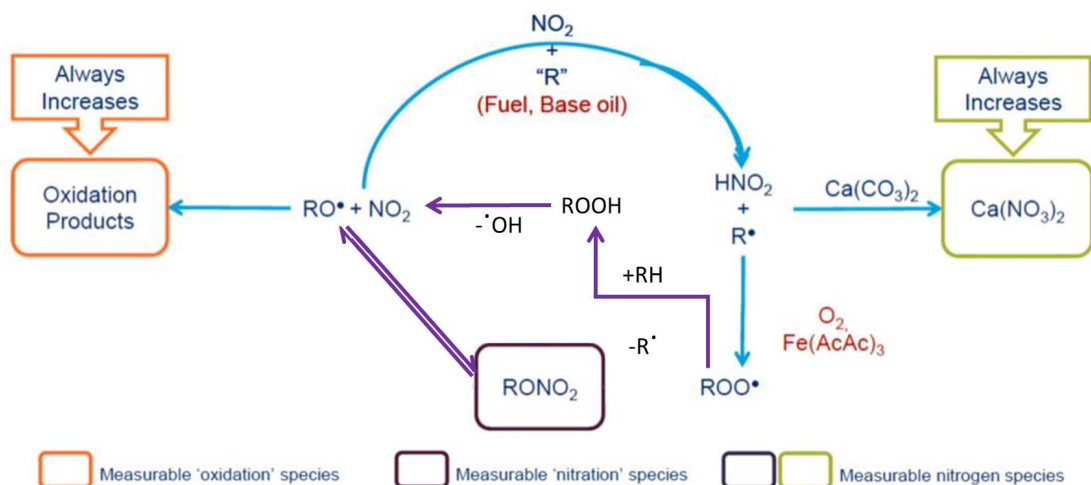


Figure 1.16: A modified version nitration mechanism as presented by Coultas to explain oxygen loss

1.9 Liquid phase reaction of hydrocarbons with NO_x

The liquid phase oxidation of lubricant using hexadecane at 160 °C as a model system has been studied by Johnson and Korcek.⁶⁴ The kinetics of NO₂ uptake were studied in detail both in the absence of oxygen and with oxidising conditions, and overall NO_x was found in both case to rapidly increase the rate of oxidation, this effect was particularly strong in the initial stages. NO_x can interact with the chain mechanism proposed for the oxidation of hydrocarbons in a variety of ways, as well as forming nitric and nitrous acids (Figure 1.17).⁶⁴

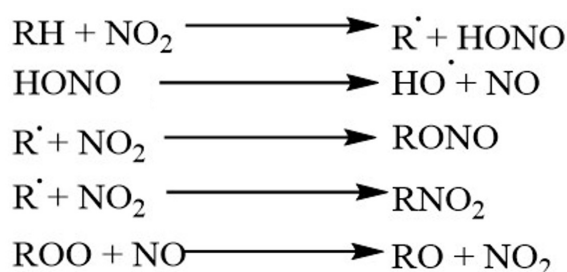


Figure 1.17: Liquid phase reactions of NO_x

However, these mechanisms are based on pre-existing literature of the reactions of NO_x with hydrocarbons which do not fit with the kinetic data presented, but Johnson *et al*⁶⁴ present no further evidence to support these mechanism or attempt to identify the products formed to ensure they are as stated.

Niki *et al*⁶⁵ studied the oxidation of alkenes initiated by a hydroxyl radical, and they proposed in this mechanism that NO will react with oxygen-centred radicals to form NO₂ and an organic radical which will react further (Figure 1.18). This work is of particular interest as, due to its strength as an oxidising agent, NO₂ is possibly involved in the oxidation of fuel and oil as it is reduced to NO, it may also be a product leading to further oxidation. This reaction cycle has also been reported to take place in the gaseous phase.

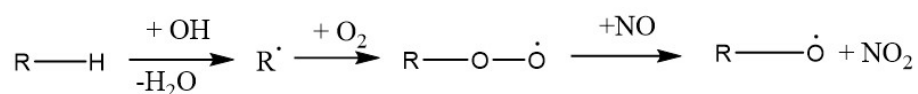


Figure 1.18: Oxidation of NO by peroxy radicals

1.10 Gas phase reactions of NO_x

Whilst there is little work to report on the liquid phase oxidation of hydrocarbons by NO_x, there is work on the gaseous phase reaction with small hydrocarbon under atmospheric conditions, these may be important to understand and analyse if similar chemistry is observed in the liquid phase. One of the key observations made in several pieces of research is the increased rates of reaction with oxygen and nitrogen dioxide together compared to oxygen on its own.⁶⁶⁻⁷⁰ This increase is proposed to be due to a catalytic cycle where the oxygen initiated reaction to the peroxide can then be reduced by NO to form NO₂, which is more reactive, however the oxidation is activated photolytically, as described by Otsuka *et al.*⁶⁹ who also noted different selectivity of the products formed with NO present. They observed a much higher yield of oxygenates formed, as well as a strong variation with products formed at different temperatures.

Mechanisms of the radical attack has also been reported to account for some of the product formation, this involves the addition of NO₂ at the carbon-centred radical to form a nitro compound or a nitrite. Further to these, radical additions to oxy radicals has shown nitrate compounds formed.^{70,71}

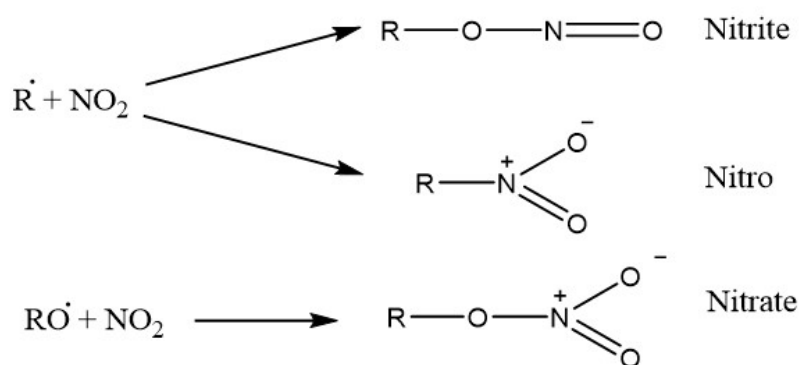


Figure 1.19: Nitrogen dioxide products in the gas phase

Similar functionalised products may be expected in the liquid phase, however the selectivity and rate will be different to those reported due to the temperatures and pressures in the combustion chamber and sump as well as difference in the reactant phases change.

The NO₂ produced as an exhaust gas has been shown to react with organic material. Diesel particulate filters are becoming widely used to reduce the amount of soot in the exhaust emission. Oxidation of the soot will regenerate the filter by removing the soot. Kandylas *et al.*⁷² studied this oxidation process and found that the NO₂ can oxidise

the soot regenerating the filter at lower temperatures than those required with oxygen directly, this study looking at NO₂ produced in the engine testing is also backed up by laboratory bench testing.⁷³⁻⁷⁵

1.11 Interactions of NO_x with antioxidants

A study into how two different types of antioxidants, phenolic and aminic reacted with NO₂, was carried out by Pochopien⁷⁶ using 1000ppm NO₂ and squalane as a carrier fluid. To explain the products observed from the antioxidants' nitration novel mechanisms were established as the products are very different from those observed with oxygen. The antioxidants prevented the nitration of the squalane for up to 130 min with phenolic and 90 mins with aminic antioxidants at 0.5% w/w. However future studies are recommended analysing the nitration products of lubricants as a large number of products that were difficult to separate were observed. Further recommendations were made to carry out nitro-oxidations were studied as these are more realistic to the engine environment.

This work confirmed earlier work carried in hexadecane which found the both phenolic antioxidants and ZDDP's were consumed quicker when NO_x was present when compared to oxidation due to only oxygen.⁷⁷

1.12 Analytical techniques for degraded oils

The products formed from these autoxidation reactions has been analysed by a range of techniques in different studies. The majority of the techniques require a separation stage first; this is due to the complex mixture of products being formed as the result of the radical mechanism. Gas chromatography (GC) is used to separate smaller volatile compounds.^{3,17,45} Liquid chromatography (LC) will separate the mixture where not all of the sample is volatile enough for GC to be an appropriate technique.¹⁷ LC can also allow coupling to different detection methods compared with GC, due to different operating conditions. More recently gel permeation chromatography has been used significantly to separate mixtures; this is a particularly strong technique for separating larger molecules, such as those formed in polycondensation.¹⁷

Infrared (IR) spectroscopy is useful to study the changes in functionality within the bulk mixture of products, although it can also be a useful technique for separated fractions. The functionality changes in the hydrocarbons upon oxidation give rise to distinctive bands. In their work with squalane Mathur *et al.*³⁶ observed four key changes in the IR

spectrum during oxidation. The OH stretching band increased in the $3550\text{-}3270\text{cm}^{-1}$, due to carboxylic acids and alcohols. Ketonic carbonyls lead to an increase in the $1800\text{-}1680\text{cm}^{-1}$ region from the C=O stretch, this is a wide region, however, any conjugation can strongly shift these bonds. An increase was observed between $1680\text{-}1600\text{cm}^{-1}$, this has been attributed to formation of unsaturated bonds.³⁶ Neighbouring unsaturated groups to the ketones showed a band formation at 888cm^{-1} .³⁶ IR has also been used to study the band observed with the presence of NO_x which show characteristic peaks at 1630cm^{-1} and 1555cm^{-1} which can be associated with nitro-oxidation.⁷⁸ The products from the nitrooxidation are suggested to be nitrate esters and nitro compounds.

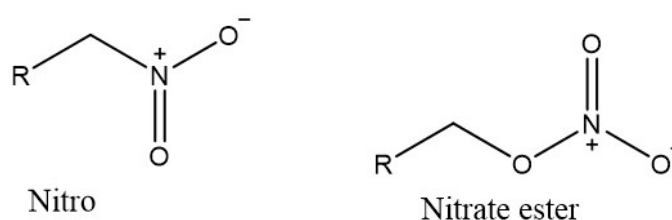


Figure 1.20: Structure of nitro and nitrate esters

^1H and ^{13}C NMR also give key signals about the functionality of the compounds formed. Ali *et al.*⁷⁹ used ^1H NMR to analyse the products of ester degradation deposits, it enabled identification of an alkene and an alkene conjugated to a ketone. The chemical shift indicated that every unit of the polymer is not conjugated. ^{13}C NMR was used by Owrang *et al.*⁸⁰ in studies of mineral oil soot production in engines; the chemical shift enabled the quantification of the amount of each functional group in the soot by peak area. This indicated that 16% of the soot was aliphatic, therefore unburnt oil still making up a considerable part of the soot. NMR is only a powerful technique with pure samples, therefore separation of the complex mixture would be required for identification of compounds.

UV-vis transitions were used by Ali *et al.*⁷⁹ with polymerised esters. The assignment of new peaks observed at 280 nm and 220 nm can confirm the formation of conjugated carbonyls as these bands are due to $n\text{-}\pi^*$ and $\pi\text{-}\pi^*$ transition. The intensity of the peak increases with the molecular weight of the polymer, thus the number of conjugated bonds therefore also increases with the molecular weight of the polymer.

Mass spectroscopy is a highly useful tool in identifying the compounds which have been formed and their elemental composition as well as structural clues from fragmentation. Mass spec is commonly coupled to LC and CG which enables the easy separation then

analysis of the product mixture. In the autoxidation of nonan-5-one by Hammond *et al.*⁴⁵ used mass spectrometry to identify the product formed. Two compounds in the GC-MS spectrum showed the same M/Z ratio however repeating the work with certain positions deuterated enabled the structures to be differentiated by GC-MS.

As shown earlier one of the key products formed in the early stages of oxidation is the alkyl hydroperoxide. The concentration of peroxide in the sample can be measured using an iodimetric titration. However instrumental methods are now also used to quantify peroxides, these include UV-vis spec, IR spectrophotometry which gives a band at 833cm^{-1} .

Above are the main techniques used to analyse degraded lubricants, however other techniques have been used. Barman³⁰ studied the difference between group I and group II mineral oils in oxidation, information on the structural changes was gained using thin layer chromatography flame ionisation detection (TLC FID) this technique allowed conclusions to be drawn upon the types of molecules which were oxidised to polar compounds in each case. Aromatic were found to be giving rise to polar compounds in group I oils and unsaturated compounds gave rise to the polar material in group II oil.

B Kowaski¹⁶ studied the effect of oxidising engine oil contaminated with vegetable oil, to do this potential difference scanning calorimetry (PDSC) was applied. It was found that PDSC was a reliable way to measure the oxidation of oil and allowed factors such as the temperature dependence of oxidation, which is equivalent to an activation energy, to be calculated. Mathur *et al.*³⁶ also calculated the activation energy by measuring the oxygen uptake at different temperatures, using the time taken for $2.6 \times 10^{-3} \text{ cm}^3 \text{ g}^{-1}$ of oxygen to be absorbed as the induction period as after this the rate of oxygen uptake was found to rise sharply which is attributed to autoxidation. From the induction period and temperature an Arrhenius plot was constructed to calculate the activation energy for the autooxidation rate determining step.

Owring *et al.*⁸⁰ studied the soot formed upon the heating of oil and compared the physical and chemical properties of soot with engine deposits, to do this the techniques of gravimetric analysis and cycling fast neutron activation analysis were employed. These methods showed a similar composition between soot and deposits in the engine, and gave indications that the mineral oil degrades *via* the autoxidised aliphatic compound.

In his work with group I and group II base oils Barman³⁰ studied the boiling point

range in GC simulated distillation and measuring the cut points, this gave an indication of the growth of species in group I and showed growth along with fragmentation of species in group II oils. Further confirmation of the observed growth in species was confirmed by carrying out size exclusion chromatography on the fresh and degraded oil samples.

1.13 Other useful analytical techniques

Whilst many techniques have been used for the study of oxidised oil there are still some which have not been reported for this application but usage for similar applications suggest that they would also be applicable. Firstly, two dimensional gas chromatography (GCxGC), has been used for a range of high resolution separations, including the separation and characterisation of petrochemical mixtures.⁸² In the multidimensional system of GCxGC the components are subject to two separations in which different factors cause the separation. This work with crude oil fractions allowed separation and identification of wide range of components from saturates and mono-aromatics to tri-aromatics and sulphurised compounds. The peak width is narrow allowing high resolution separation, and improving identification of the components.

The use of GC x GC allows enhanced separation of complex mixtures, although this is previous unreported for lubricant oxidation and nitration studies. A schematic of a GC x GC is shown in figure 1.21. The separation is achieved by the first GC working like a typical GC. A modulator collects the column effluent from the primary column, over a short period of time, typically around 5-10 seconds. Each fraction from the primary column is rapidly transferred to the secondary column at the end of each modulation. The second column is a short column (often the opposite polarity to the primary separation (typically polar)), working by a different separation mechanism. The retention time on the second column is matched to the modulation time to ensure that separation from the primary dimension is retained in the second dimension. As the separation on the second column is very short it can be deemed to be isothermal. The modulation is available in several different types, however they all serve the purpose of controlling the flow between the primary and secondary columns.

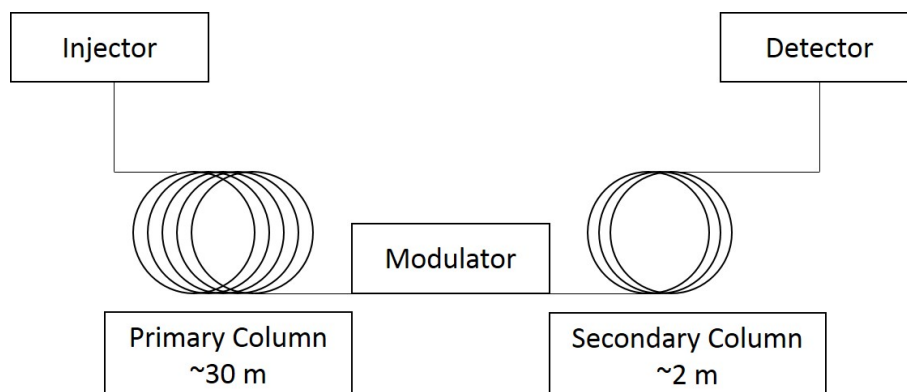


Figure 1.21: A schematic representation of GC x GC set up

As summarised in this chapter nitrogen containing species can have a significant impact upon the degradation of oil. Nitrogen chemiluminescence detection (NCD) is a detection method that can be used to quantify the nitrogen levels in a product. The sample is oxidised in NCD to form products of CO_2 , H_2O , NO and SO_2 From C, H, N and S respectively. The NO formed is the reacted with ozone to form an excited state of NO_2 , this excited state then decays to the ground state by emission of a characteristic photon at 1200 nm which is detected by a photomultiplier.⁸³ The schematic of the NCD is shown in figure 1.22. NCD has been successfully connected to gas chromatography and proved to be a useful tool in quantifying the nitrogen levels in gasoline, diesel and gas oil blends, for both individual components and the concentration in the bulk solution.^{84,85} There was some evidence of the useful nature of GC x GC NCD by Pochopien in work with antioxidants but this was not reported in great detail.⁷⁶

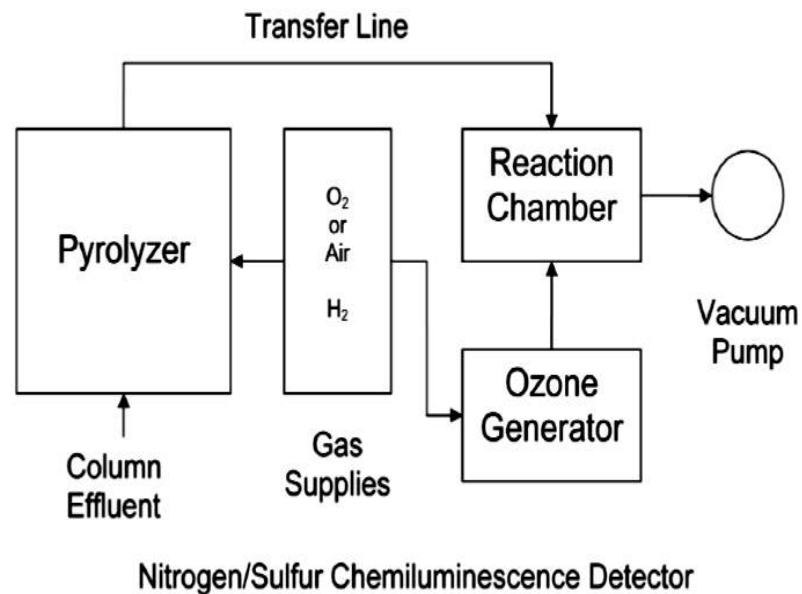


Figure 1.22: Schematic of the NCD to form excited state of NO from the organic nitrogen in the sample

1.14 Engine operation conditions

The operating conditions of an engine can have a significant effect of the chemistry which takes place, therefore for any bench testing to be reliable the conditions within the engine need to be understood. Temperature can have a large effect and can significantly vary across the engine. There is minimal actual published measurements of the engine temperature, however some evidence is discussed. The actual temperature inside a gasoline engine using a single cylinder CAT 1Y73 was found to vary between 125-180 °C dependent upon the position of the thermocouple in the cylinder and the operation conditions which varied between 1000-1200 rpm.⁸⁶ Measurements in a diesel engine with 36 points per piston show a significant variation over the range 120-350 °C with the highest at the top ring of the piston.⁸⁷

Some modelling can support that above measurements and analyse how the temperature may vary over the engine. The first temperature to consider is the highest, that is found in the piston crown and first ring, these have a desirable maximum operation temperature of 220 °C although in extreme operation this may be exceeded⁸⁸ it suggested that temperatures over 260 °C have been measured in a diesel engine.⁸⁹ The other temperature to consider is the operating temperature of the sump as the oil will be at

this temperature for a significant amount of time.

Other bench studies to test engine performance can be used to validate the conditions for this study. In work analysing oil Levermore *et al.*⁸⁹ carry their study out at 140 °C as a simulated operating temperature; the exact temperature depends upon the engine size and loading. In engine testing with a heavy duty diesel engine (sequence VD) the engine oil sump temperature was maintained at 90°C and a pressure of 330 kPa, as these were deemed normal operation conditions for the engine.⁹⁰ Oil was heated to different temperature by Diaby *et al.*¹⁴ to analyse the carbon deposits formed. The following temperatures were studied; 150°C, as the extreme sump temperature; 350 °C extreme engine temperature and 225 °C to simulate the first ring temperature on the piston head.¹⁴ However these literature sources show little reasoning in the selection of the temperature and great variation. Partly this is due to the different engines sizes and types and drive cycle. For more accurate experimental design more field evidence is required.

Lin *et al.*⁵⁹ established a link between NO_x and engine speed, as the engine speed was increased from 1000 rpm to 2200 rpm the NO_x level dropped from approximately 500 ppm to 300 ppm depending on the fuel in use. This reduction in NO_x production level was attributed to reduction in the gases residence time of high temperature combustion in the engine, as these gases lead to the production of NO_x.

Pressure can have an impact on the rate of reaction, particularly affecting the solubility of NO_x. Through the piston stroke the pressure varies significantly, this has been calculated by Han *et al.*² and is shown in Figure 1.23. Whilst the pressure is low for most of the stroke it is found to reach nearly 1.5×10^7 Pa after the compression section. It can also be seen that there is significant variation between the different rings on the piston.

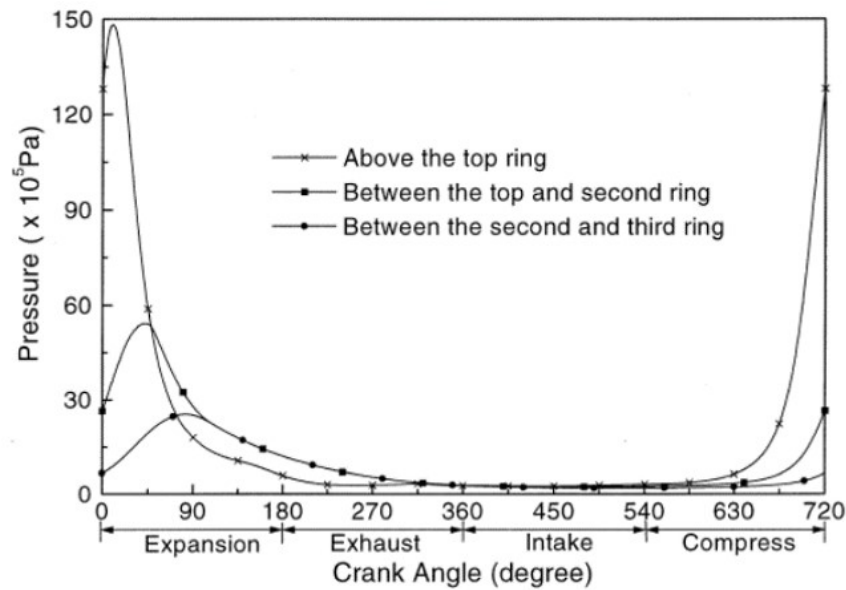


Figure 1.23: Pressure in the engine cylinder calculated by *Han et al.*²

There are two main ways NO_x can interact with the oil, firstly in the cylinder the hot oil and exhaust gases can mix causing the oil to dissolve the gases and transfer to the sump. Small amounts of the gases can also blow by the piston causing and into the sump, where they can directly interact with the oil. Blow-by gas is where the gas passes through the piston ring gaps between different part of the engine such as the valve, and valve seat also the piston ring and cylinder. The cylinder piston ring seal wears due to friction, as the wear increases the amount of blow-by gas increases significantly over the lifetime of the engine.⁹¹ Blow-by gases are a mixture of unburnt fuel and gaseous combustion products such as CO , CO_2 , NO_x , H_2O , partially combusted fuel and radicals.⁹² The high speed mixing of oil and air in the engine can cause bubbles of gas to be trapped in the oil giving a longer time and surface area for gas, liquid interface reactions. The amount of aeration will be affected by the engine speed, oil temperature and formulation of oil additives.⁹³ Entrained air was measured by S. Nemoto *et al.*⁹³ to reach levels as high as 8% volume under certain conditions.

Due to the high temperature and pressure the piston assembly is the most severe place with regard to oxidative degradation of the oil. The residence time of the oil on the piston can have a severe impact on the degradation of the oil. This was measured in a gasoline engine at 1500 rpm (50% throttle) by Stark *et al.*⁹⁴ and found to be at most approximately 60 ± 15 sec, this was measured by following the build-up of a hydrocarbon marker in the sump. By also following the build-up of oxygenated products into the sump they also calculated that the flow rate to the ring pack from the sump is 0.4 cm^3

min^{-1} cylinder $^{-1}$ with a 12% loss in the combustion chamber. This was modelled by Gamble *et al.*⁹⁵ the key factors they found to consider where, the surface area of the piston, oil thickness, flow rate, surface tension, viscosity and temperature.⁹⁵

The NO_x production in the engine oxidising the oil can be comparable to the tailpipe emissions of NO_x . The amount of blow by gas is dependent upon the wear on the engine, and the concentration of NO_x varies significantly but has been measured at between 1/7 and 1/3 the concentration of that in the tail pipe emissions.⁶³ These were measured in 1992 and found in uncatalysed car exhaust to be 1.6 g/mile (with a 0.5 g/mile variation).⁹⁶ More recently a field trial comparing the emission of school buses in 2007 found that the average NO was 6.7 g/km and 7.6 g/km when using B20 fuel rather than just petroleum diesel. Z. Huang *et al.* measure concentration of NO_2 as high as 1000ppm, dependent upon the fuel air equivalence ratio (ϕ), which is a relationship between the fuel and oxidiser, which saw maximum NO_x and NO_2 production at $\phi = 0.6$.⁵⁸ Due to the drive cycle dependence of NO_x production g/km is the current way of publish most of these measurement, which can present issues in designing a realistic bench top simulation.

The introduction of regulations on emissions form vehicles such as the EU regulation, EURO 6,⁹⁷ has controlled the emissions that an engine can produce. One way diesel engine manufactures have found to reduce the NO_x emissions is exhaust gas recirculation. The NO_x is reduced due to lower flame temperatures, decrease in inlet O_2 concentration, and an increase in the ignition delay, the downside to this reduction in NO_x is that the soot production is increased.⁷⁵ Therefore in modern engine the amount of NO_x produced is controlled by the how the engine is set up to minimise NO_x and soot emissions.⁹⁸ The EURO 6 limits for NO_x are 0.080 g/km for diesel engines and 0.060 g/km for petrol engines.⁹⁷

1.15 Conclusions

This chapter has shown that the autoxidation of hydrocarbon is well studied and the mechanism in the engine is reasonably well established for both the base oil and biofuel. The mechanistic understanding from these studies have been carried out in bench studies and transferred the engine environment with real lubricant. The development of new analytical techniques has enabled enhance separation and detector for product identification.

Nitrogen dioxide is well known to form in the engine as a reactive species which can react with the fuel and lubricant, impacting on the performance. There are some studies around the nitration of base oil on the engine environment, however the mechanisms proposed in these studies are significantly based on assumption rather than product identification. As the levels of NO_x increase in the engine due to design change it becomes increasingly important to understand the degradation mechanism.

This study will look to build upon the oxidation work and using similar methodology to understand the mechanism for degradation of hydrocarbons by nitrogen dioxide. The work in this thesis aims to identify also the major products of nitration and what the nitrogen containing products formed are. To do this GC x GC will be used with mass spectra and NCD detectors, supplemented with infra red. They will enable the major products to be identified allowing a mechanism to be proposed to support this study as well as the literature results previously reported. The study uses squalane and methyl linolate to analyse for differences between lubricant and fuel. The gas-phase change to prove the reactivity of the nitrogen dioxide and identification of any new species will be carried out using gas phase infrared. Once combined the separate aspects of this study will enable an overall picture of how nitrogen dioxide reacts with hydrocarbons in the engine. This understanding is important to enable the mechanism to be interrupted if possible to prevent degradation and the problems this causes.

Chapter 2

Experimental

2.1 Introduction

This chapter details the experimental set up, reaction procedure and the analytical techniques used during this project. Information on the specification of the chemicals that were purchased and synthesised for the reactions and identification are given.

2.2 Reaction set up

The experimental apparatus used is shown in figure 2.1 as a schematic and in figure 2.2 as a photo. This set up was used for nitration and nitro-oxidation reactions under a continuous gas flow. This set up is adapted from the equipment and techniques reported by Stark *et. al.*³ in liquid phase autoxidation studies, modified to allow the use of nitrogen dioxide in these the nitration studies. Modifications have also been made to allow mixtures of gases (NO_2 and O_2) with separate measurable flow rates for studies in nitro-oxidation.

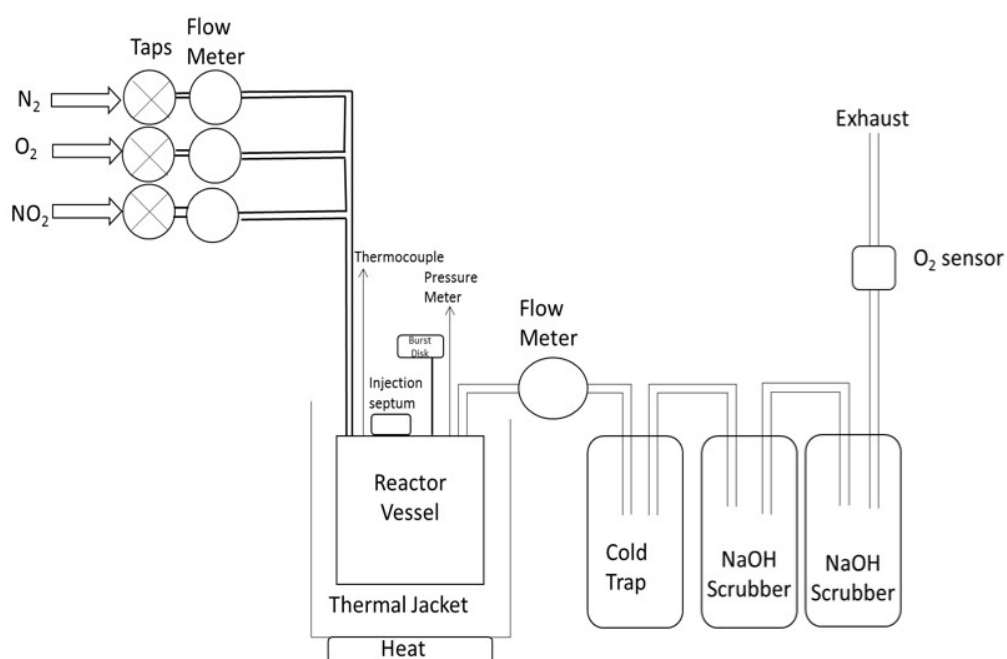


Figure 2.1: Schematic of reaction set-up used for nitration and nitro-oxidations under continuous flow of NO_2, O_2 in N_2

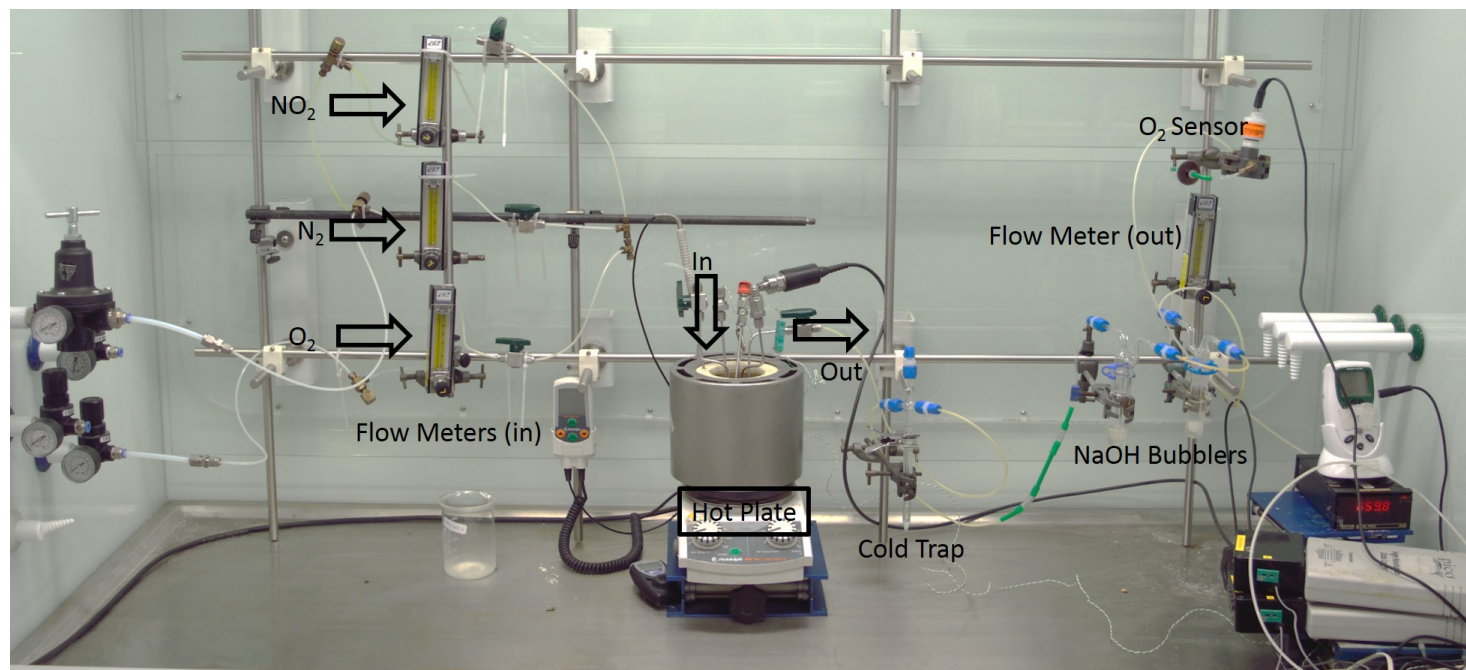


Figure 2.2: Photograph of reaction set up used for nitration and nitro-oxidations under continuous flow of NO_2, O_2 in N_2

The stainless steel reactor shown in figure 2.3 had an internal volume of 49 cm³. This was manufactured in-house at the University of York and fitted with a gas inlet and an outlet as well as adaptors to allow the reaction to be monitored via sensors and access for sampling.

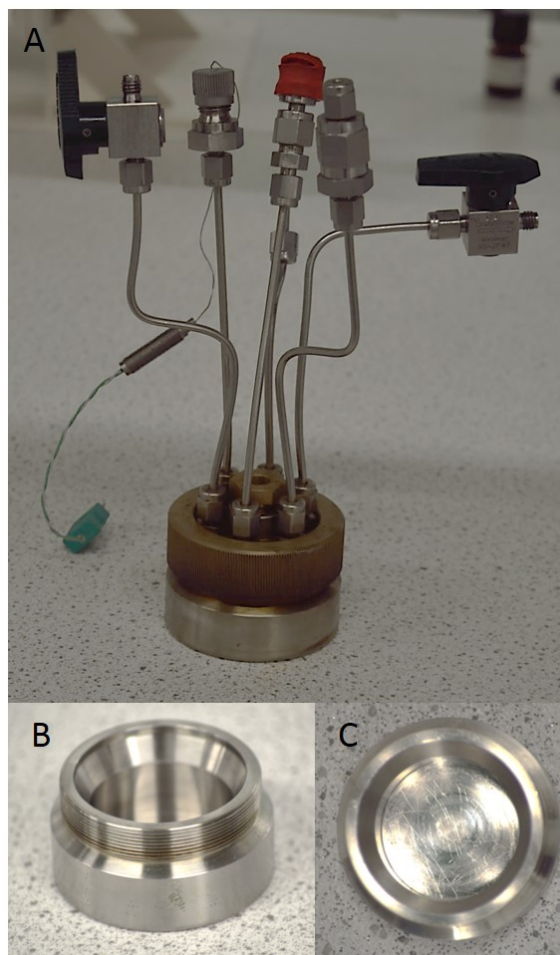


Figure 2.3: a) Photograph of reactor including lid showing inlets and outlets b) side view of reactor base c) top view of reactor

The details of the suppliers for the equipment used in the experimental set up are summarised in table 2.1

Table 2.1: The equipment used in the experimental set-up

Part	Supplier
Flow Meters 0.02-0.5 dm ³ min ⁻¹	Cole-Parmer
Non Return Valves (1/3PSI, H400SSLI/8)	Ham-let
Stainless steel reactor with 49 cm ³ internal volume with heating jacket	University of York
Hotplate with temperature controller	Heidolph
Magnetic stirring bar size 1 1/2 inch	Sigma-Aldrich
Pressure Gauge 0-2 bar, model P400	Digitron Instruments
Cold trap, capacity of 5.6 cm ³ , cooled with ice bath	University of York
Liquid traps, capacity of 25 cm ³	University of York
Oxygen (O ₂) sensor, Class 17-A	Teledyne Analytical Instruments

2.3 Materials

The detail of the main chemicals used as the reaction starting materials in this work are summarised in table 2.2. Squalane was used as a model compound for the lubricant base oil, because it is a branched alkane of appropriate molecular size for a model lubricant whilst remaining small enough for analysis via GC techniques. Methyl linolate was used as a model for the biodiesel because as a fatty acid methyl ester with a doubly allylic hydrogen, it is one of the more reactive components of biodiesel.⁹⁹

Table 2.2: Chemical used in this study

Name	Formula	CAS Number	Supplier	Purity
Reagents				
Squalane	C ₃₀ H ₆₂	111-01-3	Sigma Aldrich	99%
Pristane	C ₁₉ H ₄₀	1921-70-6	Sigma Aldrich	98%
Methyl Linolate	C ₁₉ H ₃₄ O ₂	112-63-0	Toyko Chemical Industry	95%
Polyalphaolefin	N/A	N/A	Afton Chemical	n/a
Biofuel 80% RME	N/A	N/A	Afton Chemical	n/a
Silver Nitrate	AgNO ₃	7761-88-8	Sigma Aldrich	99.00%
Solvents				
d ₈ THF	C ₄ D ₈ O	1693-74-10	Sigma Aldrich	99.50%
Toluene	C ₇ H ₈	108-88-3	Fisher chemical	99.80%
Ethyl acetate	C ₄ H ₈ O ₂	141-78-6	Fisher chemical	99.80%
Bromoalkanes				
1-bromohexane	C ₆ H ₁₃ Br	112-82-3	Sigma Aldrich	97%
1-bromooctane	C ₈ H ₁₈ Br	111-83-1	Sigma Aldrich	99%
1-bromodecane	C ₁₀ H ₂₁ Br	112-29-8	Sigma Aldrich	98%
1-bromododecane	C ₁₂ H ₂₅ Br	143-15-7	Sigma Aldrich	97%
1-bromotetradecane	C ₁₄ H ₂₉ Br	112-71-0	Sigma Aldrich	97%
1-bromopentadecane	C ₁₅ H ₃₁ Br	629-72-1	Sigma Aldrich	97%
1-bromohexadecane	C ₁₆ H ₃₃ Br	112-82-3	Sigma Aldrich	97%
1-bromooctadecane	C ₁₈ H ₃₇ Br	112-89-0	Sigma Aldrich	97%
1-bromonadecane	C ₁₉ H ₃₉ Br	4434-66-6	Sigma Aldrich	97%
Gases				
Oxygen	O ₂	7782-44-7	BOC	99.50%
Nitrogen	N ₂	93037-13-9	BOC (liquid boil off)	n/a
Nitrogen dioxide (1000ppm)	NO ₂	10102-44-0	BOC	99.5
Compressed air	n/a	n/a	n/a	n/a

2.4 Reaction procedure

The experimental set-up shown in figure 2.1 and the stainless steel reactor vessel, figure 2.3, were heated to the reaction temperature. The atmosphere of reactive gas (NO₂ with or without O₂) was allowed to equilibrate, with a total flow rate of 0.04 dm³ min⁻¹. The starting material (7 cm³) was injected through the septum into the reactor. Once the desired temperature had been reached the reaction was initiated by stirring at 600 rpm to combine the liquid and gas phases. The reaction was monitored by temperature, O₂ concentration and pressure with in-line sensors to ensure consistent conditions through the reaction. Up to seven reaction intermediate samples were taken

at regular intervals (every 20 minutes for squalane and 10 min for methyl linolate unless stated) to follow the formation of different products and the consumption of starting material. A cold trap (0°C) was used to collect the volatile products formed. The reaction was carried out over one or two hours, after which the final sample was taken. The samples taken were stored at below -10 °C prior to analysis. The duration of reaction was determined by to the reactivity of the starting material. The overall reaction parameters are summarised in table 2.3. The analysis samples where prepared on a basis of weight percentage with an ± 0.1 mg level with the solvent and the approximate dilution factor stated in table 2.4.

Table 2.3: The standard reaction parameters used

Parameters	Values
Temperature	150 ± 1 °C
Initial liquid volume	7.0 ± 0.1 cm ³
Pressure	1050 ± 10 mbar
Gas Mixtures	NO ₂ (1000 ppm in nitrogen)
	$90 \pm 2\%$ NO ₂ (1000 ppm in nitrogen) + $10 \pm 2\%$ O ₂
Sampling intervals	10 min till 60 min for methyl linolate
	20 min till 120 min for squalane
Sampling Volume	0.50 ± 0.01 cm ³
Flow Rates	$0.04 \pm 0.01 \times 10^{-5}$ dm ³ min ⁻¹

Several different samples are taken throughout the reaction and then prepared in differing ways dependant upon the analysis, the definitions for these sample as referred to in this work are given in table 2.4.

Table 2.4: Definitions of the samples taken

Sample	Definition
Reaction - Starting material	The liquid in the reactor at the beginning of the reaction before it is exposed to the reactive gases
Reaction - Intermediate samples	The samples removed from the reactor during the reaction at a regular time interval containing starting material and any degradation products formed after this time.
Reaction - End of reaction sample	The sample taken of the remain unreacted starting material and degradation products mixture at the end of the reaction
Analysis - Mass spec sample	The corresponding reaction sample dissolved in toluene at nominally 20%
Analysis - NCD sample	The corresponding reaction sample dissolved in ethyl acetate at nominally 10%

2.5 Risk assessment handling with NO₂

Due to the risks involved in work with NO₂ the following risk assessment and precautions were implemented. Working with NO₂ poses health risks, including, causing possible general delayed fatal pulmonary oedema and severe corrosion to skin, eyes and respiratory tract at high concentrations. Therefore controls are required to ensure safe working to protect the user and those in the vicinity who may also be at risk. Following information is taken from the NO₂ MSDS.

2.5.1 Risk phrases

- R8 Contact with combustible material may cause fire.
- R26 Very toxic by inhalation
- R34 Cause burns (to eyes, respiratory system and skin).

2.5.2 Safety phrases

- S1 Keep locked up.
- S9 Keep container in well ventilated place.
- S17 Keep away from combustible material.
- S26 In case of contact with eyes, rinse immediately with plenty of water and seek medical advice.
- S36/37/39 Wear suitable protective clothing, gloves and eye/face protection.
- S45 In case of accident or if you feel unwell, seek medical advice immediately (show the label where possible)

2.5.3 Exposure limits

UK: Nitrogen dioxide – Long term exposure limit (LTEL): 1 ppm max, this is the level that exposure higher concentration for a sustained period may result in health impacts
LC50/1h (ppm) - 115 ppm, this is the concentration which is lethal to 50% of the population within one hour.

2.5.4 Controlling the risk from using NO₂

- Each experiment has an individual risk assessment checked and counter signed in advance by a supervisor.
- One of the supervisors must be in the chemistry department during an experiment and notified the time and location the work will take place.
- Two members of the breathing apparatus team who are first aid trained must be available during the experiment and informed in advance.
- The safety officer is to be made aware of the location, time and duration of the experiment in advance.
- The head technician for the green chemistry labs will be notified of the location, time and duration of the experiment in advance.

2.5.5 Controls to minimise the risk during the experiment

- If the cylinder is to be removed from the fume hood it must be turned off at the main tap and a blank fitted.
- If the cylinder is not in the fume hood it must be stored in a well-ventilated cage.
- The entire experiment will take place in the fume hood this includes storage on the NO₂ cylinder.
- A NO₂ gas detector (ToxiRAE II (PGM-1150) Nitrogen Dioxide Gas Detector) will monitor the air outside the fume hood with an alarm limit of 1 ppm.
- Experiments cannot be left unattended for more than a few minutes, the sensor must stay by the fume hood with a nominated person to monitor the experiment and the sensor.
- The alarms of the fume hood (flow rate and high sash must be checked before the start of each experiment.
- The exhaust is to be secured to the back to the fume hood.
- No other experiments can take place within the fume hood.

2.5.6 Controls to minimise the risk to those outside of the laboratory

Anybody in the vicinity of the fume hood ventilation stack during the operation of the experiment is also at risk; therefore the following controls are in place:

- Access to roof controlled by a permit to work scheme.
- When informed of people on the roof all work with hazardous chemicals must stop.
- The NO₂ will be converted to NaNO₃ by passing through two liquid traps of NaOH.
- The NO₂ concentration next to the fume hood can be estimated as a maximum 16 ppb which significantly lower than the LTEL.

2.5.7 Action to take in case of accidental release

Fume cupboard extraction failure during the normal running of an experiment

If the fume hood fails this will cause the low air flow alarm to sound when the flow rate drops below 0.3 m s⁻¹. On hearing the alarm the main valve should be shut immediately

on the cylinder and the NO₂ sensor used to monitor the concentration in the lab. It can be shown that time take to fill the fume hood to the LTEL of 1 ppm would be approximately 17 minutes.

Fume cupboard extraction and alarm failure during the normal running of an experiment

If both the fume hood extraction and the low flow alarm fail a hazard warning will be given from the NO₂ gas detector which is sampling the air outside the fume hood. If this occurs the main valve should be shut immediately on the cylinder. If the NO₂ in the laboratory is above the LTEL then the laboratory shall be immediately evacuated as a precaution.

2.5.8 Risk calculation

Concentration of NO₂ emitted from exhaust stack

Typical Volume of flow rate of 1000 ppm NO₂ in nitrogen = $0.04 \times 10^{-4} \text{ dm}^3 \text{ min}^{-1}$

Volume flow of NO₂ = $4 \times 10^{-5} \text{ dm}^3 \text{ min}^{-1}$

Volume flow in exhaust from 1 fume hood with sash height at 0.2 m and 1 m width with a flow rate of $0.5 \text{ m s}^{-1} = 6 \text{ m}^3 \text{ min}^{-1} = 6 \times 10^3 \text{ dm}^3 \text{ min}^{-1}$

Concentration of NO₂ = $4 \times 10^{-5} \text{ dm}^3 \text{ min}^{-1} \div 6 \times 10^3 \text{ dm}^3 \text{ min}^{-1} = \text{c.a } 6.6 \text{ ppb}$

Time to fill a fume hood

Volume of Fume hood with dimensions = $1 \text{ m} \times 1 \text{ m} \times 0.7 \text{ m} = 0.7 \text{ m}^3 = 7 \times 10^2 \text{ dm}^3$

Volume flow of NO₂ = $4 \times 10^{-5} \text{ dm}^3 \text{ min}^{-1}$

Time to fill fume hood to LTEL (1 ppm) = $(7 \times 10^2 \text{ dm}^3 \div 4 \times 10^{-5} \text{ dm}^3 \text{ min}^{-1}) \div 1 \times 10^6 = 17.5 \text{ min}$

Time to fill area surrounding the fume hood

Approximate area around the fume hood = $3 \text{ m} \times 3 \text{ m} \times 3 \text{ m} = 27 \text{ m}^3 = 2.7 \times 10^4 \text{ dm}^3$

Volume flow of NO₂ = $4 \times 10^{-5} \text{ dm}^3 \text{ min}^{-1}$

Time to fill area to LTEL (1ppm) = $(2.7 \times 10^4 \text{ dm}^3 \div 4 \times 10^{-5} \text{ dm}^3 \text{ min}^{-1}) \div 1 \times 10^6 = 675 \text{ min} = 11.25 \text{ hours}$

2.6 Infrared spectroscopy (IR)

FT-IR spectra were measured on the reaction samples using a Bruker Vertex 70 FT-IR spectrometer set up to carry out attenuated total reflectance (ATR) experiments. The instrument was set to measure in the mid-IR range ($4000\text{-}600\text{ cm}^{-1}$) with a resolution of 4 cm^{-1} and 16 scans taken per spectrum. The data was collected and analysed using Opus version 5.5.

2.7 Gas phase infrared spectroscopy

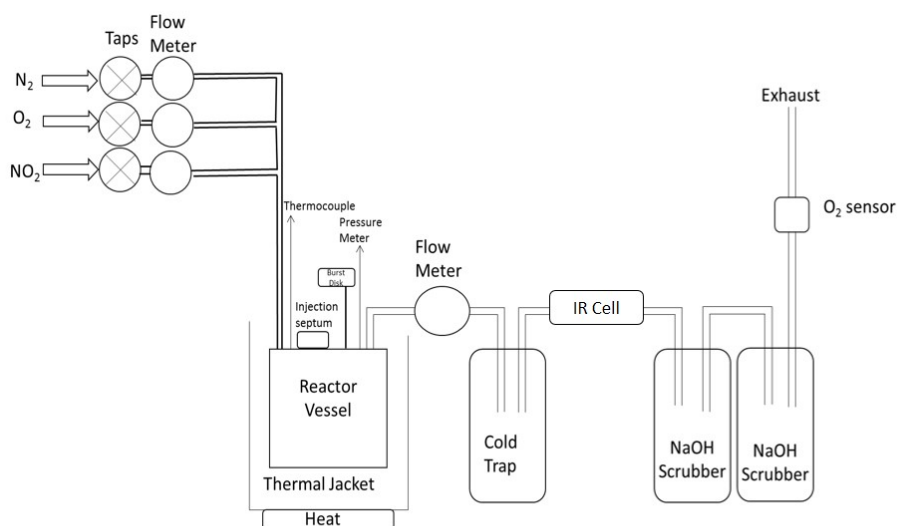


Figure 2.4: Schematic of reaction set up for gas phase IR

The experimental set up was modified to incorporate a gas phase IR measurement prior to scrubbing of the unreacted NO_2 in the exhaust gases. Measurements of the spectra were recorded by FT-IR using a gas cell with KBr windows and a 10 cm path length. 64 scans were taken between 4000 cm^{-1} and 400 cm^{-1} with a resolution of 0.5 cm^{-1} , against the background with the cell filled with nitrogen only. An NO_2 spectrum was also taken for comparison (NO_2 blank) which was prepared by flowing (in N_2) through the cold reactor to flush the IR cell, once cell had filled with the gas mixture the spectra was measured as per the reaction samples.

2.8 Gas chromatography mass spectrometry (GC-MS)

GC-MS was used to identify some of the products formed in the oxidation, the samples were approximately diluted to nominally 20% by mass, with the dilution factor accurately recorded in toluene. Toluene and tetrahydrofuran (THF) were identified as suitable solvents based on the solubility, however, toluene was found to be preferable due to its lower volatility. GC-MS was performed on a Perkin Elmer Clarus 500 GC coupled with a Clarus 560 S quadrupole mass spectrometer. Injections were completed by an Perkin Elmer auto-sampler system with a volume of 1 μl . The GC was fitted with a 5% -Phenyl-methylpolysiloxane (DB5HT(Phenomenex)) capillary column (30 m \times 250 μm \times 0.25 μm nominal). The carrier gas used was helium with an initial head pressure of 22.35 psi. The temperature of the injector was 300 $^{\circ}\text{C}$ with the flow rate controlled and set to 1.00 $\text{cm}^3 \text{min}^{-1}$. A split-splitless injector was used and the sample analysed using a split ratio of 50:1. The initial oven temperature was maintained at 60 $^{\circ}\text{C}$ for 1 minute. The temperature was then ramped at a rate of 8 $^{\circ}\text{C} \text{min}^{-1}$ until 360 $^{\circ}\text{C}$ and held for 10 minutes. The Clarus 500 quadrupole mass spectra was operated in the electron ionisation mode (EI) at 70 eV, a source temperature of 300 $^{\circ}\text{C}$, and the quadrupole at the scan range of 30 - 1200 m/z. The data was collected with the PerkinElmer enhanced TurboMass (Ver5.4.2) chemical software.

2.8.1 Silylation of the alcohol

2.8.2 GC x GC – time of flight (TOF) MS

The GC x GC NCD analysis was carried out on an Agilent 6890 GC x GC coupled with a Pegasus III TOF-MS (LECO). Injections were carried out at 200 $^{\circ}\text{C}$ using a liquid auto-sampler (Gerstel) with a volume of 1 μL . The first column in the primary oven was a 5% phenyl polysilphenylene-siloxane (BPX5 (30 m \times 250 μm \times 0.25 μm). The primary oven had an initial temperature of 40 $^{\circ}\text{C}$ held for five minutes after which it was ramped at 5 $^{\circ}\text{C} \text{min}^{-1}$ to 260 $^{\circ}\text{C}$ then held for seven mins. The secondary oven used a (BPX50 (2 m \times 100 μm \times 0.1 μm) 50% phenyl polysilphenylene-siloxane and the oven was programmed with an initial temperature of 55 $^{\circ}\text{C}$ for five min when it is ramped at 5 $^{\circ}\text{C} \text{min}^{-1}$ to 270 $^{\circ}\text{C}$ then held for seven min. This system has a dual cryogenic jet modulator between both columns. Helium was used as the carrier gas. The TOF-MS had a detector delay of four minutes, after which 200 spectra were acquired per seconds over a mass range of, m/z 40-500 at a rate of 200 Hz. The acquisition voltage is 1515 mV. The electron energy at the ionisation source is -70 eV. The data was analysed using LECO chromaTOF software.

2.8.3 GC x GC nitrogen chemiluminescence detection (NCD)

The GC x GC MS analysis was carried out on a Agilent 7890 coupled with a Agilent 255 nitrogen chemiluminescence detection (NCD). Injections were carried out at 200 °C using a liquid auto-sampler (Gerstel) with a volume of 1 μ L . The first oven contained a 5% phenyl polysilphenylene-siloxane (zebron - DB5) (30 m x 320 μ m x 0.25 μ m) column programmed to an initial temperature of 40 °C for two mins when it is ramped at 7 °C min⁻¹ to 260 °C then held for two mins. The secondary oven contained a 50% phenyl polysilphenylene-siloxane (BPX50 (2m x 100 μ m x 0.1 μ m) column, the oven was programmed with an initial temperature of 55 °C for 2 mins when it is ramped at 5 °C min⁻¹ to 275 °C then held for 2 mins. Helium was used as the carrier gas. The NCD had a detector delay of 2 min, after which data was record for emissions at 1200 nm at 200 Hz for the entirety of the analysis

2.9 Synthesis of nitroalkanes

Synthesis of nitroalkanes was adapted from a method reported by Ballini *et al.*,¹⁰⁰ figure 2.5. 1-bromoalkane (1 mmol) was added to water (2 ml) this was stirred and reacted with of silver nitrate, AgNO₃, (0.62g, 4 mmol) for 24 hours in the dark. The reaction was filtered to remove excess and the product extracted with ethyl acetate, and then dried over magnesium sulphate. The final product was isolated by filtration of the magnesium sulphate, then removal of the ethyl acetate under vacuum. The product was dissolved in deuterated THF to prepare NMR sample to confirm the conversion, as discussed in section 4.6.

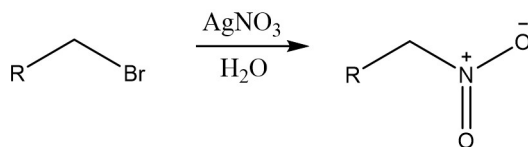


Figure 2.5: The reaction scheme for conversion of primary bromides to nitroalkanes

Chapter 3

Major products of nitration and nitrooxidation of squalane

3.1 Introduction

The major products from the nitration and nitrooxidation of squalane are discussed in this chapter. The major products identified are alkanes, ketones, alcohols and lactones. GC×GC mass spectra and FT-IR analysis are the techniques used to identify the products. Mechanisms for the formation of these products from the starting material are proposed.

3.2 Previous work to identify the products from nitration of alkanes

Previous studies in to the nitration of alkanes in the liquid phase have not identified the functional groups of products, with the exception of nitrate esters.^{1,64,78} These previous studies have focused on monitoring the loss of the starting material to give reaction kinetics. Other studies have also examined the bulk elemental analysis of the products.^{55,62} In studies of the products *via* infrared the formation of nitrate esters has been indicated by the increase in the absorbances from these products however full identification of structure has not been completed, neither have any other species been identified.

Work in the gas phase under atmospheric conditions has identified the addition of nitrogen dioxide to small alkyl radical *via* the nitrogen or oxygen to form the nitroalkanes and alkyl nitrites. Under the conditions used in this study, to simulating the engine environment, the reactions and therefore the observed products may differ.^{67,71,101,102}

This chapter examines separation of products by GC x GC coupled with an TOF MS detector to identify the major products from the nitration of squalane. Once identified these degradation products are used to build an understanding into their mechanism of formation.

3.3 FT-IR analysis of squalane nitration and nitrooxidation

FT-IR has been carried out of samples taken at 20 minute intervals throughout the reaction of NO₂ with squalane as described in the experimental section. The first spectra, figure 3.1, is compared to a blank background, which shows the overall absorbances for the wave number range measured in the spectra. In figure 3.2, the spectra of squalane samples taken every 20 minutes are compared to a reference background of squalane,

these shows the changes from the starting material in more detail as the strong C-H stretches absorbances are removed .

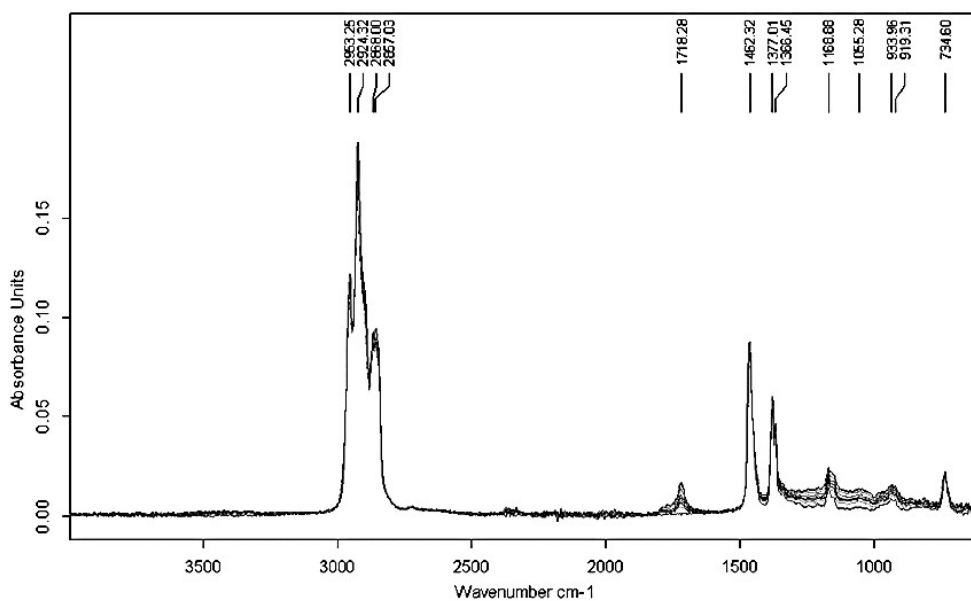


Figure 3.1: FT-IR spectrum of squalane nitration at 150 °C of the liquid samples at 20 minute intervals between 0 and 120 mins

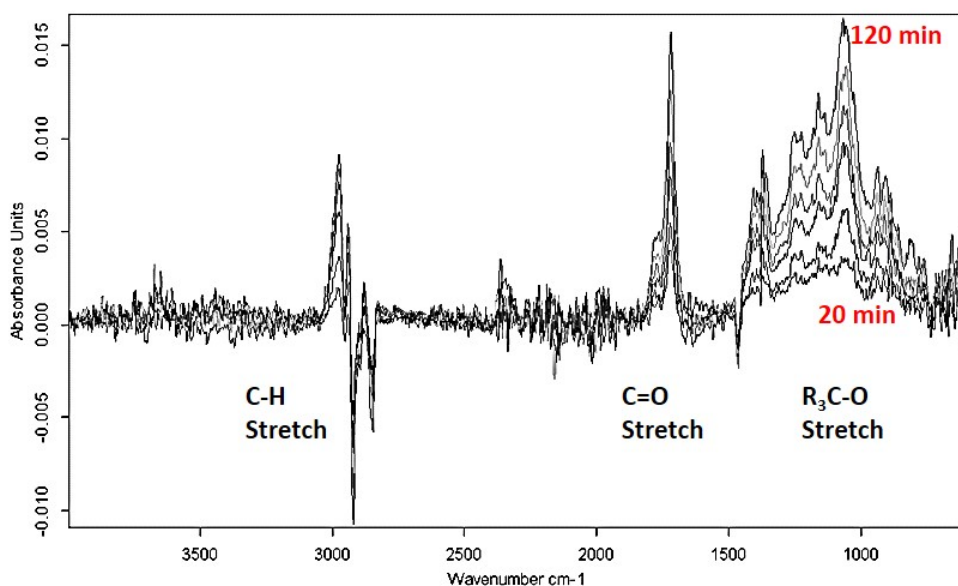


Figure 3.2: FTIR of squalane nitrooxidation at 150 °C of the liquid samples at 20 minute intervals, measured against a background of squalane

The most significant change in the IR spectra is the increase in intensity with reaction time of the peak at *ca.* 1716 cm^{-1} . This wavelength of adsorbance corresponds to that of

a C=O stretch, which can be assigned to ketone functional groups. Other functionalities have the carbonyl, C=O, stretch notably carboxylic acids, esters and aldehydes. However characteristic bands associated with these functional groups are not present: C-O stretch for acids ($\sim 1300\text{ cm}^{-1}$) and esters ($\sim 1250\text{ cm}^{-1}$), C-H stretch in aldehydes ($\sim 2720\text{ cm}^{-1}$).

The second assignable change is the increase in the broad peak centred at 1168 cm^{-1} , which corresponds to the absorption for the C-O stretch in a tertiary alcohol. There are some weak changes between $3500\text{-}3000\text{ cm}^{-1}$, which could be assignable to the alcohol OH bond, however this is broad and weak, which is normal for OH, making the identification less certain.

Other minor changes can be observed in the peaks which are attributable to changes in the C-H bond in the alkanes, particularly the band observable between $3000\text{-}2800\text{ cm}^{-1}$.

3.4 GC x GC MS analysis of squalane nitration and nitrooxidation

FT-IR analysis give evidence for some of the general functional groups present in the liquid sample mixtures. GC X GC-TOF-MS can aid the separation and identification of the individual compounds formed in the nitration and the nitrooxidation of squalane.

Previous work into nitration and nitrooxidation has either monitored the starting material loss or bulk analysis of the functionality. Due to the complex array of products expected to form it was examined whether using two dimensional gas chromatography could give separation of a high enough resolution of the products to identify a majority of the products formed. It was hoped that the TOF mass spectra analysis could provide structural analysis of the products and mass ions to give the molecule weight. This mass spectra analysis can be confirmed using the characteristics of the primary and secondary retention times to relate to similar functionality products. This product identification has the potential to give information which has not been collected in previous work carried out on engine oil nitration, once completed this could enable greater understanding of significant products of degradation and hence help elucidate the mechanistic pathway for the degradation.

Analysis of the nitration of squalane, figure 3.3, shows a large proportion of unreacted squalane as well as several products, with two trends in secondary separation suggesting a range of products with the same functionality.

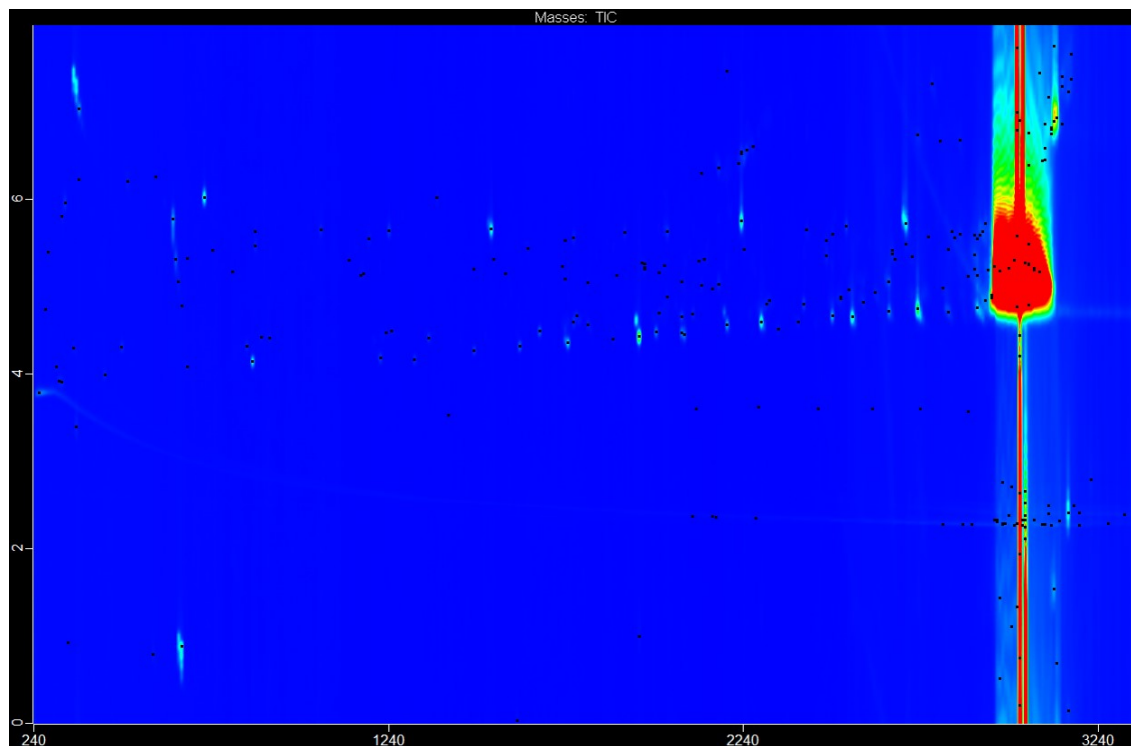


Figure 3.3: GC x GC-TOF-MS of squalane nitration at 150 °C after sample two hours

Nitrooxidation of squalane, figure 3.4, shows the same products as nitration, although at a higher concentration relative to the unreacted squalane when compared to the nitration. Some products are also present with an higher secondary retention time than in the nitration reaction, indicating more polar products.

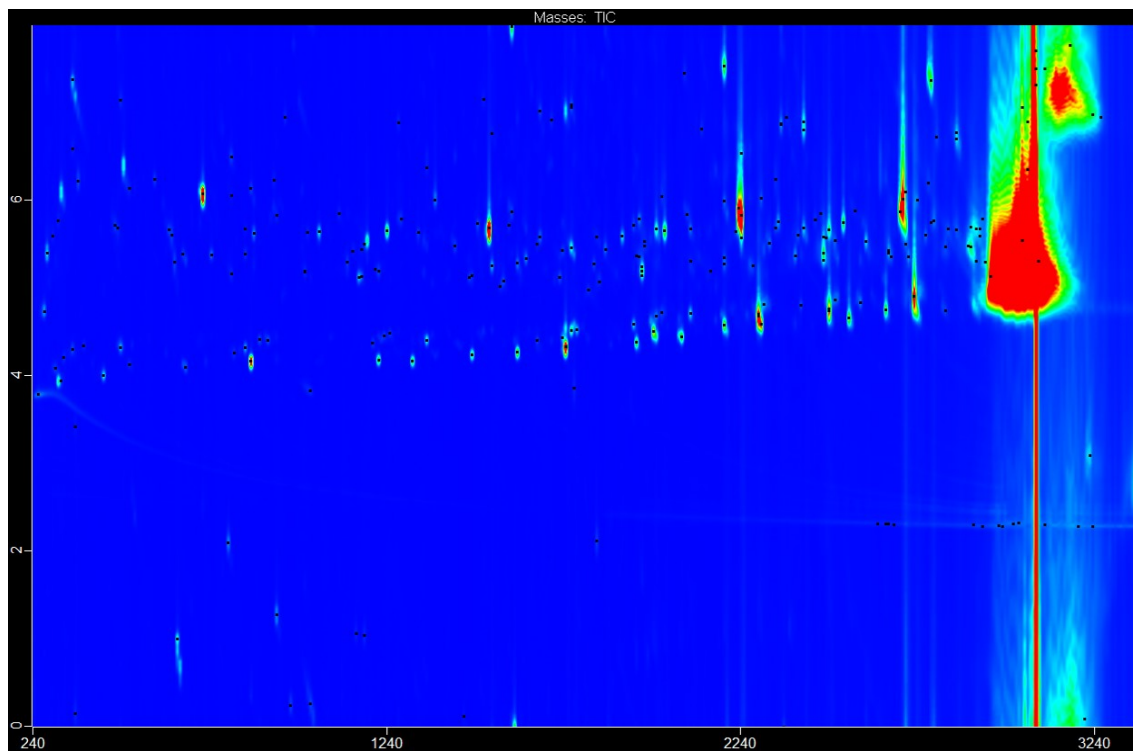


Figure 3.4: GC x GC-TOF-MS of squalane nitrooxidation at 150 °C after two hours

3.5 Product identification by GC x GC MS analysis

The products identified in the nitration and nitrooxidation of squalane are a range of alkanes, ketones from fragmentation of squalane, and alcohols. Lactones have also been identified as products in the nitrooxidation. These products are labelled in figure 3.5 and the identification is discussed in sections 3.5.1, 3.5.2 and 3.5.3.

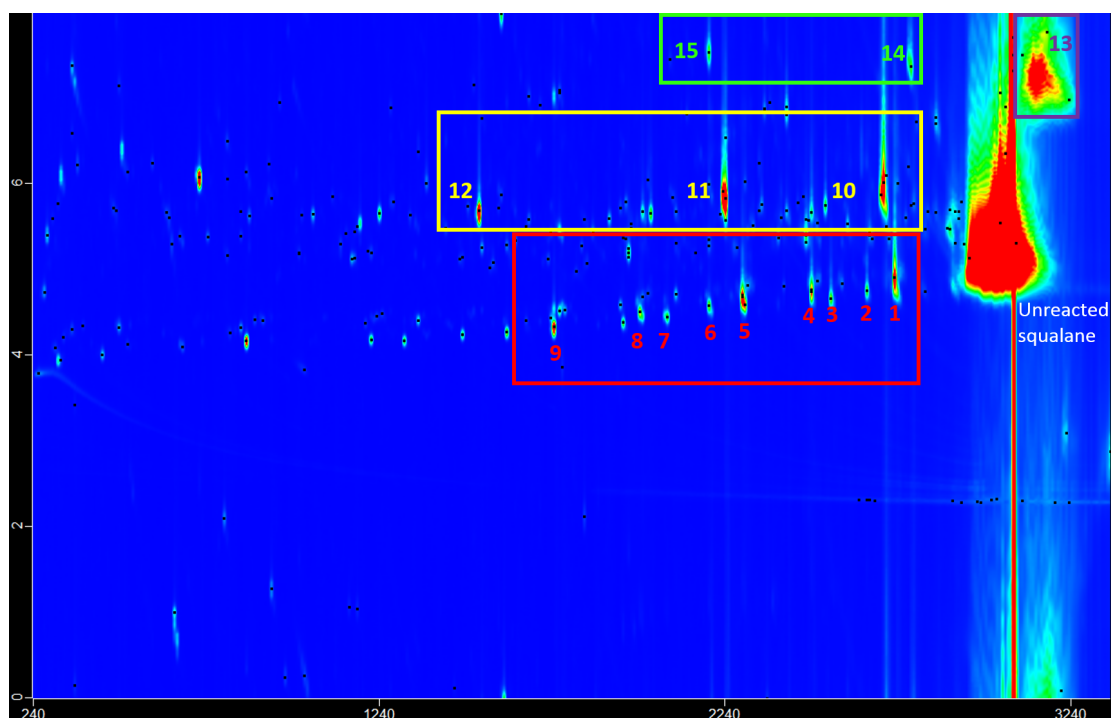


Figure 3.5: GC x GC TOF MS of nitrooxidation with identified products numbered, Red - alkanes, Yellow - Ketones, Purple - Alcohol, Green - Lactones

3.5.1 Alkanes

The group of product with a secondary retention time of approximately four seconds have been characterised as alkanes based on the mass spectra data. Nine alkanes formed from the fragmentation of squalane have been identified with sizes between C_{17} and C_{27} . The mass fragmentation pattern are summarised in table 3.1. Where the mass ions are not available to confirm the molecule size the retention indices have been used to give further evidence.

Table 3.1: Mass spectrum fragmentation pattern peaks for identified alkanes

Product number	Product Name	This work EI-MS m/z spectra	Previous published literature, ³ EI-MS m/z spectra
1	2,6,10,15,19-pentamethyl docosane	43 (100) 57 (80) 71 (50) 85 (27) 99 (10) 113 (8) 127 (4) 141 (4) 155 (2) 169 (1) 183 (1) 197 (2) 211 (0.5) 225 (0.5) 239 (0.1) 253 (0.3) 267 (0.2) 281 (0.05) 295 (0.1)	43 (46) 57 (100) 71 (96) 85 (62) 99 (28) 113 (27) 127 (21) 141 (8) 155 (12) 183 (7) 197 (2) 211 (3) 227 (2) 239 (1) 252 (0.3) 267 (0.5) 281 (0.5) 295 (0.1)
2	2,6,10,15,19-pentamethyl heneicosane	43 (78) 57 (100) 71 (64) 85 (31) 99 (21) 113 (9) 127 (7) 141 (4) 155 (3) 169 (1) 183 (3) 197 (1) 211 (1) 225 (0.5) 239 (1) 253 (0.3) 267 (0.2) 281 (0.2) 295 (0.1)	
3	2,6,10,15,19-pentamethyl eicosane	43 (83) 57 (100) 71 (51) 85 (21) 99 (6) 113 (3) 127 (6) 141 (2) 155 (1) 169 (0.5) 183 (0.5) 197 (0.5) 211 (0.1) 225 (0.1)	
4	2,6,10,15 - tetramethyl eicosane	43 (90) 57 (100) 71 (52) 85 (25) 99 (10) 113 (8) 127 (5) 141 (2) 155 (3) 169 (1) 183 (2) 197 (1) 211 (0.5) 225 (0.2) 239 (0.5) 253 (0.5) 267 (0.1) 281 (0.2)	

5	2,6,10,15-tetramethyl octadecane	43 (85) 57 (100) 71 (76) 85 (39) 99 (16) 113 (11) 127 (5) 141 (4) 155 (4) 169 (2) 183 (2) 197 (1) 211 (0.5) 225 (1) 239 (1) 253 (0.05) 267(0.1) 281 (0.1) 295 (0.05) 310 (0.02)	43(46) 57 (100) 71 (96) 85 (62) 99 (28) 113 (27) 127 (21) 141 (8) 155 (12) 183 (7) 197 (2) 211 (3) 227 (2) 239 (1) 252 (0.3) 267 (0.5) 281(0.5) 295 (0.1)
6	2,6,10,15-tetramethyl heptadecane	43 (74) 57 (100) 71 (63) 85 (33) 99 (11) 113 (11) 127 (10) 141 (4) 155 (4) 169 (2) 183 (2) 197 (1) 211 (0.5) 225 (1) 239 (1) 253 (0.05) 267 (0.1) 281(0.05) 296 (0.05)	43, 57, 71, 85, 99, 113, 127, 141, 155, 169, 183, 197, 211, 253, 281 (NIST)
7	2,6,10,15-tetramethyl hexdecane	43 (93) 57 (100) 71 (67) 85 (30) 99 (11) 113 (8) 127 (6) 141 (3) 155 (2) 169 (1) 183 (2) 197 (1) 211 (0.1) 225 (0.1) 239 (0.5) 253 (0.1) 267 (0.1) 282 (0.05)	43, 57, 71, 85, 99, 113, 127, 141, 155, 169, 183, 197, 211, 266 (NIST)
8	2,6,10-trimethyl hexdecane	43 (86) 57 (100) 71 (66) 85 (23) 99 (8) 113 (9) 127 (4) 141 (2) 155 (2) 169 (1) 183 (3) 197 (1) 211 (0.1) 225 (0.1) 239 (0.1) 253 (0.1) 268 (0.1)	43, 57, 71, 85, 99, 113, 127, 141, 155, 168, 183, 196, 210,225,239, 253,268 (NIST)
9	2,6,10-trimethyl tetradecane	43 (100) 57 (91) 71 (51) 85 (30) 99 (9) 113 (7) 127 (3) 141 (1) 155 (3) 169 (1) 183 (1) 197 (0.2) 211 (0.1) 225 (0.1) 240 (0.1)	

Mass fragmentation of alkanes

The fragmentation patterns are compared to published data for these compounds from previous work published by Stark *et al.*³ (compounds 1,5) or available in the National Institute of Standards and Technology (NIST) database (compounds 6,7,8). For compounds where published data was not available (2,3,4,9) the fragmentation pattern has been identified for the key fragments. The fragmentation for product 2, (2,6,10,15,19-pentamethyl heneicosane), is given in figure 3.6 as an example, these can be found in appendix for the other compounds.

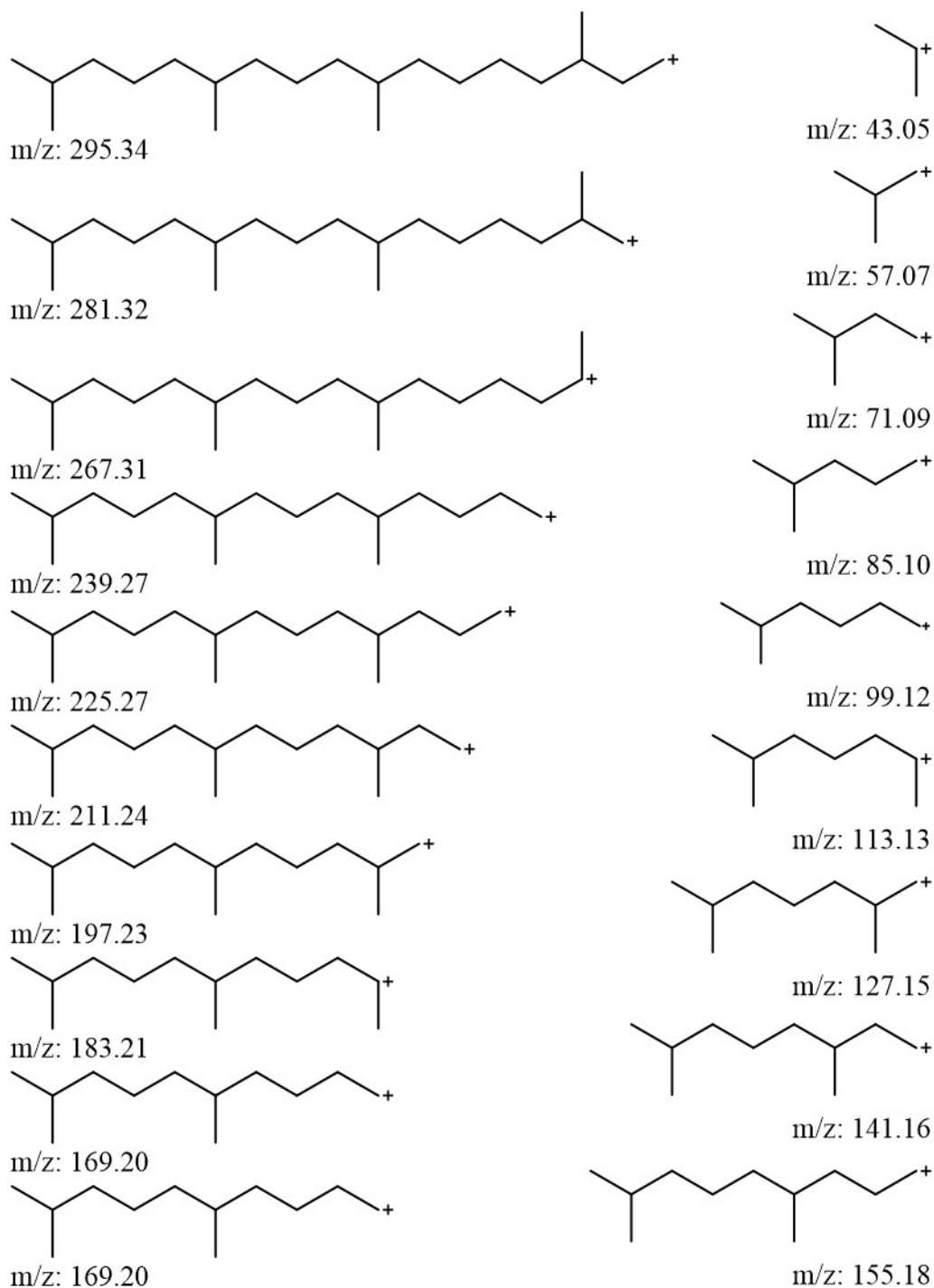


Figure 3.6: fragmentation pattern of 2,6,10,15,19-pentamethyl heneicosane in TOF-MS (product 2)

Analysis of retention indices for confirmation of molecular size

As some of the mass ions are not present in the mass spectra, the size of the molecules can be uncertain from the MS analysis also, so to give further evidence for the molecular size, a linear plot can be made using those fragment molecules of known size as well as

the unreacted squalane as a reference point. If the molecules are all alkanes at the size identified they would be expected to fit the linear relationship according to retention index established by Kovat.¹⁰³ Figure 3.7 shows the plot of molecular size against primary retention time, the plot shows a linear relationship, this gives further evidence to molecular size of the alkane products identified.

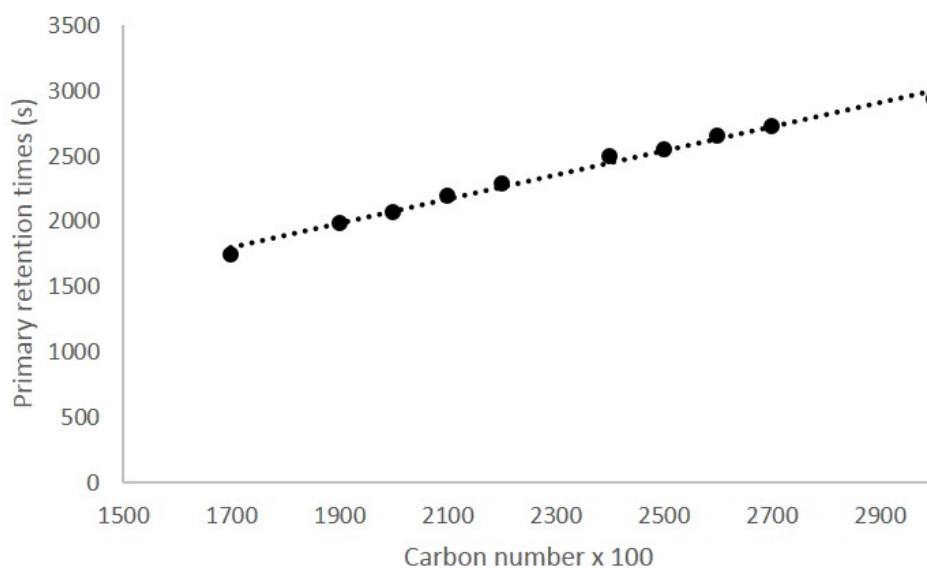


Figure 3.7: Analysis of retention times of alkanes identified by GC x GC-TOF-MS to confirm molecular size

Product identification of alkanes

The structure of the alkanes identified are shown in figure 3.8, the degree and position of branching has been eluded using fragmentation pattern and confirmed based on the products size and the structure of the squalane starting material.

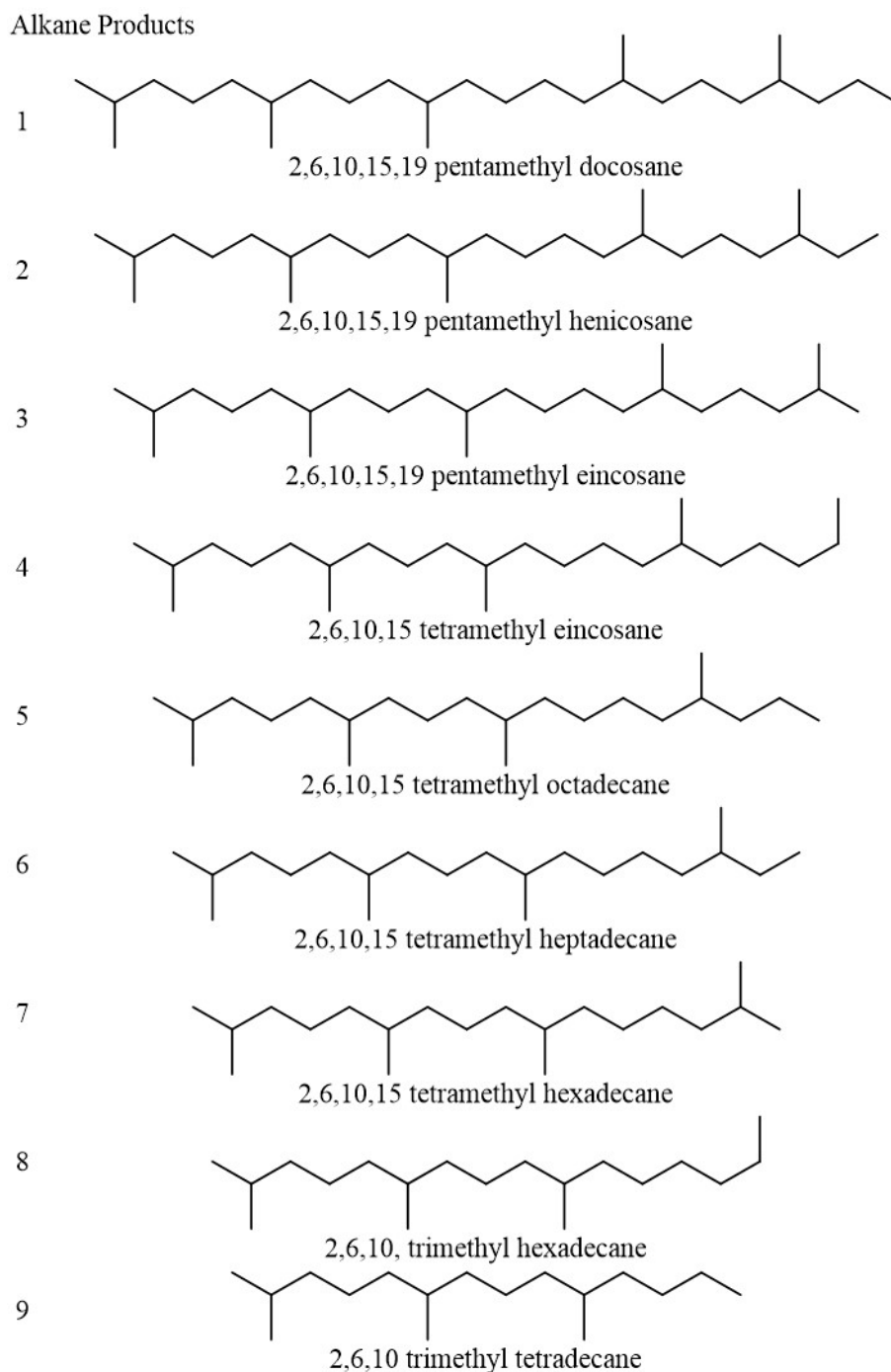


Figure 3.8: Structures of alkanes identified by GC x GC TOF MS

Mechanism of alkane formation

The mechanism for the alkane formation is proposed in in figure 3.12. This involves an initiation step of hydrogen abstraction by nitrogen dioxide to form nitrous acid (HONO), propagation steps to form an alkoxy radical followed by a fragmentation, the final step in the alkane formation is a hydrogen abstraction to form the stable alkane products. This mechanism is discussed in more detail in chapter 7.

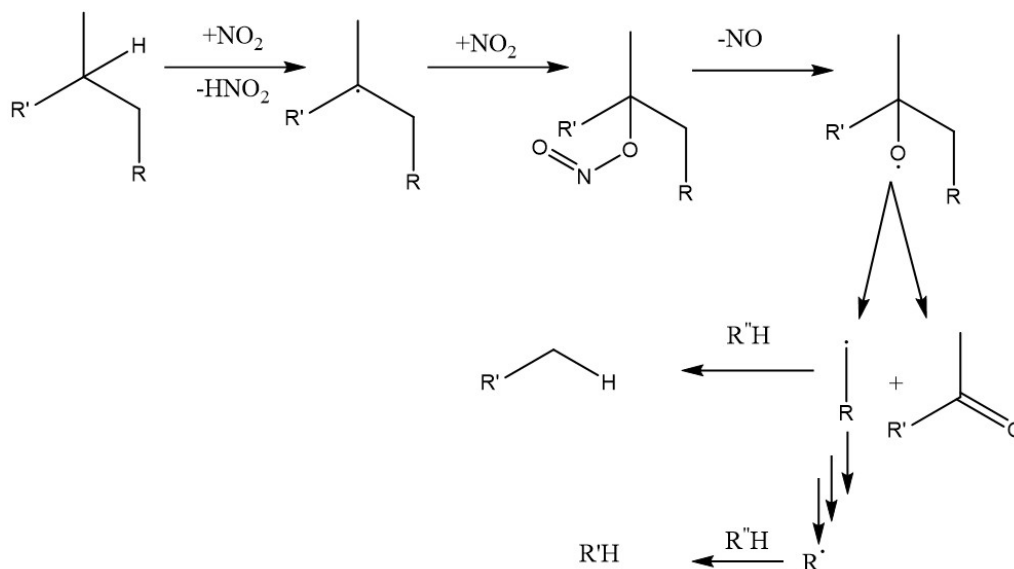


Figure 3.9: Mechanism of alkane fragments formation from squalane during nitration

Alkane ratio

The ratio in which the alkanes form can give insight into the selectivity of the reaction. Total ion count from the mass spectra is not the most accurate method of quantification, however, can be used to give an estimate. The ratio of the identified alkanes, scaled to product 1 which has the largest concentration, is summarised in table 3.2.

Table 3.2: The ratio of alkanes formed during the nitrooxidation of squalane at 150 °C for 2 hours

Product	Ratio
1	1
2	0.2
3	0.2
4	0.6
5	0.8
6	0.2
7	0.1
8	0.3
9	0.7

These ratios show a higher formation of products from the direct fragmentation at the tertiary centre, (products 1, 5, 9). There is also a slight tendency to form the higher

molecular weight species, however, this most likely is caused by the volatility of the smaller species formed evaporating from the reactor.

3.5.2 Ketones

Three products with the secondary retention of approximately six seconds time have been characterised as ketones. The mass fragmentation patterns are summarised in table 3.3. The fragmentation patterns are compared to published data for these compounds from previous work published by Stark *et al.*³ and were available in the NIST database.

Mass fragmentation of ketones

The mass fragmentation for the ketones all give a fragment with a $m/z = 58$, this is characteristic mass with odd electron, even mass fragments are uncommon. In carbonyl compounds the McLafferty rearrangement can occur, involving an intermolecular hydrogen abstraction from the γ position can occur to give an even mass fragment, for ketones in position two the resulting fragment has a $m/z = 58$. The mechanism of this fragmentation is shown in figure 3.10. The McLafferty ions are relatively stable resulting in a strong relative intensity.¹⁰⁴

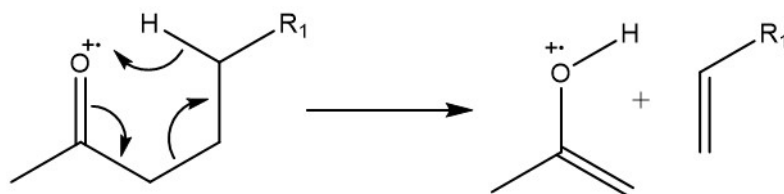


Figure 3.10: Mechanism of McLafferty ion formation for ketones

Table 3.3: Mass spectrum fragmentation pattern peaks for identified ketones

Product Number	Product Name	EI-MS m/z spectra	Previous published literature, ³ EI-MS m/z spectra
10	6,11,15,19-tetramethyl eicosan-2-one	43 (100) 57 (47) 58 (40) 71 (34) 85 (23) 95 (17) 109 (13) 123 (5) 138 (5) 151 (1) 179 (1) 193 (0.1) 222 (0.5) 249 (0.1) 264 (0.1) 334 (0.5) 352 (0.1)	43 (59) 58 (100) 71 (44) 83 (34) 85 (30) 95 (46) 109 (62) 123 (23) 138 (22) 151 (5) 179 (2) 193 (6) 222 (8) 249 (1) 264 (1) 282 (2) 334 (40) 352 (0.1)
11	7,11,15-trimethyl hexadecan-2-one	43 (100) 58 (63) 71 (35) 83 (10) 85 (10) 95 (12) 109 (15) 123 (5) 137 (5) 138 (5) 151 (2) 179 (1) 193 (1) 222 (2) 249 (0.1) 264 (0.5) 282 (0.1)	43 (62) 58 (100) 71 (40) 85 (23) 95 (24) 109 (48) 123 (17) 137 (24) 151 (4) 179 (9) 193 (3) 222 (29) 249 (1) 264 (7) 282 (0.1)
12	6,10-dimethyl undecan-2-one	43 (100) 58 (77) 71 (27) 85 (14) 95 (11) 109 (11) 123 (3) 140 (2) 180 (2) 198 (1)	43 (60) 58 (100) 71 (29) 85 (18) 95 (19) 109 (22) 123 (6) 140 (7) 180 (11) 198 (0.1) 43(98) 58 (100) 71 (32) 85 (16) 109 (11) 123 (4) 140 (6) 180 (8) 198 (1)(NIST)

For the three identified ketones all of the mass data matches with published spectra shown in table 3.3. The McLafferty ion and mass ions are identifiable for all three compounds.

Product identification of ketones

The structures of the compounds identified can be seen in figure 3.11. It is also likely that 6 methyl heptan-2-one and propane are also formed, however, these could of evaporated from the reaction mixture due to their lower boiling points.

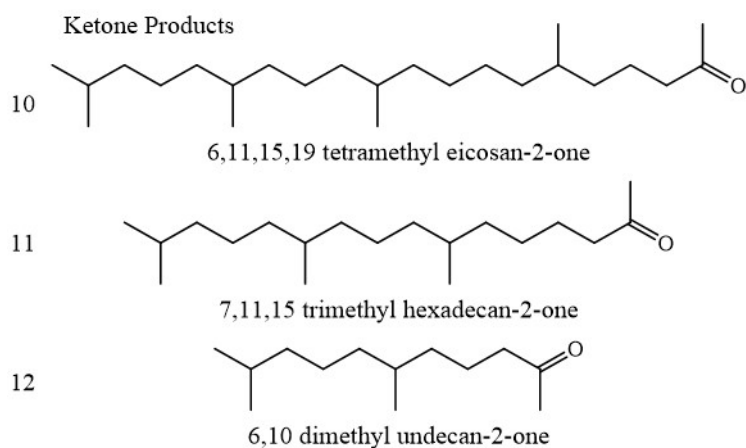


Figure 3.11: Structures of ketones identified by GC x GC-TOF-MS

Mechanism of alkanes and ketones formation

The mechanism for alkane formation is proposed in figure 3.12. This involves an initiation step of hydrogen abstraction by nitrogen dioxide to form nitrous acid (HONO) and a carbon centred radical. The propagation steps are the addition of NO_2 via the oxygen to form an alkyl nitrite. This nitrite is then able to decay breaking the CO-NO bond to form an alkoxy radical followed by a fragmentation. The final step in the alkane formation is a hydrogen abstraction to form the stable alkane products. A more detailed discussion as part of the complete mechanism is made in chapter 7.

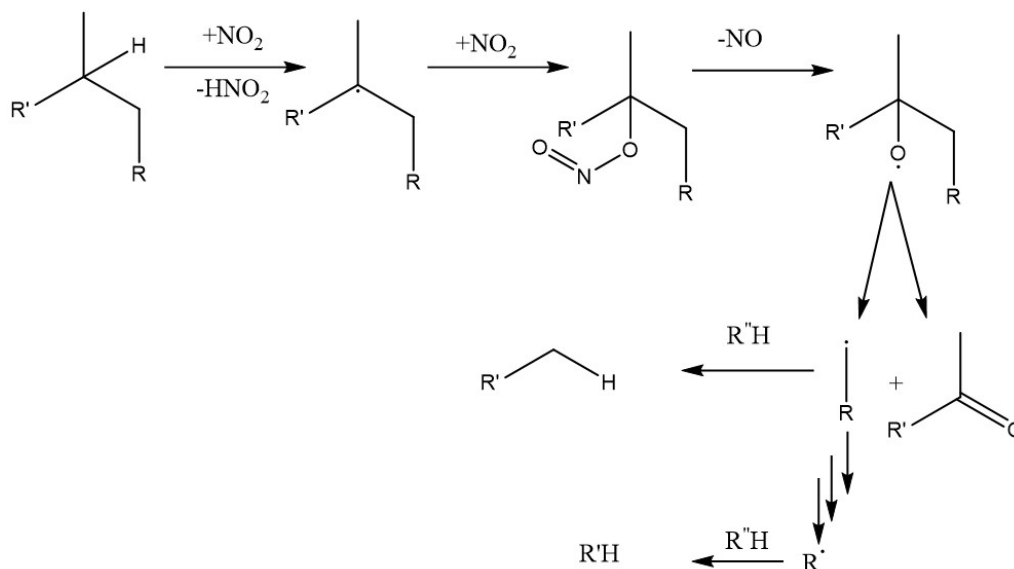


Figure 3.12: Mechanism of alkane and ketone fragments formation from squalane during nitration

3.5.3 Alcohols and lactones

The other product identified after both nitration and nitrooxidation is the alcohol of squalane which is the most intense product peak in comparison to the unreacted squalane. In the nitro-oxidation the heavier oxidation products of lactones have also been identified as products.

The mass spectra fragmentation data is summarised in table 3.4. Lactones had previously been identified by Stark et al.³ as a product of squalane autooxidation. Alcohols had been identified as a product of the similar work on pristane $C_{19}H_{40}$ but not previously from the autooxidation of squalane. The mass ion for the squalane alcohol ($m/z = 438$) is not present due to the low stability in mass fragmentation, loss of the ion is expected through dehydration. Analysis of this product peak by silylation with GC-MS shows derivatization and hence demonstrate the alcohol functionality.

Mass fragmentation of alcohols and lactones

Table 3.4: The mass spectra fragmentation of squalane alcohol and lactone products

Product Number	Product Name	EI-MS m/z spectra	Previous published literature, ³ EI-MS m/z spectra
13	2,6,10,15,19,23 hexamethyltetracosanol	43 (100) 55 (80) 57 (90) 69 (82) 71 (62) 83(43) 85(33) 97 (35) 99 (15) 111 (31) 123 (17) 125 (19) 139 (10) 143 (11) 151 (4) 165 (2) 179 (3) 196 (2) 209 (3) 222(1)	
14	4,9,12,16 tetramethyl octadecano- γ lactone	43 (65) 55 (37) 69 (25) 71 (21) 99 (100) 114 (20) 126 (8) 141 (2)	
15	4,8,12 trimethyl tridecano- γ lactone	43 (32) 55 (16) 69 (10) 71(10) 99 (100) 114 (7) 126 (2)	43 (38) 55 (16) 69 (10) 71 (6) 99 (100) 114 (8) 126 (4)

Alcohols

The identity of the highest product concentration which elutes after squalane is discussed here. The increase in retention time is either due to addition of carbons to squalane, which is highly unlikely, or a functionality of squalane for which the type is unknown. In order to identify the large product peak, proposed to be an alcohol, a sample of squalane was oxidised under an atmosphere of oxygen at 200 °C. This formed the same product, with identical retention times and mass fragmentation patterns, additionally this reaction formed the product at higher concentration allowing for easier analysis. Figure 3.13 shows a truncated the area of the GC-MS chromatogram with the unreacted squalane at 26.5-26.6 min and the peak of interest as 28.13 minutes.

On silylation the peak at 28.13 min has disappeared, and three new peaks are visible with retention times of 26.67, 27.94 and 28.06 min. The reaction with a silylation agent shifting the retention times provides evidence that the product is either an alcohol or an acid.

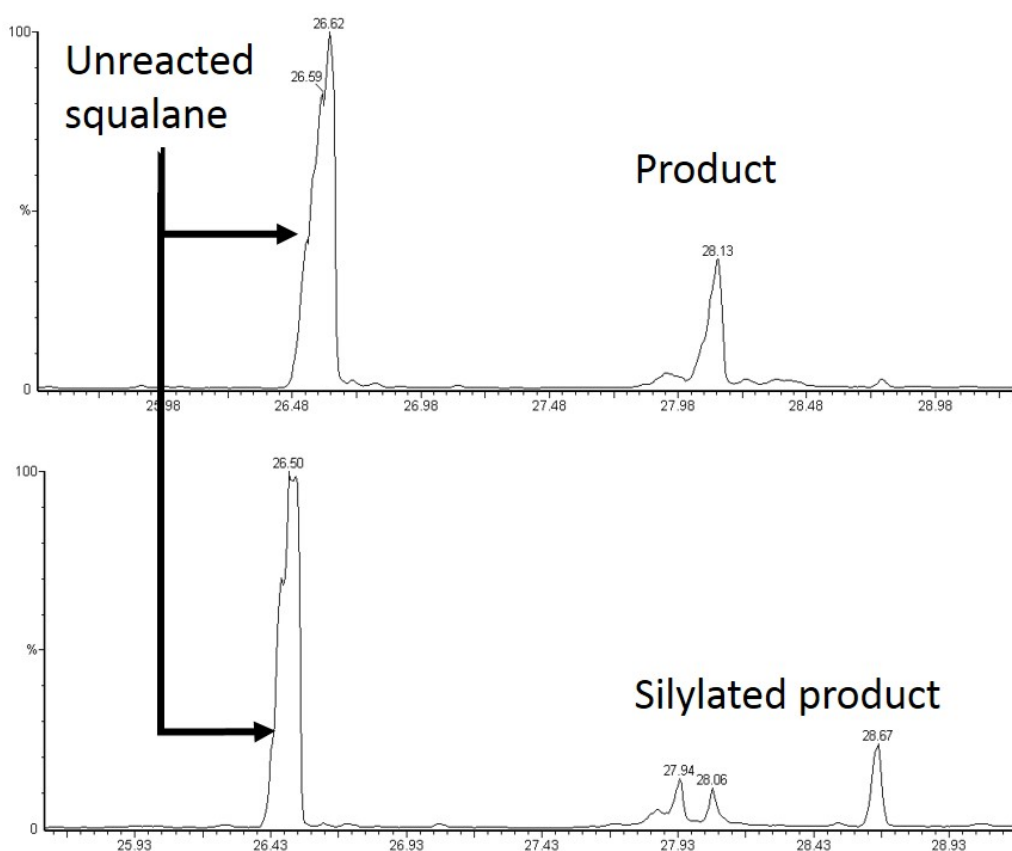


Figure 3.13: TIC of the GC-MS analysis of the squalane oxidation (top) and after silylation (below)

For each of the three new peaks formed upon silylation in figure 3.13 the mass fragmentation can be used to aid identification of the initial species. The fragmentation patterns are very similar to each other and that of product 13, with the exception of the stable fragments added at the following m/z ratio 131, 201, 271 and 355. These fragmentation patterns can be seen for each of these peaks in figure 3.14. Silylation often causes the formation of stable fragments during mass spectrum analysis, this can give further information on the products structures.

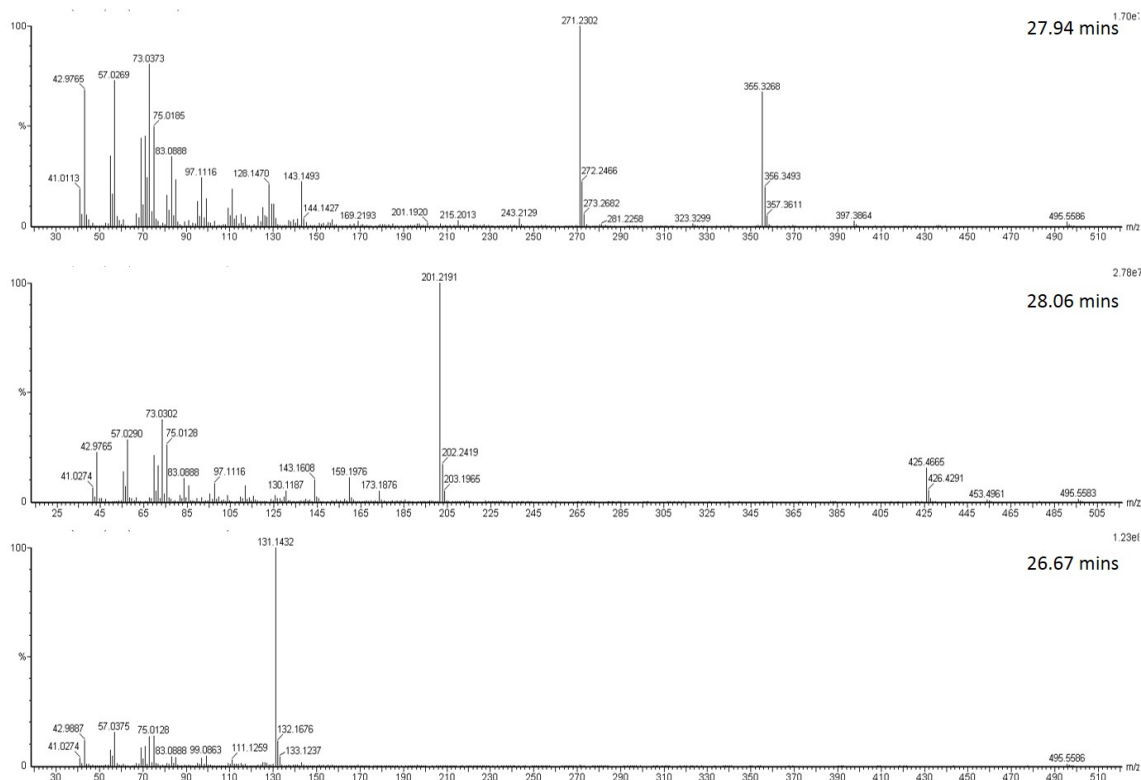


Figure 3.14: Mass spectra of the three peaks formed on the silylation of oxidised squalane

The stable fragment in the mass spectra, figure 3.14, can be assigned to the silylated alcohols of squalane to give structural information. The expected positions of alcohols formed are the three tertiary alcohol (positions 2,6, and 10) due to the bond strength of the tertiary C-H bond, there is also eight secondary and three primary positions in which the alcohol could be positioned. The assignments of the fragment structure are shown in figure 3.15, with the fragments identifying structural isomers as tertiary alcohols in position 2 ($m/z = 131$), position 6 ($m/z = 201$) and position 10 ($m/z = 271, 355$). These fragments also confirm the original product must be an alcohol rather than an acid due to the tertiary position of the fragmentation, it is only possible to form an acid in a primary position. The carboxylic acid functional group contains a C=O and C-OH, a total of 3 bonds to the carbon which is tetravalent, therefore carbon can only bond to

one other atom.

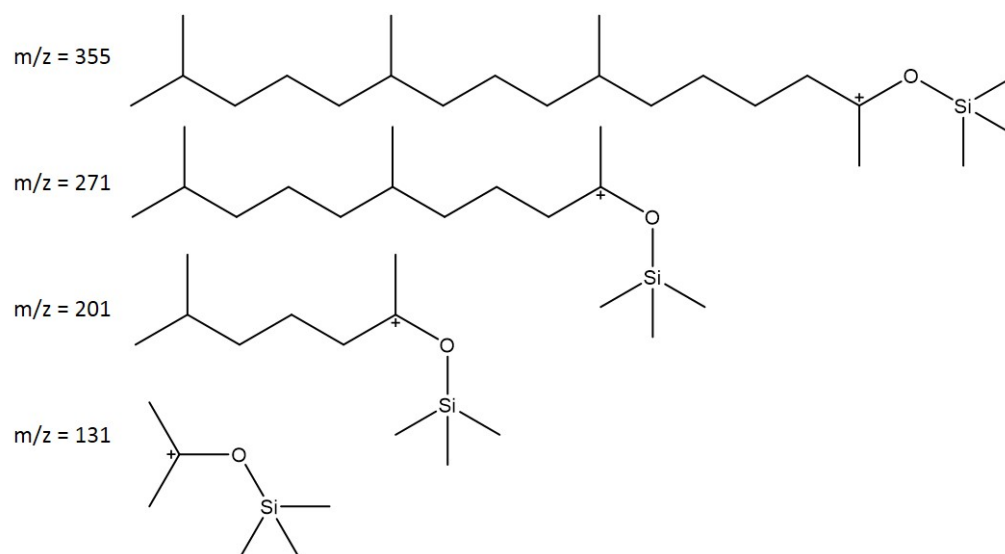


Figure 3.15: Structures of alcohols identified by GC x GC TOF MS

Using the fragments from the silylation has allowed the different alcohols of squalane to be resolved by GC-MS and identified. Three different isomer have been identified as 2-squalanol, 6-squalanol, 10-squalanol. These structures of these tertiary alcohols are shown in figure 3.16.

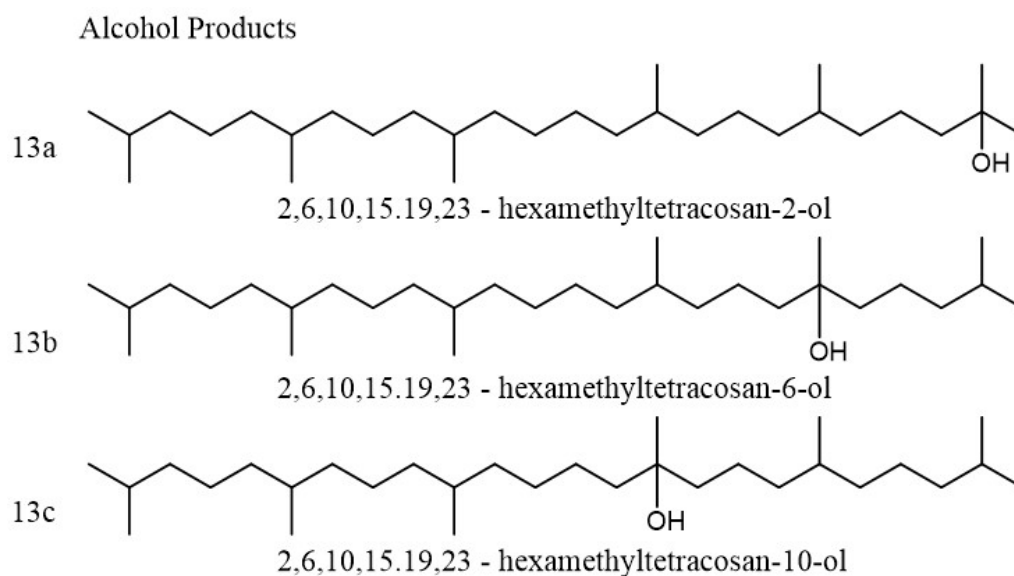


Figure 3.16: Structures of silylated alcohols identified by GC x GC TOF MS

The alcohols can be formed by following the same reaction pathway as shown in figure 3.12, to form the oxy radical, however instead of fragmentation to form the ketone and

the alkane radical, a hydrogen abstraction occurs to form the alcohol and continue the chain reaction. This mechanism is shown in figure 3.17.

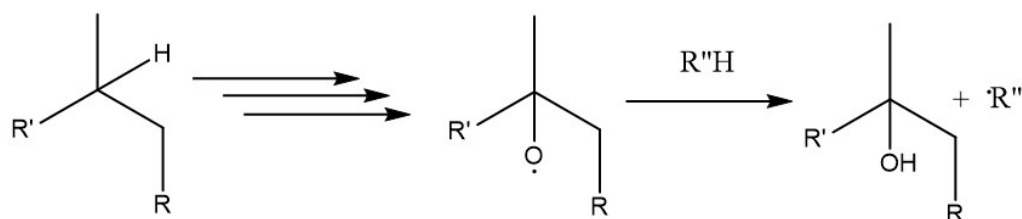


Figure 3.17: Scheme of alcohol formation from squalane during nitration

Previous similar studies into autooxidation of alkanes have identified alcohol as the products. Work with squalane by Stark *et al.*³ was unable to identify product via GC-MS due to the instability resulting of the dehydration during analysis giving a mass ion at 420 m/z which is the mass ion for the alkene. By using silylation as derivitisation technique for the alcohol has proved to be a useful technique. Firstly we have been able to prove the most major products of both oxidation and the nitration reaction. The benefit of silylation is the difference in boiling point between the positional isomers which enabled separation via GC, this has confirmed the alcohols are formed in all three of the unique tertiary points in squalane. The isomer separation gives more evidence for the selectivity for the initiation being form the tertiary centres due to the weaker C-H bonding and insignificant reactions form the primary and secondary C-H bonds. Without silylation the isomer identification would of not been possible by GC-MS

Lactones

Lactones have been identified previously as products of the autooxidation of squalane by Stark *et al.*³ In this work, the nitro-oxidation reactions two lactones have been identified based on the fragmentation, these are found with a secondary retention time in the GCxGC analysis.

The mass spectra data is summarised in table 3.4, the lactones give a characteristic fragment with a $m/z = 99$, $C_5H_7O_2$ this fragment is assignable to lactone ring, shown in figure 3.18.

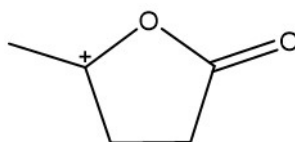


Figure 3.18: Characteristic fragmentation of lactones

The structure of the two lactones are shown figure 3.19 have been identified based on the comparison data, key fragments and the secondary retention times.

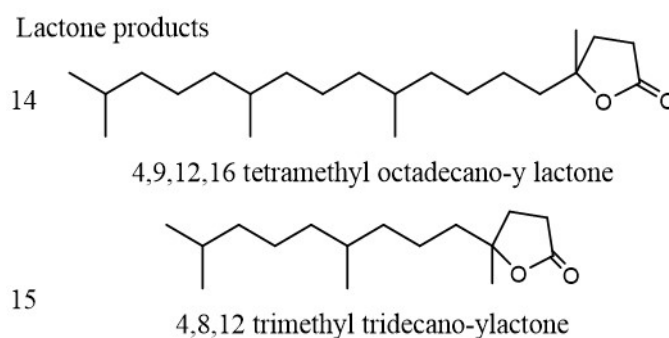
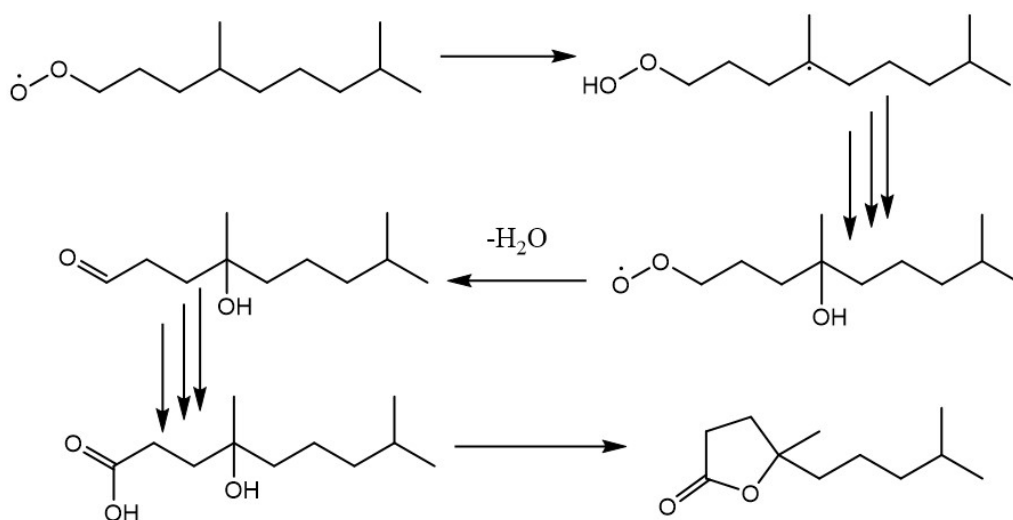


Figure 3.19: Structures of lactones identified by GC x GC TOF MS

A previously discussed mechanism by Goosen *et al.*⁴⁸ for lactone formation in autooxidation by reaction with oxygen was not viable for squalane due to the tertiary centres unable to undergo a second hydrogen abstraction. Therefore Stark *et al.*³ presented a new mechanism, figure 3.20 to allow for the formation of lactones from squalane via autooxidation.

Figure 3.20: Mechanism of lactone formation from squalane by autooxidation as proposed by stark *et al.*³

A comparative mechanism can be drawn, using NO_2 as the source of oxygen to form the acid and alcohol formation, which then undergo intermolecular esterification to form the lactones. This mechanism is presented in figure 3.21, suggesting that nitrogen dioxide is able to form lactones. Although the lactones are only observed in the nitro oxidation, it is likely that a mixture of both steps of mechanisms, figure 3.20 and 3.21, take place to form the lactone, with the overall formation controlled by the concentration of each gas and rate of diffusion of oxygen and nitrogen dioxide. The reason for this expectation is due to the barrierless radical radical reactions in both cases.

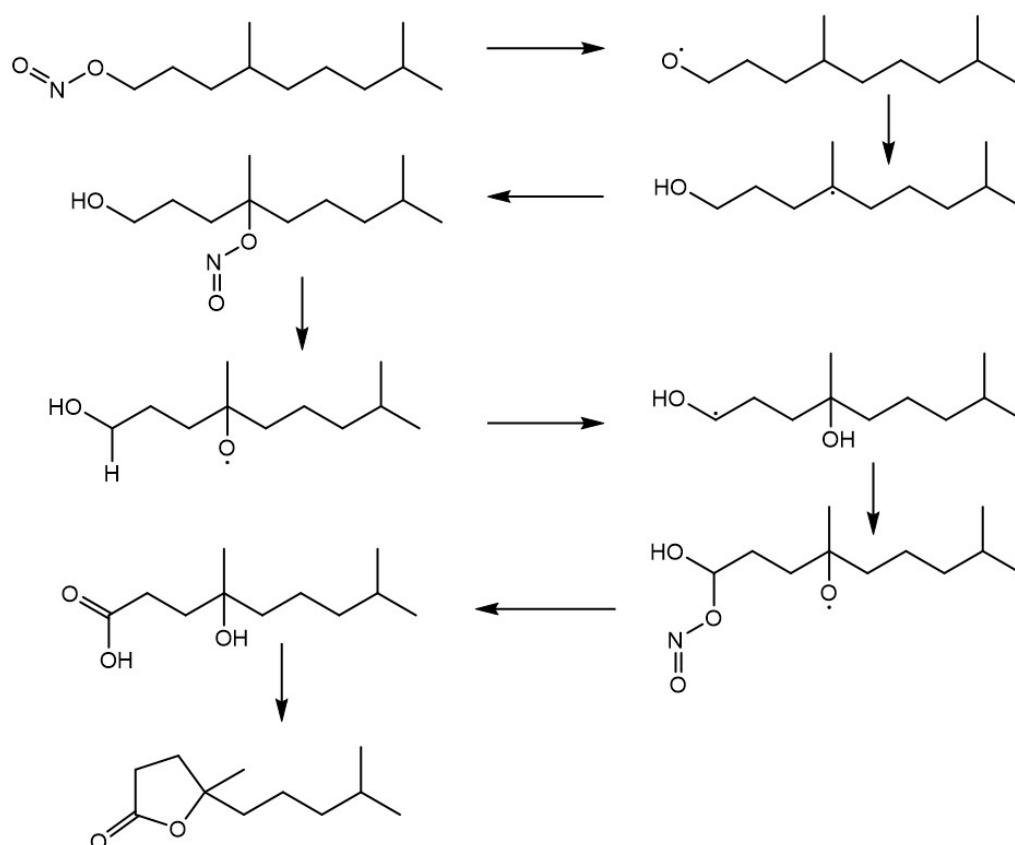


Figure 3.21: Mechanism of lactone formation from squalane by autooxidation with squalane

3.6 Conclusions

The major products of nitration and nitrooxidation of squalane have been identified using GC x GC-MS analysis. The products identified are a range of alkane fragments, the alcohols of squalane, ketone fragments and lactones. The mechanisms for the formation of these oxygenated degradation products of squalane upon reaction with nitrogen dioxide have been proposed.

None of products previously reported containing nitrogen have been observed in the products by GC x GC MS. All the products identified in nitration or oxidation, alkanes, ketones, alcohols and lactones, no unique products of nitrooxidation have been observed. The work previously discussing the mechanism for the degradation of these type of alkanes in these systems have not identified the expected products.^{1,64,78} One area of study requiring further work to explain is that as the degradation mechanism relies on nitrogen dioxide, so identifying which nitrogen contain species are formed as a result would be beneficial. From the GC x GC MS the identification of the new forms nitrogen containing compounds has not been possible.

Chapter 4

Identification of nitrogen containing products

4.1 Introduction

In chapter 3 the major products of nitration and nitrooxidation were identified using GC x GC-MS as alkanes and ketone fragments, squalane alcohol and lactones. Products containing nitrogen have not been identified by GC x GC-MS. If nitrogen containing species are formed, their non-identification could be due to the concentrations being below the limits of detection of the mass spectrum detector, or decay during to the gas chromatography, amongst other reasons. In this chapter infrared spectroscopy and GC x GC - NCD have been used with the aim of identifying nitrogen containing components.

4.2 Previous work to identify nitrogen containing degradation products of base oils

Previous work in the literature studying the nitration of base oils found elevated nitrogen levels in bulk oil by elemental analysis, suggesting that nitrogen containing products are formed. It was either not possible or not of interest to the studies to separate and identify the products containing nitrogen. This results in a weak conclusion in identifying the formation of nitrogen containing products due to nitrogen dioxide. These published studies are therefore unable to strongly support any mechanistic conclusions.^{1,63,77}

In a study of antioxidants in squalane, Pochopien was able to show that once the antioxidant had been consumed nitrated products were formed and detectable by GC x GC-NCD, although individual components were not identified.⁷⁶ These reactions were carried out on a similar reaction set up to the one used in this study. This, therefore, gives evidence that GC x GC-NCD is a technique which would enable the detection and quantification of nitrogen containing products.

4.3 Maximum nitrogen concentration

The maximum nitrogen content of the degraded squalane sample can be calculated to work out the maximum possible percentage of nitrated squalane (nitro squalane or squalane nitrite) to give the nitrogen mass content based on the nitrogen input to the reaction as nitrogen dioxide.

Using the ideal gas law, Equation 4.1, Equation 4.2, the amount of nitrogen dioxide flowed into the reactor can be calculated with the parameters for the gas flow for this reaction (n.b. the temperature is that of the flow meter not that of the reactor).

$$pV = nRT \quad (4.1)$$

$$\frac{pV}{RT} = n \quad (4.2)$$

where

p = pressure, 1 atm

V = volume, $40 \text{ ml min}^{-1} \times 120 \text{ min} = 4800 \text{ ml} = 4.8 \text{ dm}^3$

n = moles of gas

R = molar gas constant, $8.314 \text{ J K mol}^{-1}$

T = temperature, 25°C

These can be substituted into equation 4.2 and the moles of gas calculated.

$$n = \frac{1 \text{ atm} \times 4.8 \text{ dm}^3}{8.314 \text{ J K mol}^{-1} \times 25^\circ\text{C}} = 0.2 \text{ mol} \quad (4.3)$$

The flow of gas into the reactor is 1000 ppm (0.1%), therefore the total flow of gas can be scaled to calculate the amount of NO_2 .

$$0.2 \text{ mol} \times 0.1 \% = 2 \times 10^{-4} \text{ mol NO}_2$$

The amount on nitrogen dioxide flowed through the reactor needs to be compared to the amount of squalane in order to calculate the maximum possible percentage of nitrated material. The moles of the squalane in the liquid sample can be calculated using equation 4.4, equation 4.5

$$m = \frac{7 \text{ ml}}{0.810 \text{ g mL}^{-1}} = 5.67 \text{ g} \quad (4.4)$$

$$n = \frac{5.67 \text{ g}}{422 \text{ g mol}^{-1}} = 0.0135 \text{ mol} \quad (4.5)$$

Using the moles of nitrogen dioxide and squalane, assuming 100% of the nitrogen dioxide is added to squalane, the ratio of the two components can be used to give the maximum theoretical percentage of nitrated squalane (equation 4.6).

$$\frac{0.0002 \text{ mol}}{0.0135 \text{ mol}} = 0.014 = 1.4\%(mol) \quad (4.6)$$

In nitrated squalane the molar ratio of nitrogen is low due to the molecular size of squalane. The molecular masses can be used to calculate the nitrogen weight percentage for nitrosqualane. For pure nitrated squalane the weight percent is calculated in 4.7.

$$\text{mass ratio of nitrogen in nitrated squalane} = \frac{14 \text{ g mol}^{-1}}{467 \text{ g mol}^{-1}} = 0.03 = 3\% \quad (4.7)$$

Using the maximum nitrated squalane percentage the maximum nitrogen percentage can be calculated (equation 4.8).

$$\text{Maximum molar ratio of nitrogen} = 0.014 \times 0.03 = 0.00042 = 0.042\% \quad (4.8)$$

Using the calculated percentages the appropriate analytical techniques can be selected to ensure the sensitivity is high enough for the low concentrations. The theoretical maximum does not account for nitrogen lost via other pathways such as the initiation reaction to form HONO, or flowed through the reactor without reaction, therefore it is likely to be significantly higher than the actual concentration. Before consideration of the assumptions made the nitrogen level is already too low for many analytical techniques such as nitrogen NMR. Many techniques would also be too overloaded by non-nitrated species to detect the nitrated species. Therefore GCxGC NCD is a suitable technique as it is able to detect nitrogen containing species to below ppb level. Secondly the detection of only nitrogen containing products allows the analysis sample to be sufficiently concentrated without risk of over loading the detector with other species.

4.4 Infrared absorption bands due to nitro functional groups

Infrared spectra of nitroalkanes show two bands due to the nitro group; an asymmetric stretch at 1575 - 1500 cm^{-1} and a symmetric stretch at 1360 - 1290 cm^{-1} . The asymmetric stretch gives the stronger absorbance of the two bands. Library spectra of tertiary nitroalkanes were not available therefore these were measured for a standard compound to allow comparison to the reaction products. Figure 4.1 shows the infrared spectrum for methyltrispropanol (4-(3-hydroxypropyl)-4-nitro-1,7-heptanediol) (CAS Number 116747-80-9)(blue) in in figure 4.1 with the nitro absorbance bands assigned. As methyltrispropanol was unavailable for direct comparison, a comparison is made with

2-methyl propan-1-ol (red) in figure 4.1 due to similar functionality of a primary alcohol group and a tertiary carbon centre. It can therefore be expected to give a similar spectrum to nitromethanetrispropanol without the bands due to the nitro groups. The comparison of these spectra in combination with the literature values for primary nitro compounds has enabled reliable identification of the nitro absorbance bands of tertiary nitro centres.

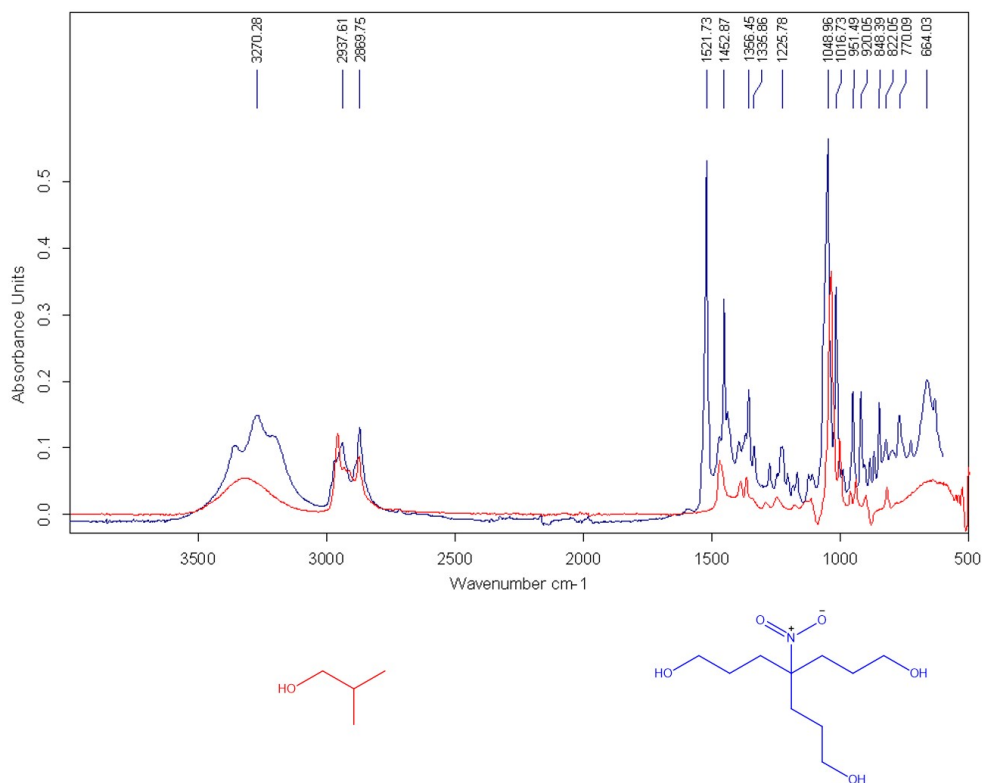


Figure 4.1: Infrared spectra of nitromethanetrispropanol (blue) and 2-methyl propan-1-ol (red)

In figure 4.1 the asymmetric stretch is visible at 1521 cm^{-1} as a strong narrow band. The symmetric stretch at 1355 cm^{-1} is also visible but less characteristic due to overlapping bands in the finger print region.

In order to clearly assign these nitro alkane bands figure 4.2 shows the IR spectrum of nitro methane. In this simplest nitroalkane the bands for the nitro stretch are clearly visible and assigned with minimal inference, due to the low number of the C-H bands from the methyl group, the finger print region is relatively clean.

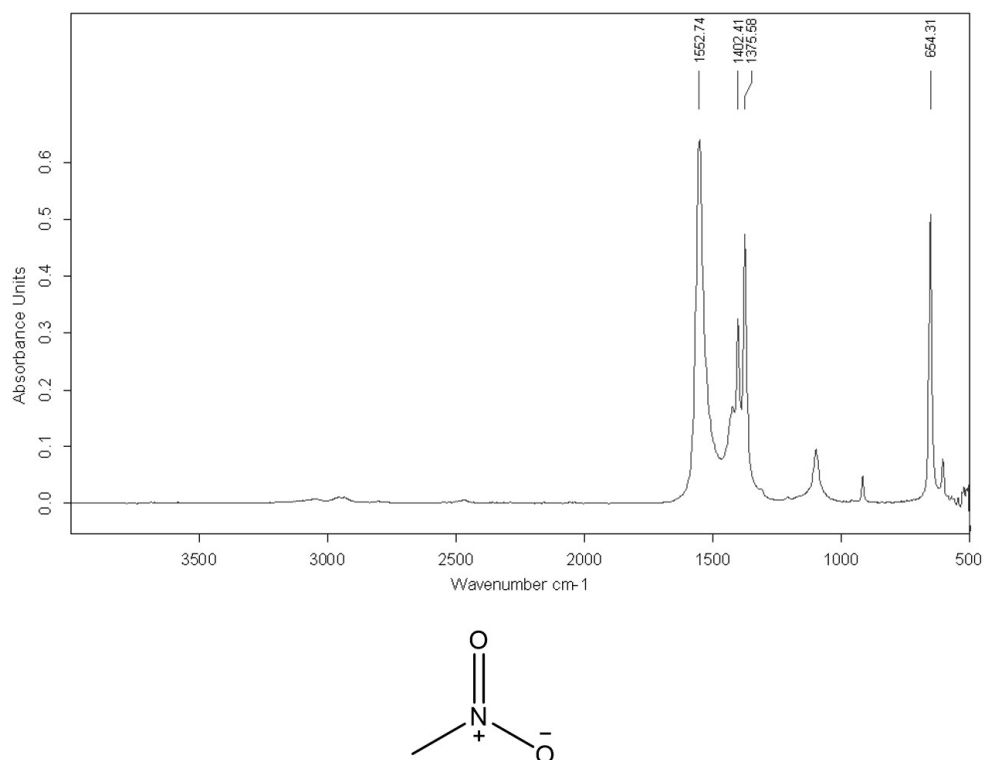


Figure 4.2: Infrared spectrum of nitromethane

The nitro group absorbance can be assigned in nitromethane and 1552 and 1375 cm^{-1} for the asymmetric and symmetric stretches respectively. Using the previous spectra (figure 4.1,4.2 the reaction mixture obtained during the nitration of squalane can be analysed for the presence of these bands.

Using ATR-FT-IR no change was observed in the regions assigned to the nitro bands ($1575 - 1500 \text{ cm}^{-1}$ and $1360 - 1290 \text{ cm}^{-1}$) in the degraded squalane sample obtained by nitration reactions where the path length is approximately one wavelength for the light. This is possibly due to the low concentration of nitrated products. Therefore the instrument set-up was altered from ATR to allow a cell to be used for measurement with a path length 0.5 mm. The increase in pathlength increases the absorbance in accordance with the Beer Lambert law. The increases in absorbance increases sensitivity allowing lower concentrations to be analysed. The negative side to using a long path length is that wavenumber regions containing strong absorptions due to high concentrations, such as C-H bands, cannot be analysed due to saturation in both the background and sample.

The asymmetric stretch at $1575 - 1500 \text{ cm}^{-1}$ is in a region clear of many other absorbance bands in the spectrum therefore can be analysed using the IR cell. The symmetric stretch at $1360 - 1290 \text{ cm}^{-1}$ overlaps with the C-H bands in the fingerprint region therefore cannot

be seen in IR cell analysis. Analysis of only one of the two nitro stretches gives limited confirmation for the presence of the nitro alkanes but can provide some evidence to the formation of these compounds to support further analysis.

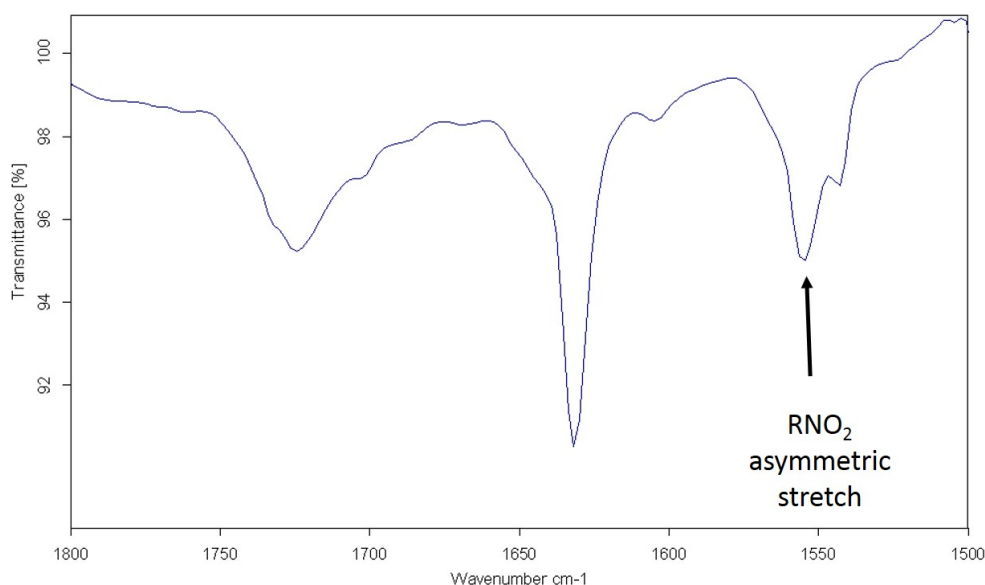


Figure 4.3: FTIR spectrum of squalane nitration end of reaction sample for 2 hours at 150 °C

Figure 4.3 shows the spectrum for the infra red analysis of a cell of a reaction sample of squalane which has been nitrated at 150 °C for two hours. This sample analysis shows an absorbance band 1550 cm^{-1} , in the region for the asymmetric stretch of the nitro group. This gives limited evidence for the formation of nitro alkane products in the products of squalane nitration. The band shape shows two overlapping peaks, this may give evidence for more than one nitro alkane to be present in the sample causing slightly different bond strength and therefore absorbance frequency. As the reaction mixture has already been shown to contain many products via GC x GC-TOF MS it is likely that the nitrogen containing products are also a mixture, consistent with the hypothesis for the peak shape.

4.5 GC x GC-NCD analysis of squalane nitration and nitrooxidation

Due to the low levels of nitrogen as calculated in section 4.4 even if squalane is fully nitrated, NCD is a suitable method for detecting nitrogen containing products due to its high sensitivity and selectivity to nitrogen. Coupled to GC x GC this provides the separation to allow individual compounds to be isolated and identified. Trends in the secondary retention time will also allow compounds with similar functional groups to be identified.

An example GC x GC - NCD chromatogram obtained for the end of reaction sample of the nitration of squalane at 150 °C for two hours is shown in Figure 4.4.

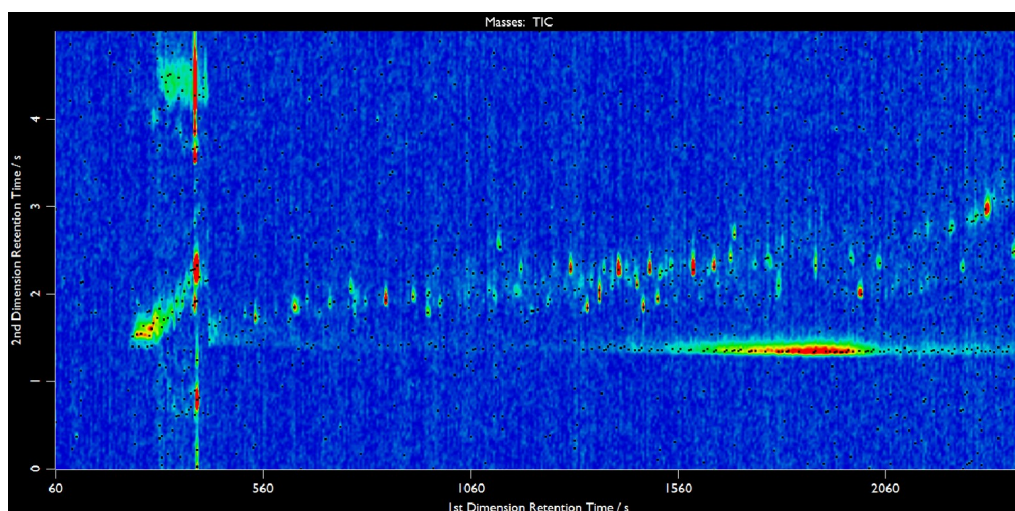


Figure 4.4: GC x GC-NCD analysis of squalane nitrated at 150°C for 2 hours

The chromatogram shows a complex mixture of products containing nitrogen. The most prominent feature is a series of peaks (up to six peaks which are not completely resolved) with a primary retention time around 400 seconds with a range of secondary retention times. The peaks are tailing in the second dimension suggesting these products are retained strongly by the polar column.

The area with a primary retention time over 560 seconds and a secondary retention time over 1.5 seconds shows a range of products. These products are suspected to be alkanes containing nitrogen functionality. These peaks have been compared to the nitroalkane standards, which have been synthesised in this project and analysed in the GC x GC-NCD to enable the identification of nitroalkane products formed during nitration.

The equivalent analysis has been carried out on reaction samples following nitrooxidation of squalane for two hours at 150°C. The products identified and the features of the 2D chromatogram are the same which provides evidence that no unique functional groups are formed under nitrooxidation conditions. The only slight difference is in the abundance of the products due to the increase in reaction rates due to the oxygen induced radicals.

The regions identified in the nitration and nitro oxidation chromatograms are highlighted in figure 4.5. Where it was possible to identify the products these identifications are discussed in the following sections.

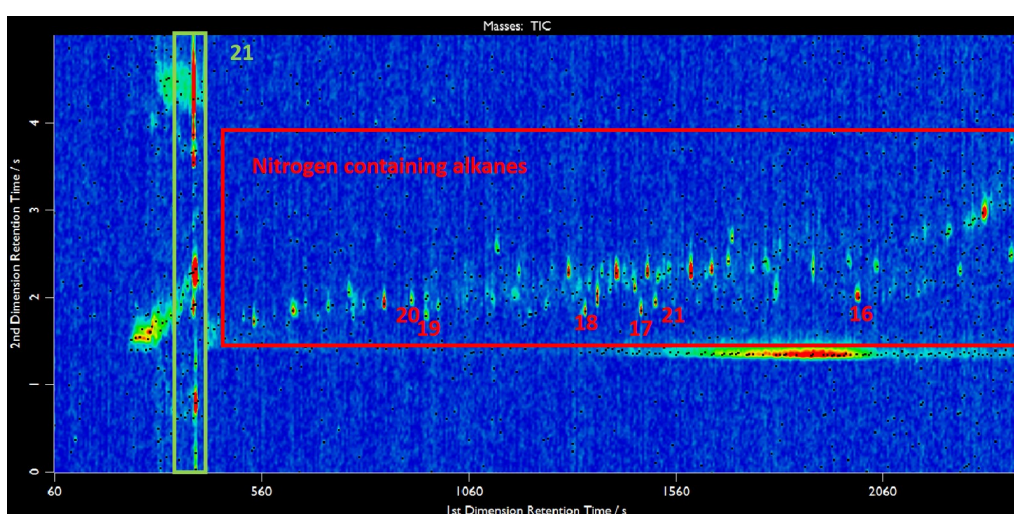


Figure 4.5: Numbered products and regions of GC x GC NCD analysis of squalane nitrated at 150°C for 2 hours

4.6 Synthesis of nitroalkanes

In order to identify the nitroalkanes which may be formed during the nitration of squalane, nine standards were synthesised from bromoalkanes. The retention times for these standards allow the secondary retention time for nitroalkanes to be identified. The primary retention time will allow investigation into whether the retention time shows a proportional increase with the molecular weight of the hydrocarbon. A proportional relationship allows the Kovats retention index to be calculated.¹⁰³ The retention index can then be applied to nitroalkanes to estimate the carbon number for any nitro alkanes detected.

Conversion from the bromoalkane to the nitro alkane was confirmed using ¹H NMR

spectroscopy, a sample spectrum is shown in figure 4.6. The chemical shift of H_a is observed at 3.4 ppm, which changes to 4.3 ppm for H_e on conversion of the bromo group to the nitro functional group (shown in 4.6).

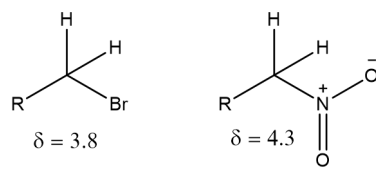


Figure 4.6: ^1H NMR shift changes between a bromide and nitro alkane

An example of the crude ^1H NMR spectrum of 1-nitrotetradecane is shown in figure 4.7. The peaks can be identified as those of 1-nitrotetradecane (green), 1-bromotetradecane (red) and ethyl acetate (blue).

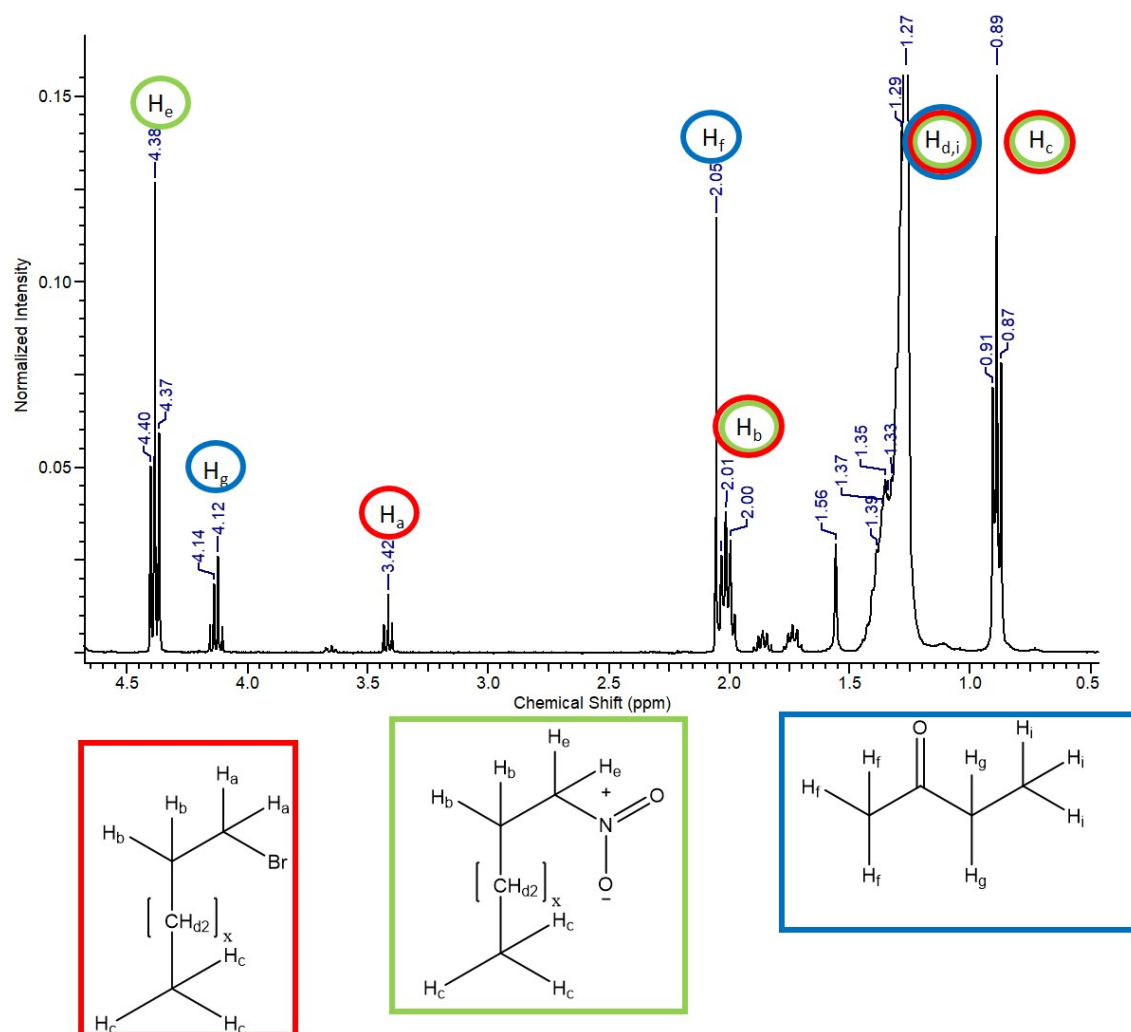


Figure 4.7: Crude ^1H NMR spectrum of nitroalkanes synthesized from bromoalkanes

The compounds synthesised ranged from C₅ to C₁₉, all of which are shown in figure 4.8. For the purpose of this work, the nitro alkanes were not purified from the starting materials or solvents as only the nitrated species will give a signal in GC x GC-NCD.

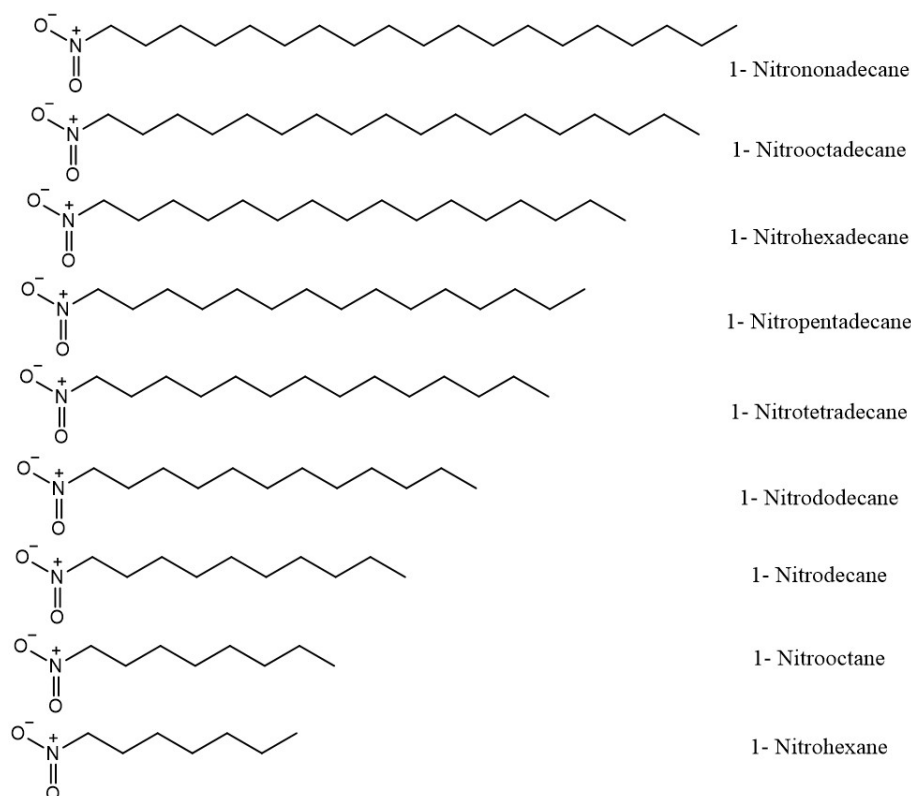


Figure 4.8: Nitroalkanes synthesised from bromoalkanes

4.7 Retention indices calculation of nitroalkanes in GC X GC NCD

Retention indices were first used by Kovat¹⁰³ to compare the retention times in different gas chromatography systems. This principle uses the linear relationship between the molecular size (carbon number) and retention index, which is well established. For temperature programmed GC Kovats presented equation 4.9. The linear relationship has not previously been confirmed for nitroalkanes, and therefore the Kovats retention index has not been calculated. The standards will enable the application of Kovats retention indices to nitro alkanes.¹⁰³

$$I = 100N + 100 \frac{(T_{R(X)} - T_{R(N)})}{(T_{R(N+1)} - T_{R(N)})} \quad (4.9)$$

where

N = Carbon Number

X = Compound under Investigation

T_R = Retention Time

I = Retention Index

This can be modified to allow the linear relationship of multiple related compounds to be used to calculate the retention index of unknown peaks (equation 4.11)

$$T_{R(X)} = I(100X) + T_{R(0)} \quad (4.10)$$

$T_{R(0)}$ is the gas hold up time, which is the theoretical time a completely unretained compound would take to travel between the injector and the detector.

The nine synthesised primary nitroalkanes and a commercially available tertiary compound (2-methyl-2-nitrotridecane) were used to calculate the linear relationship between C_n and T_R of the nitroalkanes. The carbon numbers used and the retention times are shown in table 4.1.

Table 4.1: The nitro compounds used for the retention index calculation

Compound	Carbon Number	Primary Retention Time /s
1-nitrohexane	6	940
1-nitrooctane	8	1115
1-nitrodecane	10	1355
1-nitrododecane	12	1575
1-nitrotetradecane	14	1770
2-methyl-2-nitrotridecane	14	1660
1-nitropentadecane	15	1860
1-nitrohexadecane	16	1940
1-nitrooctadecane	18	2100
1-nitrononadecane	19	2180

The carbon number and retention times could then be plotted to calculate the retention index based on the linear relationship given in equation 4.11. This relationship between retention time and carbon number can be seen in figure 4.9.

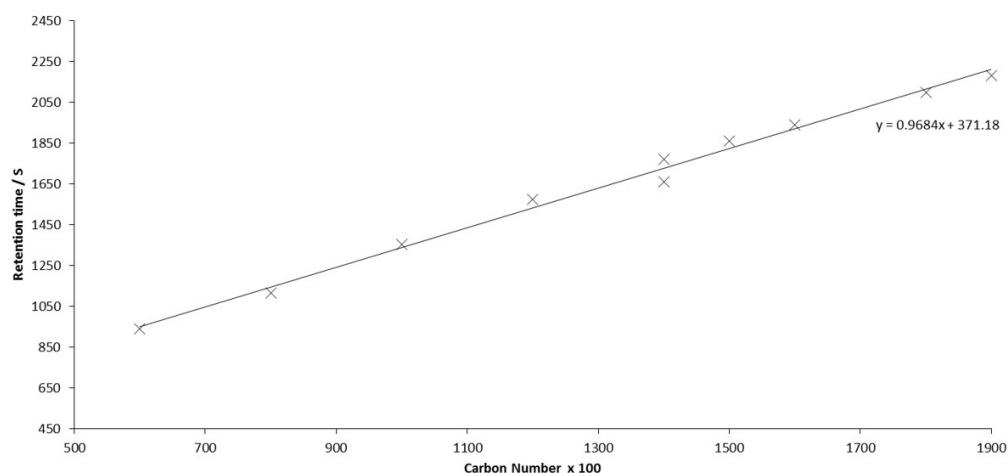


Figure 4.9: Retention indices of nitroalkanes in the GC x GC NCD

This can be calculated from the gradient of the graph gives the experimental values for the GCxGC used for the analysis in this project

$$I = 0.97$$

$$T_{R(0)} = 372 \text{ s}$$

The retention time shows a strong linear relationship with the primary alkanes shown in figure 4.9. Comparisons of 1-nitrotetradecane and the 2-methyl-2-nitrotridecane show the effect of branching. The branching gives a reduction of the retention time compared to primary compound with equal carbon number. This presents limitations to the application of Kovats retention index as the compounds are also able to form secondary and tertiary derivatives. To account for the effect of branching the estimated carbon number should be rounded up to the nearest carbon number.

4.8 Carbon number calculation

A series of peaks have been identified as having a secondary retention time, around 1.9 - 2.1 seconds, which is consistent with the trends seen for the nitroalkane standards synthesised. The major peaks which were assigned to nitroalkanes, as labelled (products 16-21) in figure 4.5, are identified in this section.

Using the retention index equation (4.11) described in section 4.7 the carbon number of the nitroalkanes products can be calculated using the primary retention time.

$$T_{R(X)} = I(100X) + T_{R(0)} \quad (4.11)$$

with the calculated values

$$I = 0.97, T_{R(0)} = 372 \text{ s}$$

An example is shown below for the largest nitroalkane.

using equation 4.11 and a primary retention time = 2000 s

$$\frac{2000 - 372}{0.97} = 100X$$

$$1678 = 100X, X = 16.8$$

The carbon number of the nitro alkane can then be calculated.

$$X \approx 17$$

The size calculated for the six nitroalkanes identified by the secondary retention times is summarised in table 4.2.

Table 4.2: The calculated carbon number based on the primary retention time of the nitroalkanes from the nitrated squalane

1st retention time /s	2nd retention time /s	Estimated Carbon Number
2000	2.105	17
1510	1.980	12
1460	2.110	11
1340	1.890	10
955	1.805	6
855	1.970	5

Using the calculated molecular sizes and the structure of the squalane starting material the structures of these nitroalkanes can be estimated. Products 16 to 20 are primary nitroalkanes. Product 21 is a secondary nitroalkane; the fragmentation of squalane to form a twelve carbon species requires two fragmentations; these can be initiated from the tertiary carbon in the two and ten position resulting in fragmentation.

The structures of the identified nitroalkanes can be seen in figure 4.10.

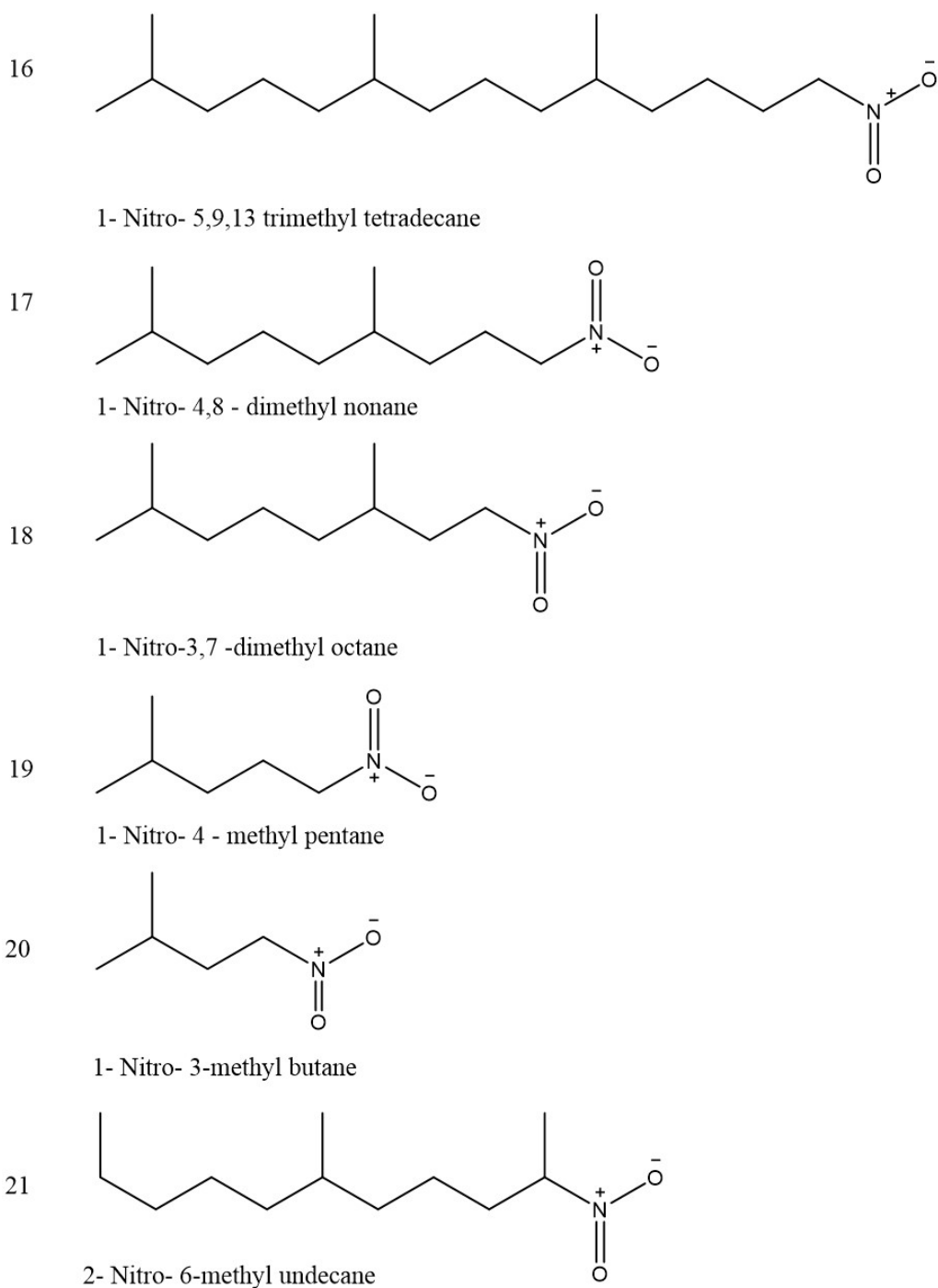


Figure 4.10: Chemical structures of the proposed nitro alkane products from the nitration and nitrooxidation of squalane

The formation of the nitro alkane can take place *via* the mechanism proposed in figure 4.11. The initiation can be started by either nitrogen dioxide or oxygen. The reaction then precedes to form an oxygen centred radical, this radical can fragment to give a carbon centred radical and a ketone. This fragmentation has been previously reported for the oxygenated compounds and is adapted here for nitration. This mechanism is

in line with the shorter alkanes identified in chapter 3 by GCxGC-TOFMS. The carbon centred radical addition with nitrogen dioxide occurs *via* the nitrogen to form the nitro alkanes. Decarboxylation can also occur to shorten the carbon chain, resulting in the formation of a primary nitro alkane. The addition of NO_2 is well reported and is the expected product from these reactions based on previous studies.

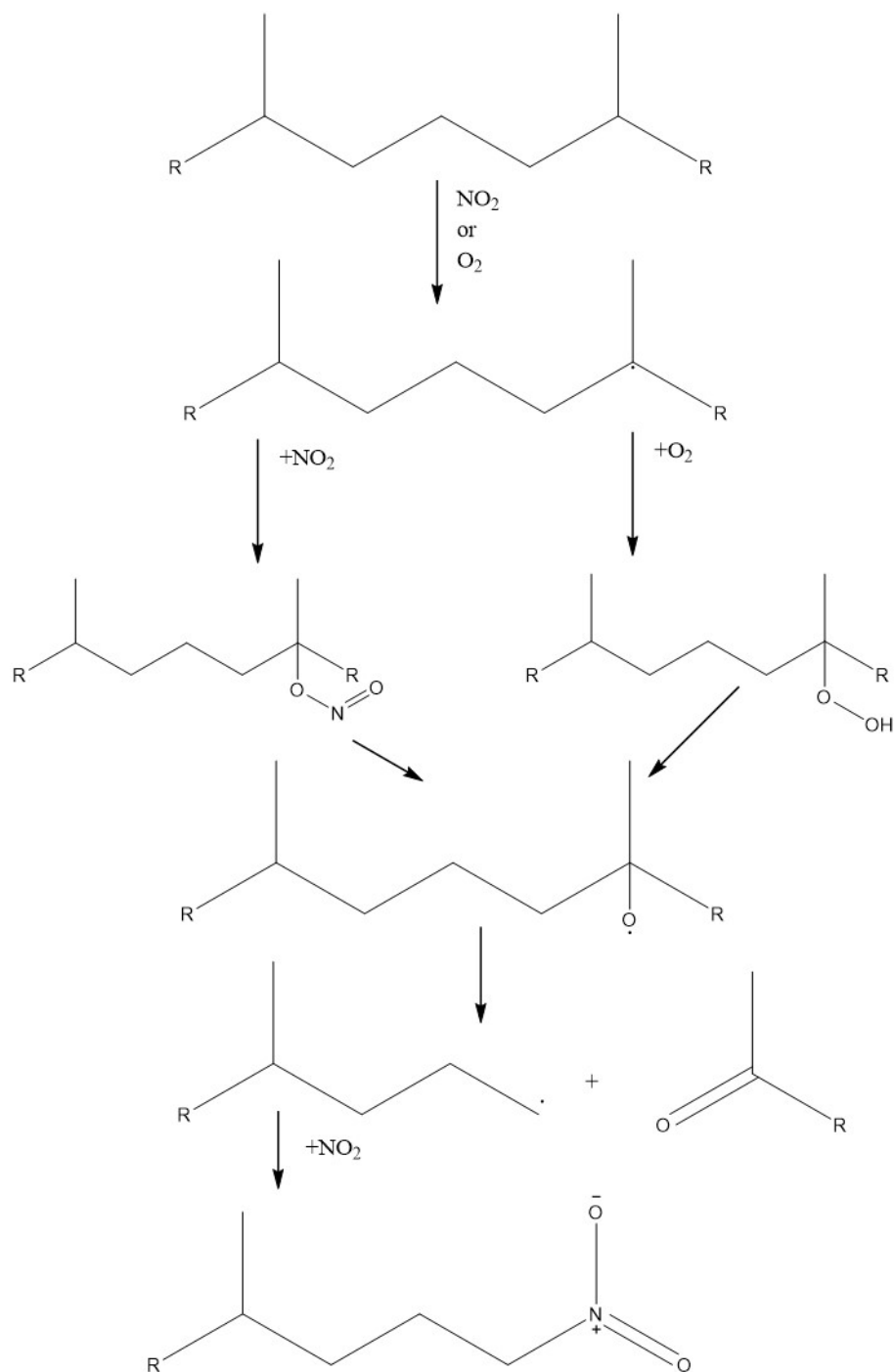


Figure 4.11: The scheme to form primary nitroalkanes from the fragmentation of squalane

The largest size of nitro-alkane that can be detected using the GCxGC method can also be calculated by equation 4.11 using maximum primary retention time of 2500 sec.

$$\frac{2500 - 372}{0.97} = 100X$$

$$100X = 2194$$

$$X = 21.94$$

Therefore it is estimated that the nitro alkanes with a carbon number < 22 can be detected using this method. This calculation suggests that the largest possible nitro-products are not able to be detected using the GCxGC NCD method, including those resulting from the addition of nitrogen dioxide to the tertiary centre to form nitro squalane ($C_n = 30$).

4.9 Quantification of the nitro alkane products

The identified nitro alkanes have been quantified using peak area and the equimolar response for nitrogen from the NCD detector. The response was calibrated using standards of nitromethane, nitrobenzene, 2-methyl-2-nitrotridecane and found to be equal at equal concentration. Therefore, due to availability and safety, nitrobenzene was identified as the most suitable standard for calibration. The concentrations of these products over time for both the nitration and nitrooxidation are shown in figure 4.12 and 4.13 respectively.

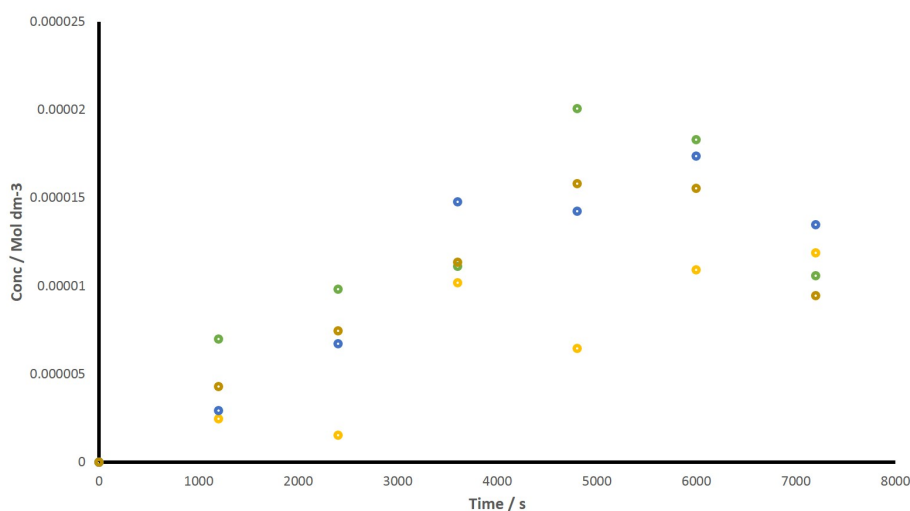


Figure 4.12: The quantification of the identified nitro alkanes from NCD for the nitration of squalane at 150 °C for two hours. Product 17 - Green, 18 - Blue, 19 - Brown, 21 - Yellow,

The species all follow the same growth trends, an approximately steady linear increase in the concentration, with time, until a maximum is reached after 80 minutes. After this the concentration decreases with further samples. This suggests that there is a loss mechanism, either chemical reaction or evaporation. After 80 minutes the rate of loss is faster than the rate of formation.

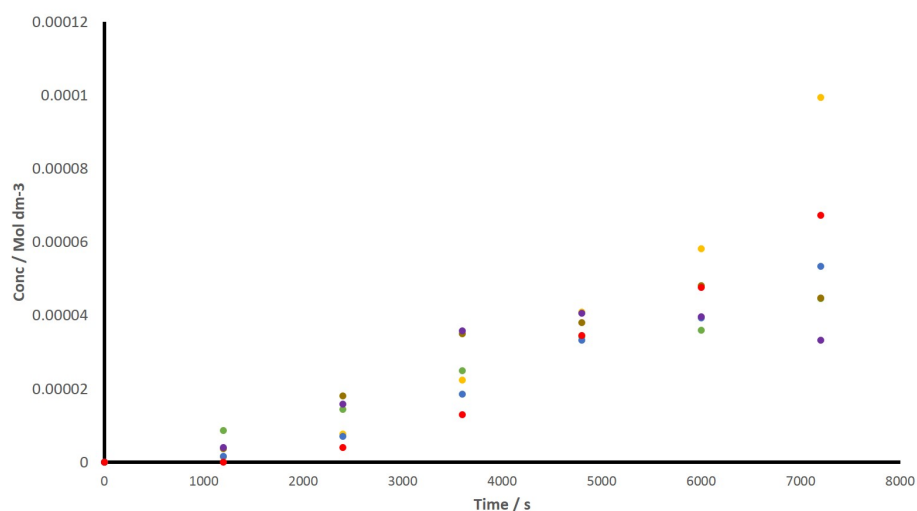


Figure 4.13: Quantification of the identified nitro alkanes from NCD for the nitro oxidation of squalane at 150 °C for two hours. Product 16 - Red, 17 - Green, 18 - Blue, 19 - Brown, 20 - Purple, 21 - Yellow

During the nitrooxidation it can be observed that the product concentration increase with time. Some of the products increase to a maximum, such as product 20 (1-nitro-3-butane), similar to the trend seen in the nitration reaction. However some products do not follow the same trends as in the nitration reactions and show continuous growth over time. The likely cause of this difference is the increase in radicals due to the increase of initiator (reactive gas, NO_{2O_2}).

From the plot of nitro product concentration over time a difference can be seen between the nitro and the nitrooxidation reactions products. For all products a significantly higher concentration of the products is formed in the nitrooxidation compared to nitration. This increase in concentration can be attributed to higher concentration of initiator (reactive gas). In nitration experiments there is only 1000 ppm NO_2 and for nitrooxidation there is a total initiator concentration of 101000 ppm (100000 ppm O_2 + 1000 ppm NO_2), which is a factor of ≈ 100 times higher.

4.10 Identification of nitromethane

In the GCxGC NCD analysis in fig 4.5 the features in the region with a primary retention time of 400 seconds are identified as product 21 in figure 4.5. From the primary retention time the product can be expected to have a relatively high volatility, and therefore a

small molecular size is likely. The spread and the secondary dimension tailing resulting in several peak suggests that the product is also highly polar.

The likely species formed from this type of reaction are either nitric acid or nitro methane. To identify the products, standards were run for comparison, nitric acid did not show clear features in the chromatogram. A chromatogram for nitro methane is shown in figure 4.14

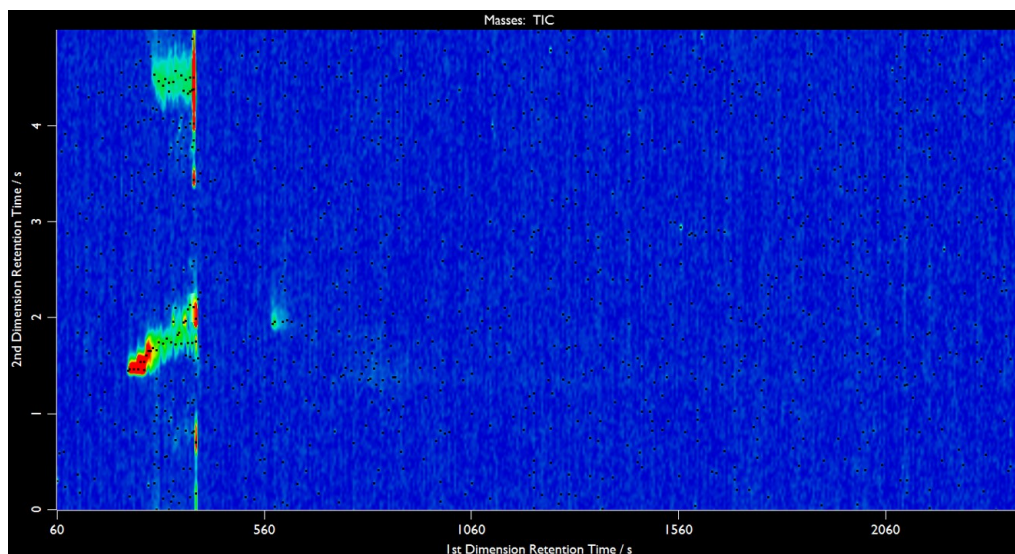


Figure 4.14: GC x GC NCD analysis of nitromethane

The key peaks from the area identified as product 21 from the nitration of squalane are summarised in table 4.3.

Table 4.3: Retention times for nitromethane peaks and product 21

Nitro methane		Product 21	
Primary retention time /s	Secondary retention time /s	Primary retention time /s	Secondary retention time /s
395	0.705	395	0.740
395	1.995	400	1.915
395	3.435	395	3.795
390	4.380	395	4.280
390	4.506	395	4.602
390	4.905	400	4.815

Comparisons between the product peaks and the nitromethane standards (table 4.3) show strong similarity; some of the peaks show a small variation in the secondary

degree retention time, which can be accounted for by the peak shape and tailing in this separation.

The area identified as product 21 can be assigned as nitromethane. The identification of nitromethane has previously not been identified or suggested as a product of nitration alkanes, however this is species with the highest concentration amongst the nitrogen containing products identified in this work.

A possible route to the formation of nitromethane can be the loss of a methyl radical following an attack in position two of squalane, as shown in figure 4.15; this is comparable to the mechanism proposed in other reactions forming nitromethane.

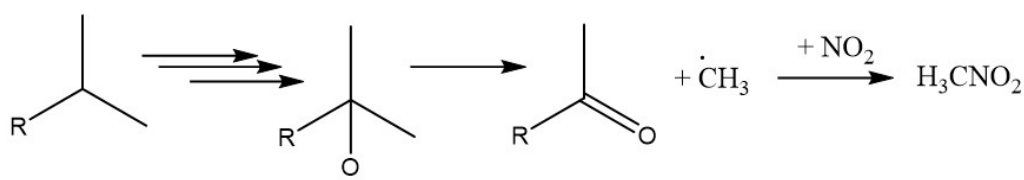


Figure 4.15: Formation of nitromethane from attack at position two of squalane

The mechanism in figure 4.15 relies on the loss of a methane radical; this is typically unfavourable due to the low stability of the methyl radical. The fragmentation would be expected to form propan-2-one and the larger primary radical.

4.11 Quantification of detected nitrogen containing species

Only some of the nitrated products have been identified and quantified individually. In order to quantify the overall nitrogen containing products, the equimolar response due to the nitrogen in the NCD can be used with a total peak area. This allows the nitrogen which has been incorporated into the liquid sample to be estimated. This can be compared to the total nitrogen dioxide input into the reactor.

The total area of nitrogen containing alkanes, which is the area within the red box in figure 4.5, have been summed using the analysis software GC image Version 2.1.

The dilution factor for the samples is nominally 10% in ethyl acetate, however the mass is used to measure the dilution accurately. In order to take into account the

dilutions the following calculations have been carried out for all the samples.

$$\text{Dilution factor} = \frac{\text{Mass of sample}}{\text{Mass of sample} + \text{Mass of ethyl acetate}}$$

$$\frac{\text{Peak area}}{\text{Dilution factor}} = \text{Normalised peak area}$$

$$\frac{\text{Normalised peak area}}{\text{calibration factor}} = \text{Concentration (mol dm}^{-3}\text{)}$$

The quantification of the nitrogen containing alkanes is shown in figure 4.16. The total concentration is shown for the nitration and the nitrooxidation reactions.

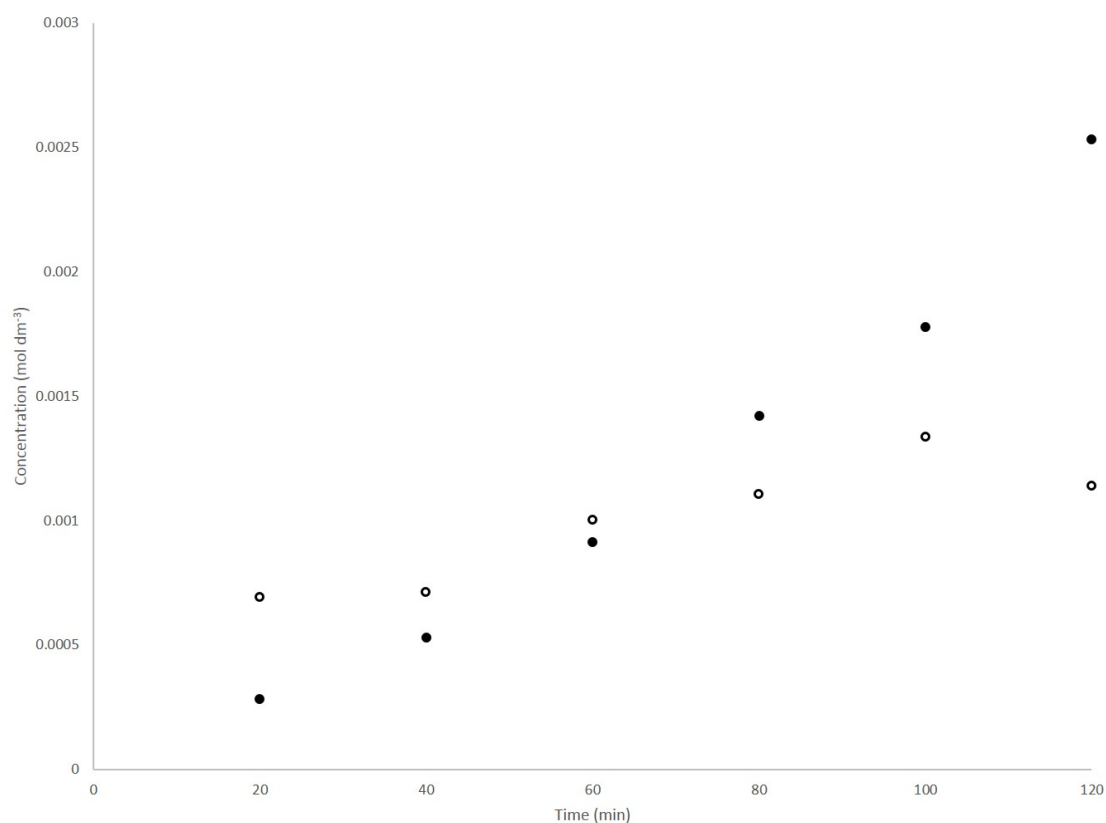


Figure 4.16: Quantification of total nitrogen containing alkanes from nitration - hollow and nitrooxidation - filled

The trends for the total nitrogen containing species during nitration and nitrooxidation reactions can be seen to have the same trends as for the individual species quantified in (figure 4.12). The nitrooxidation shows higher levels of nitrogen, with steady increase in nitrogen containing products. The increased level of oxygen in the nitrooxidation reaction results in a higher concentration of reactive gases to act as initiators in the radical reactions. The observed difference in the concentration can be attributed to the

concentration of the reactive gases.

Another major region of nitrogen containing products is that of the nitro methane, which consist of several large tailing peaks in the GC x GC-NCD, and calculating the concentration from the total peak area for this regions can allow quantification of the nitromethane. The concentrations of nitromethane for nitrooxidation are shown in figure 4.17.

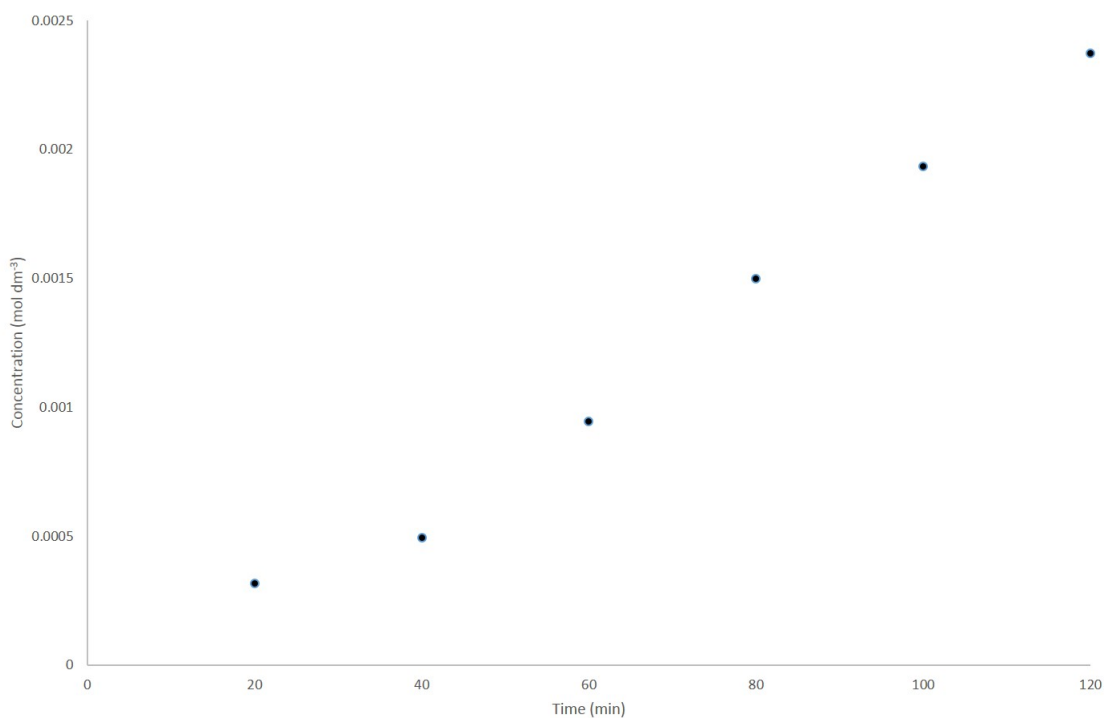


Figure 4.17: Quantification of nitromethane from the nitrooxidation of squalane

During the nitrooxidation a steady increase in nitromethane concentration during the reaction is observed. The concentration of nitromethane under nitrooxidation is by far the highest product identified at $0.0024 \text{ mol dm}^{-3}$, compared to a total nitrogen containing alkane concentration of $0.0025 \text{ mol dm}^{-3}$. The concentration of nitromethane is almost equal to the total amounts of other species containing nitrogen, visible by the GCxGC NCD.

4.11.1 Percentage identified nitrogen

The amount of nitrogen identified for the reactions compared to the input of nitrogen in the form of nitrogen dioxide can be calculated.

The example shown in this section is for the nitrooxidation of squalane as this has the highest concentration of nitrogen.

First the concentration of nitrogen has to be converted to a total amount nitrogen for the sample.

The sample volume is 7 cm^{-3} .

For nitrogen containing alkanes the total concentration of $0.0025 \text{ mol dm}^{-3}$

$$\frac{\text{concentration (mol dm}^{-3}\text{)}}{1000} \times \text{Sample volume (cm}^{-3}\text{)} = \text{Amount of nitrogen (mol)}$$

$$\frac{0.0025 \text{ mol dm}^{-3}}{1000} \times 7 \text{ cm}^{-3} = 0.0000175 \text{ mol} = 1.75 \times 10^{-5} \text{ mol}$$

For nitromethane the identified concentration is $0.0024 \text{ mol dm}^{-3}$

$$\frac{0.0024 \text{ mol dm}^{-3}}{1000} \times 7 \text{ cm}^{-3} = 0.0000168 \text{ mol} = 1.68 \times 10^{-5} \text{ mol}$$

The summing of these amounts of nitrogen can give an total amount of identified nitrogen

$$\text{Amount of nitrogen containing alkanes} + \text{Amount of nitromethane} = 1.75 \times 10^{-5} \text{ mol} \times 1.68 \times 10^{-5} \text{ mol} = 3.43 \times 10^{-5} \text{ mol}$$

The total amount of nitrogen input into the reaction as nitrogen dioxide is calculated in section 4.3 as 0.0002 mol

The percentage of nitrogen identified can be calculated

$$\frac{\text{total Amount of identified nitrogen (mol)}}{\text{Amount of nitrogen input as NO}_2} \times 100 = \text{identified nitrogen percentage}$$

$$\frac{3.43 \times 10^{-5} \text{ mol}}{2 \times 10^{-4} \text{ mol}} = 17.15\%$$

For the nitration of squalane the identified nitrogen has been calculated

This gives a identified nitrogen percentage of 8.5%

The unidentified nitrogen could be lost as unreacted NO_2 , nitrous acid (HONO) formed

in the initiation *via* hydrogen abstraction and other nitrogen containing products lost in the gas phase from reactions, such as NO, and small volatile alkanes containing nitrogen. The large nitro alkanes larger than $C_n=22$ will not be measurable using this method, as they are unsuitable for analysis by this GC x GC NCD method. The difference between the nitration and the nitrooxidation is likely due to be lower reactivity of the overall gas system, therefore more NO_2 is vented into the exhaust system unreacted.

4.12 Nitration of pristane

As it has been calculated in section 4.8 that the maximum nitro alkane size identifiable with this GC x GC NCD method will be less than $C_n=22$ carbons meaning the largest potential alkane cannot be identified. Pristane has been used instead of squalane during nitration to give evidence for the larger alkanes, in particular the direct addition of NO_2 to the tertiary centres; with 19 carbons these should be identifiable for pristane *via* GC x GC NCD. Any direct addition direct addition should be measurable as the estimated maximum species for the method used during this study is with a carbon number of 22. Using the retention index it can be estimated that the direct addition to form nitro pristane would elute with a primary retention time of approximately 2215 s. No species have been identifiable in the GC x GC NCD analysis with the appropriate retention time to be assigned as nitro pristane.

This result give evidence that the direct addition of nitrogen to the tertiary to form tertiary nitro compounds does not occur or these are not the most stable products favoured by the equilibrium. Other causes for the observation absence than favoured thermodynamics may be due to the steric hindrance or decay to form a different product. The decomposition pathways are summarised for the gas phase reaction by Nazin *et al.*, with the most prominent pathways being the elimination reaction via a five member transition state to form HONO or the nitro-nitrite conversion. These proposals are of limited use to the system as they are carried out at significantly higher temperatures and further work would be applicable to transfer them, to the liquid phase hydrocarbons in this study.

4.13 Conclusions

GC x GC NCD has been used to identify six nitro alkanes and nitromethane as the nitrogen contain products for nitration and nitrooxidation of squalane. In order to identify these species the retention indices for nitroalkanes have been calculated once the linear

relationship was species have been proven. The species have been identified based on the retention indices molecular size and the functionality from comparison of the secondary retention time with standard for nitro alkanes. Previously in liquid phase reaction the nitrogen containing products have been assumed. The only evidence has been the infra red absorbance measure by Coultas assigned as the the nitrate ester. The use of the NCD to identify the products in the first conclusive evidence that the nitrogen is reacted to form organic nitrogen in the products.

The total amount of nitrogen reacted with squalane to form nitrated products has been calculated. Of the nitrogen input as nitrogen dioxide 8.5% has been measured as organic nitrogen in the end of reaction sample for the nitration and 17.15% in the nitro oxidation. The nitration of pristane enabled the full range of potential nitro alkanes to be analysed showing that tertiary nitro compounds do not form as the expected major nitrogen contain compound as expected from previous studies by Korcek.⁶⁴

No previous work has reported the identification of any nitromethane however this has been the significant nitrogen containing product identified from the degradation of squalane. The nitromethane has been identified by comparison with a standard sample. A mechanism based on this evidence has been proposed and is novel as there has been no evidence requiring the justification for the formation of nitromethane previously reported.

Chapter 5

Analysis of the reaction gases

5.1 Introduction

This chapter analyses the exhaust gases produced during the nitration of squalane. Gas phase infrared spectroscopy is the technique employed to measure the changes in the gas phase species. The products condensed in the cold trap are also analysed *via* infrared spectroscopy. The concentration of the nitrogen dioxide input is seen to be reduced in the output as well as new gas phase products formed in the reactions.

5.2 Previous work into reaction gas analysis

Previous work under the engine conditions of this study has been unable to show any changes in the exhaust gases, either by the consumption of nitrogen dioxide or the formation of new gaseous species. The majority of these studies have worked on the assumption that the nitrogen dioxide reacts with the hydrocarbon to form nitrous acid or then may add to a carbon-centred radical. Although these assumptions may be correct, other reactions may involve the gaseous species, as either the reactant or the products, which have not been accounted for.^{1,64,76}

Atmospheric chemistry studies have shown that hydrocarbons can react with NO_2 in the gaseous phase, although under the conditions and reagents studied in this work the reactions are not expected to be significant in the gas phase.⁶³ As the gaseous reactions are not prevalent during this work the observations and reactions may also not be applicable to this system. The nitration analysis so far in this work has shown the formation of smaller hydrocarbons which may be more volatile than squalane. These may form secondary products in the gaseous phase, although due to the residence time of the gas in the reactor being only one minute it is expected that the formation of secondary products from the gas phase will be negligible.

5.3 Gas phase IR of exhaust gases

The reaction conditions used to study the gas phase changes have been varied, and are summarised in table 5.1 . The slower flow rate increased the residence time of the gases in the reactor, longer residence times will likely lead to greater changes in compositions. The larger changes will increase the chances of observations as they are more likely to be above the limit of detection.

The nitrogen dioxide reference was measured by flowing the gas through the cold

reactor to fill the infra red cell. This spectrum has then been used as a reference for comparison with the reaction spectra.

Table 5.1: The reaction conditions used for gas phase infrared spectroscopic analysis

Colour in figure 5.1	Flow rate / ml min ⁻¹	Temperature / °C
Black	NO ₂ Blank	
Blue	10	200
Red	10	150
Pink	40	200

The spectra were measured after one hour with continuous flow of the gases. This was expected to be long enough to completely flush the gas phase infra red cell which has a residence time of 20 minutes at the lower flow rate. The gas phase spectra shown in figure 5.1 shows a decrease in nitrogen dioxide during the reaction, with new species formed which are identified as water, carbon monoxide and carbon dioxide. There are also some absorbances due to the C-H stretch of gaseous emissions of volatile hydrocarbons formed in the reaction.

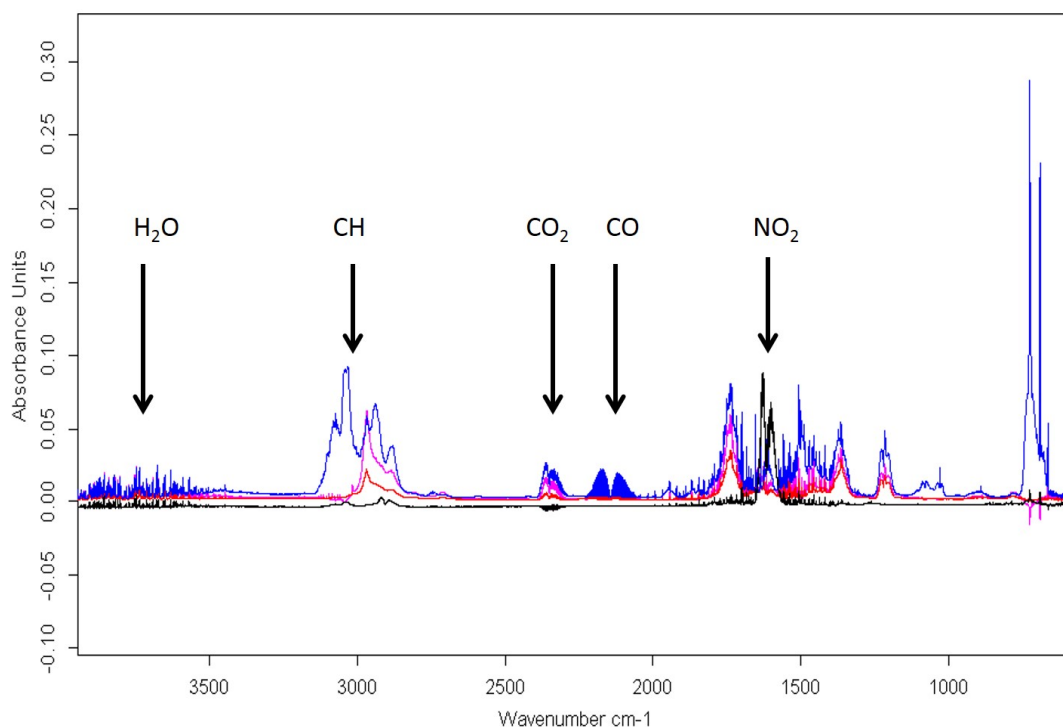


Figure 5.1: The gas phase infra red spectrum of the exhaust gases under the conditions summarised in table 5.1

The identified bands in the gas phase spectra are analysed in more details in sections 5.4, 5.5 and 5.6.

5.4 Gas phase IR of nitrogen dioxide

The evidence for the loss of nitrogen dioxide in all of the reactions studied can be seen in figure 5.2. By comparing the starting material spectrum (black) to those obtained at the end of the reactions, a strong decrease can be seen in the band intensity. The unreacted nitrogen dioxide has a peak height of approximately 0.08 absorbance units and for the end of reaction the peak height has decreased to below 0.01, ($\sim 12.5\%$ of the NO_2 blank). With approximately 87.5% decrease in the intensity of the nitrogen dioxide peak it can be estimated that at the end of the reaction the 1000 ppm starting concentration, has been reduced to less than 125 ppm. In the hottest temperature of the reaction and slowest flow rate (blue spectra) it appears all of the nitrogen dioxide is consumed.

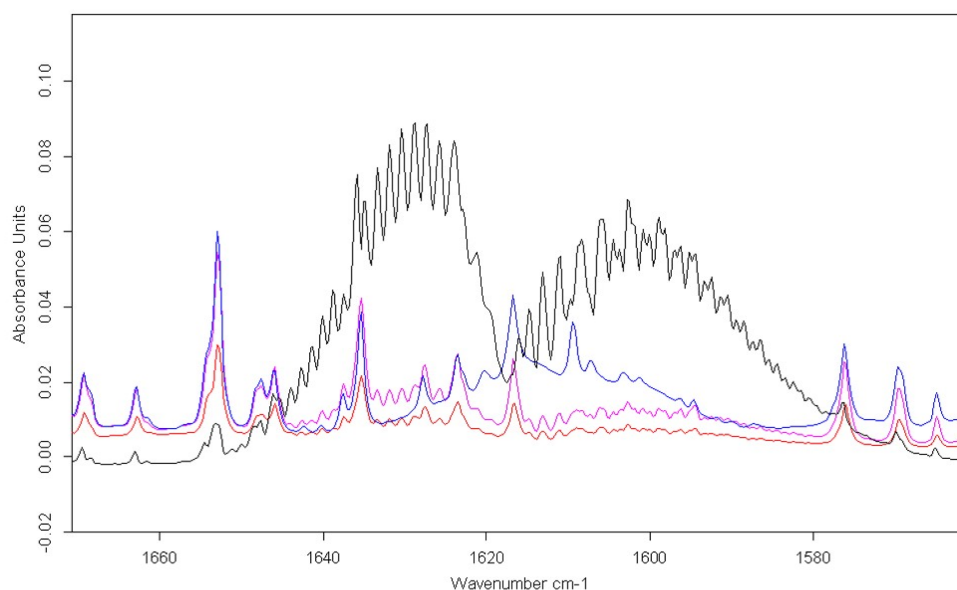


Figure 5.2: The gas phase infra red spectrum of NO_2 region of the exhaust gases under the conditions summarised in table 5.1

5.5 Gas phase IR of nitric oxide

From the oxygen containing products identified so far it is hypothesised that the nitrogen containing products in the form of nitrites can decay to form nitric oxide (NO). Nitrogen dioxide also forms an equilibrium with nitric oxide and oxygen although this is dependent

upon the conditions and very slow.¹⁰⁵ The infrared can detect the formation of nitric oxide with bands at 1870 cm^{-1} ,¹⁰⁶ with a published spectrum shown in figure 5.4. The absorbance coefficient for the nitric oxide significantly lower than for nitrogen dioxide, the coefficients have been measured as $1.23 \times 10^{-7}\text{ ppm}^{-1}\text{ cm}^{-1}$ at 1870 cm^{-1} for nitric oxide and $4.8 \times 10^{-7}\text{ ppm}^{-1}\text{ cm}^{-1}$ at 1628 cm^{-1} nitrogen dioxide.¹⁰⁷ The difference in absorbance coefficient will result in a 75 % decrease in the band from NO_2 to NO for the same concentration.

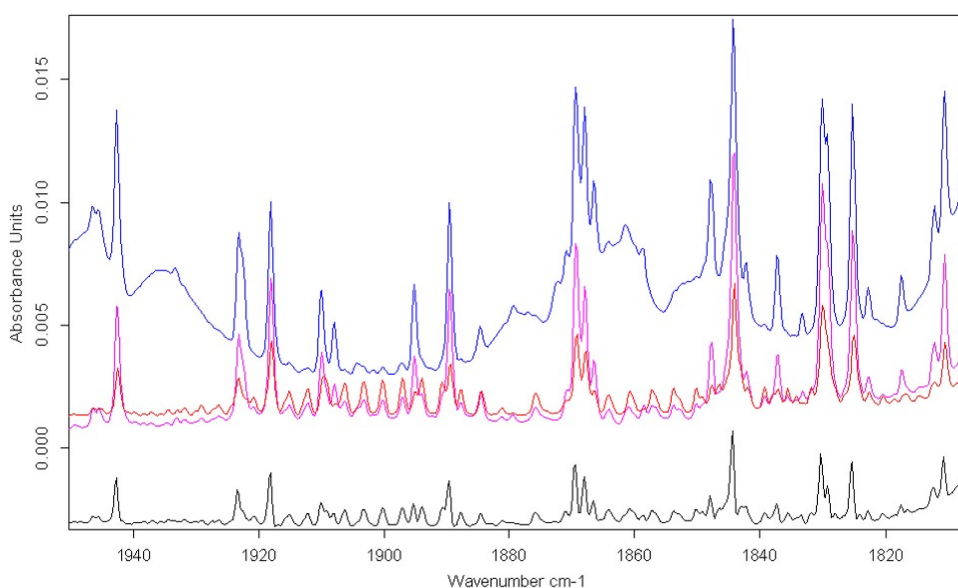


Figure 5.3: The gas phase infra red spectra of NO region of the exhaust gases under the conditions summarised in table 5.1

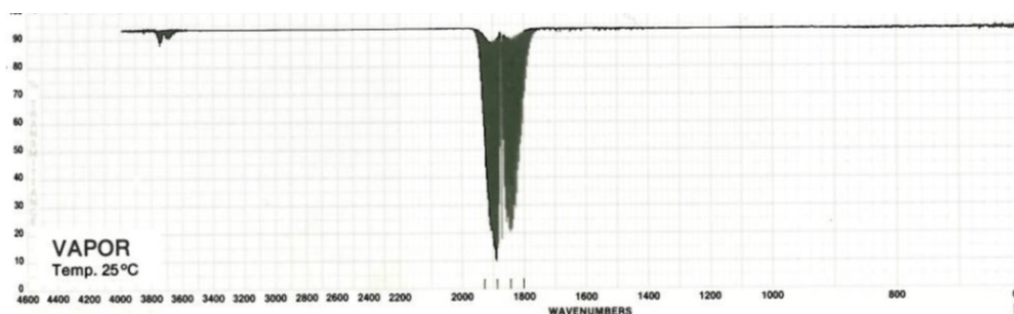


Figure 5.4: Infra red spectrum of NO reported by Pouchert¹⁰⁶

Some low intensity vibrational bands can be seen in figure 5.4 with P and R branches with a band centre at $\sim 1870\text{ cm}^{-1}$. This may be nitric oxide at a low concentration. However the absorbance coefficient and the low concentration, combined with other

bands from other species, means the presence of the nitric oxide cannot be conclusively confirmed from the measurements in these test.

5.6 Gas phase IR spectra of carbon monoxide and carbon dioxide

Two new strong bands have been formed in the reaction, shown in figure 5.6. These bands have P and R branches showing rotational fine structure with band centres at 2145 and 2340 cm^{-1} respectively. Analysis of the literature for species with similar absorbances, shown in figure 5.5, shows matching wavenumbers for carbon monoxide (2146 cm^{-1} , figure 6.6a)⁵ and carbon dioxide (2350 cm^{-1} , figure 6.6b).⁴

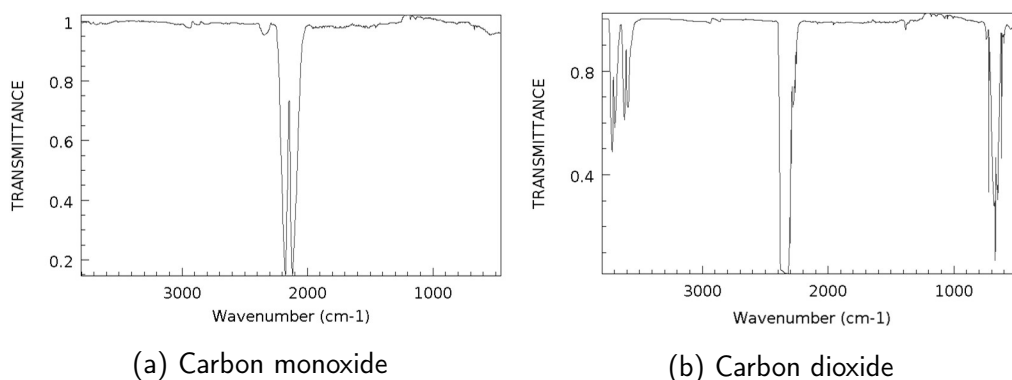


Figure 5.5: Infra red spectra of carbon monoxide and carbon dioxide reported by Coblentz^{4,5}

These literature spectra show strong similarities with those obtained for the end of reaction gases shown figure 5.6. These show fine rotational structure which is not seen in the literature spectra. This is due to the higher resolution of the instrument used to obtain the spectra. The vibrational bands and band centre are equivalent between the literature and experimental spectra in these reactions. This leads to the conclusions that carbon monoxide and carbon dioxide are produced in nitration reactions of squalane.

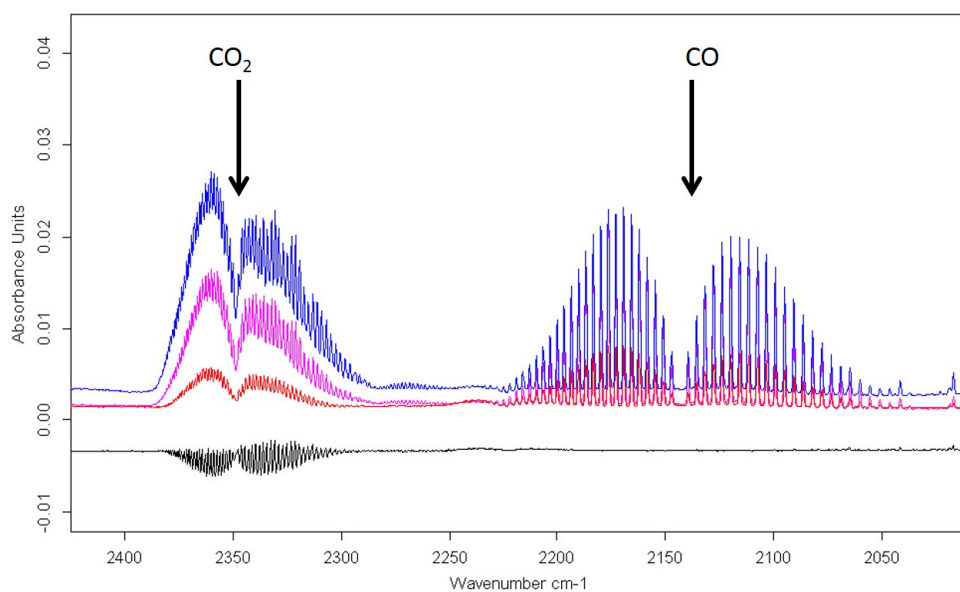
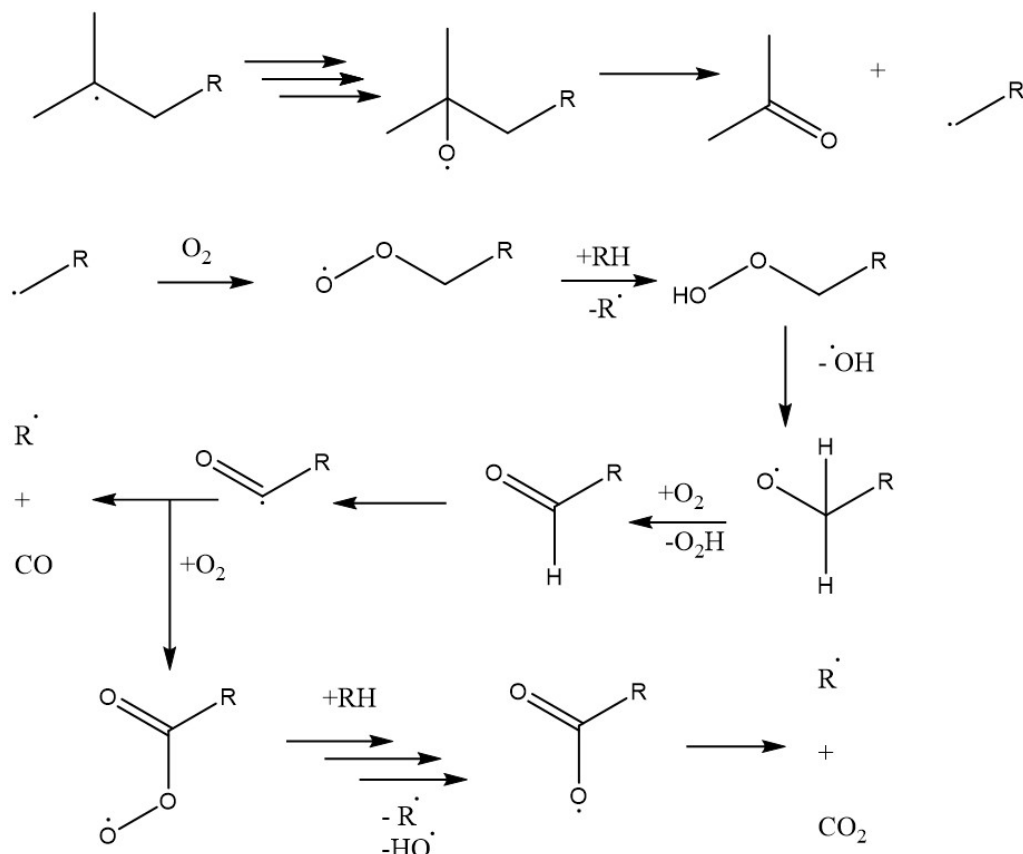


Figure 5.6: The gas phase infra red spectra of CO and CO₂ region of the exhaust gases under the conditions summarised in table 5.1

Carbon monoxide and carbon dioxide were not species predicted to form from the nitration of squalane, however these species have been observed in the autooxidation of alkanes.⁴⁷ In order to understand the mechanism by which these compounds are formed the closest comparison in the literature is shown in figure 5.7 as proposed previously^{6,7} for autoxidation of hydrocarbons.

Figure 5.7: Scheme of carbon monoxide and carbon dioxide formation by autoxidation^{6,7}

The mechanism forms an acyl radical which can decay to give carbon monoxide or oxidise further. During the further oxidation the radical form of the acid is formed which can decarboxylate to produce carbon dioxide. Formation of both the carbon monoxide and carbon dioxide, also forms an alkyl radical. Alkyl radicals terminate to shorter chain fragments, which have been identified in this work using GCxGC MS. This mechanism can be altered to have nitrogen dioxide as the reactive gas and source of oxygen; instead of the formation and decay of peroxides, the mechanism centred around the formation and decay of nitrites. The proposed mechanism for the formation of carbon dioxide from the nitration reactions is shown in figure 5.8

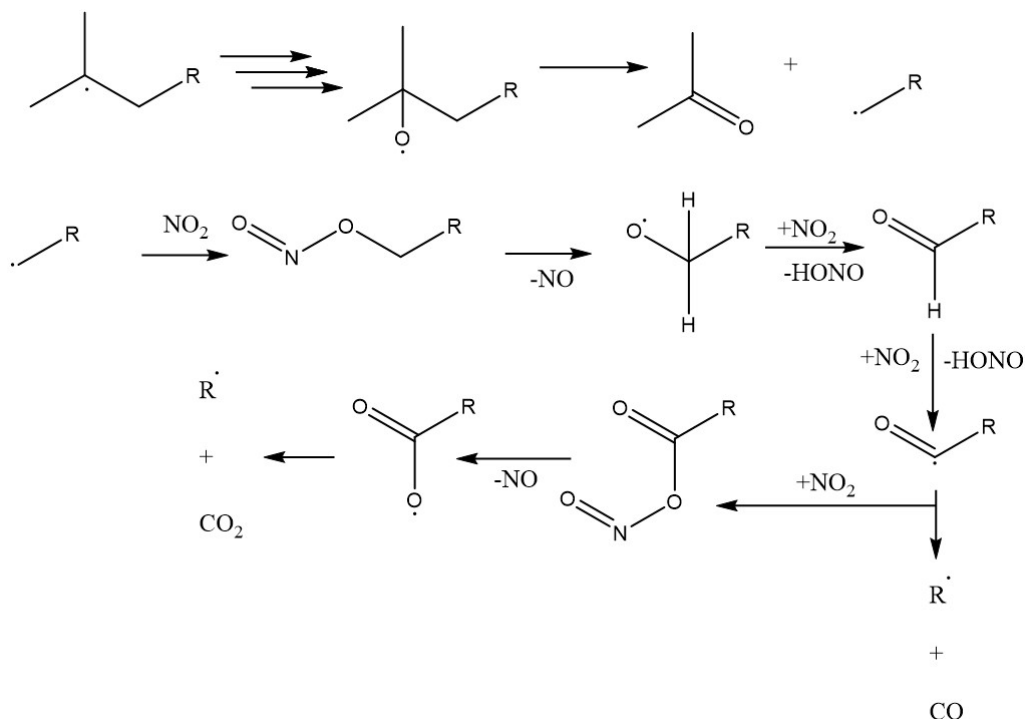


Figure 5.8: Scheme of carbon monoxide and carbon dioxide formation under nitration

The decarboxylation gives evidence for the shortening of the carbon chains after fragmentation from the tertiary carbon centres. This is required to form the range of primary nitroalkanes identified in chapter 3.

5.7 Summary of gas phase infra red analysis

There are other gaseous species which may be formed, in particular those containing nitrogen which are of a mechanistic interest. The gas phase infra red spectrum has been analysed for these species. The comparison for these species and the peak absorption wavenumbers reported in literature are summarised in table 5.2.

Table 5.2: Summary of the infra red signal of species analysed for in the gas phase infra red spectra

Gas Phase Compounds	IR	
	Signals /cm ⁻¹ ¹⁰⁸	Present
NO	1893, 1850	Possible at v. low conc
NO ₂	1629, 1590	Decreased from starting material
N ₂ O	2236, 2178, 1298, 1258	No
HONO	1263, 852, 790	No
N ₂	N/A	N/A
H ₂ O	3854, 3744, 1558, 1653	Yes
CO	2172, 2199	Yes
CO ₂	2364, 667	Yes
NH ₃	1046, 967, 930, 888	No
CH ₃ NH ₂		No

The changes identified in the gas phase of the reaction analysed infra red spectroscopy are the decrease in nitrogen dioxide concentration and the formation CO, CO₂, which have already been discussed, formation of H₂O and a possible low concentration of NO. No other species containing nitrogen have been identified using gas phase infra red.

5.8 Infra red spectroscopic analysis of the contents of the cold trap

In order to analyse the species which evaporate from the reactor, the exhaust gases from the nitration of squalane at 150 °C over a two hour reaction were condensed out into a cold trap maintained at 0 °C. This condensed sample has been analysed by ATR-FTIR and an example spectrum is shown in figure 5.9 in red; this is also overlaid with the spectrum for H₂O (pink).

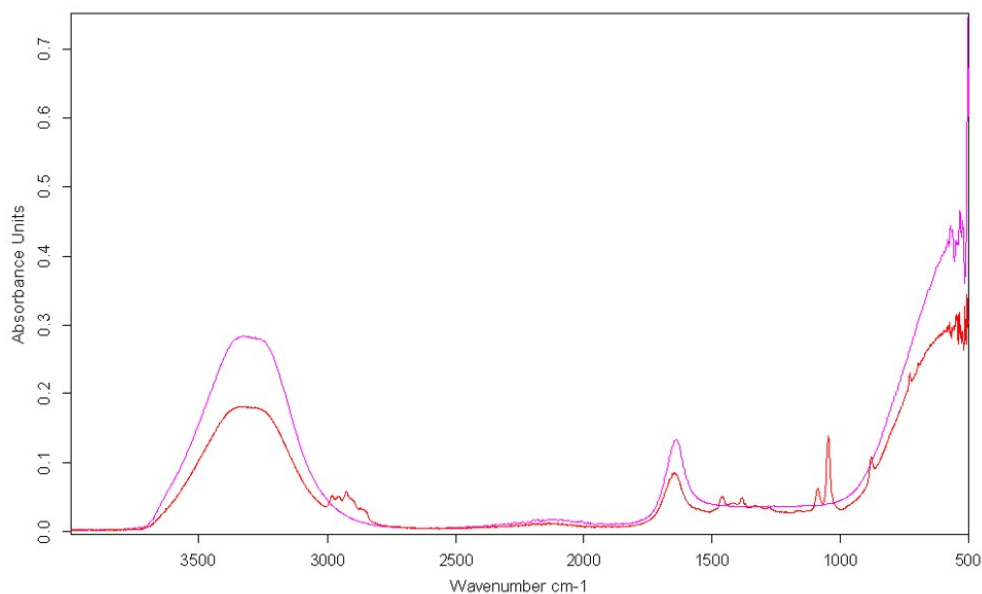


Figure 5.9: Infra red spectrum of the sample collected in the cold trap during nitration of squalane for two hours at 150 °C compared to spectrum of H₂O, sample - red , water - pink

The major peaks in the spectrum at approximately 3300 and 1600 cm⁻¹ are common for both sample and H₂O. Other small difference can be noted, these can be attributed to the C-H bands from small organic species which have been evaporated.

Under all conditions, other than weak concentrations at low temperatures, nitrous acid (HONO) is known to decay rapidly forming nitric oxide and a reactive hydroxyl radical. Nitrous acid is the expected product from the initiation of the radical reaction for the hydrogen abstraction by nitrogen dioxide. As HONO is not identified in this study an alternative initiation needs to be presented or a loss mechanism for the HONO. One loss mechanism is fragmentation of the HONO to start a chain branching of the radical reaction *via* the hydroxyl radical abstracting a hydrogen forming water. The mechanism for the formation of water from HONO is shown in figure 5.10.

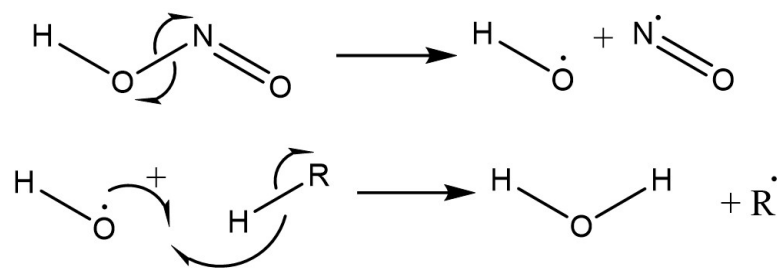
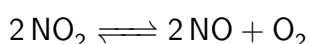


Figure 5.10: Scheme for the formation of water from nitrous acid decay

5.9 Production of the oxygen due to the decay of nitrogen oxide

One mechanism for the formation of oxygenated products is the decay of NO_2 *via* an equilibrium with nitric oxide and oxygen. The oxygen formed in this equilibrium can then act as the oxidant in the reaction *via* the mechanism previously proposed in autooxidation studies. Nitrogen dioxide is known to decay at elevated temperatures; the reaction kinetics have been studied by Rosser and Wise.⁹



As expected the reaction was found to be second order with respect to nitrogen dioxide (equation 5.1) with the rate constant defined as in equation 5.2.

$$r = k [\text{NO}_2]^2 \quad (5.1)$$

$$k = 10^{12.6} \times e^{\frac{-26900}{RT}} \text{ cm}^3 \text{ mol}^{-1} \text{ s}^{-1} \quad (5.2)$$

Using equation 5.2 the rate constant for the production of oxygen in the conditions for the reactions carried out in this study can be calculated, these are summarised in table 5.3

Table 5.3: Rate constants for the decay of nitrogen dioxide to nitric oxide and oxygen between 150 °C and 200 °C using the Arrhenius parameters of Rosser and Wise⁹

Temp / °C	Temp / K	Rate Constant / $\text{cm}^3 \text{ mol}^{-1} \text{ s}^{-1}$	Rate Constant / $10^{-5} \text{ dm}^3 \text{ mol}^{-1} \text{ s}^{-1}$
150	423	0.05	5.03
160	433	0.11	10.54
170	443	0.21	21.35
180	453	0.42	41.91
190	463	0.80	79.92
200	473	1.48	148.28

Using the ideal gas law, (equation 4.1) the total number of moles per dm^3 of gas at 1 atm and 298 K can be calculated to be 0.04089 mol; the NO_2 used in this work is

1000 ppm (0.1%) therefore the concentration can be stated as $4.1 \times 10^{-5} \text{ mol dm}^{-3}$.

The rate of gas flow through the reactor is $40 \text{ cm}^3 \text{ min}^{-1}$, with the reactor having internal volume of 49 cm^3 . The average residence time of the gas in the reactor can be approximated by

$$\text{Residence time} \approx \frac{\text{Reactor Volume}}{\text{Flow Rate}} = \frac{49 \text{ cm}^3}{40 \text{ cm}^3 \text{ min}^{-1}} = 1.225 \text{ min} = 73.5 \text{ s} \quad (5.3)$$

The integrated rate law for a second order reaction (equation 5.4) can be used to calculate the concentration change of NO_2 within the reactor.

$$\text{NO}_2 = \frac{[\text{NO}_2]_0}{1 + kt [\text{NO}_2]_0} \quad (5.4)$$

If it is assumed that the NO_2 is only lost via the equilibrium with NO and O_2 , then the loss of NO_2 can be used to calculate the concentration of O_2 in the reactor. The concentration at varying temperature is shown in figure 5.11.

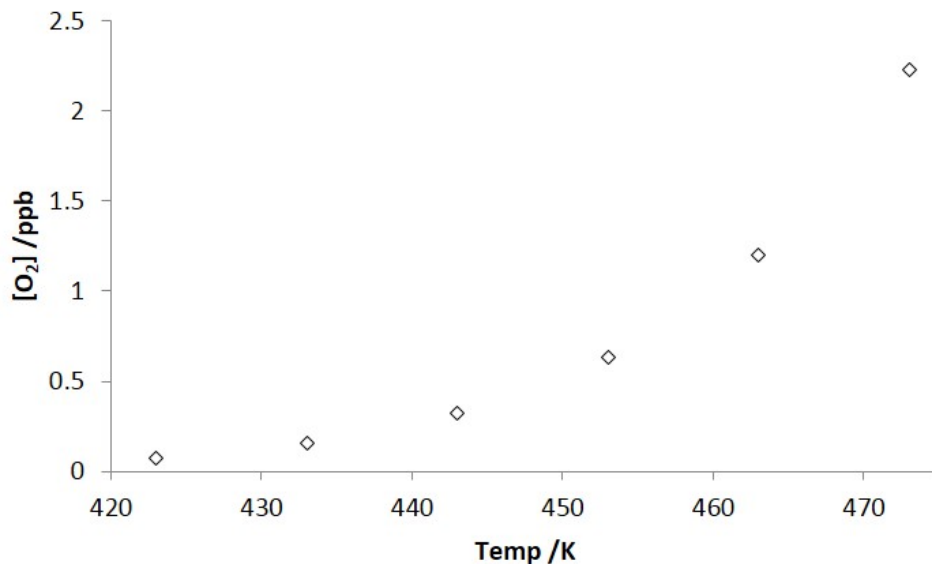


Figure 5.11: The concentration of oxygen formed by the decay of nitrogen dioxide with varying temperature

From figure 5.11 it can be seen that the highest concentration of oxygen reached in these studies at $150 \text{ }^\circ\text{C}$ can be estimated to be $<1 \text{ ppb}$. This concentration is significantly lower than that required to give the level of oxidation seen in the samples,

therefore it is likely that oxidation by oxygen is negligible and NO_2 causes the oxidation. It also suggests that the oxygen levels produced from NO_2 remain low at the higher temperatures that may be seen within an engine.

5.10 Conclusions

Gas phase infra red measurements of the exhaust produced during the nitration of squalane have shown a decrease in the concentration of nitrogen dioxide to approximately 125 ppm or less from a starting concentration of 1000 ppm. This result was expected as nitrogen dioxide was the most likely initiator, although there has been no direct evidence for this previously. The reactivity of NO_2 was only supported by the degradation starting materials or the increased level of nitrogen in the products. Bands are also present due to the formation of CO and CO_2 , for which a mechanism of carbonyl formation and the following decarboxylation is proposed. This is a novel conclusion which has only previously been identified or hypothesised in autooxidation studies in the literature but not with nitration reactions.

The presence of water can also be detected in the gas phase infrared spectra produced during nitrations as well as the cold trap; it is proposed that this is formed during the decay of HONO to form a hydroxyl radical, which is highly reactive toward hydrogen abstraction. This decay gives evidence for why HONO is not identified despite being one of the expected products from initiation stage of the mechanism. The calculations of the decay of the nitrogen dioxide have indicated that the decay to oxygen appears negligible, and oxidation is driven by nitrogen dioxide.

Chapter 6

Nitration and nitrooxidation of methyl linolate

6.1 Introduction

The level of biofuels used in transport fuels is increasing and currently a minimum of five percent is standard in the UK. The amount of biofuel in diesel is currently controlled by EU legislation and the engine manufacturers warranties.⁹⁷ During recent history the price of crude oil has been rising overall and due to reduction in supply as peak oil is passed this is likely to rise higher. Biodiesel is made up of fatty acid methyl esters comprising of mixtures of mono unsaturated compound such as methyl oleate (methyl-octadec-9-enoate), poly unsaturated compounds such as methyl linolate (methyl-9,12-octadecadienoate) and saturated compound such as methyl stearate. The saturated compounds are of low concern with regard to oxidative stability. However the unsaturated compounds are expected to be susceptible toward radical oxidation, due to the weak C-H bond in α the position to the double bond.

Methyl linolate (figure 6.1) is used here as a model compound for poly unsaturated components of the biodiesel, which is the most reactive component due to the extremely weak doubly allylic C-H bond as indicated in figure 6.3.

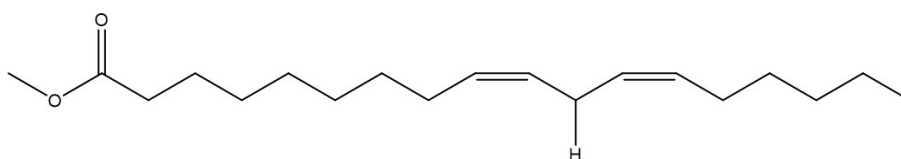


Figure 6.1: The structure of methyl linolate

The squalane model has shown that the previous hypothesis for the products of base oil nitration were not correct and different functional products have been formed. To test whether the hypothesis stands true for biodiesel the major products of the nitration of methyl linolate have been identified using GC x GC MS and found to not contain nitrogen functionality. In order to understand the organic nitrogen containing components the samples have also been analysed using GC x GC-NCD to identify and quantify these products.

6.2 Previous work into the nitration of methyl linolate

Previously the nitration of biodiesel has not been carried out to give an understanding of the products formed. The expected functional groups have been based on the same assumptions as for the for base oil. These studies contain no product identification which

can make it difficult to confirm if their conclusions are correct.

Although there are limited studies into there nitration there in several piece of work studing the oxidation of biodiesel as it is a current area of concern in the automotive industry. Work by Dugmore and Stark contains a study into the autoxidation of methyl linolate and found it to not behave in direct comparison with base oil during oxidation.¹⁰⁹ It was concluded that under certain conditions to behave with antioxidant properties. Although these conclusions may not be true for nitration it gives evidence that it is not enough to assume these two systems will behave in the same way.

6.3 Identification of the major product of nitration of methyl linolate

The methyl linolate was nitrated for one hour at 150 °C as described in chapter 2. The end of reaction sample was then prepared as a mass spec sample for analysis. The mass spec sample of nitrated methyl linolate was separated by GC x GC and analysed by TOF MS using the method given in section 2.8.2 in The two dimensional chromatogram for the analysis of the nitrated methyl linolate is shown in figure 6.2

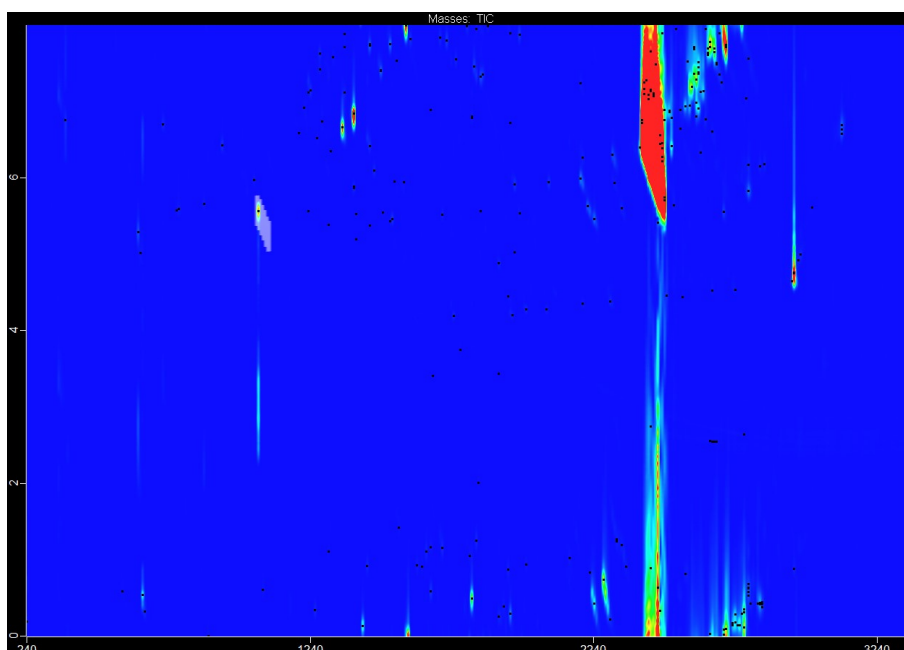


Figure 6.2: GC x GC chromatogram of methyl linolate nitration at 150 °C of the liquid samples at 20 minute intervals

Four products have been identified by GC x GC-TOF MS from the nitration of methyl

linolate. The most reactive site due to the weakest C-H, as indicated in figure 6.1 only occurs once in the methyl linolate and products are likely to result from initiation at this single site. The high level of selectivity may account for the lower number of products formed for methyl linolate when compared to squalane.

The radical formed from hydrogen abstraction in the initiation step of methyl linolate is resonance stabilised. There are two resonance structures which can lead to the observed products by further chain reactions which are discussed along with their identification in the following sections. The resonance structures are more stable than the initial radical due to the double bond shift to form a conjugated structure. The initiation and resonance of methyl linolate is shown in figure 6.3.

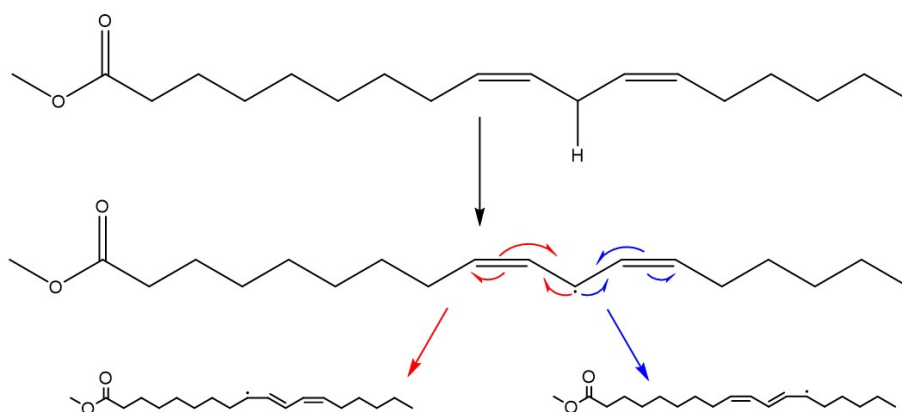


Figure 6.3: Initiation of methyl linolate by hydrogen abstraction and resultant resonance structures

The mass spectra used to identify products and the library spectra are shown in the following sections and the mechanisms for the formation of these products from methyl linolate are shown

6.3.1 Mass spectrum identification of dec-2,4-dien-1-al

The mass spectra for product 1 from methyl linolate is compared to the NIST spectra for dec-2,4-dien-1-al shown in figure 6.4. This is used to identify the product with the key fragmentation alongside a proposed mechanism for the formation from methyl linolate.

The spectra for the product in figure 6.4a shows significant mass fragments at $m/z = 41$ and 81 with a mass ion of $m/z = 152$. This has the same characteristics as the spectra for dec-2,4-dien-1-al shown in figure 6.4b, the identification of these key fragments from the mass spectra can be seen in figure 9.4 in the appendix.

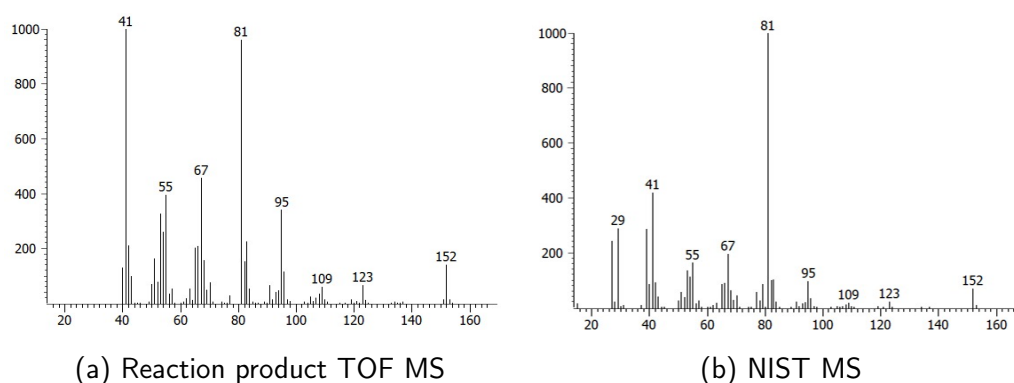


Figure 6.4: Comparison of the mass spectra to identify dec-2,4-dien-1-al

The identification using mass spectra shows the product as dec-2,4-dien-1-al this is a compound which can be formed simply via a radical mechanism from methyl linolate. The mechanism can be initiated via hydrogen abstraction to form the radical (as shown in figure 6.3). In turn this will form a nitrite which can decay to give an oxy radical and in turn the aldehyde product (as shown by the mechanism in shown in figure 6.5). This product is highly stable as a conjugated system is formed between the alkenes and carbonyl.

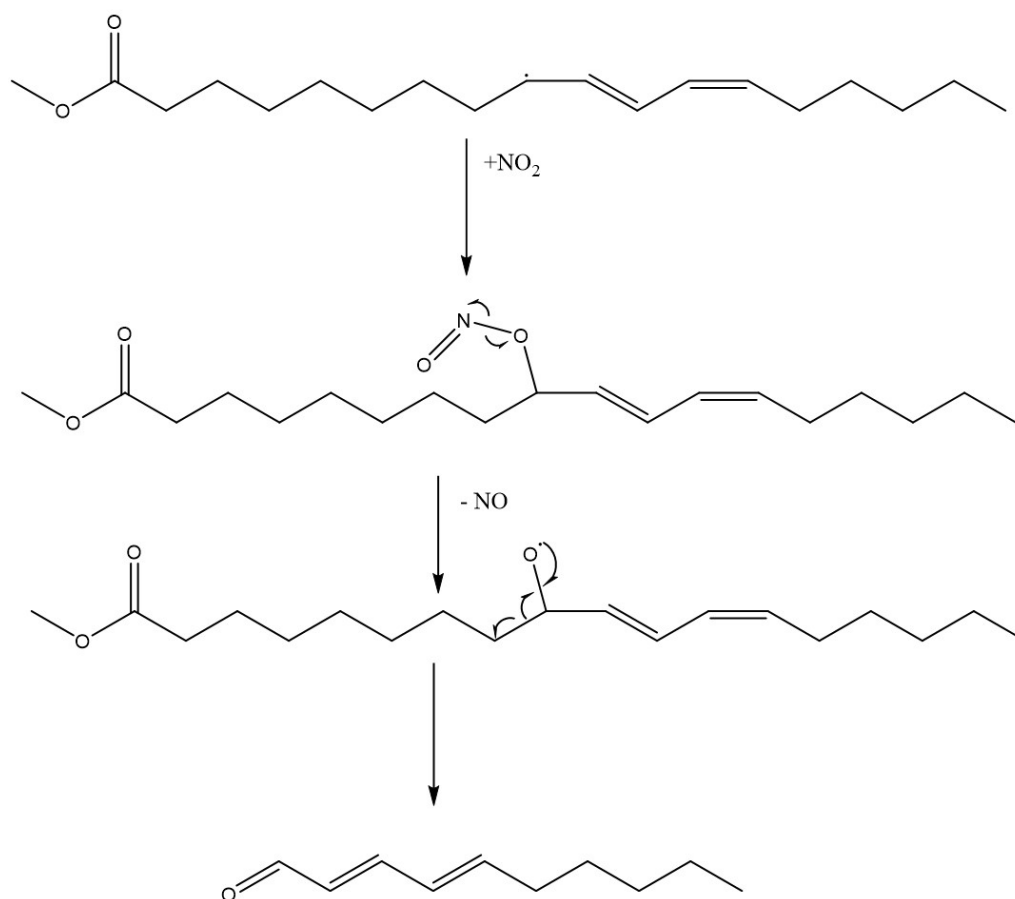


Figure 6.5: Mechanism for the formation of dec-2,4-dien-1-al from methyl linolate during nitration

6.3.2 Mass spectrum identification of the formation of methyl octanoate

The mass spectra for the product and methyl octanoate library, shown in figure 6.6, both show key mass fragments at $m/z = 87$ and 127 with a McLafferty ion for a methyl ester at m/z of 74 . Although the mass ion is not stable enough to be visible, the fragmentation, particularly the McLafferty rearrangement ion and the fragment at $m/z = 127$ give evidence for the overall structure from both sides of the ester where the fragmentation has occurred. The mass ion is also not present in the the library showing it instability during EI fragmentation

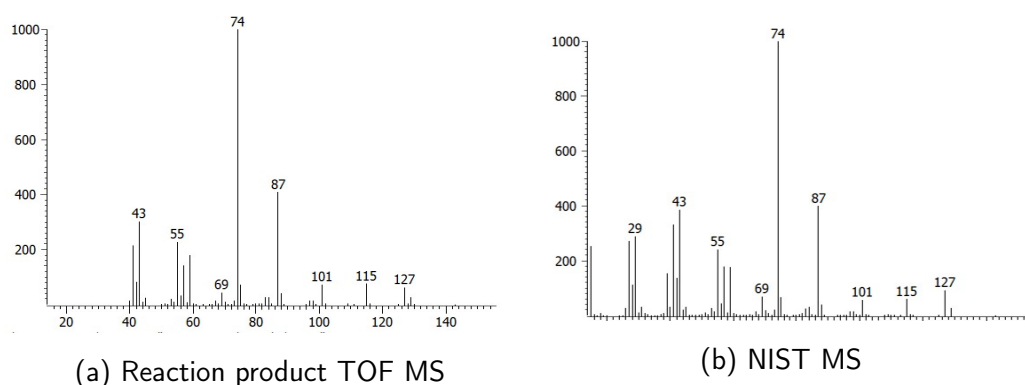


Figure 6.6: Comparison of the mass spectra to identify methyl octanoate

Methyl octanoate can be formed from methyl linolate by hydrogen abstraction for the initiation followed by the fragmentation of the C-C bond, to give the primary radical, which can form the product via hydrogen abstraction as shown in figure 6.7.

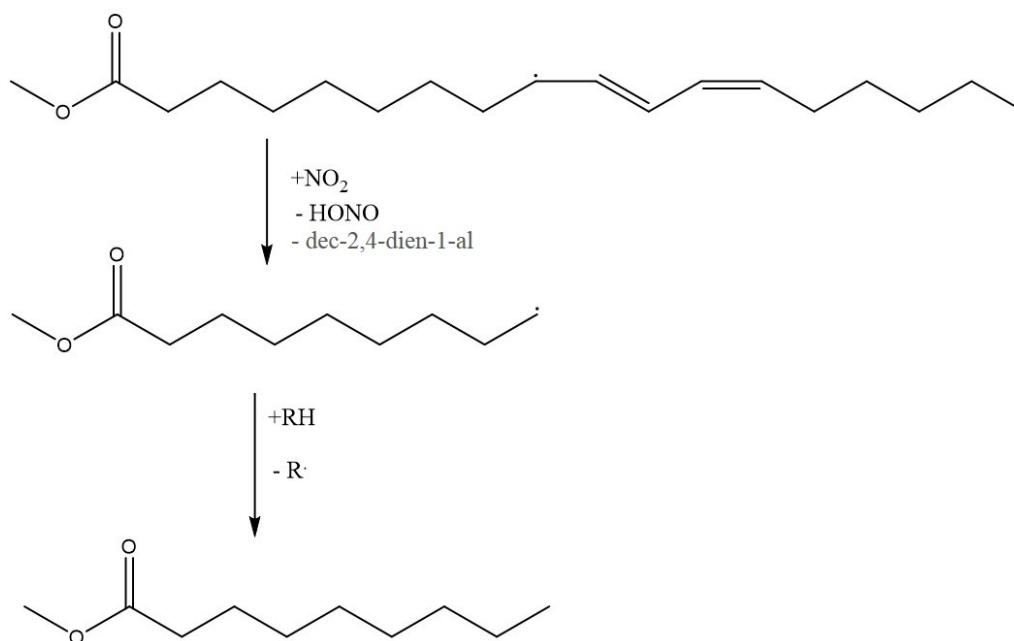


Figure 6.7: Mechanism for the formation of methyl octanoate from methyl linolate during nitration

The mechanism in figure 6.7 relies on the fragmentation of a C-C bond after forming the radical. The second possible pathway for the formation of methyl octanoate is the fragmentation as shown in figure 6.5, where the fragmentation to form dec-2,4-dien-1-al gives a radical which then can be terminated via a hydrogen abstraction (propagation step) to give methyl octanoate. The identification of both halves of the radical fragmentation gives further evidence to validate the identification of these compounds using TOF MS. The

formation of the conjugated ketone will give the enthalpic benefit to be the driving force for the reaction and with the entropic increase due to the increase in species. These free energy benefits will overcome the breaking of a C-C bond and forming of a primary radical which can be less energetically favourable.

6.3.3 Mass spectrum identification of the formation of methyl nonano-1-al

The product mass spectra shown in figure 6.8a is compared to that of methyl octano-1-al shown in figure 6.8b. These have the same feature and key mass fragments which are assigned to show the evidence for the product and the mechanism from methyl linolate to present this as a viable product.

In both spectra the McLafferty rearrangement ion can be seen for the methyl ester with a m/z of 74 with other key mass ions at m/z of 87, 111, 143 and 155. these are all assigned in figure 9.6. The mass at 111 is the corresponding alkene from the formation of the McLafferty ion which has subsequently been charged. The mass ion at 186 is not stable enough to be detectable how the McLafferty ion and the m/z 155 fragment give evidence for the overall molecular size.

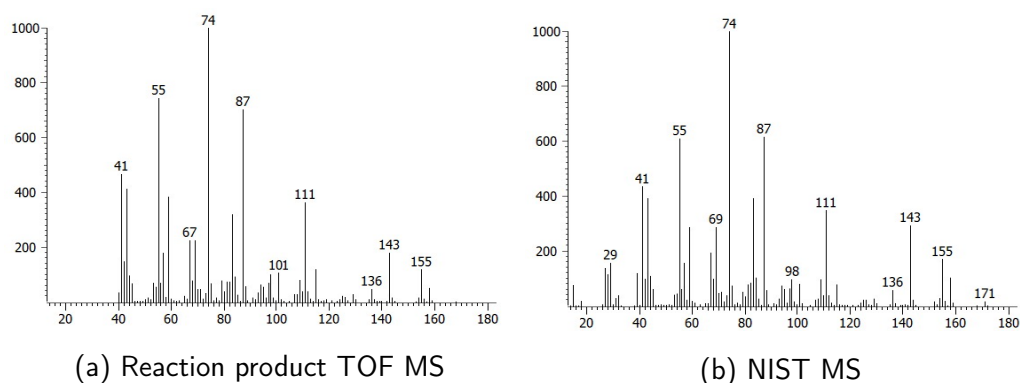


Figure 6.8: Comparison of the mass spectra to identify methyl nonano-1-al

The formation of methyl octano-1-al from methyl linolate can be presented as the initiation via hydrogen abstract, which can undergo addition of nitrogen dioxide to form a nitrite. The nitrite can decay to give an oxy radical which in turn can fragment to give the aldehyde product. The formation of methyl octano-1-al from methyl linolate is shown in figure 6.7.

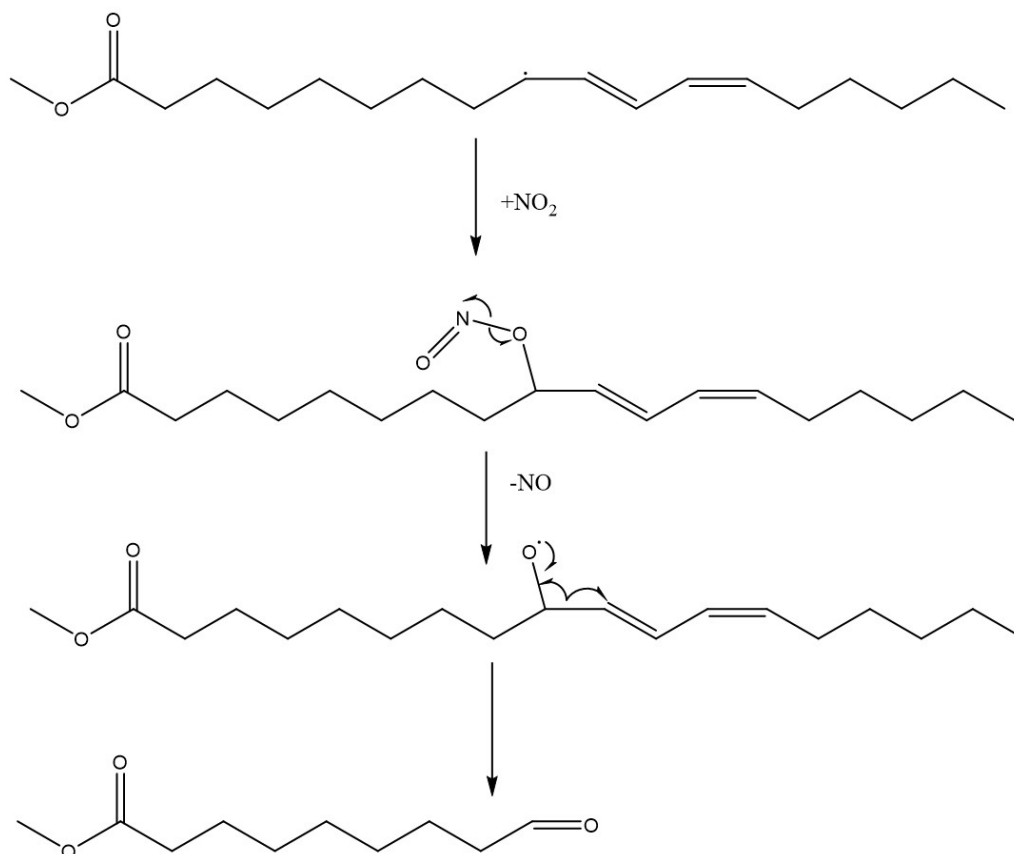


Figure 6.9: Mechanism for the formation of methyl nonano-1-al from methyl linolate during nitration

This proposed mechanism forms a vinyl radical which is energetically unfavourable. Therefore, an alternative mechanism for the formation of this product could be a concerted reaction to form the nitroso compound, shown in fig 6.10. The nitroso compound is highly conjugated, therefore, a driving force for the reaction. However, the nitroso product has not been identified to give further evidence to the mechanism.

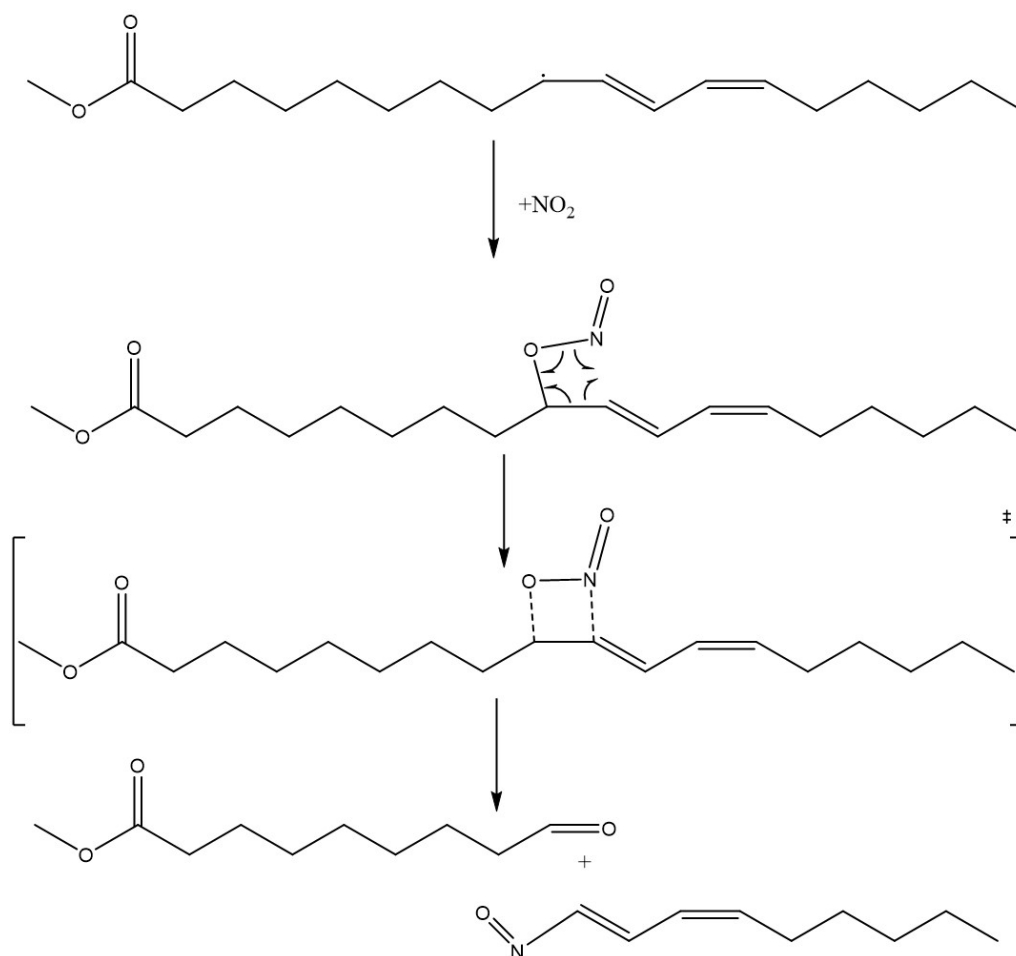


Figure 6.10: Alternative mechanism for the formation of methyl nonano-1-al from methyl linolate during nitration

6.3.4 Mass spectrum identification of the formation of methyl dec-2-eno-1-al

Product four has been identified by comparison of the mass spectra shown in figure 6.11a with that of methyl dec-2-eno-1-al shown in figure 6.11b. Comparisons have been made for the key ion in the fragmentation patterns, the mechanism for the formation of this product from methyl linolate is also made.

In the mass spectra shown in figure 6.11 key fragments at $m/z = 55, 74, 83, 98$ and 138 are also assigned in figure 9.7. The fragmentation pattern matches with that of the known mass spectra methyl dec-2-eno-1-al. The mass ion with an $m/z 198$ is not visible in either the product or the literature spectra. However the overall structure can be determined with the fragmentation of the chain at the ester, with the m/z at 138 due to the conjugated alkene and aldehyde and the methyl ester McLafferty ion (m/z

74).

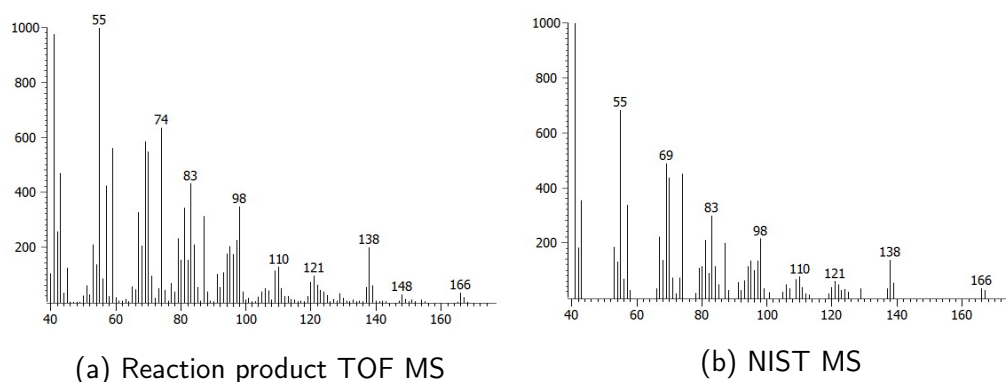


Figure 6.11: Comparison of the mass spectra to identify methyl dec-2-eno-1-al

Methyl-dec-2-eno-1-al could be formed from the addition of nitrogen dioxide to the double bond. The nitro compound can then abstract a hydrogen via a 6 membered ring transition state, to form HONO, shifting the double bond. The radical formed can react with NO_2 to form a nitrite which can decay *via* the CO-NO bond to give a oxy radical, the oxy radical can then form the C=O double bond and fragment the C-C bond to form the aldehyde product observed. The mechanism for the formation of this product is shown in figure 6.12.

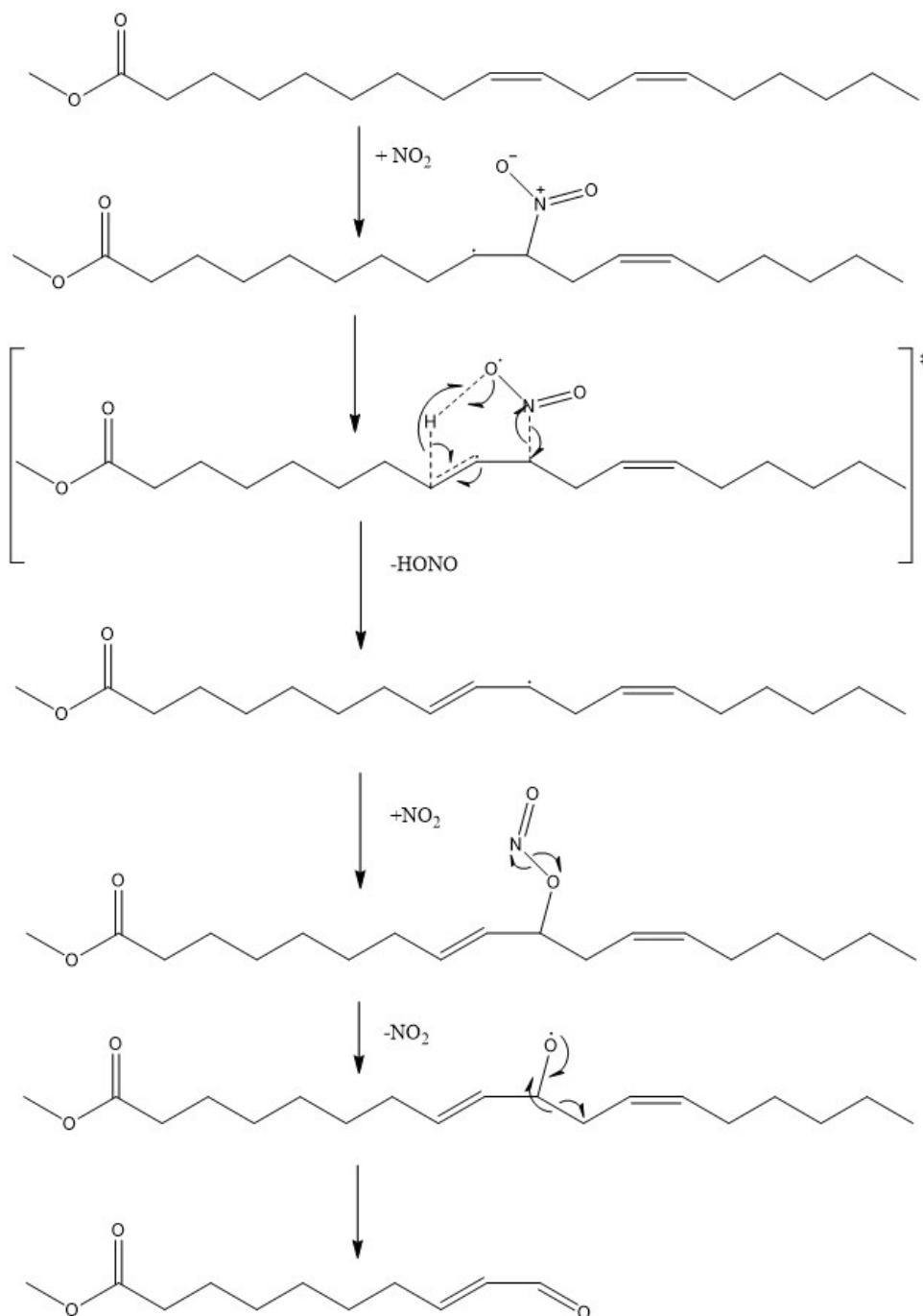


Figure 6.12: Mechanism for the formation of methyl dec-2-eno-1-al from methyl linolate during nitration

6.4 NCD analysis of the nitration and nitrooxidation of methyl linolate

As found with squalane in chapter 3 none of the major products formed contained any nitrogen. Therefore GC x GC-NCD has been applied to analyse for the presence

of organic nitrogen compounds as a product of the reaction between nitrogen dioxide with methyl linolate. This technique is highly sensitive for organic nitrogen containing compounds and will be useful along side the GC x GC-TOFMS analysis to create more complete picture of the degradation products.

The two dimensional chromatogram for the nitration of methyl linolate is shown in figure 6.13. The chromatogram shows over 20 unique responses by the detector giving evidence that a range of organic nitrogen compounds products are formed in the nitration of methyl linolate containing nitrogen.

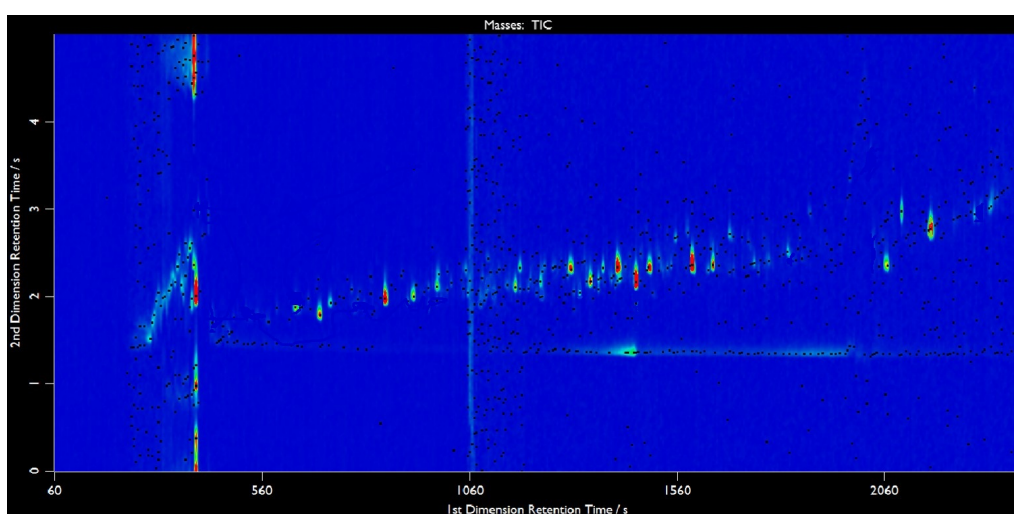


Figure 6.13: GCxGC NCD analysis of methyl linolate nitration at 150 °C for 1 hour

The reaction of methyl linolate under the nitrooxidation conditions has also been analysed using GC x GC-NCD, this is a more realistic system with respect to the reactive gases that will be experienced by the biodiesel in the engine. The analysis will allow understanding if any products are formed as a result of both gases being present. The NCD chromatogram for the nitro oxidation of methyl linolate is shown in figure 6.14.

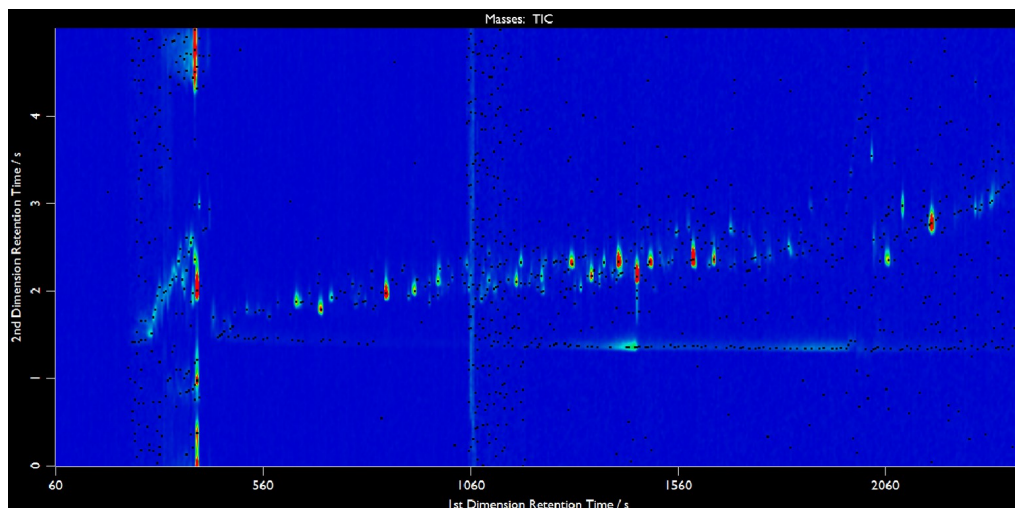


Figure 6.14: GCxGC NCD analysis of methyl linolate nitrooxidation at 150 °C for 1 hour

The NCD chromatogram shown in figure 6.13 can be seen to show responses due to a range of nitro alkanes, based on comparisons with the standard samples run previously which gave the trend in the secondary retention time of approximately 2.1 seconds. The previously identified linear relationship between molecular size and the primary retention time can be used to estimate these product size.

The region at around 400 seconds has a selection of peaks which can be compared to the standard run for the nitromethane analysis, given in section 4.10. These show the same characteristic peaks presenting evidence that nitromethane is formed as product of nitrogen dioxide and methyl linolate in these reaction conditions.

The NCD results shown in figure 6.14 show the same key features as the nitration shown in figure 6.13. Chromatogram features allow identification of nitromethane. The range of nitrogen containing alkane are similar with no new secondary retention times due different functional groups. Two new nitroalkanes are detected in the nitrooxidation with primary retention times of 980 sec and 1230 sec, discussions will be made as to whether the products are only formed in nitrooxidation or the enhanced concentration due to oxygen initiation make these products reach a concentration at which they become detectable.

6.5 Identification of the nitro alkane products of nitration of methyl linolate

The standards of nitroalkanes earlier synthesised to test for the linear relationship between nitro alkane carbon chain length and the primary retention time can be used for to determine the chain length of the products discussed in this chapter. The nitroalkane standards showed a retention time of approximately 2.1 seconds for this GC x GC method. Five products with secondary retention times times at 2.1 seconds have been identified in the nitro oxidation with three of the peaks present in the nitration samples.

Based on the secondary retention time in the GCxGC NCD, five nitroalkanes have been identified from the reaction between methyl linolate and nitrogen dioxide. The retention times and the corresponding estimated carbon chain lengths for the nitroalkanes are summarised in table 6.1.

Table 6.1: Calculated carbon numbers from the primary retention times of products from the nitration nitrooxidation of methyl linolate at 150 °C for 1 hour

Primary retention time	Secondary retention time	Estimated carbon number
1460	2.135	11
1350	2.14	10
1230	2.12	9
1170	2.1	8
980	2.11	6

In order to check the nitroalkanes identified as products of methyl linolate nitration and nitrooxidation the mechanism of formation for the products from methyl linolate has been determined. Four of the products are proposed to form *via* a simple hydrogen abstraction mechanism. The radical carbon chain has then fragmented to give a primary radical stabilised by resonance with the alkene which then has undergone nitrogen dioxide addition *via* the nitrogen to form the identified nitroalkane.

The product with the retention time of 1460 seconds and a estimated chain length of eleven carbons appears to be different mechanism. Firstly the initiation hydrogen abstraction and resonance of the alkene with the double bond is the same initiation process of for the other products identified. The next stage is the addition nitrogen dioxide to the radical to form a secondary radical of methyl linolate. The addition

product has a second reactive hydrogen due to the conjugation to the diene, result in an abstraction of the second hydrogen, followed by the fragmentation of the carbon chain to give the identified product. The structure of the products and the mechanism for their formation from methyl linolate is shown in figure 6.15.

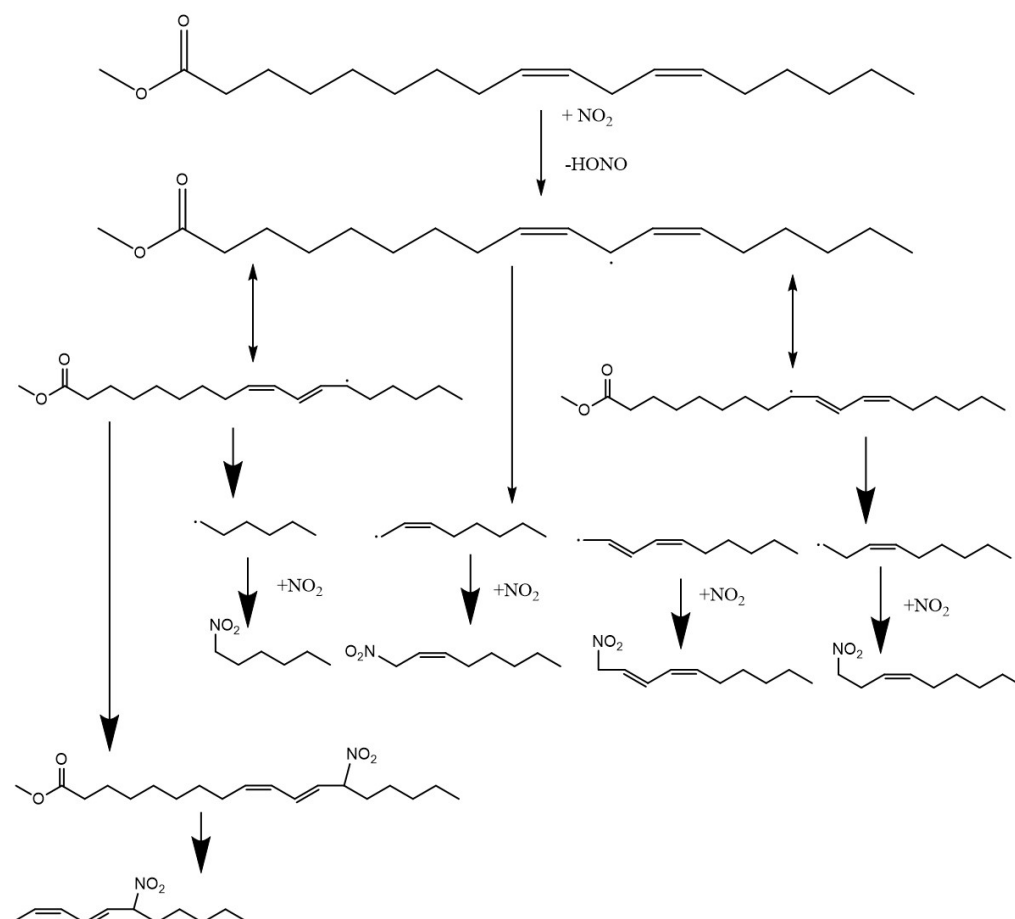


Figure 6.15: Mechanism for the formation of the the nitro alkanes from methyl linolate nitration and nitrooxidation

Using the calibration for the equimolar response factor for organic nitrogen in the NCD detector, the concentration of the nitroalkanes can be calculated. The formation of products formed in the nitration can be compared with that in nitrooxidation. The quantification of these product based on the nitrogen response is shown in figure 6.16.

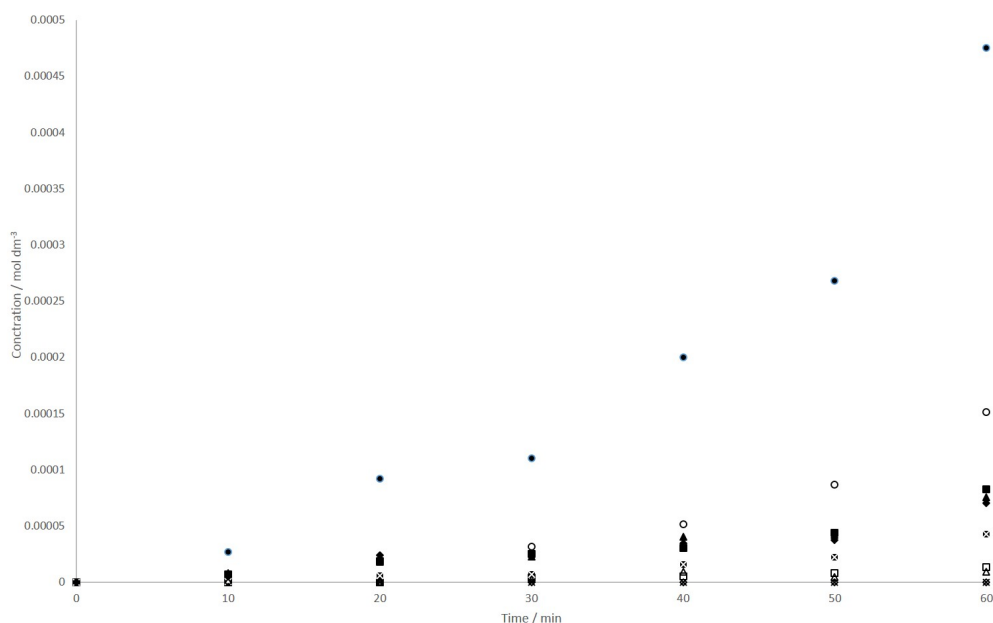


Figure 6.16: The concentration of nitroalkanes identified from the nitration (hollow) and nitrooxidation (solid) of methyl linolate

The steady growth over time is seen with the 6-nitro-undec-2,4-diene (circle) which is formed produced in the highest concentration. The difference between the nitration and the nitrooxidation can be seen as the nitrooxidation gives a higher concentration of all of the products. The two products only identified during the nitro oxidation, 1-nitro hexane (star) and 1-nitro non-2-ene (diamond) are the lowest concentration of the nitroalkanes identified. This evidence suggest that these are not unique products to the nitrooxidation but do not form fast enough to be seen using GC x GC-NCD and sample preparation used in after the nitration reactions as carried out in this work.

6.6 Stability of the identified nitroalkanes

In order to asses the stability of the identified nitrogen containing products the reactive gases were replaced with a nitrogen only flow creating an inert atmosphere, with all other reaction conditions remaining the same for an hour at the end of the reaction. A sample was taken after the hour and analysed by GC x GC-NCD. The concentrations of the nitroalkanes through the reaction and after the hour have been compared. If the products formed are stable the concentration of these products should be approximately the same after 60 min and 120 min. The plot showing the calculated concentrations is shown in figure 6.17.

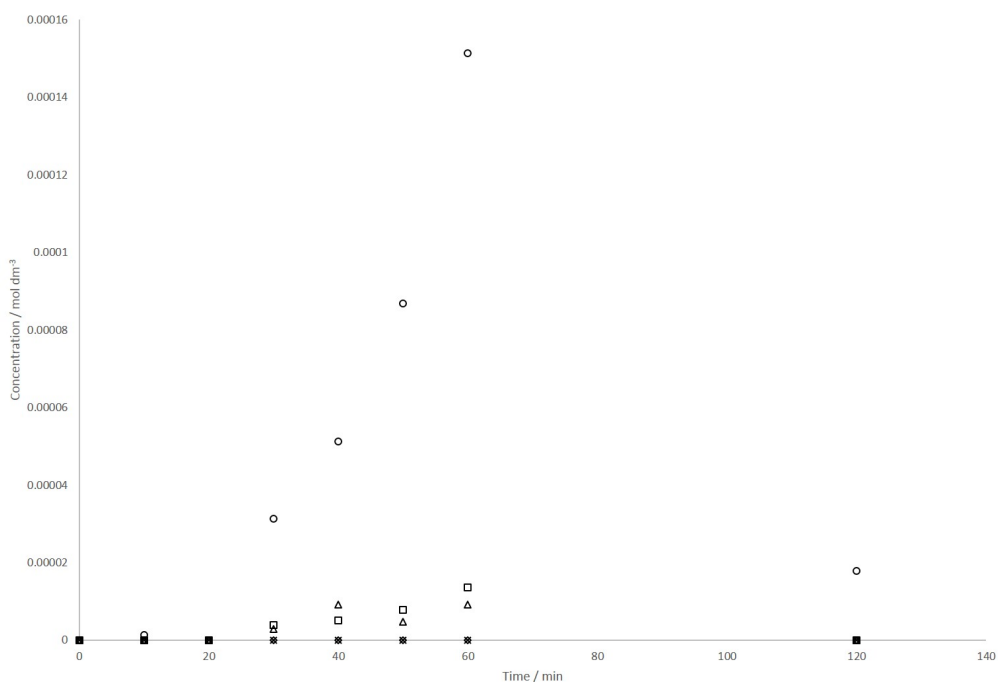


Figure 6.17: The concentration of nitroalkane products identified from the nitration of methyl linolate at 150 °C after heating under nitrogen for 1 hour

The three identified products from the nitration of methyl linolate show a significant decrease in concentration with 1-nitro-dec-2,4-diene and 1-nitro-oct-2-ene (square and triangle respective) fully decaying away from the end of the reaction mixture. 6-nitro-undec-2,4-diene (circle) has the highest initial concentration and after an hour has decayed to approximately 12% of the maximum concentration at the end of the nitration conditions.

The decay can explain why two nitroalkanes are only identified in the nitrooxidation reaction, 1-nitrohexane and 1-nitro-non-2-ene. These products have the lowest concentration in the nitration oxidation where all of the nitroalkene products are seen to form at faster rates due to the higher concentration of reactive gases. If the rate of the formation is slower than the rate of decay then a measurable concentration of the products will not build up in the sample.

6.7 Quantification and stability of other nitrogen containing products

Other nitrogen containing compounds can be identified with a secondary retention time at 2.3 seconds, which is typically due to the products being more polar. These products with a secondary retention time have not been matched with any standards for known compounds containing nitrogen, the most likely functionality is nitrate esters or nitro products from fragmentation including the ester portion. Although the compounds are unknown, the equimolar response of the NCD, can allow the amount of nitrogen incorporated into them to be quantified. The rate of formation of these species during nitration (figure 6.18) and nitrooxidation (figure 6.19) are shown below.

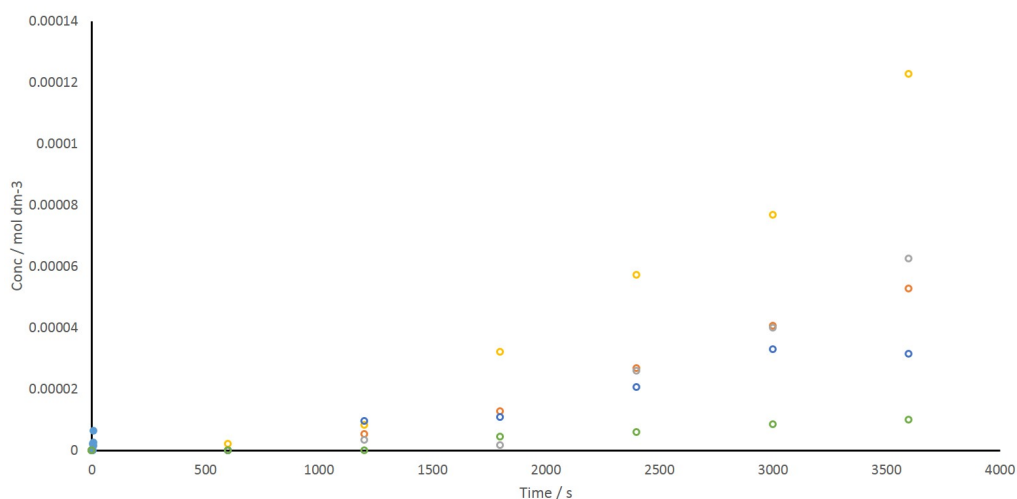


Figure 6.18: Quantification of other nitrogen containing species by NCD from the nitration of methyl linolate for 1 hour at 150 °C, each data set is a unique product identified in the NCD

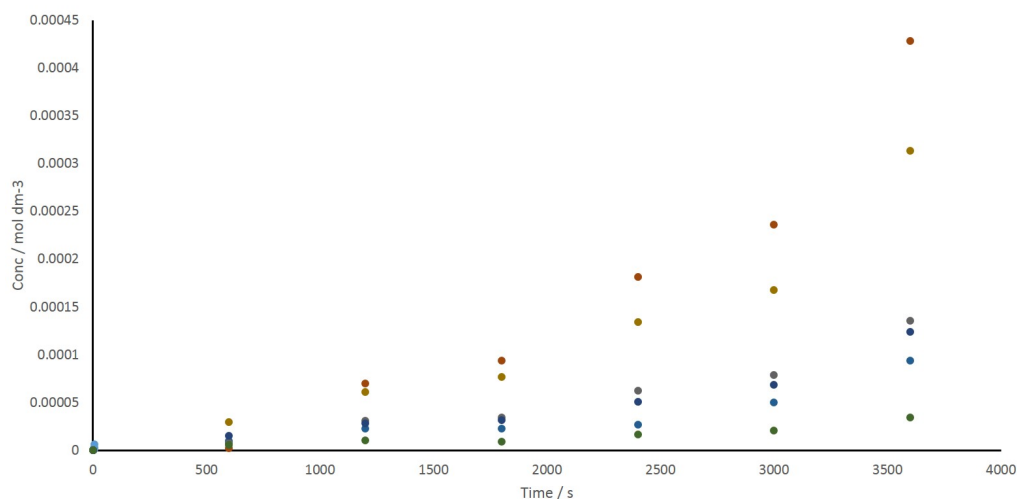


Figure 6.19: Quantification of other nitrogen containing species by NCD from the nitrooxidation of methyl linolate for 1 hour at 150 °C, each data set is a unique product identified in the NCD

The concentration of these products with time show a steady increase. The rate of formation of the product is slightly higher for the nitrooxidation than the nitration. The concentration of all products have similar concentrations, (less than 1.5×10^{-4} mol dm⁻³ for nitration reaction) to the identified nitro alkanes quantified in section 6.5. The difference between the nitration and the nitrooxidation is less significant for these products compared to the identified nitroalkene. This difference suggest the rate of formation is less dependant on the initiation than the nitration formation.

The increase in the secondary retention time with a polar secondary column in the GC x GC analysis usually due to an increase in unsaturation or a more polar functional group. The unsaturation option is less likely in this system. The functional groups which are most likely to be attributable to these peaks either nitroso or nitrate esters.

The stability of these products can be analysed in the same way for the nitroalkenes, maintaining the end of reaction sample at temperature and under a flow of the inert gas whilst monitoring the concentrations by NCD.

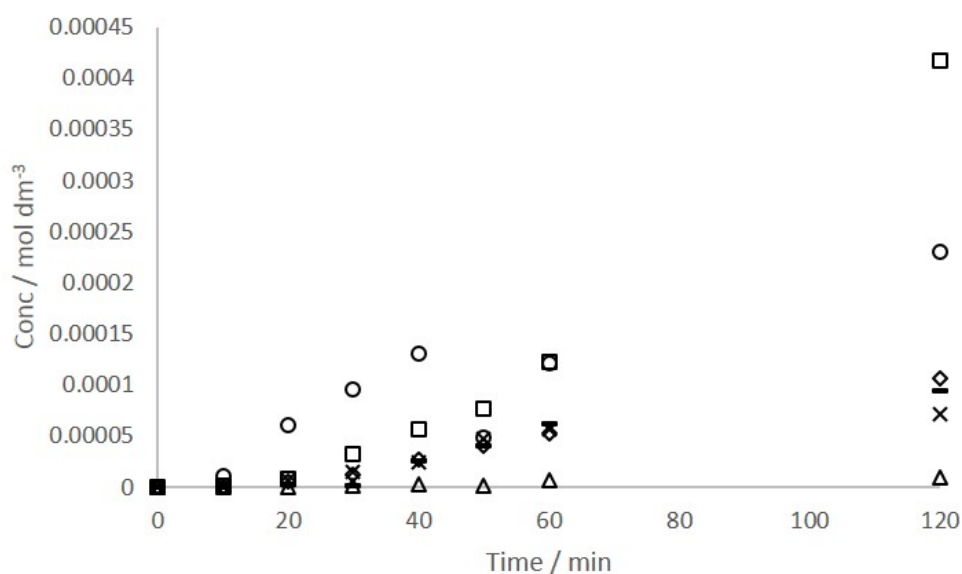


Figure 6.20: Quantification of other nitrogen containing species by NCD from the nitration of methyl linolate for 1 hour at 150 °C with heating under nitrogen for 1 hour

Figure 6.20 show the calculated concentration for the products with a secondary retention times of 2.3 seconds in the nitration reactions extended to analyse stability. These concentrations are shown to increase with time during the nitration, continuing to increase when reactive atmosphere of the nitrogen dioxide is replaced with nitrogen dioxide. This indicates that the formation of these compounds is not from nitrogen dioxide directly. The nitrogen dioxide is the only reactive source of nitrogen input into the reactions. Therefore the nitrogen dioxide can be proposed to be converted another reactive species in the reaction mixture. This secondary species is then able to react further to form nitrogen containing species.

6.8 Total amount of nitrogen containing products in nitrogen and nitrogen dioxide

The use of the equimolar response of nitrogen in the NCD detector can be used to quantify the total nitrogen in the sample as well as in the individual species. This process has been carried out to identify the total organic nitrogen in the degradation of squalane and the same method is applied to methyl linolate

The total area of nitrogen containing alkanes, has been summed using the analysis

software GC image Version 2.1.

The samples used for analysed on the GC x GC-NCD have a nominal dilution factor of 10% in ethyl acetate, however, the accurate mass is recorded used to measure the dilution accurately. In order to take into account the dilutions the calculations have been carried out for all the samples using the method explained in section 4.11.

The quantification of the total nitrogen containing alkanes from the degradation of methyl linolate is shown in figure 6.21. The total concentration of organic nitrogen containing compounds is shown for the nitration and the nitrooxidation reactions.

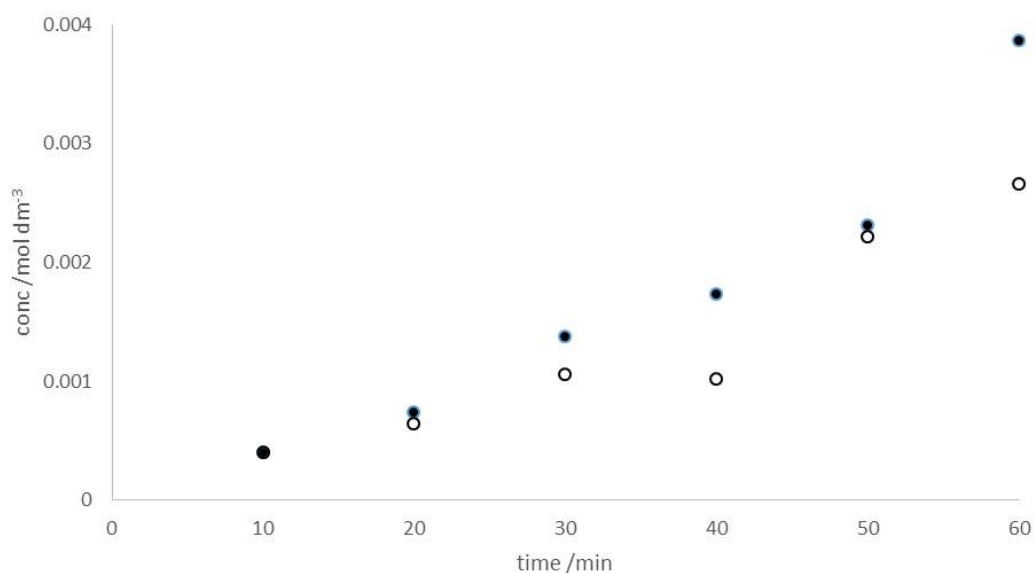


Figure 6.21: Quantification of total nitrogen containing products form nitration - hollow and nitrooxidation - filled, of methyl linolate

Following the trends observed during the squalane analysis the increase in reactive gas which acts as an initiator in the radical reaction can be seen to have an impact on the concentrations. This increase in initiation can be seen in the results as the difference in the between the total nitrogen containing alkanes under the nitration and nitrooxidation conditions. The same trends can also be seen for the individual species the quantified (figure 6.21), where the nitrooxidation shows higher levels of nitrogen at the end of reaction, with a steady increase in nitrogen during the reactions.

Nitromethane is also major part of the chromatogram, consisting of several large tailing peaks in the GCxGC NCD. This can also be quantified using the total peak area,

as carried out to quantify the nitrogen containing alkanes, to allow quantification of the nitromethane. The concentrations of the nitromethane for nitration and nitrooxidation are shown in figure 6.22.

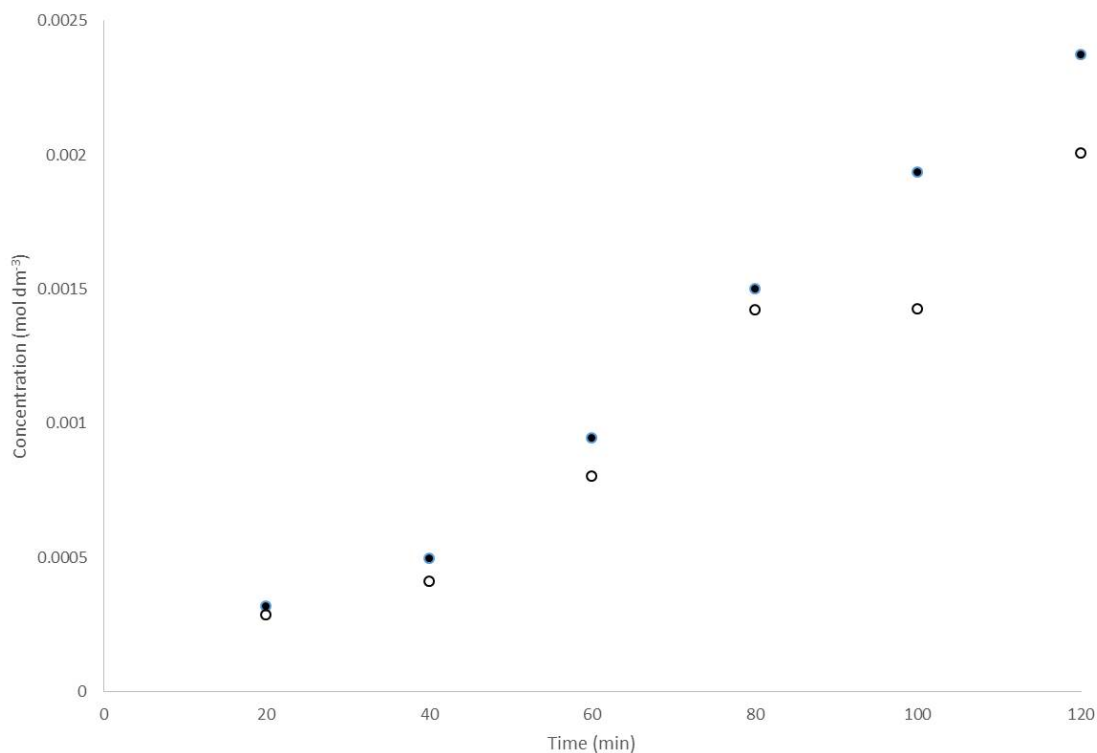


Figure 6.22: Quantification of nitro methane form nitration - Hollow and nitrooxidation - Filled

The nitrooxidation shows a steady increase in nitromethane concentration during the reaction. The concentration of nitromethane is by far the highest product identified containing with a quantification for the nitrooxidation of $0.0024 \text{ mol dm}^{-3}$ compared to a total nitrogen containing alkane concentration of $0.0045 \text{ mol dm}^{-3}$. The concentration of nitromethane is more than half the concentration to the total amounts of other species containing nitrogen combined, for the nitrooxidation and is closer for the nitration. The difference in concentration compared to other species can be visible seen from the GC x GC-NCD chromatograms.

6.8.1 Percentage identified nitrogen

The amount of nitrogen identified for the reactions compared to the input on nitrogen dioxide can be calculated, using the method carried to calculate the and described in section 4.11.1. These calculations are summarised in table 6.2. This gives an addition

of 42% of the nitrogen in the nitrooxidation and 29% for nitration of methyl linolate over one hour at 150 °C. The input of nitrogen dioxide over the reaction is 0.0001 mol with a liquid sample size of 5 ml.

Table 6.2: Total nitrogen quantification and percentage for nitration and nitrooxidation of methyl linolate

	Concentration /mol dm ⁻³ organic nitrogen	mol organic nitrogen	Concentration /mol dm ⁻³ nitromethane	mol nitromethane	Total N mol	Percentage
Nitrooxidation	0.0039	0.0000195	0.0045	0.0000225	0.000042	42
Nitration	0.0027	0.0000135	0.0031	0.0000155	0.000029	29

As with squalane, some of the nitrogen is unaccounted for, for which the losses can be justified as unreacted NO₂, nitrous acid (HONO) formed in the initiation *via* hydrogen abstraction and other nitrogen containing products which are of highly volatile therefore evaporate into the gas phase from the reactor such as NO and small alkanes containing nitrogen. The largest potential nitrogen containing species formed in any addition reactions will not be measurable using this method, as they are unsuitable for analysis by this GC x GC-NCD method.

6.9 Conclusion

The products of the nitration of biodiesel have not been previously identified for the conditions similar to those experienced in the engine sump by the lubricant which becomes diluted with fuel during operation. The study has identified the major product by GC x GC-TOF MS however no nitrogen containing products were identified *via* this technique. Therefore GC x GC-NCD has also been used to separate and identify the products containing organic nitrogen. During both the nitration and the nitrooxidation reactions the most abundant product containing organic nitrogen is nitromethane. Five nitroalkanes have been identified using the retention index as products of the nitration reactions. Products with other nitrogen containing functionality have also been observed and discussed in this study as to the most likely functionality being, nitroso or nitrate ester. All of these products are quantified based on the equimolar response of the NCD in the both nitration and nitrooxidation. The total nitrogen incorporated into the liquid samples for the nitrogen dioxide had also been estimated based on the total response. For the products quantified the stability of the functionality has been analysed and found that the nitro alkanes are not stable as shown a decrease in the concentration after remaining at elevated temperatures in an inert atmosphere.

This work is the first study to identify that the nitrogen containing products are formed. The identification of the products gives evidence allowing the degradation mechanism to be identified. This is the only investigation to use a GC x GC-NCD for this type of analysis. The technique allows a high degree of separation and the detection is highly sensitive toward organic nitrogen containing compounds. Employment of this technique has allowed the more detailed identification compared to previous studies in this field.

Chapter 7

Discussion

7.1 Introduction

This chapter looks to interpret the results and data gained in the previous chapters for the nitration and nitrooxidation of branched alkanes and methyl linolate as model compound for the base oil and biodiesel respectively. The chemical changes observed are used to explain the radical mechanisms which result in formation of the observed products. The complete mechanism for interaction of NO_2 with alkanes is given as an autonitration cycle. The effect of nitration in each stage of the reaction is discussed to give the behaviour of nitrogen dioxide in each stage. The conclusions made in this investigation make a significant link from the chemical structures identified to understand the complete degradation pathway which result in the negative impact on the performance of the lubricant in the engine as discussed in section 1.4

7.2 Initiation

The first stage of any radical reaction is the initiation. The initiation for the nitration reaction is the abstraction of hydrogen by the nitrogen dioxide to form HONO nitrous acid. The loss of nitrogen dioxide is shown in section 5.4 via gas phase infra red on the reaction gases

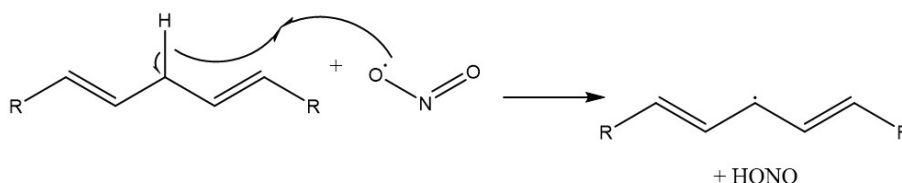


Figure 7.1: Initiation of alkanes by NO_2

The initiation is often considered the rate determining step for the overall reaction for oxidation, and the same for is true for nitration.¹⁰ The initiation is the rate determining step for the nitration, due to the associated activation energy from the required the breaking of a the C-H bond. The activation energy for the reaction is controlled by the C-H bond strength. The remainder of the reaction mechanisms are based around radical-radical additions which are barrierless. Therefore an increase in NO_x concentration in the engine environment is likely to cause an increase in nitration. The increase in initiation is due to within a fixed maxwell-boltmans distribution (fixed temperature), the same fraction molecules will have the required energy to react, resulting in an increase in the total number of NO_2 with the sufficient energy to react. As the NO_2 increase concentration the total number of collisions will increase that result is

successful initiation will increase.

The selectivity for the reaction is due to the weakest C-H bonds, as found in the branched alkanes at the tertiary centres and the allylic CH bonds in the fatty acids. The weaker the C-H bond the faster the initiation due to the lower activation energy.

7.3 Propagation

Once the radicals have been formed in the initiation stage several propagation reactions can occur until the final stable products are formed and the radicals are terminated from the reaction.

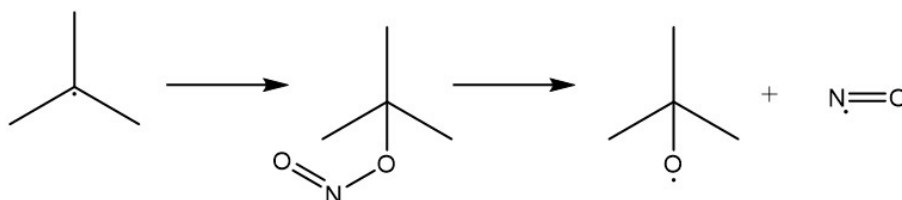


Figure 7.2: Proposed propagation steps for the nitration of branched alkanes

The propagation of the radical chain reaction occurs by the addition of the nitrogen dioxide to the carbon-centred radical via the oxygen to form alkyl nitrites.

As nitrogen dioxide is a radical in its ground state, the addition to the carbon centred radical is a barrierless addition as with all radical-radical additions. Therefore the addition will happen irreversibly on the collision of the two radicals.

Rate of the reaction is proportional to the rate of diffusion through of the gas through the liquid sample to result in a collision with the radical species. The solubility of the nitrogen dioxide in the liquid media will have a large impact on the rate as well as the concentration and pressure of the gas in the system.

The solubility of the gas in a liquid varies depend on the partial pressure as defined by Henry's law, which states that the concentration of a gas (a) in the liquid phase (C_a) is proportional to the partial pressure in the gas phase (P_a), related by Henry's constant (K_H) as given in equation 7.1.

$$K_H = \frac{[C_a]}{[P_a]} \quad (7.1)$$

This equation can also be modified to account for the difference in temperature by including Henry's constant at standard conditions and the enthalpy of solution ($\Delta_{soln}H$) shown in equation 7.2

$$K_H = K_H^\ominus \times e^{\frac{\Delta_{soln}H}{R}(\frac{1}{T} - \frac{1}{T^\ominus})} \quad (7.2)$$

The vapour pressure of the liquid sample will have an impact of any gas phase reaction. For squalane and methyl linolate the vapour pressures are too low for this to be a viable factor, however this may be more significant for the smaller alkyl radicals formed. With the small molecules formed, the addition of nitrogen dioxide may have significant impact on the vapour pressure. The increase in vapour pressure can cause products formed in the gas phase to condense into the liquid phase.

Nitrogen dioxide can add to the carbon-centred radicals *via* the nitrogen or the oxygen due to the resonance of the radical structure as shown in figure 7.3. The selectivity between the two reactive states has been discussed in both experimental and computation work. Overall, the nitrogen-centred radical is found to be the thermodynamically favourable radical and therefore the favoured product, in similar molecules. The energy difference varies depending upon the technique, however it is found to be in the order of 10 kJ mol^{-1} , when comparing product energy of nitro^tbutane with ^tbutyl nitrite.¹¹⁰ Other work also discussed the kinetic selectivity due to the 2:1 oxygen to nitrogen ratio, with the random collision between these two radicals resulting in an addition is more likely to result in the addition via the oxygen to form the alkyl nitrite. Overall, the selectivity between the addition to form the alkyl nitrite or the nitroalkane has been found to be negligible with both products observed in these studies.

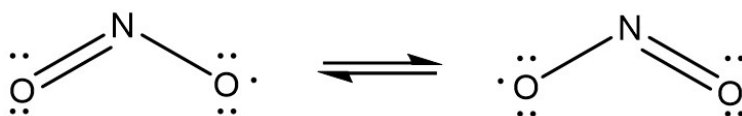


Figure 7.3: Nitrogen dioxide resonances

The alkyl nitrite is likely to be an unstable product under the conditions examined due to the CO-NO bond strength which has been shown in the available literature data to be of comparable strength, or weaker than the CO-OH bond in a peroxide. This weak bond allows the decay of the alkyl nitrite to form the alkoxy radical and nitric oxide as shown in figure 7.4 In autooxidation the formation of the alkyl peroxides is known to occur in the mechanism and then decay rapidly. The peroxides are often not observed products in the studies of autooxidation as is in the autoxidation of squalane by Stark

*et. al.*³ due to the rapid decay. As peroxides decay too rapidly to be observed this can also explain why no alkyl nitrites are observed in this study, however the stable products which can be attributed to the decay forming the alkoxy radical which can react further to generate the identified species.

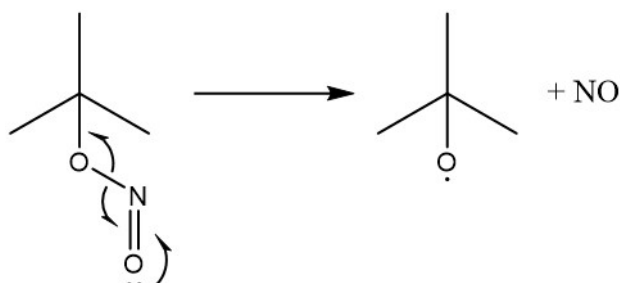


Figure 7.4: Mechanism for tertiary nitrite decay

7.4 Chain branching

The radical chain also contains many options for chain branching to continue the chain reaction in another alkyl species. The first of these is the decay of nitrous acid formed in the initiation, as well as the radicals formed in the propagation stage.

The product of the initiation stage is nitrous acid (HONO), which is only stable at low concentrations in cold temperatures, otherwise it decays rapidly as shown in figure 7.5. The decay products are NO and a hydroxyl radical. The nitric oxide (NO) is very unreactive towards hydrocarbons at the temperature studied and therefore the engine conditions and can be considered inert. The hydroxyl radical (OH) is highly reactive and will cause the initiation of another radical *via* the formation of water by the abstraction of the hydrogen from C-H bond. The hydroxyl radical formed by HONO fragmentation is a chain branching reaction resulting in more oxidation or nitration.

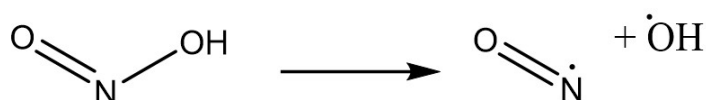


Figure 7.5: HONO fragmentation

The nitric oxide (NO) formed as a product of the decay of the alkyl nitrite and the nitrous acid can itself be considered to be inert toward the alkyl species in this system. However, at elevated concentrations it may occur that some of the nitric oxide is oxidised by oxygen or hydroxyl radicals to nitrogen dioxide *via* the reactions shown in figure 7.6.

This may explain why the level of nitric oxide in the gas phase infrared does not account for all the HONO and nitrite decay.

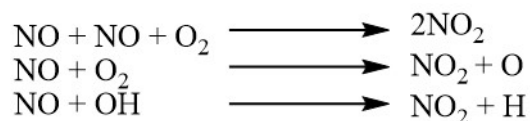


Figure 7.6: Oxidation of NO to NO₂

This regeneration of nitrogen dioxide may cause a cycle of initiation by nitrogen dioxide, shown in figure 7.7. This cycle is likely to be minimal in the system used in this study as low concentration of nitrogen dioxide have be observed in the gas phase infrared of the exhaust gas. However it can have a large impact dependant on the gas system and temperature of the system in a real engine.

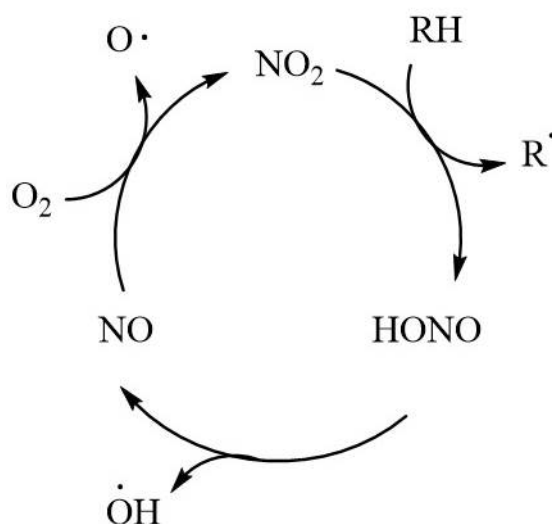


Figure 7.7: NO_x cycle

The alkoxy radical formed in the propagation stage can fragment in to smaller species, often to form a ketone and a alkyl radical as shown in figure 7.8. This fragmentation is driven by the increase in entropy by the increase of species from one to two. The formation of the ketone creates a C=O double bond, this has an enthalpic stabilising effect and driving force for the reaction. The entropy and enthalpy effects overcome the formation of a less stable primary alkyl radical.

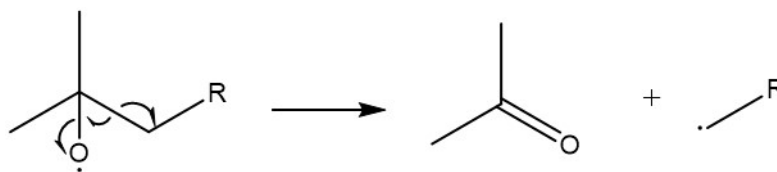


Figure 7.8: Fragmentation of a tertiary alkoxy radical to form a ketone

The formation of several of the products identified, such as the alcohol and alkane fragments, are formed by the same final step. The radical form of the products are formed during the propagation stages. The stable product identified are formed by the abstraction of a hydrogen. The hydrogen abstraction follows the same rules as the initiation with the weakest C-H bond being the one which is broken. The formation of the new hydrocarbon radical continues the chain reaction creating further oxidation products and degradation of the sample.

7.5 Termination

The termination of the radical reaction can occur in two main ways to remove radicals from the reaction and prevent further radical reactions occurring result in more degradation.

Firstly, radical-radical addition can occur to create larger alkyl species. This addition will be barrierless if two radicals collide. This is more likely to occur as the concentration of the radicals in the liquid sample increase. The concentration of radicals will be affected by the concentration of initiator species, time, temperature and the stability of the radicals formed. The addition of radicals has not been observed as products in this study. However, the cause of this is that heavy molecular weight species are not volatile enough to be detected and identified *via* GC x GC MS as the squalane starting material was toward this upper volatility limit.

The second form of termination which is observed in this work is addition of nitrogen dioxide to the alkyl radicals *via* the nitrogen atom to form nitroalkanes. The nitroalkanes are observed to be stable in the conditions of this work. This addition removes the radicals from the reaction preventing further nitration as it has been shown to be irreversible at these temperatures. The nitroalkane products observed are from the fragmentation, giving primary radicals. The addition directly to the tertiary centre does not appear to occur, as demonstrated in the work with pristane, the most likely reason for this is steric hindrance controlling the orientation of the addition of the nitrogen dioxide to favour the nitrite product. This addition of the nitrogen dioxide to the alkyl

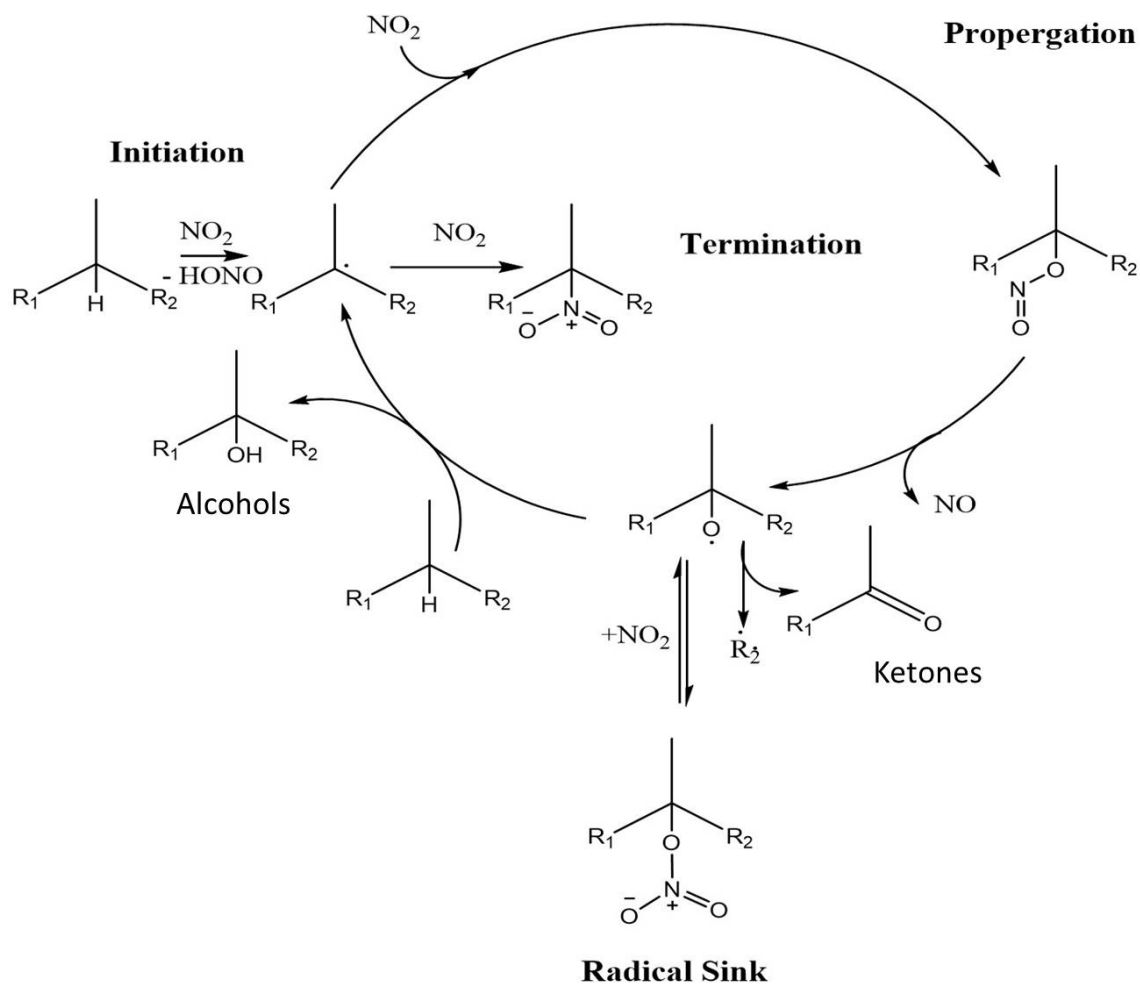
radical is a barrierless addition as a radical-radical reaction. The control of the rate of this termination is the rate of the diffusion of nitrogen dioxide through the liquid sample. Once the radicals collide with the nitrogen dioxide in the correct orientation the termination reaction will occur.

The addition of the nitrogen dioxide to the alkoxy radical to form the nitrate ester can occur and is reported as a termination product in similar work.¹ However, the CO–NO₂ bond is weak, with a bond strength for isoC₃H₇O–NO₂ of 175.7 kJ mol⁻¹. This bond strength is comparable to alkyl peroxide or alkyl nitrite, which are known to be unstable. If any nitrite esters are formed this can be considered to be a radical sink with the products removing radicals from the reaction. The nitrite esters can decay to reform the alkoxy radical and nitrogen dioxide reactant which they originate from.

7.6 Overall mechanism

The mechanisms for initiation, propagation, chain branching and termination discussed in sections 7.2 - 7.5 to give a overall autonitration cycle of alkanes at elevated temperatures which is shown in figure 7.9. This cycle is can be compared with the published and accepted autoxidation cycle with oxygen as the reactive gas.

The autonitration cycle shows all the stages between initiation and termination for the hydrocarbons that are observed as products. Whilst this cycle contains the some of reactions previous published on the nitration reactions this mechanism goes further. The work by Korcek *et. al.*⁶⁴ states the final products as nitro alkanes, alkyl nitrites without evidence. In this study we have identified that these are intermediate rather than the final products. Although the final product identified in this study differ from those proposed by Korcek *et. al.*⁶⁴ they present no product identification, however their proposals are based on the rate data gained. The rate determining step for this reaction scheme is the initiation stage by hydrogen abstraction therefore the rate data gained for the loss of starting alkanes will be similar. Therefore the reactions proposed in figure 7.9 making up the autonitration proposed in will also fit with the rate data gained by Korcek *et. al.*⁶⁴ In conclusion when comparing the two pieces of work the evidence for the final products given in this study give greater evidence for the mechanism which is also supported by korchek *et. al.*⁶⁴ rate data. Further reactions have been included to create the cycle continuing the chain radical reaction.

Figure 7.9: Autonitration cycle of hydrocarbons by NO_2

This mechanism can be compared to the only literature mechanism which has been presented by Coultas at UNITI conference in 2015, shown in figure 7.10.¹ This work is based on the measurement of the nitrate ester in a bench test, for which the method is unknown, complimented by engine tests run different temperature. Again this is based on simple bulk data with out product identification. This work gives further evidence to support the conclusions that nitration can result with stable products traditionally considered to be from oxidation. However, there are issues in the mechanism. There are steps missing between the peroxy radical and the nitrate ester. To correct this it would require the alkoxy radical to be formed before the nitrate ester. This study therefore gives the evidence that nitrate esters are formed as a radical sink in the engine condition.

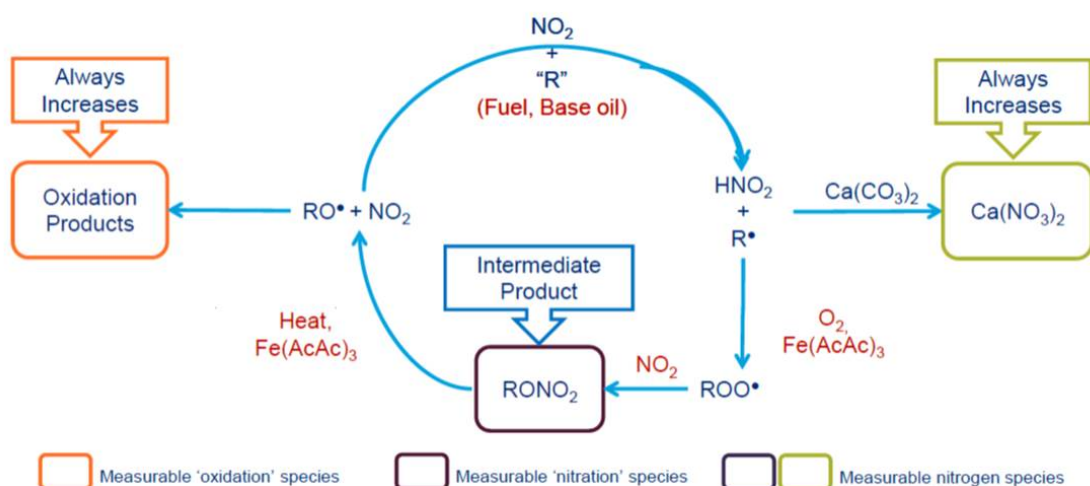


Figure 7.10: Mechanism the nitration of engine oil as proposed by Coultas¹

Despite the flaws in the mechanism both can be used together to support the idea that the mechanism of nitration and oxidation are related and that traditional oxidation products can result from nitration. The key stages and the final stable products are the same. This proves the concept that the mechanism established in this study can be applied to the engine environment.

Other studies in this area treat nitration and oxidation separately therefore the conclusions drawn are different to the mechanism from this work. However some of these studies are still applicable, the study by Korcek *et. al.*⁶⁴ supports the initial stage with the rate determining step being the initiation stage. The kinetic data previously generate is able to be used to support the conclusions made from this study.

7.7 Nitromethane

The highest concentration of nitrogen containing product identified is nitromethane. In terms of its impact on the performance of the oil as it is degraded by nitrogen oxides the presence of nitromethane may have minimal impact. Nitromethane is unlikely to be persistent in the engine oil with a boiling point of 100 °C it can be expected to evaporate from the sump once the engine is at running temperatures. There is a current trend to increase the sump temperature to increase the fuel economy, this could also cause a larger increase in the evaporation of the nitromethane, reducing the concentration in the oil. Nitromethane can also still remain in the oil as it is pumped into the crankcase environment, this would result in the combustion of the nitromethane. Nitromethane has a flash point of 35 °C therefore will undergo combustion easily. In

order to increase the efficiency of the combustion nitromethane is added to the gasoline in high performance engines such as a racing cars. This combustion presents a loss pathway for the nitromethane from the lubricant.

7.8 Comparison with oxidation

As a results of this study a mechanism for the nitration of hydrocarbons has been proposed. This project has also looked into nitrooxidation. When compared to previous studies for the oxidation, the nitration as part of this study, the nitrooxidation shows no unique reactions, only combinations of the reactions previously discussed.

The combination of the two mechanisms will also occur in all systems including bench reactions carried out for this study and in the engine environment. The initiation will be dependant on the temperature and the concentration of the reactive gases in the system. Once the radicals have been formed the addition of the oxygen or nitrogen dioxide is barrierless, therefore will be controlled by the rate of diffusion of the gases throughout the liquid system and the partial pressure of each reactive gas making up the atmosphere. Therefore, it can be justified that oxidation will result in more lubricant degradation than nitration due to the approximate maximum concentration of NO_2 being 0.1% when compared to the oxygen with a concentration of 10% in the blow by gases which is 100 times higher.

The proposed mechanism can be compared the published mechanism for the oxygen showing some over lapping points. The first overlapping point is the initiation step to form the alkyl radical which gives the same product regardless of the initiation method. For the initiation by the nitrogen dioxide the by-product is HONO, which can decay to give nitric oxide which can be considered inert and a hydroxide radical, which is the highly reactive. With the initiation by oxygen the by-product is the hydroperoxyl radical which can cause a second initiation to form hydrogen peroxide. Hydrogen peroxide is unstable and can decay to form two hydroxyl radicals. The hydroxide radical is likely to form water a stable product by a hydrogen abstraction giving another initiation. Therefore, for the comparison of the two mechanism, nitrogen dioxide initiation gives two possible alkyl radicals, however when oxygen is the initiator this can be as high are four possible initiations. The second comparable point is the propagation stage to form alkoxy radical with nitrogen dioxide no reactive by products are formed. With oxygen in the propagation stage, the main the mechanism leads the formation and decay of an alkyl peroxide giving which gives another a total of two further initiations. Therefore, in

total for two molecules of the reactive gas to form the alkoxy radical product from the initiation and propagation there is a total of one further possible initiation with nitrogen dioxide which can be compared to a possible five initiations when carried out by oxygen.

7.9 Effects on lubricant performance the engine

The degradation of the lubricant can cause significant impact on the performance of the lubricant in the engine. Firstly the most simple impact of the degradation is the fragmentation to form smaller more volatile compounds will result in a reduction of oil volume. The reduction of the oil volume can have a negative impact for two reasons. Firstly, the reduction in volumes increase the percentage of the time the lubricant will spend in the piston environment instead of the sump environment in which the temperatures are milder and the physical stress is less. The second impact of the volatile loss of the degraded lubricant is the concentration of additives in the lubricant. High concentrations of the additive can have negative impacts such as increased wear or reduced fuel economy. The increase in concentration of components such the viscosity modifier and dispersant can increase the viscosity, this increase viscosity can result ineffective circulation of the lubricant throughout the engine.

The second impact of the degradation is down to the functionality of the products formed. The major products are the alcohols and ketones which have been shown to undergo addition reactions such as the aldol reactions to form species of higher molecular weight. As discussed in section 7.5, the termination by radical-radical addition can also occur. These species of higher molecular weight can form resulting in a increase in viscosity which will impact the performance as it flows inefficiently around the engine. Under autoxidation the viscosity increase is observed as an exponential after an induction period. Based on the similarity between the published mechanism for autoxidation and the proposed mechanism for nitration in this study it can be expected that the viscosity increase during nitration will also result in an exponential rise.

The products of both the nitration and nitrooxidation contain functional groups in common with oxidation. Oxidation products have been shown to have an impact of the engine. The increase in surface activity due to the polar functionality on the large hydrocarbons and the interaction on the oxygen toward engine metals such iron and copper lead to an increase in corrosion. Used engine oil with a high degree of oxidation have been analysed *via* ICP and found to contain higher concentration of these metal ions. As the functional groups for the nitration and nitrooxidation identified are the same

as oxidation it can be assumed that the nitration and nitrooxidation will also cause an increase corrosion of the metal surfaces in the engine.

7.10 Measurement of the nitrate esters

The lubricant industry is keen to measure the life time of oil and its level of degradation due to oxidation and nitration. The standard way to measure these parameters is using the infra red peak area at 1710 cm^{-1} for oxidation and 1750 cm^{-1} for nitration. The peak at 1750 cm^{-1} corresponds to the nitrate ester and the peak area 1710 cm^{-1} corresponding to the carbonyl $\text{C}=\text{O}$. The significant nitrogen containing products identified in this study are nitroalkanes, in particular nitromethane.

The nitroalkanes will not be measured using this method. Evidence has been shown that alkyl nitrites have been shown to decay to form a ketone . Although the nitrate esters have not been identified as one on the major products in this work it does have the potential as a radical sink, due to the weak CO-NO_2 it likely that the position of equilibrium for the formation of the nitrate esters lies toward the radicals for the conditions of these reactions. Under different conditions found in engine sump, such as if the temperature is lower, the build up of the nitrate ester has the potential to be larger. Once any nitrate esters are heated to higher temperatures these can rapidly decay reacting to form the carbonyl products. As nitration and oxidation happen in parallel and both result in the oxy radicals which can form carbonyl species or form nitrate esters in the radical sinks. Although other products are formed as both of the degradation processes the rate determining step the rate determining step for the reactions is the initiation via hydrogen abstraction. The measurements of degradation using peak area by infrared have a significant variation in the measurements and sources of error, however the consideration of both the nitration and oxidation can give a approximation proportional to the overall degradation.

Chapter 8

Comparison of the model system
with the materials used
commercially

8.1 Introduction

In order to elucidate the pathways between the reactants and products model compounds have been used for the base oil and biodiesel. For the understanding developed from the results of model system to be applicable to the real lubricant evidence needs to be gained that the same observations can be made and learning transferred. Polyalphaolefins (PAO) are a synthetic base oil used in high quality engine oils. PAO has tertiary carbons in a similar ratio to squalane, therefore it is chemically the closest base oil to squalane. PAO can be analysed using gas chromatography therefore it can be directly compared to the work on the model system.

The work previously carried out to understand nitration has neither taken place on model system or complete lubricant oil. No published work has looked to apply any learning from models systems directly from the real system using the same analysis. This chapter will look to make these comparisons to support the conclusions drawn in the model and ensure the real world applicability.

The second part of this comparison will also look to use previously generated engine data to compare to whether it adds further supports the mechanism. These conclusions are reliant on previously generated data, therefore key area of focus will be on infra red measurements of oxidation and nitration The investigation will be looking to support the hypothesis that these mechanisms are reliant on the radical initiation and heavily linked and therefore cannot be considered as separate degradation mechanisms.

8.2 PAO

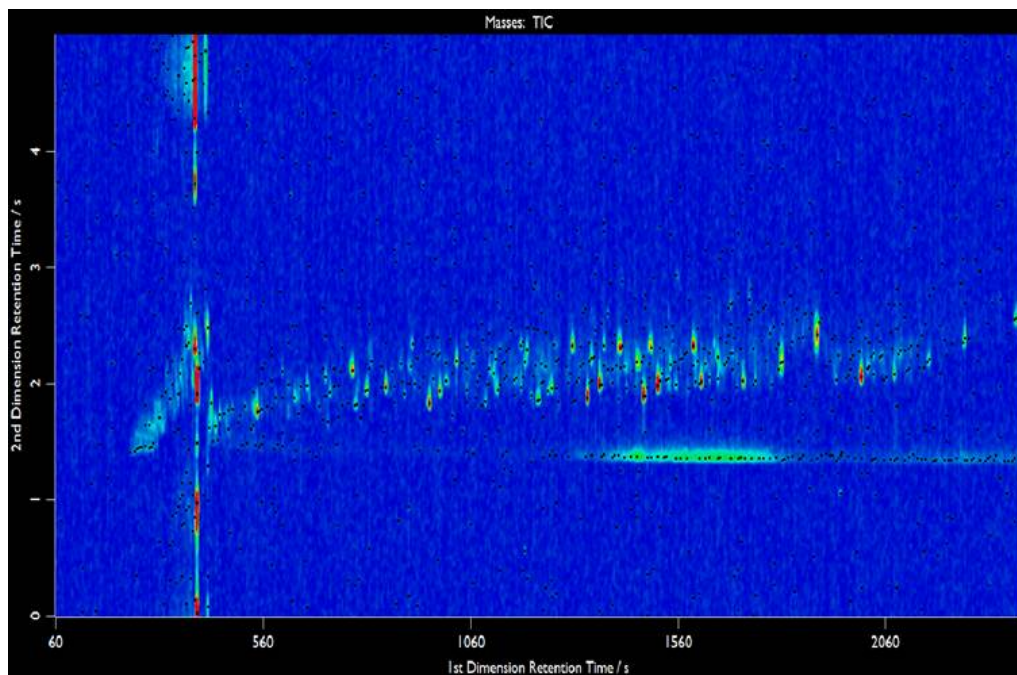
Polyalphaolefins are polymers synthesised *via* addition polymerisation from 1-alkenes. The structure of the finished products depends on the source of the alkene.¹¹¹ For engine oil application the viscosity is on the most important parameters. The viscosity is controlled by the polymerisation chain length with the longer the chain length forming higher viscosities. The viscosity of the polymers at 100 °C is used for the classification of the PAO by suppliers. For this study a 4 cst PAO will be used as this has the lowest molecular weight of those used in engine oils. The use of the lowest molecular weight will ensure that it is the closest volatility to squalane and that the gas chromatography as an analytical techniques employed in this work will be transferred.

8.3 PAO nitration and nitrooxidations by GC x GC NCD

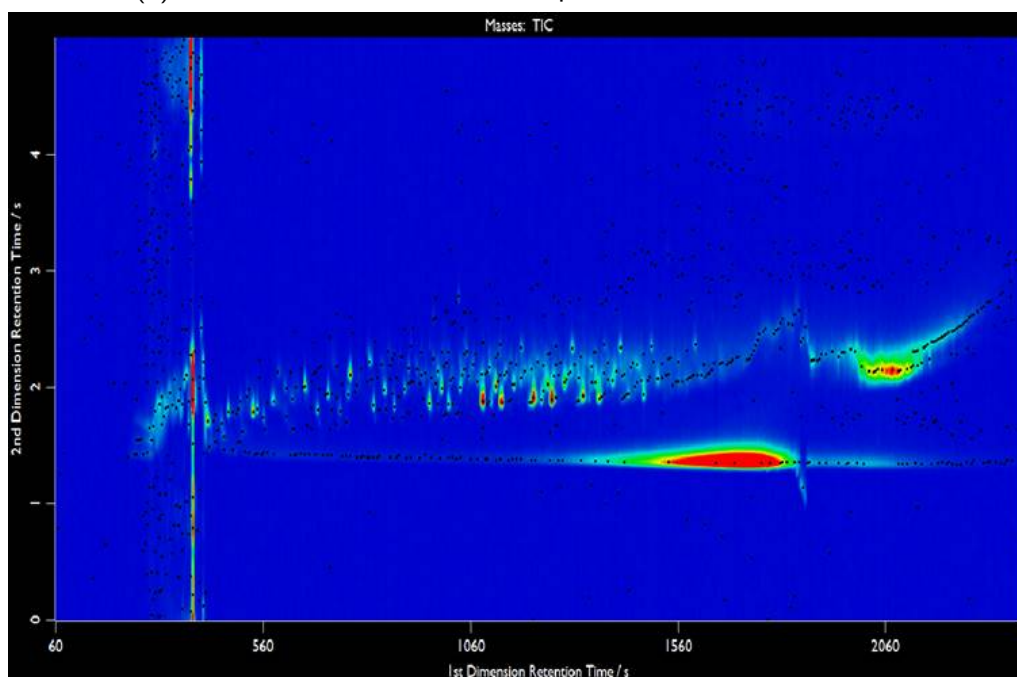
A comparison between the squalane and PAO is shown in figure 8.1 for the nitrooxidation, at 150 °C for two hours, as analysed by GC x GC-NCD. This allows a comparisons of the key features identified in the nitrooxidation of squalane end of reaction sample (figure 8.1a), with the features from the analysis of the end of reaction sample from the nitration of PAO (figure 8.1b). The most degradation has been observed during the nitrooxidation, this is presented in this section as any differences will be more significant and therefore observable. In the engine environment the nitrooxidation conditions are closest to the gas system that the lubricant will experience, therefore it is the system for which the learning of this study are most applicable.

In the nitration and nitrooxidation of squalane the highest concentration of nitrogen containing organic products was identified as nitromethane by comparisons with standards. This feature has primary retention time of approximately 470 secs. The feature can be observed as the highest concentration of organic nitrogen in the nitrooxidation of PAO, proving that PAO also forms nitromethane as a degradation product.

The next set of organic nitrogen containing products identified from the degradation of squalane was the nitroalkanes identified with a secondary degree retention time of approximately 2.1 seconds. The primary retention time for the products of reactions with PAO differ from the model system of squalane. This is due to the differences in the starting material with regard to the overall molecular weight, the degree and position of branching. The position on the branching will impact the molecular weight of the products if fragmentation occurs, the impact of this change will be seen in the primary retention time. The functionality of the products established from the secondary retention time, gives evidence the same mechanism can be applied to PAO system form the model system. The difference in the chromatogram and the number of products can be justified form the variation in the starting material. This difference supports the use of the model system to be appropriate to enable the level of understanding achieved in this project.



(a) NCD of the nitrooxidation of squalane at 150°C for 2 hours



(b) NCD of the nitrooxidation of PAO at 150°C for 2 hours

Figure 8.1: Comparison between squalane and PAO nitrooxidation

8.4 Biodiesel

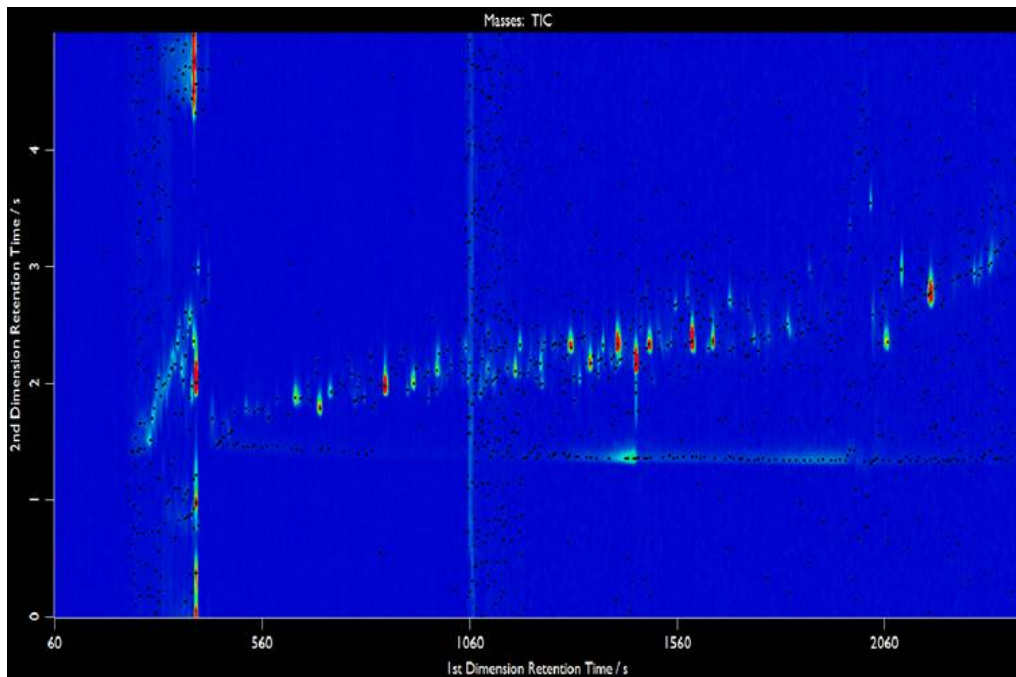
Due to its nature as a plant based material biodiesel varies between batches. One of the largest cause of the variation is from the biodiesel source, two most common of

which are rape seed (RME), soy bean (SME). The biofuel used in this study are 80% SME and 20% RME. In terms of chemistry the variables are in the length of the alkyl chain on the fatty acid methyl ester, with a majority falling between C16 and C20. The differences in alkyl chain chain are not expected to impact the reactivity of the biodiesel with regard to nitration.^{24,112} With regard to reactivity the bigger impact will come from the degree of unsaturation in the fatty acid methyl ester. Saturated linear chains will be expected to be fairly unreactive towards nitration. A majority of the biofuel contains monounsaturated alkyl chains which will increase the reactivity. The main driver for the overall differences reactivity in the concentration of the polyunsaturated components such as methyl linolate as these are highly reactive.

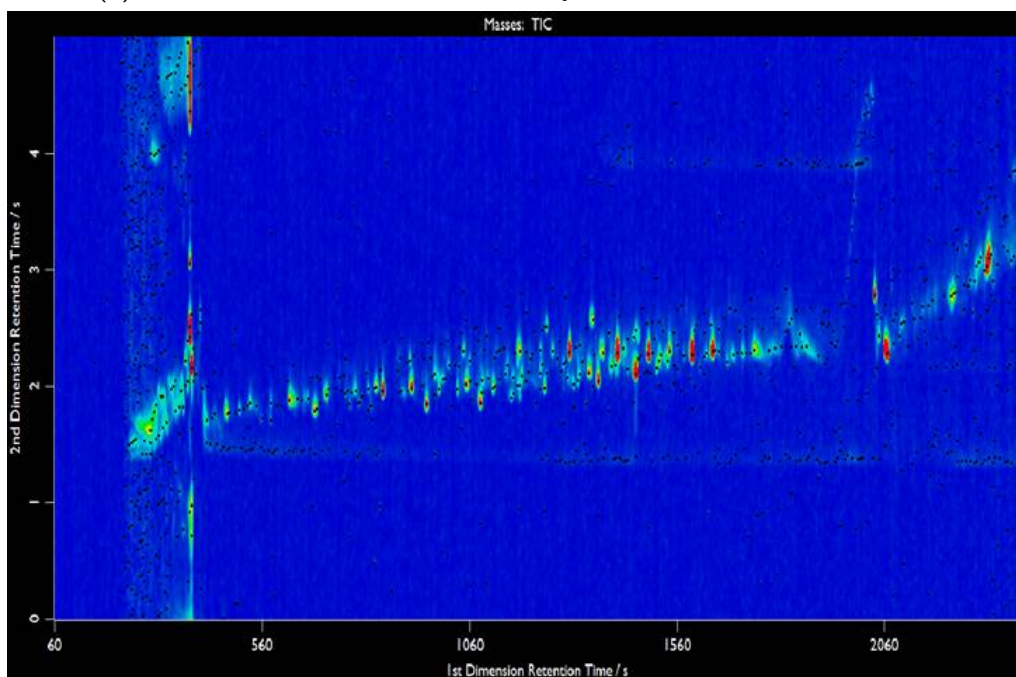
8.5 Biofuel nitration and nitrooxidations by GCxGC NCD

Figure 8.2 shows the comparisons between chromatograms on the GCxGC NCD from the nitrooxidation of the model system methyl linolate in figure 8.2a and the biofuel nitrooxidation in figure 8.2b. As with the base oil system, the highest concentration of organic nitrogen in the degraded samples of biodiesel is the nitromethane. It can be seen with the primary retention time of approximate 470 s.

In terms of the other organic nitrogen based on the secondary retention time, the model system, methyl linolate, shows strong similarity to the biodiesel. The similarity in the chromatograms shows that the same functionality is formed in the degradation reactions with the both the methyl linolate and biodiesel. The similarity is not unexpected due to the closeness of the methyl linolate to all of the constituents of biodiesel. Methyl linolate is also found in biodiesel and as it one of the more reactive constituents. Many of the products both identified and non identified are in both the chromatograms. The products and functionality similarity provide the evidence the mechanism is applicable and the conclusions have not been compromised by running on a model methyl linolate only system.



(a) NCD of the nitrooxidation of methyl linolate at 150°C for 1 hours



(b) NCD of the nitrooxidation of biodiesel at 150°C for 1 hours

Figure 8.2: Comparison between nitrooxidation methyl linolate and biodiesel NCD

8.6 Field trials of lubricants in heavy duty diesel engines

In order to understand how fast the lubricant degrades and if this causes any issues in the engines operation field trials are carried out. These field trial a carried out in commercial vehicles during normal operation. Throughout the field trial the lubricant is sampled and routine lubricant analysis is carried out. The routine analysis focuses on viscometric, metal content and infrared changes. Part of this analysis is the measurement of the oxidation or nitration by the industry standard infrared methods (DIN 51453). Afton Chemical has a library chemical analysis from different field trials. The data collected is of limited use due to the fact that only certain changes in the lubricant are measured. However, this data can be used to study to whether the conclusions made in this study can explain some of the observations made in the field trial.

The field trials consist of three oil fills for each truck with regular sampling. An example for one truck of the changes in the nitration and oxidation are plotted in figure 8.3, against the distant travelled for each oil sample.

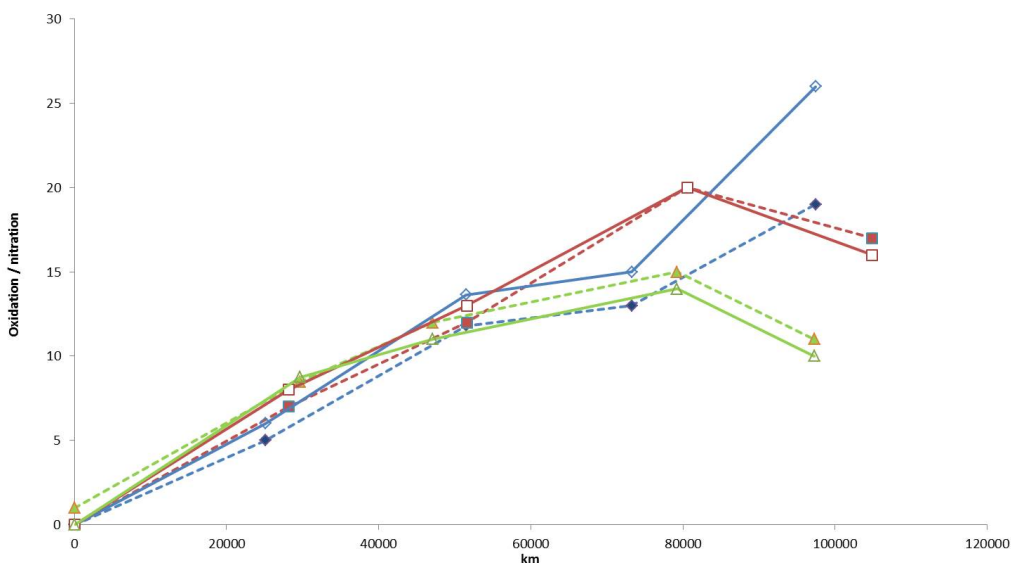


Figure 8.3: Oxidation and nitration value by IR from a field trial of heavy duty trucks, Solid line - Nitration, Dashed line - oxidation

Due to the variation in drive cycle the and conditions experienced by the lubricant the nitration and oxidation varies between the vehicles, oils drains and samples. Due to difference it is important the more than one vehicle and oil drain is studies to ensure any conclusions are valid. Despite these differences the it can be seen that the nitration and oxidation trends closely mirror each. Due to the close relationship between the nitration

and oxidation; it can be proposed that the controlling factor for the mechanisms are common. In both the oxidation mechanism which has been published and the nitration cycle presented at part of this study the rate determining step is the initiation of the radical. The mechanism also contain common points including the alkyl radical, and the alkoxy radical as well as the products. These points give opportunity for interchange between the two mechanism which are normally presented separately. The connection between the mechanism and the rate determining step proves the overall nitration or oxidation is dependant on the initiation whether it is due to the nitrogen dioxide and oxygen.

These conclusions change the way that nitration and oxidation should to be considered. Currently in the automotive industry considers the mechanisms and the measurements individually. However the field trial data used here shows the connection observed in this bench study is applicable in engines. From the mechanistic study nitrite ester are presented as a radical sink, this is supported by the data generated by Coultas.¹ Therefore to correctly quantify the degradation completely by the increase in infrared absorbance due to degradation products of carbonyl and nitrate esters would need to be considered in combination as the are meaningless independently.

8.7 Conclusions

This section has looked to take the conclusions made from the model bench study and confirm they can be applied to real systems. The application of the model compounds has enabled a the level of detail to be obtained, these learnings have been confirmed in using PAO and biofuel. The GC x GC-NCD has been applied to these degraded systems to compare the functionality of the compounds observed. The connection between the nitration and oxidation has been confirmed looking into the available data from field trials carried out by Afton chemical. This uses the oxidation and nitration measurement carried out by infrared in line with the industry standard technique. The connection between both of these degradations mechanisms supports the hypothesis that the rate determining step is the initiation stage of the reaction.

Chapter 9

Conclusions and Future Work

9.1 Conclusions

The increase in concerns around emissions due climate change and air quality is resulting in legislation requiring car manufacturer to have increased fuel economy and a reduction in harmful emissions. These requirements have lead to changes in engine designs. To increase the fuel economy there has been a trend towards smaller engines with optimised designs to meet the same power and performance with hotting running conditions, which can increase the degradation of the lubricant. Previously, minimal literature has been published on the mechanism for the reaction between hydrocarbons in the liquid phase and nitrogen dioxide, although proposals had been made without support by effective product identification.

This study has examined nitration and nitrooxidation in bench tests with conditions based on those experienced by the lubricant in the engine environment. The products from this degradation have been analysed using gas chromatography with mass spectra and nitrogen chemiluminescence detectors. This analysis has been coupled with infrared spectroscopy of both the liquid phase and the exhaust gases from the reactor. Squalane has been used as a model hydrocarbon for a base oil, and methyl linolate as a model for biofuel. The use of model systems allows the identification of the mixture of the degradation products from the starting materials and therefore giving evidence to assign the mechanism. Conclusions from squalane and methyl linolate model compounds have been confirmed as translatable, using Polyalphaolefin baseoil and biodiesel.

The uses of gas chromatography as a separation techniques coupled with the high level of analysis has allowed products with functional groups containing nitrogen and oxygen to be observed. Mass spectra has enabled the identification of ketones, alcohol and alkane fragments as the products of the nitration of squalane. The NCD detector has allowed the identified of nitromethane and nitroalkanes as products by the comparison with standards and the retention indices.

The gas phase infrared was firstly able show a decrease in the concentration of the nitrogen dioxide of up to 100 % dependant on the reaction conditions. Gas phase products were also identified with the formation of carbon oxides from the nitration reactions. Infrared analysis on the liquid shows absorbencies which are at the wavelengths associated with the nitrate ester and water as the products of the nitration reactions.

The detailed product analysis, has enabled a new mechanism to be proposed. The

mechanism for autonitration has comparable stages to the published and accepted mechanism for autoxidation of lubricants in the engine. This mechanism fits with the data generated in previous work, however it allows a deeper understanding to be presented for the nitration and nitrooxidation. This mechanism is initiated by hydrogen abstraction to form HONO, this is in line with previous studies.¹⁰¹ The nitrogen dioxide then adds to the alkyl radical to form nitroalkanes or alkyl nitrite. The mechanism then is based the novel stages which differ when compared to the previously published work. The decay of the nitrite under these conditions due to the weak bond to form a alkoxy radical. The alkoxy radical then is able to react as published for autoxidation to form ketones, alcohol and alkanes.

Some of the expected products were not able to be identified using the techniques applied. The equilibrium position of the nitration is thought to favour addition of the nitrogen dioxide to the radical to form the nitroalkanes or alkyl nitrite. Comparison of the published bond strength of the CO-NO bond in the alkyl nitrites with the CO-OH of a peroxide has shown the decay of the these products will happen rapidly as is known to occur with the peroxides.¹³

The comparison of this study with other data generated by Coultas¹ and by Afton Chemical in field trials show the connections between the oxidation and nitration mechanism when measured by the industry standard methods. This data supports the conclusions that these mechanisms are connected with the initiation stage being the rate determining step.

This study has provided greater understanding about how increased levels of nitrogen dioxide can cause further oxidation to the lubricant. This also supports the idea that the level of NO₂ needs to be considered when designing engine systems to maximise the lifetime of the lubricant. Due to the relationship between the oxidation and the nitration it can also be suggested that radical scavenger antioxidants will also help control nitration reactions. These conclusions are also supported by the work on antioxidants and nitrations carried out by Pochopien.⁷⁶

9.2 Future work

The biggest area for further investigation is the product identification accounting for the nitrogen loss. The identification of nitrogen has been one of the hardest areas in this project with the NCD enabling approximately 20% of the reacted nitrogen to be

quantified. The identification of this level of nitrogen has been a major contributing factor to understanding the mechanism. However, the identification of the currently unidentified nitrogen and the form this takes may give add another level of understanding.

From the results and the literature it is not widely accepted whether the interconversion of nitroalkanes and alkyl nitrites can occur in an accessible reaction pathway or not. The monitoring of these species at different temperatures to give the reaction kinetics would be able to answer if this reaction occurs in these conditions and in other regimes. This understanding would indicate whether nitroalkanes would continue to increase in concentration in line with this study or there would be decay via the nitrite pathway over a longer time frame.

This study has focused branched alkanes as a model for highly refined base oil. Base oil used in engine contains other constituents, including rings, aromatics and heteroatoms. Dependant on the source of the crude oil and the amount of refining the impacts the level of other functionality beyond the alkanes in the base oil. The other functional groups such as aromatics are likely to be able to degrade *via* in a different mechanism, closer to the work presented by Pochopien.⁷⁶ The methyl linolate model for biodiesel is likely to apply to lower lever of unsaturation and in unsaturated species beyond biodiesel. However, work confirming how the mechanism differs for aromatics and heteroatom containing species can complete the picture for all base oil constituents.

The biggest difference between the system in this study and and engine oil is the addition of additives. Engine oils are a complex system containing many additives to the oil. Antioxidants have been shown by Pochopien to interact with nitrogen dioxide.⁷⁶ Other additives, such as dispersant and detergents, which are the highest concentration of additives in the a full formulated oil have been shown to impact oxidation. Therefore the application of different analytical techniques, such as LC-MS, could lead to an understanding of how the mechanism presented in this study is affected by additives. An understanding for the direct interaction between nitrogen dioxide and additives would also help to build complete understanding for the degradation of engine oils.

Nitrogen levels have been found to be high in deposits in the engine when the levels of NO_x is increased. The mechanism presented here is not able to explain these observation.⁴⁹ This difference can be due to the time line of these experiments, the mechanism presented from the results of this study is based on the short term nitration. However the long term nitration may also differ as the mechanism may alter with higher

molecular weight and polar species which lead to deposits formation.

List of Abbreviations

API	American petroleum institute
ATR IR	Attenuated total reflection infrared
CO	Carbon monoxide
CO ₂	Carbon dioxide
DFT	Density Functional Theory
FT IR	Fourier transform infra red
GC	Gas Chromatography
GC x GC	Two dimensional Gas Chromatography
MS	Mass spectrometry
NCD	Nitrogen chemiluminescent Detection
NIST	National Institute of Standards and Technology
NMR	Nuclear magnetic resonance
NO ₂	Nitrogen Dioxide
NO	Nitric oxide
NO _x	Nitric Oxides
PAO	Poly Alpha Olefin
PDSC	Pressure differential scanning calorimetry
R	Alkane fragment
ToF MS	Time of flight Mass spectrometry

Appendix

A1 : Appendix for chapter 3

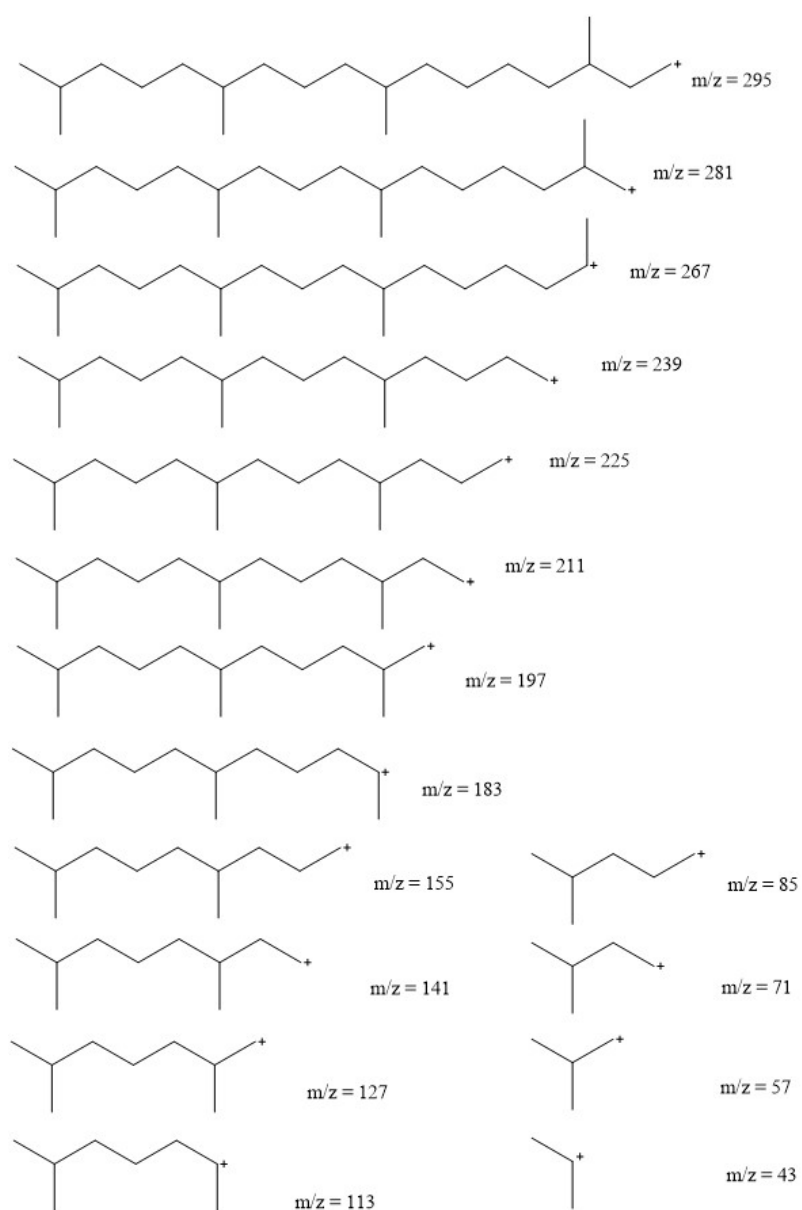


Figure 9.1: Fragmentation pattern to identify 2,6,10,15,19 pentamethyl henicosane

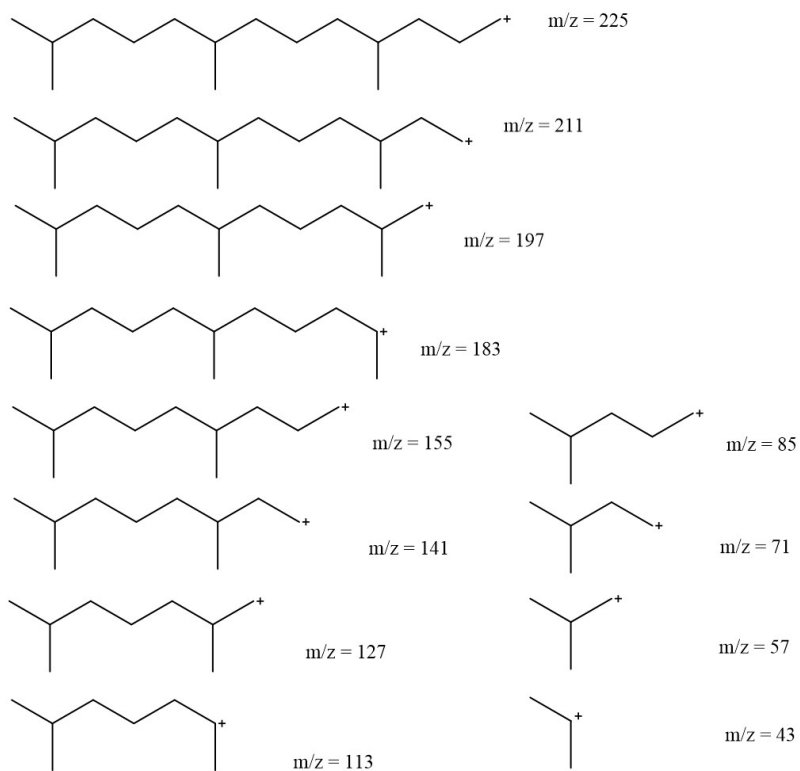


Figure 9.2: Fragmentation pattern to identify 2,6,10,15,19 pentamethyl eicosane

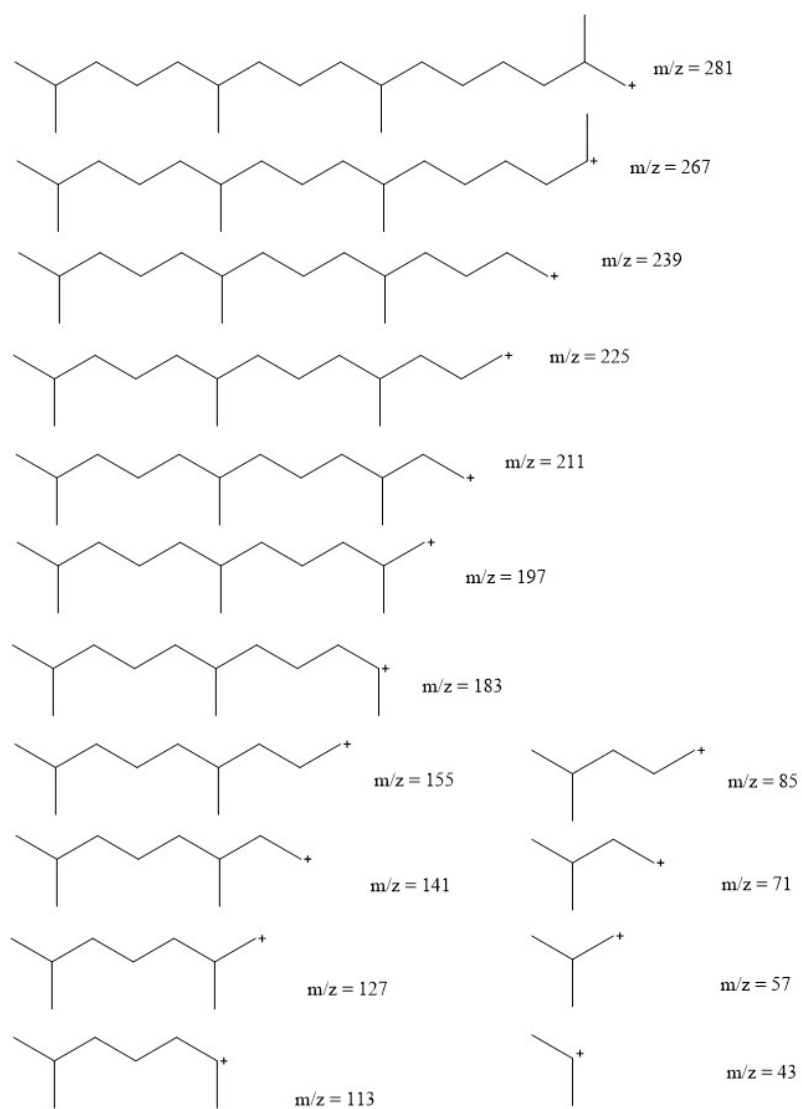


Figure 9.3: Fragmentation pattern to identify 2,6,10,15 tetraamethyl eicosane

A2 : Appendix for chapter 4

Table 9.1: Calculated concentrations of NO₂ and O₂ in the reactor

Temp / °C	Temp / K	[NO ₂] / 10 ⁻⁵ mol dm ⁻³	[O ₂] / 10 ⁻¹¹ mol dm ⁻³	[O ₂] / ppb
150	423	4.089330	0.31	0.08
160	433	4.089329	0.65	0.16
170	443	4.089328	1.31	0.32
180	453	4.089325	2.58	0.63
190	463	4.089321	4.91	1.20
200	473	4.089312	9.11	2.23

A3 : Appendix for chapter 6

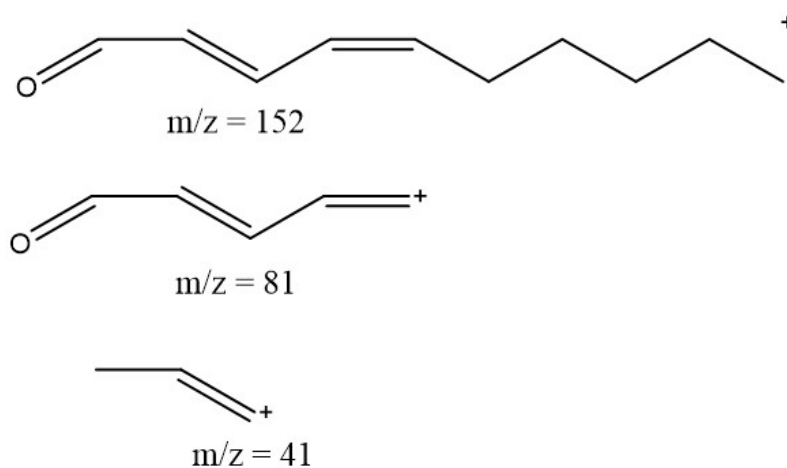


Figure 9.4: Fragmentation pattern to identify dec-2,4-dien-1-al

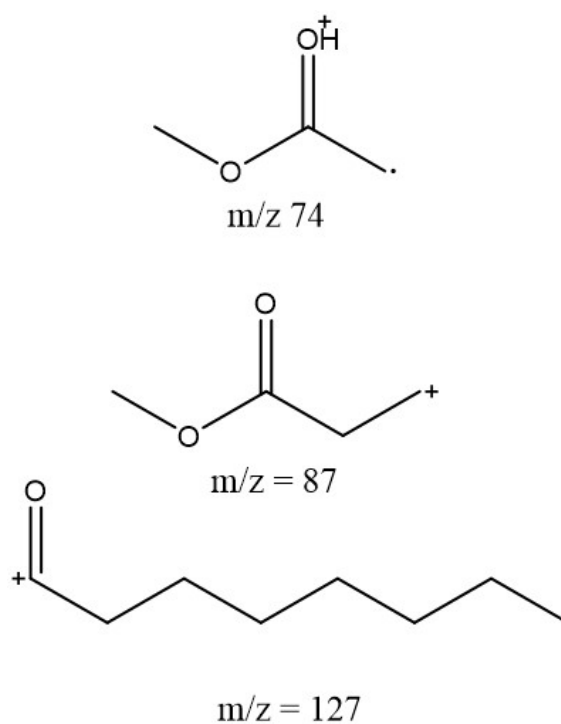


Figure 9.5: Fragmentation pattern to identify methyl octanoate

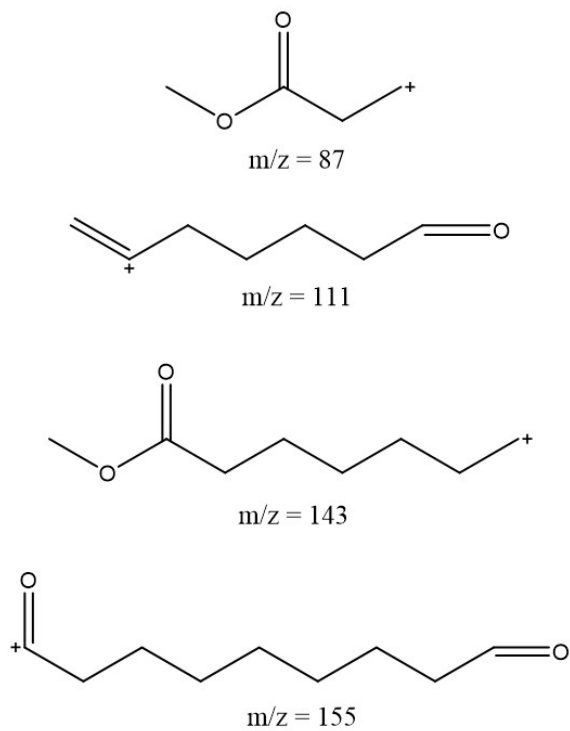


Figure 9.6: Fragmentation pattern to identify methyl nonano-1-al

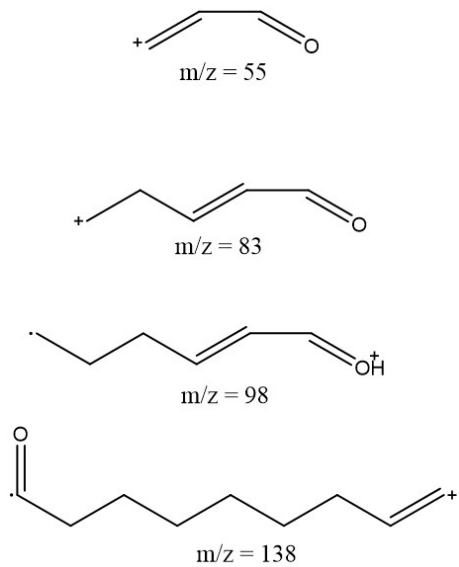


Figure 9.7: Fragmentation pattern to identify dec-2-eno-1-al

Bibliography

- [1] D. Coultas, *UNITI Mineral Oil Conference Proceedings*, 2015.
- [2] D. Han and J. Lee, *Tribology international*, 1998, **31**, 753–760.
- [3] M. Stark, J. Wilkinson, J. R. Lindsay Smith, A. Alfadhl and B. A. Pochopien, *Industrial & Engineering Chemistry Research*, 2011, **50**, 817–823.
- [4] C. inc, P. Linstrom and W. Mallard, in *NIST Chemistry WebBook, NIST Standard Reference Database Number 69*, National Institute of Standards and Technology, Gaithersburg MD, 1964, p. 8753.
- [5] Coblenz Coblenz inc, P. Linstrom and W. Mallard, in *NIST Chemistry WebBook, NIST Standard Reference Database Number 69*, National Institute of Standards and Technolog, Gaithersburg MD, 1964, p. 8755.
- [6] E. Bell, W. Vaughan and F. Rust, *Journal of the American Chemical Society*, 1957, **97**, 3–6.
- [7] F. van der Klis, M. H. van den Hoorn, R. Blaauw, J. van Haveren and D. S. van Es, *European Journal of Lipid Science and Technology*, 2011, **113**, 562–571.
- [8] API, *Engine Oil Licensing and Certification System- API 1509*, 2011, 1–28.
- [9] W. A. Rosser and H. Wise, *The Journal of Chemical Physics*, 1956, **24**, 493.
- [10] R. Mortier and S. Orszulik, *Chemistry and Technology of Lubricants*, Springer, 2nd edn., 1997, pp. 98–140.
- [11] M. Fenske and C. Stevenson, *Industrial & Engineering Chemistry*, 1941, **33**, 516–524.
- [12] M. Nakada, *Tribology International*, 1994, **27**, 3–8.
- [13] G. H. Denison, *Industrial & Engineering Chemistry Research*, 1944, **36**, 477–482.

- [14] M. Diaby, M. Sablier, a. Le Negrate, M. El Fassi and J. Bocquet, *Carbon*, 2009, **47**, 355–366.
- [15] J. Kagawa, *Toxicology*, 2002, **181-182**, 349–53.
- [16] B. Kowalski, *Thermochimica acta*, 1995, **250**, 55–63.
- [17] N. Fox and G. Stachowiak, *Tribology International*, 2007, **40**, 1035–1046.
- [18] European Union, *Official Journal of the European Union*, 2009, 16–62.
- [19] J. Salimon, N. Salih and E. Yousif, *Journal of Saudi Chemical Society*, 2011, **15**, 195–201.
- [20] S. Bekal and N. R. Bhat, *Energy Sources, Part A: Recovery, Utilization, and Environmental Effects*, 2012, **34**, 1016–1026.
- [21] S. K. Saxena, V. Chhibber, H. C. Joshi and O. Anand, *Advances in Pure and Applied Chemistry*, 2012, **1**, 18–19.
- [22] P. Nagendramma and S. Kaul, *Renewable and Sustainable Energy Reviews*, 2012, **16**, 764–774.
- [23] J. Peters and S. Thielmann, *Energy Policy*, 2008, **36**, 1538–1544.
- [24] G. P. Pousa, A. L. Santos and P. A. Suarez, *Energy Policy*, 2007, **35**, 5393–5398.
- [25] W. Lowe, *Synergistic antioxidant additive composition*, 1978.
- [26] H. Low, *Industrial & Engineering Chemistry Product Research and Development*, 1966, **244**, 80–86.
- [27] S. M. Hsu, *Tribology International*, 2004, **37**, 553–559.
- [28] S. Korcek and R. K. Jensen, *A S L E Transactions*, 2008, **19**, 83–94.
- [29] D. C. Kramer, J. N. Ziemer, M. T. Cheng, C. E. Fry, R. N. Reynolds, B. K. Lok, M. L. Sztenderowicz and R. R. Krug, NLGI Annual Meeting, 1999.
- [30] B. Barman, *Tribology International*, 2002, **35**, 15–26.
- [31] A. Adhvaryu, S. Z. Erhan, S. K. Sahoo and I. D. Singh, *Fuel*, 2002, **81**, 785–791.
- [32] S. McCoy, *Ph.D. thesis*, University of Kentucky, 2007.
- [33] S. Z. Erhan, B. K. Sharma, Z. Liu and A. Adhvaryu, *Journal of Agricultural and Food Chemistry*, 2008, **56**, 8919–25.

- [34] N. Dörmő, K. Bélafi-Bakó, L. Bartha, U. Ehrenstein and L. Gubicza, *Biochemical Engineering Journal*, 2004, **21**, 229–234.
- [35] H. Johnston and W. Giauque, *Journal of the American Chemical Society*, 1929, **51**, 3194–3214.
- [36] A. B. Mathur, V. Kumar and G. N. Mathur, *Polymer Photochemistry*, 1982, **2**, 161–165.
- [37] J. Pfaendtner and L. J. Broadbelt, *Industrial & Engineering Chemistry Research*, 2008, **47**, 2897–2904.
- [38] N. Porter, S. E. Caldwell and K. Mills, *Lipids*, 1995, **30**, 277–90.
- [39] A. Monyem and J. V. Gerpen, *Biomass and Bioenergy*, 2001, **20**, 317–325.
- [40] R. Hamilton, C. Kalu, E. Prisk, F. Padley and H. Pierce, *Food Chemistry*, 1997, **60**, 193–199.
- [41] S. Hsu, E. Klaus and H. Cheng, *Wear*, 1988, **128**, 307–323.
- [42] S. Hsu and R. Gates, *Tribology International*, 2005, **38**, 305–312.
- [43] J. Lahijani, F. Lockwood and E. Klaus, *ASLE transactions*, 1982, **25**, 25–32.
- [44] C.-S. Koh and J. B. Butt, *Industrial & Engineering Chemistry Research*, 1995, **34**, 524–535.
- [45] C. J. Hammond, J. R. Lindsay Smith, E. Nagatomi, M. S. Stark and D. J. Waddington, *New Journal of Chemistry*, 2006, **30**, 741.
- [46] S. Blaine and P. E. Savage, *Industrial & Engineering Chemistry Research*, 1991, **30**, 2185–2191.
- [47] R. Jensen and S. Korcek, *Journal of the American Chemical Society*, 1981, **103**, 1742–1749.
- [48] A. Goosen and S. Kindermans, *South African Journal of Chemistry*, 1997, **50**, 9–16.
- [49] R. Spindt, *Journal of the Air Pollution control Association*, 2012, **6**, 127–133.
- [50] P. Flynn, G. Hunter, L. Farrel, R. Durrett, O. Akinyemi, a.O. Zur Loye, C. Westbrook and W. Pitz, *Proceedings of the Combustion Institute*, 2000, **28**, 1211–1218.

- [51] J. Kasper, *Journal of the Air & Waste Management Association*, 1996, **46**, 127–133.
- [52] D. Iverach, K. Basden and N. Kirov, *Symposium (International) on Combustion*, 1973, **14**, 767–775.
- [53] B. G. Gowenlock and G. B. Richter-Addo, *Chemical Reviews*, 2004, **104**, 3315–40.
- [54] P. F. Flynn, R. P. Durrett, G. L. Hunter, A. O. Loye, J. E. Dec and C. K. Westbrook, *Society of Automotive Engineers International Congress and Exposition*, 1999.
- [55] J. Wüning, *Progress in Energy and Combustion Science*, 1997, **23**, 81–94.
- [56] C. Fenimore, *Symposium (International) on Combustion*, 1971, **13**, 373–380.
- [57] T. Hanson and A. Egerton, *Proceedings of the Royal Society of London. Seris A, Mathematical and Physical Sciences*, 1937, **163**, 90–100.
- [58] Z. Huang, S. Shiga, T. Ueda, H. Nakamura, T. Ishima, T. Obokata, M. Tsue and M. Kono, *Journal of Automobile Engineering*, 2003, **217**, 935–941.
- [59] C.-Y. Lin and H.-A. Lin, *Fuel Processing Technology*, 2007, **88**, 35–41.
- [60] G. Josefsson, I. Magnusson, F. Hildenbrand, C. Schulz and V. Sick, *Symposium (International) on Combustion*, 1998, **27**, 2085–2092.
- [61] J. Wang, Z. Huang, B. Liu and X. Wang, *Frontiers of Energy and Power Engineering in China*, 2009, **3**, 204–211.
- [62] H. Diamond, H. C. Kennedy and R. G. Larsen, *Industrial & Engineering Chemistry*, 1949, **41**, 495–501.
- [63] K. Iwakata, Y. Onodera, K. Mihara and S. Ohkawa, *SAE Technical Paper*, 1993, **932839**, year.
- [64] M. D. Johnson and S. Korcek, *Lubrication Science*, 1991, **3**, 95–118.
- [65] H. Niki and P. Maker, *The Journal of Physical Chemistry*, 1978, **82**, 135–137.
- [66] S. Sillman, *Atmospheric Environment*, 1999, **33**, 1821–1845.
- [67] R. Atkinson, S. M. Aschmann, W. P. L. Carter, A. M. Wlner and J. N. Pitts, *Journal of Physical Chemistry*, 1982, **86**, 4563–4569.

- [68] J. Arey, S. M. Aschmann, E. S. C. Kwok and R. Atkinson, *Journal of Physical Chemistry*, 2001, **105**, 1020–1027.
- [69] K. Otsuka, R. Takahashi, K. Amakawa and I. Yamanaka, *Catalysis Today*, 1998, **45**, 23–28.
- [70] K. R. Darnall, W. P. L. Carter, A. M. Winer, A. C. Lloyd and J. N. J. Pitts, *Journal of Physical Chemistry*, 1976, **80**, 1948 – 1950.
- [71] R. Atkinson, S. Aschmann and A. Winer, *Journal of Atmospheric Chemistry*, 1987, **5**, 91–102.
- [72] I. P. Kandylas, O. A. Haralampous and G. C. Koltsakis, *Industrial & Engineering Chemistry Research*, 2002, **41**, 5372–5384.
- [73] F. Jacquot, V. Logie, J. F. Brillhac and P. Gilot, *Carbon*, 2002, **40**, 335–343.
- [74] A. Setiabudi, B. A. van Setten, M. Makkee and J. A. Moulijn, *Applied Catalysis B: Environmental*, 2002, **35**, 159–166.
- [75] A. Maiboom, X. Tauzia and J.-F. Hétet, *Energy*, 2008, **33**, 22–34.
- [76] B. A. Pochopien, *Ph.D. thesis*, University of York, 2012.
- [77] M. D. Johnson, S. Korcek and M. J. Rokosz, *Lubrication Science*, 1994, **6**, 247–266.
- [78] J. Coates and L. Setti, *ASLE Transactions*, 1986, **29**, 394–401.
- [79] A. Ali, F. Lockwood, E. E. Klaus, J. L. Duda and E. J. Tewksbury, *ASLE transactions*, 1979, **22**, 267–276.
- [80] F. Owrang, H. k. Mattsson, J. Olsson and J. Pedersen, *Thermochimica Acta*, 2004, **413**, 241–248.
- [81] R. Holman and C. Nickell, *Journal of the American Oil Chemists' Society*, 1958, **35**, 422–425.
- [82] J. Blomberg, P. J. Schoenmakers, J. Beens and R. Tijssen, *Journal of High Resolution Chromatography*, 1997, **20**, 539–544.
- [83] X. Yan, *Journal of Chromatography*, 2002, **976**, 3–10.
- [84] B. Chawla, *Journal of Chromatographic Science*, 1997, **35**, 97–104.

- [85] P. Zeuthen, K. G. Knudsen and D. Whitehurst, *Catalysis Today*, 2001, **65**, 307–314.
- [86] R. I. Taylor and P. G. Evans, *Proceedings of the Institution of Mechanical Engineers, Part J: Journal of Engineering Tribology*, 2004, **218**, 185–200.
- [87] Z. Qian, H. Liu, G. Zhang and D. J. Brown, *Knowledge-Based Intelligent Information and Engineering Systems*, 2006, **4251**, 1198–1205.
- [88] J. Ong, *Computers in industry*, 1990, 255–258.
- [89] D. M. Levermore, M. Josowicz, W. S. Rees and J. Janata, *Analytical chemistry*, 2001, **73**, 1361–5.
- [90] J. Habeeb and W. Stover, *ASLE transactions*, 1986, 37–41.
- [91] H. Chang, Y. Zhang and L. Chen, *Applied Thermal Engineering*, 2003, **23**, 2285–2292.
- [92] S. Verhelst and C. Sheppard, *Energy Conversion and Management*, 2009, **50**, 1326–1335.
- [93] S. Nemoto, K. Kawata and T. Kuribayashi, *JSAE Review*, 1997, **18**, 271–276.
- [94] M. Stark, R. Gamble, C. Hammond, H. Gillespie, J. L. Smith, E. Nagatomi, M. Priest, C. Taylor, R. Taylor and D. Waddington, *Tribology Letters*, 2005, **19**, 163–168.
- [95] R. Gamble, M. Priest and C. Taylor, *Tribology Letters*, 2003, **14**, 147–156.
- [96] J. Dasch, *Journal of the Air & Waste Management Association*, 1992, 37–41.
- [97] The European Commission, *Official Journal of the European Union*, 2012.
- [98] K. Satoh, L. Zhang, H. Hatanaka, T. Takatsuki and K. Yokota, *JSAE review*, 1997, **18**, 369–375.
- [99] T. I. Dugmore and M. S. Stark, *Fuel*, 2014, **124**, 91–96.
- [100] R. Ballini, L. Barboni and G. Giarlo, *The Journal of organic chemistry*, 2004, **1**, 6907–6908.
- [101] P. Gray and A. Yoffe, *Chemical Reviews*, 1955, **9**, 1069–1154.
- [102] T. Turney and G. Wright, *Chemical Reviews*, 1959, **59**, 497–513.

- [103] E. S. Kovats, *Advanced Chromotography*, 1965, **1**, 227–249.
- [104] F. McLafferty, *Analytical Chemistry*, 1959, **31**, 82–87.
- [105] I. K. Newhall, *Symposium (International) on Combustion*, 1969, **12**, 604 – 613.
- [106] C. J. Pouchert, *The Aldrich Library of FT-IR Spectra - Vapour Phase Volume 3*, 1989, pp. 1689–1690.
- [107] R. Cueto and W. Pryor, *Vibrational Spectroscopy*, 1994, **7**, 97–111.
- [108] George Socrates, *Infrared and Raman Characteristic Group Frequencies: Tables and Charts*, John Wiley & Sons, 2004, p. 18.
- [109] T. Dugmore, *Ph.D. thesis*, University of York, 2011.
- [110] P. Neogi and T. Chowdhuri, *Journal of the Chemical Society, Transactions*, 1916, **30**, 701–707.
- [111] S. Ray, P. V. C. Rao and N. V. Choudary, *Lubrication Science*, 2012, **24**, 23–44.
- [112] S. K. Hoekman, A. Broch, C. Robbins, E. Cenicerros and M. Natarajan, *Renewable and Sustainable Energy Reviews*, 2012, **16**, 143–169.